

NAVAL POSTGRADUATE SCHOOL

MONTEREY, CALIFORNIA



THESIS

**APPLICATION OF PRESSURE-SENSITIVE
PAINT IN SHOCK-BOUNDARY LAYER
INTERACTION EXPERIMENTS**

by

Douglas L. Seivwright

March, 1996

Thesis Advisor:

Raymond P. Shreeve

Approved for public release; distribution is unlimited.

19960607 105

DTIC QUALITY INSPECTED 3

REPORT DOCUMENTATION PAGE

Form Approved OMB No. 0704-0188

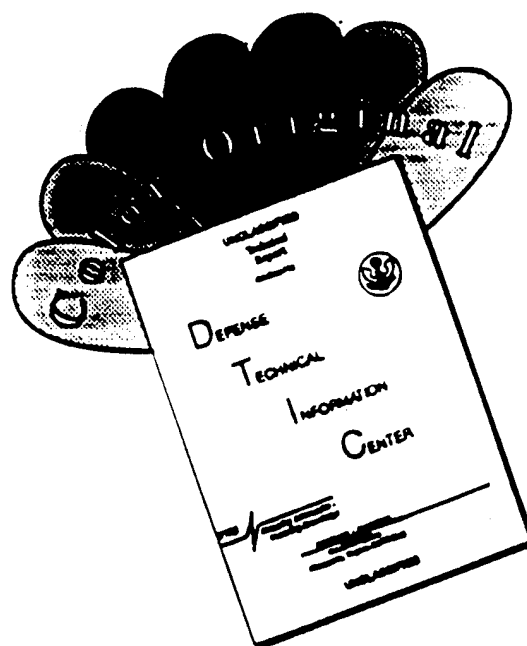
Public reporting burden for this collection of information is estimated to average 1 hour per response, including the time for reviewing instruction, searching existing data sources, gathering and maintaining the data needed, and completing and reviewing the collection of information. Send comments regarding this burden estimate or any other aspect of this collection of information, including suggestions for reducing this burden, to Washington Headquarters Services, Directorate for Information Operations and Reports, 1215 Jefferson Davis Highway, Suite 1204, Arlington, VA 22202-4302, and to the Office of Management and Budget, Paperwork Reduction Project (0704-0188) Washington DC 20503.

1. AGENCY USE ONLY (<i>Leave blank</i>)	2. REPORT DATE	3. REPORT TYPE AND DATES COVERED	
	March 1996	Master's Thesis	
4. TITLE AND SUBTITLE APPLICATION OF PRESSURE-SENSITIVE PAINT IN SHOCK-BOUNDARY LAYER INTERACTION EXPERIMENTS			5. FUNDING NUMBERS
6. AUTHOR(S) Seivwright, Douglas L.			8. PERFORMING ORGANIZATION REPORT NUMBER
7. PERFORMING ORGANIZATION NAME(S) AND ADDRESS(ES) Naval Postgraduate School Monterey CA 93943-5000			
9. SPONSORING/MONITORING AGENCY NAME(S) AND ADDRESS(ES)			10. SPONSORING/MONITORING AGENCY REPORT NUMBER
11. SUPPLEMENTARY NOTES The views expressed in this thesis are those of the author and do not reflect the official policy or position of the Department of Defense or the U.S. Government.			
12a. DISTRIBUTION/AVAILABILITY STATEMENT Approved for public release; distribution is unlimited.			12b. DISTRIBUTION CODE
13. ABSTRACT (<i>maximum 200 words</i>) A new type of pressure transducer, pressure-sensitive paint, was used to obtain pressure distributions associated with shock-boundary layer interaction. Based on the principle of photoluminescence and the process of oxygen quenching, pressure-sensitive paint provides a continuous mapping of a pressure field over a surface of interest. The data measurement and acquisition system developed for use with the photoluminescence sensor was evaluated first using an underexpanded jet blowing over a flat plate. Once satisfactory results were obtained, the system was used to examine shock-boundary layer interaction in a blow-down supersonic wind tunnel at Mach numbers of 1.4 and 1.7. Details of the measurement technique, and discussion of the flow fields which were examined, are reported.			
14. SUBJECT TERMS APPLICATION OF PRESSURE SENSITIVE PAINT IN SHOCK-BOUNDARY LAYER INTERACTION EXPERIMENTS			15. NUMBER OF PAGES 203
			16. PRICE CODE
17. SECURITY CLASSIFICATION OF REPORT Unclassified	18. SECURITY CLASSIFICATION OF THIS PAGE Unclassified	19. SECURITY CLASSIFICATION OF ABSTRACT Unclassified	20. LIMITATION OF ABSTRACT UL

NSN 7540-01-280-5500

Standard Form 298 (Rev. 2-89)
Prescribed by ANSI Std. Z39-18 298-102

DISCLAIMER NOTICE



**THIS DOCUMENT IS BEST
QUALITY AVAILABLE. THE COPY
FURNISHED TO DTIC CONTAINED
A SIGNIFICANT NUMBER OF
COLOR PAGES WHICH DO NOT
REPRODUCE LEGIBLY ON BLACK
AND WHITE MICROFICHE.**

Approved for public release; distribution is unlimited.

**APPLICATION OF PRESSURE-SENSITIVE PAINT
IN SHOCK-BOUNDARY LAYER INTERACTION EXPERIMENTS**

Douglas L. Seivwright
Lieutenant, United States Navy
B.S., Embry-Riddle Aeronautical University, 1985

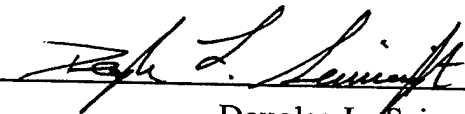
Submitted in partial fulfillment
of the requirements for the degree of

MASTER OF SCIENCE IN AERONAUTICAL ENGINEERING

from the

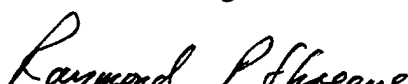
NAVAL POSTGRADUATE SCHOOL
March 1996

Author:

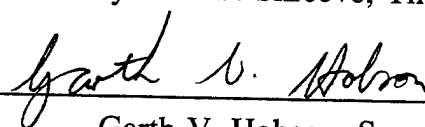


Douglas L. Seivwright

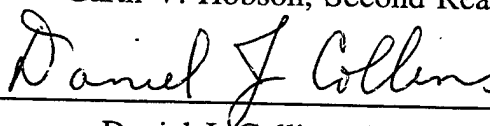
Approved by:



Raymond P. Shreeve, Thesis Advisor



Garth V. Hobson, Second Reader



Daniel J. Collins, Chairman
Department of Aeronautics and Astronautics

ABSTRACT

A new type of pressure transducer, pressure-sensitive paint, was used to obtain pressure distributions associated with shock-boundary layer interaction. Based on the principle of photoluminescence and the process of oxygen quenching, pressure-sensitive paint provides a continuous mapping of a pressure field over a surface of interest. The data measurement and acquisition system developed for use with the photoluminescence sensor was evaluated first using an underexpanded jet blowing over a flat plate. Once satisfactory results were obtained, the system was used to examine shock-boundary layer interaction in a blow-down supersonic wind tunnel at Mach numbers of 1.4 and 1.7. Details of the measurement technique, and discussion of the flow fields which were examined, are reported.

TABLE OF CONTENTS

I. INTRODUCTION	1
A. DESCRIPTION OF THE CONCEPT	2
B. APPROACH TO THE PROBLEM	3
II. THEORY OF MEASUREMENT	5
A. BACKGROUND	5
B. LUMINESCENCE	5
C. ABSORPTION AND EMISSION MECHANICS	6
1. Perturbation Theory	7
2. Spontaneous Emission	10
3. Triplet and Singlet States	10
4. Intramolecular Processes Involving Excited States	12
D. OXYGEN QUENCHING	16
E. MATHEMATICAL MODEL DEVELOPMENT	17
1. Temperature Effects	20
2. Aerodynamic Application	21
III. EARLY DEVELOPMENT USING A FREE-JET APPARATUS	23
A. APPARATUS AND FLAT PLATE ASSEMBLY	23
1. Freestream Flow Field of the Underexpanded Sonic Jet	27
a. Further Flow Field Studies	33

B. OPTICAL MEASUREMENT SYSTEM	41
1. Luminescence Coating	41
a. Reflective Backing	43
2. Illumination Source	43
a. Filters	45
3. Detection System	46
C. EXPERIMENTAL PROGRAM	48
1. Flat Plate Preparation	48
2. Experimental Procedure	49
3. Image Data Reduction	51
a. Image Processing	51
(1) Averaging	52
(2) Dark Current	54
(3) Registration	54
(4) Ratioing	63
b. Calibration	70
c. Field Pressure Map	77
IV APPLICATION TO SHOCK-BOUNDARY LAYER INTERACTION IN A SUPERSONIC WIND TUNNEL	83
A. DESCRIPTION OF FACILITY	83
1. Nozzle Blocks	86
a. Performance Evaluation of the Mach 1.7 Nozzle Blocks	86

B. INSTRUMENTATION	90
C. EXPERIMENTAL PROCEDURE	90
D. DISCUSSION AND RESULTS	94
V. CONCLUSIONS AND RECOMMENDATIONS	103
APPENDIX A. RUSSELL-SANDERS COUPLING	107
APPENDIX B. LUMINESCENCE COATING CHARACTERISTICS	109
A. TEMPERATURE SENSITIVITY	109
B. PHOTODEGRADATION	110
C. TIME RESPONSE	112
D. COATING THICKNESS / INDUCTION PERIOD	112
APPENDIX C. EPIX SOFTWARE SUMMARY	115
A. IMAGE DATA ACQUISITION	115
B. IMAGE PROCESSING	120
1. Averaging	120
2. Subtraction	121
3. Registration	123
4. Ratioing	126
5. Thresholding	127
6. Pseudo-coloring	128
APPENDIX D. DARK CURRENT	131

APPENDIX E. SUPERSONIC NOZZLE DESIGN PROGRAM	135
A. INVISCID CONTOUR SOFTWARE (Program char6)	136
1. Category 1: Characteristic Lengths and Nozzle Types	137
2. Category 2: Nozzle Flow and Geometry Specifications	140
3. "outpt1" Example and Description	143
B. MODIFICATION FOR VISCOUS EFFECTS (Program nbl6) ...	146
1. Category 1: Functional Modes	148
2. Category 2: Flow Conditions and Nozzle Dimensions	151
3. File "outpt3" Format Description	155
C. PROGRAM LISTINGS	159
REFERENCES	179
INITIAL DISTRIBUTION LIST	183

LIST OF FIGURES

Figure 1 Schematic Representation of the Pressure-Sensitive Luminescent Coating Concept	3
Figure 2 Energy Level Diagram for the Representation of Fluorescence and Phosphorescence	8
Figure 3 Energy Levels of Molecular Excited States and Transitions Between Them	13
Figure 4 Summary of Transition Types and Associated Rates	18
Figure 5 Schematic of the Underexpanded, Sonic Jet Nozzle and Supporting Facility	23
Figure 6 Underexpanded Jet Nozzle Apparatus	24
Figure 7 Schematic of the Pressure Port Arrangement on the Plate Surface	25
Figure 8 Bracket and Model Assembly	26
Figure 9 Bracket and Model Assembly Mounted to the Face of the Sonic Jet	26
Figure 10 Sketch of Jet Structure Behind a Highly Underexpanded Nozzle	27
Figure 11 Underexpanded Free Jet at 65 psig Plenum Pressure	28
Figure 12 Flow Visualization and Pressure Distribution Across Flat Plate at 65 psig ...	29
Figure 13 Flow Visualization and Pressure Distribution Across Flat Plate at 80 psig ...	30
Figure 14 Flow Visualization and Pressure Distribution Across Flat Plate at 90 psig ...	31
Figure 15 Flow Field Comparison Without (Top) and With (Bottom) the Flat Plate	32
Figure 16 Flow Visualization at 30 psig	34

Figure 17 Flow Visualization at 38 psig	35
Figure 18 Flow Visualization at 65 psig	36
Figure 19 Details of Separation Bubble	37
Figure 20 Flow Visualization at 25 psig	39
Figure 21 Flow Visualization at 40 psig	39
Figure 22 Flow Visualization at 68 psig	40
Figure 23 Flow Visualization at 75 psig	40
Figure 24 Schematic of Pressure Measurement System	41
Figure 25 Excitation and Emission of Platinum Octaethylporphyrin	42
Figure 26 Modification of Focusing Assembly of the Light Source	44
Figure 27 Spectral Response Curve for the COHU Camera Model 4910	47
Figure 28a Single Image of the Underexpanded Jet Across the Flat Plate at 65 psig	55
Figure 28b Graphical Representation of a Single Line of Pixels of a Single Image	56
Figure 29a Ten Averaged Images of the Underexpanded Jet Across the Flat Plate	57
Figure 29b Graphical Representation of a Single Line of Pixels of Ten Averaged Images	58
Figure 30a One Hundred Averaged Images of the Underexpanded Jet/Flat Plate	59
Figure 30b Graphical Representation of a Single Line of Pixels of One Hundred Images	60
Figure 31 Wind-On Image of the Underexpanded Jet at 65 psig Across a Flat Plate	64
Figure 32 Wind-Off Image for the 80 psig Condition	65
Figure 33 Three Dimensional Intensity Plot of the Surface of the Plate	66

Figure 34 Ratioed Image of the Wind-On and Wind-Off Images for the Flat Plate/Jet Interaction	68
Figure 35 Result of a Ratioed Image Following Improper Registration Technique	69
Figure 36 Calibration Line of Pixels for the 65 psig Case Prior to Spatial Averaging ...	72
Figure 37 Calibration Line of Pixels for the 65 psig Case After Spatial Averaging	73
Figure 38 Calibration Curve for the Underexpanded Jet/Flat Plate at 65 psig	74
Figure 39 Calibration Curve for the Underexpanded Jet/Flat Plate at 80 psig	75
Figure 40 Calibration Curve for the Underexpanded Jet/Flat plate at 90 psig	76
Figure 41 Graphical Representation of the Red, Green, and Blue Lookup Tables	78
Figure 42 Pressure Map of the Underexpanded Jet at 65 psig Across a Flat Plate	79
Figure 43 Pressure Map of the Underexpanded Jet at 80 psig Across a Flat Plate	80
Figure 44 Pressure Map of the Underexpanded Jet at 90 psig Across a Flat Plate	81
Figure 45 Schematic of the Supersonic Wind Tunnel and Supporting Facility	84
Figure 46 Supersonic Wind Tunnel Apparatus	84
Figure 47 Nozzle Blocks and Test Section Exploded View	85
Figure 48 Tunnel Pressure Distributions as a Result of Varying Rod Diameters	88
Figure 49 Cross-Sectional View of the Mass Bleed-Off System	89
Figure 50 Mass Bleed-Off Tube Mounted in the Tunnel	89
Figure 51 Spectrometer Results for the Optical Window	91
Figure 52 Instrumentation Setup for the Supersonic Wind Tunnel Shock-Boundary Layer Experiment	92
Figure 53 Schematic of the Normal Shock-Boundary Layer Interaction	95

Figure 54 Mach 1.4 Pressure Map of the Shock-Boundary Layer Interaction	96
Figure 55 Graphical Representation of the Pressure Distribution of the Shock-Boundary Layer Interaction at Mach 1.4	97
Figure 56 Mach 1.7 Pressure Map of the Shock-Boundary Layer Interaction	98
Figure 57 Graphical Representation of the Pressure Distribution of the Shock-Boundary Layer Interaction at Mach 1.7	99
Figure 58 Calibration Curve for the Mach 1.4 Interaction	100
Figure 59 Calibration Curve for the Mach 1.7 Interaction	101
Figure B1 Luminescence Intensity as a Function of Temperature	110
Figure B2 Effect of Temperature on Coating Calibration Curve	111
Figure B3 Illustrative Example of the Effect of Photodegradation on Response Time	111
Figure B4 Induction Period of the Luminescent Coating with Thicknesses in Excess of 17 Micrometers	113
Figure C1 "Main Menu" for EPIX Interactive Image Analysis Software	116
Figure C2 "Video Resolution" Sub-Menu	116
Figure C3 "Video Digitize/Display" Menu	117
Figure C4 "Motion Sequence Capture/Display" Sub-Menu	118
Figure C5 "Image Processing" Sub-Menu	122
Figure C6 "Two Image Arithmetic" Sub-Menu	123
Figure C7 "Pixel Peek, Poke and Plot" Sub-Menu	124
Figure C8 "Image, Copy, Resize, Rotate" Sub-Menu	125
Figure C9 "Contrast & Lookup Table" Sub-Menu	128

Figure C10 "Define Lookup Table" Sub-Menu	129
Figure D1 Representation of the Effect of Dark Current on the Creation of Charge	132
Figure E1 Illustrative Example of the Introductory Remarks for Program "char6"	136
Figure E2 Schematic of Supersonic Nozzle Design by Method of Characteristics	138
Figure E3 Example Showing the Format of File "outpt1"	144
Figure E4 Nozzle Wall Correction for Boundary Layer	147
Figure E5 Example Showing the Format of File "outpt3"	156

ACKNOWLEDGMENTS

I would like to take this opportunity to express my deep appreciation to those people who have contributed to this seemingly endless endeavor. To Professor Raymond Shreeve for his invaluable guidance and knowledge, and for instilling in me the qualities that are necessary to successfully investigate the scientific unknown. To Rick Still for his incredible technical expertise, creativity, and steady influence. I thank Thad Best for his support and sound judgment. Finally, I would like to thank my wife, Angelica, whose patience, support, and encouragement has shown me that there is no obstacle that cannot be overcome to attain your dreams and desires.

I. INTRODUCTION

One of the major thrusts of military aircraft engine design is towards achieving higher pressure ratios per compressor stage in order to reduce the number of stages and thereby reduce engine weight. This requires higher aerodynamic loading on the blades, and/or higher relative flow velocities over the blading. Where the relative Mach number is supersonic, shock waves will occur in front of and within the blade passages. The interaction of strong shocks with blade surface boundary layers can lead to high losses and reduced turning. Thus shock-boundary layer interaction, and methods to alleviate its attendant negative effects on compressor blade performance, warrant careful investigation. It was the need to make surface pressure measurements in a model simulation of shock-boundary layer interaction in a fan blade passage, which motivated the present study.

Currently, aerodynamic (surface) pressure measurements are made by installing a prearranged distribution of pressure ports in a wind-tunnel model or prototype aircraft. Since the installation of taps is an expensive process, the location and number of taps is normally predicated on a pre-selected area of interest. Obviously, this arrangement offers little flexibility if the area of aerodynamic interest is broad and fine spatial resolution is needed. Even with a substantially instrumented region, the information obtained is spatially discrete. It is often difficult to decide where to position the taps before the model is tested.

Within the last six years, the Central Aero-Hydrodynamic Institute in Moscow, the University of Washington (with support from Boeing and NASA) and McDonnell Douglas Aerospace have independently developed a new technique to measure surface pressures which is based on photoluminescent coatings [Ref. 1 through Ref. 9]. The pressure-sensitive coatings contain photoluminescent probe molecules. With the proper excitation of light, the molecules luminesce with an intensity which is inversely proportional to the local surface pressure. As a result, pressure-sensitive paints offer almost limitless spatial resolution, in addition to being applicable to surface locations which may not be accessible for pressure ports.

A. DESCRIPTION OF THE CONCEPT

Figure 1 illustrates the general concept of the method. A luminescent molecule dissolved in an oxygen-permeable plastic resin is applied to a surface of interest. When illuminated by ultraviolet radiation the coating luminesces with an intensity that depends on the oxygen partial pressure seen by the active molecule. Thus the oxygen partial pressure can be determined from the emitted light intensity and since the mole fraction of oxygen in air is a known constant, the air pressure may then be readily calculated. The result of this oxygen dependence is that the airflow-induced surface-pressure field (and the corresponding oxygen partial-pressure field), gives rise to a luminescence intensity distribution. The intensity field can be imaged using a video camera, the image digitized, processed and stored on a computer. The end result is a map of the surface pressure field.

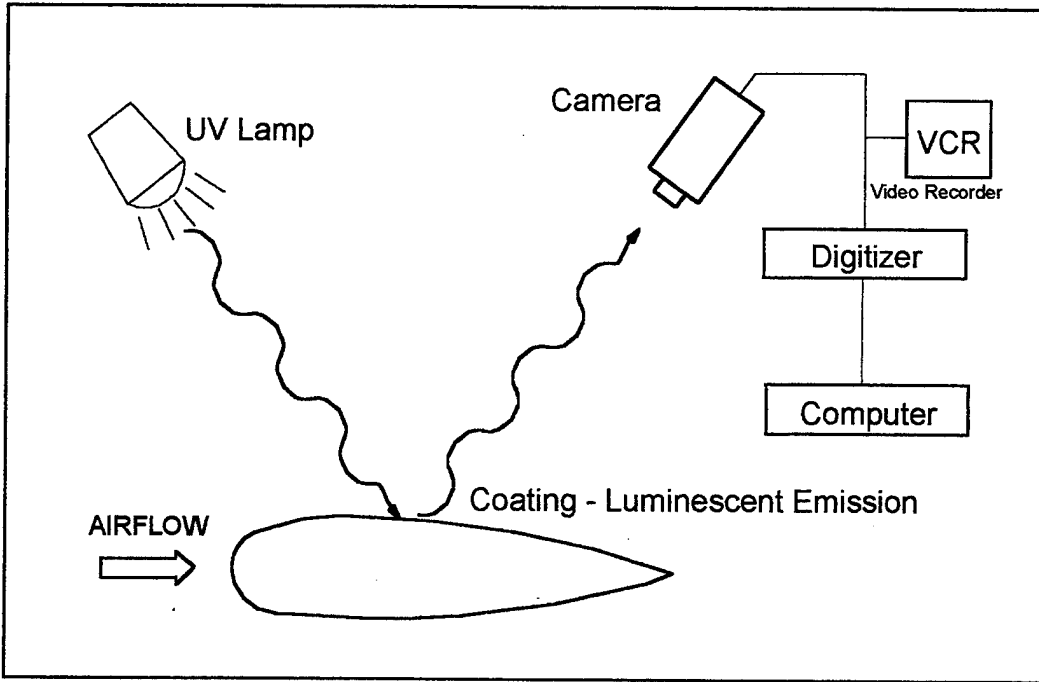


Figure 1. Schematic Representation of the Pressure-Sensitive Luminescent Coating Concept¹

The processing of the surface pressure image relies on a calibration curve for the coating material, which is based on the Stern-Volmer relation.[Ref. 1: p. 34]

B. APPROACH TO THE PROBLEM

The present work was focused on the development of a working pressure-measurement system, utilizing pressure-sensitive paints, for use in the Gas Dynamics and Turbopropulsion Laboratories at the Naval Postgraduate School. Although the system's initial application was tailored for use in the study of shock-boundary layer interaction in a pilot transonic cascade wind tunnel, and subsequently in a larger supersonic wind-tunnel, its use for other compressible flow studies was anticipated.

¹See Ref. 1, page 34, Figure 1

The initial development was carried out using an existing flat-plate model in an underexpanded sonic jet. This was an arrangement that would produce effects similar to those to be measured in the tunnel, (i.e. shock waves impinging on a surface, creating a near-discontinuity in a pressure distribution) but be visually unrestricted since no walls and windows were present. Subsequently, measurements were made of the interaction of the starting shock wave with the side-wall boundary layer in the test section of a blow down wind tunnel. Results were obtained at $M=1.4$ and $M=1.7$ using different fixed nozzle blocks. The blocks for $M=1.7$ were designed and built for the present study, and the design is detailed in Appendix E.

In reporting the work, Section II first provides some preliminary background work done in photoluminescent barometry in addition to the theory of photoluminescent coatings. Section III describes the development program using the sonic free-jet. Section IV provides results of applying the system in the supersonic wind tunnel, and Section V gives conclusions and recommendations. Since the system represents a powerful new tool for two laboratories, the attempt has been made to include all information and details necessary to both use and extend the present system.

II. THEORY OF MEASUREMENT

A. BACKGROUND

Photoluminescence and the process of quenching by oxygen is a photo-chemical interaction that is well documented and reasonably well-understood. In 1980, Peterson and Fitzgerald first recognized its potential as a means to make qualitative assessments in flow visualization studies [Ref. 3]. They reported on a technique in which fluorescent dye, when applied to a surface and excited by a blue light, illuminated in varying degrees of intensity, depending on the introduction of nitrogen or oxygen. When nitrogen was injected through a wall static-pressure tap, a bright streak of luminescence, moving in the direction of the surface flow, was observed. The nitrogen, in close proximity to the fluorescent dye, reduced the effect of the quenching (by displacing the oxygen) and allowed the intensity of the luminescence to increase. The introduction of oxygen, on the other hand, enhanced the quenching process and decreased the luminescence, producing a dark streak. This demonstrated that the concept of quenching could be used to acquire surface pressure measurements.

B. LUMINESCENCE

According to the laws of thermodynamics, a system in an excited energy state due to the absorption of radiation, must be such that the reverse process of emission of radiation can occur. If no other process is available to allow the system to return to its initial state,

then emission must take place. Light emission excited by light absorption is called photoluminescence.

Luminescence is a broad term which encompasses both fluorescence and phosphorescence. The basic, underlying difference between these two processes is the time of emission with respect to the end of excitation; fluorescence has a relatively short lifetime, approximately 10^{-9} - 10^{-7} seconds, whereas phosphorescence's lifetime persists for 10^{-4} - 10^{-2} seconds. It is the phosphorescent emission that was used in the present work to quantitatively measure the static pressure on a surface of interest.

C. ABSORPTION AND EMISSION MECHANICS

Quantum mechanics provides the necessary theoretical tools to describe the absorption and emission processes of light that were previously unexplainable by wave theory [Ref. 10: p. 457]. Instead of considering light as a wave train of infinite length, the radiation is instead composed of discrete photons (or quanta) whose energies are equal to $h\nu$, where h is the universal Planck constant, 6.63×10^{-27} erg sec. The concepts of light being consider as a wave train and that of discrete photons are linked in that the energy of the quantum is proportional to the light excitation frequency, ν . This led to the hypothesis that radiation of frequency ν could not be emitted or absorbed in arbitrary amounts, but only in quanta of energy $\epsilon = h\nu$. During an emission process following light absorption, less energy release by emission could occur, but would radiate at a lower frequency.

An absorbing molecule can exist in discrete, sharply defined levels in which transitions between states occur in certain definite steps. The lowest of these states is the ground state. States of higher energy are called excited states. There is a large number of possible excited states, but usually only several of those of the lowest energy are produced with visible or ultraviolet light. A simplistic description of the nature of these excited states is that a single electron has been promoted from an orbital occupied in the ground state to an orbital that is vacant while in the ground state.

Figure 2 illustrates several energy levels of an arbitrary molecule which are represented by the horizontal lines. The vertical distance between two of these lines is proportional to the corresponding difference in energy, $h\nu$; the level N represents the ground state. By absorption of light frequency ν_{NF} the molecule is raised to the state F and if no other energy levels exist between N and F, the molecule can return to N only by re-emission of a photon of light of the same frequency. Theoretically this is the simplest case of photoluminescence; it is called "resonance radiation". However, if, as indicated in Figure 2, several other levels C, D, ... are located between N and F, other transitions to C, D, ... can occur, resulting in the emission of spectral lines of frequency ν_{FC} , ν_{FD} , ... These frequencies must be smaller than ν_{FN} and therefore photoluminescence can have no greater frequency or shorter wave-length than the exciting light. [Ref. 11: p. 2]

1. Perturbation Theory

For a molecule that absorbs or emits quanta of radiation under the influence of an electric field, perturbation theory of quantum mechanics provides the theoretical model

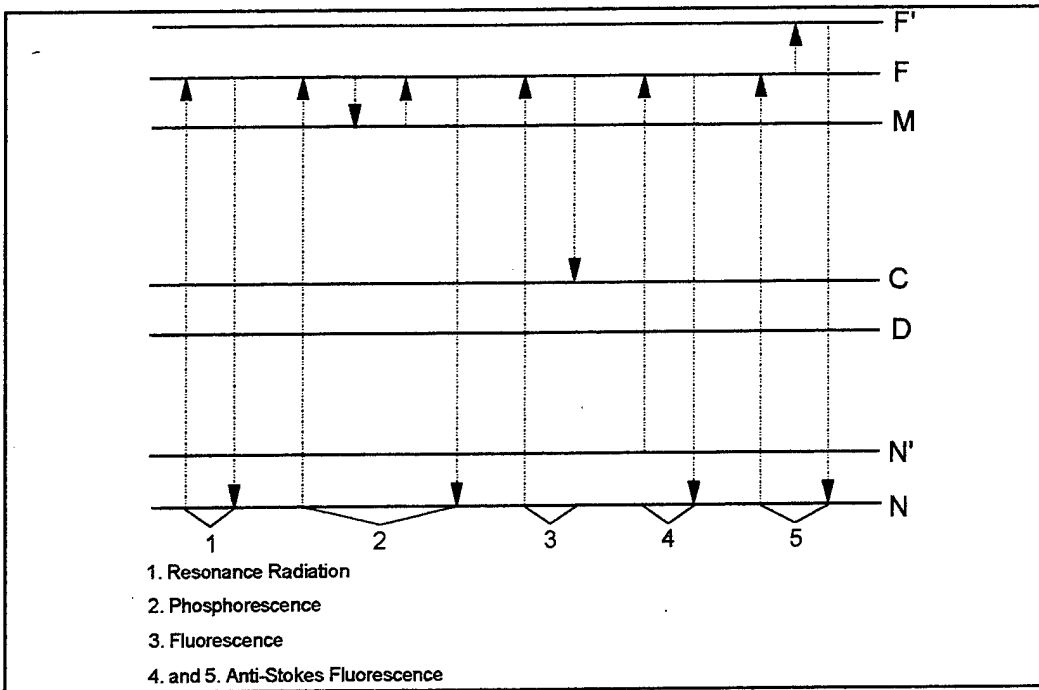


Figure 2. Energy Level Diagram for the Representation of Fluorescence and Phosphorescence²

that defines the physical interaction. The general solution of the wave equation for a molecule in the presence of a perturbing field results in certain derived relations that govern the changes of the molecule. One such outcome mandates that for radiation to be absorbed and transition from a stable ground state of energy to an electronically excited state of energy to occur, the frequency of the quantum must be proportional to the difference in energy between the states, a situation previously discussed. Once this condition is met, the probability of the transition is governed by the value of the transition moment integral, a second corollary from the solution of the perturbed wave equation:

²Figure 2 is found in Ref. 11, page 4, as Figure 2

$$m = \int \Psi_u \mathbf{M} \Psi_l d\tau$$

Here, Ψ_u and Ψ_l are the total wave functions for the upper and lower states respectively (the wave functions result from the unperturbed solution of the Schrödinger wave equation) and \mathbf{M} is defined as the dipole moment operator [Ref. 10: p. 583]. Evaluation of this integral determines the probability of an optical transition between two states. Detailed analysis has shown that transitions are probable only between states characterized by wave functions of a certain class. The results have been summarized in the form of selection rules which are formulated in terms of the quantum numbers that describe the electronic states involved [Ref. 12: p. 51].

Perhaps the most important is the rule governing spin multiplicity. This states that the spin of an electron must not change during an electronic transition. As will be seen later, although from a theoretical standpoint transitions between states of different "multiplicity" do not intercombine, in practice they are observed, but the probability is usually much lower than an allowed transition. Thus, selection rules are good empirical guides, but they are not inviolable.[Ref. 13: p. 36]

Although the selection rules considered have been based on the absorption and emission of light by a molecule under the influence of a perturbing field, a second set of selection rules similar to the first but derived under a different set of circumstances govern radiationless processes. These processes, in addition to the spontaneous emission of light, compete with the excited state of a molecule in depleting its acquired energy and allowing it to return to its ground state.

2. Spontaneous Emission

An excited state may undergo a third radiation-related transition to a lower state by means of spontaneous emission, i.e., fluorescence and phosphorescence. In this process, an excited species loses energy in a spontaneous manner in the absence of an electric field. It is a random process: the rate-of-loss of excited species following a kinetic first-order reaction. If a process follows first-order kinetics described by a rate constant "k", the mean radiative lifetime, (the time τ taken for the intensity to fall to $1/e$ of its initial value), is given by

$$\tau = 1/k$$

When a radiative transition occurs between states of similar multiplicity, it corresponds, according to the selection rules, to an allowed transition. Such transitions are characteristic of fluorescence emission having lifetimes equal to $\tau = 10^{-8}$ seconds. However, there are transitions in which τ is much higher, 10^{-3} seconds. When selection rules suggest a low probability for a transition to occur, such as between states of different multiplicity, the transition, though theoretically forbidden, can occur, but the process is relatively slow. This is representative of phosphorescent emission. [Ref. 10: p. 585]

3. Triplet and Singlet States

In the absence of a magnetic field, the energy of a single unpaired electron characterized by its given values of "n" (the principle quantum number) and "l" (the azimuthal quantum number) must be further refined to explain the observed fine structure of atomic spectra. The additional amount of energy that the spectroscopic evidence

indicates is attributed to the interaction that occurs between the angular momenta from the intrinsic spin and orbital motion of the electron. When several electrons within an atom (or molecule) are present, the resultant orbit and resultant spin angular momenta components can combine in several ways resulting in several energy levels for a single configuration of an atom (or molecule). This interaction is known as Russell-Sanders coupling, the result of which is the "multiplicity" of energy levels that a given electron configuration of an atom may possess. Thus, a single energy level for a given electron configuration for an atom (or molecule) is referred to as singlet state, two energy levels as a doublet, three energy levels a triplet, etc. [Ref.14: p. 79] A more thorough discussion is given in Appendix A.

Nearly all molecules have a ground-state electronic configuration in which the spin of each electron is opposed to, or paired up with, the spin of another electron which otherwise has the same spatial quantum numbers, a consequence of the Pauli exclusion principle. In this instance the total angular momentum of each electron within the pair, composed of the spin and orbital momenta, tend to cancel with each other. When all the pairs of electrons within the molecule are considered, the net result is zero total angular momentum (vector), producing a single energy level for the given electron configuration. Molecules will have, in addition to a ground state that is usually a singlet state, a number of excited states that also have all the electrons paired and that are, therefore, also singlet states. [Ref. 15: p. 16]

Whether or not the ground state is a singlet state for molecules with an even number of electrons, there will be excited states in which a pair of electrons have their spins in the same direction, giving the molecule a net total angular momentum (vector). In this case, the coupling interaction results in three energy levels for the configuration, and thus the designation triplet state.

Therefore, promotion of an electron to an upper state can in principle give rise to two types of energy states, the triplet and singlet, while still maintaining the same electron configuration. Therefore, for every singlet state there is a corresponding triplet state, with the triplet state displaying a lower energy level. Figure 3 illustrates the two types of electronically excited states, where the spin orientations for each state are depicted as arrows next to the appropriate state. The additional lines within each electronic state refer to the various vibrational and rotational energy levels the molecule may acquire with the absorption of energy.

4. Intramolecular Processes Involving Excited States

With the absorption of a quantum, a molecule is raised from a singlet ground to a singlet excited state. The selection rules stipulate that the absorption of electromagnetic radiation does not "unpair" the electrons of a molecule (transitions occur between states of like multiplicity) thus preventing direct absorption of light from a singlet to a triplet state. The molecule, having been raised to an upper vibrational level within the excited state, begins to lose the excess vibrational energy by collisions with surrounding molecules. The

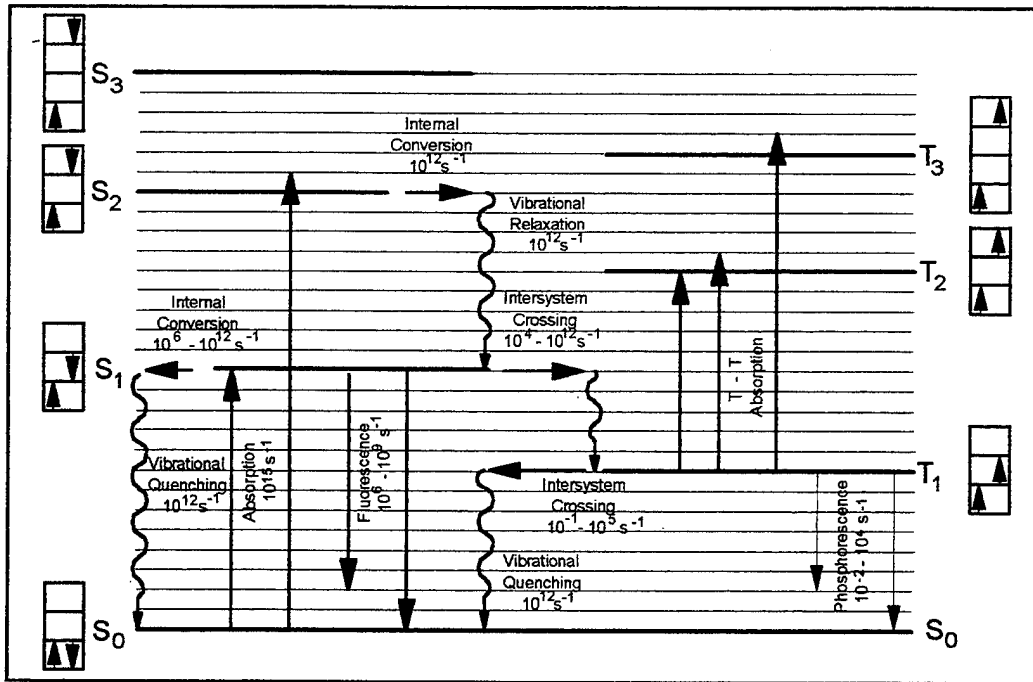
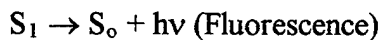
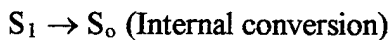


Figure 3. Energy Levels of Molecular Excited States and Transitions Between Them³

radiationless process of internal conservation then occurs whereby the molecule passes from a low vibrational level of the upper state to a high vibrational level of a lower state having the same total energy. Once internal conversion is complete, this cycle of events repeats itself leading to the net result of the molecule falling to the lowest vibrational level of the first excited singlet state as illustrated in Figure 3. [Ref. 15: p. 9]

At this point, the molecule may return to the ground state by one of three paths:



³ Figure 3 is found in Ref. 16, page 71, as Figure 5-1.

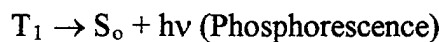
The internal-conversion process, involved with the intramolecular energy transfer between the first excited singlet and ground state, takes place at a much slower rate (10^{-9} seconds) as compared with the same process occurring between the upper excited singlet states to the first excited singlet state (10^{-12} seconds). The increase in inefficiency in energy transfer is explained by the relatively large energy separation between S_1 and S_0 as compared to the energy differences between the upper excited states. This allows fluorescence (10^{-9} to 10^{-7} seconds) and, with the combined effect of the spin-forbidden nature of the states, the process of intersystem crossing (10^{-9} seconds) to effectively compete with the internal conversion process.

When a molecule returns to the ground state via the first excited triplet state, it undergoes a conversion process known as intersystem crossing. Intersystem crossing is a non-radiative process between states of different multiplicity. It is theoretically forbidden with regard to the formal selection rules, but in practice, these transitions do take place (although with extremely low probability). This is made possible through the "breakdown" of the spin-orbit coupling model discussed in Appendix A. In the absence of magnetic or electric fields the total angular momentum of the molecule remains constant, and the ability to discern between specific states such as singlet and triplet is possible. However, when an electromagnetic field is present, though the total angular momentum vector remains constant, the spin and orbital degrees of freedom become time dependent, and it becomes meaningless to speak of specific states [Ref. 16: p. 12]. This ultimately leads to the mixing of states. The interaction is enhanced by heavier elements

due to an increase of the magnetic field developed by the nucleus, as in the case of platinum octaethylporphyrin (PtOEP).

The lowest vibrational level of the lowest triplet state is generally situated at an energy level below that of the lowest excited singlet state, but its upper vibrational levels reach to the bottom of the singlet level, and intersystem crossing occurs with the molecule crossing over to one of these upper vibrational levels of the lowest triplet state. From here the molecule rapidly loses its excess vibrational energy and falls to near the lowest vibrational level of the triplet state.

Again, the molecule may return to the ground state from this point by one of the following paths:



As before, it might be expected that the analogous process of intersystem crossing from the lowest vibrational level of the triplet state to the ground state would take place with equal facility as the transition from $S_1 \rightarrow T_1$. In fact it is usually some $10^6 - 10^9$ times slower. If radiationless $T_1 \rightarrow S_0$ transitions occurred with rate constants of 10^{-8} seconds, the molecule would have no time to emit $T_1 \rightarrow S_0$ phosphorescence by the spin-forbidden radiative process. On the other hand, if the $S_1 \rightarrow T_1$ intersystem crossing process were as slow as that of the $T_1 \rightarrow S_0$ radiationless process, then it could not compete effectively with fluorescence. Phosphorescence would then be a rare phenomenon and the photochemical behavior would be very different. The difference between the rates of the

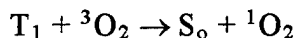
$S_1 \rightarrow T_1$ and $T_1 \rightarrow S_o$ radiationless processes is, as was the case with internal conversion, a function of the energy differences between S_1 and T_1 , and, T_1 and S_o . [Ref. 15: p. 41]

D. OXYGEN QUENCHING

The exceptionally long radiative lifetimes of molecules in the lowest triplet state make them vulnerable to a variety of radiationless processes that deactivate the molecule, allowing it to return to the ground state. As an example, they are very susceptible to collisions with molecules, and in such cases may encounter molecules of a specific nature which are particularly effective in removing excitation energy.

Previous reference was made to the fact that most molecules with an even number of electrons have a ground state in which their electrons occupy orbitals in pairs. These molecules were said to have singlet states. There are however some molecules containing an even number of electrons for which the states of lowest energy have two unpaired electrons occupying different orbitals. The most important of these is molecular oxygen, of which the ground state is a triplet. Molecular oxygen is very effective in removing triplet excitation energy, and can act at exceedingly low concentrations. [Ref. 15: p. 36]

The energy transfer that takes place when an excited triplet PtOEP molecule collides with a triplet oxygen results in a ground-state singlet PtOEP molecule and a singlet excited oxygen molecule. The reaction is expressed as follows:



The reaction occurs very rapidly but is consistent with the formal selection rules. It is this bimolecular reaction that results in the quenching of the phosphorescence. The University

of Washington found that when PtOEP was embedded in an oxygen-permeable silicon resin and subject to atmospheric pressure, the quenching reaction had a rate comparable to that of phosphorescence. Variations in atmospheric pressure from 0 to 1 atmospheres demonstrated a suitable drop in phosphorescence yield of PtOEP that would allow it to be useful as a measurement tool in the study of static pressure changes in aerodynamic wind tunnel testing. [Ref. 9: p. 18]

E. MATHEMATICAL MODEL DEVELOPMENT

Oxygen quenching of luminescence by collisional deactivation of the emission process is the basis for developing a prediction model. It is important to note that the end result of this development, the Stern-Volmer relation, is strictly valid only for free molecules in solution. However, it has been found that it describes accurately the quenching process that occurs in the present situation. The basis for the present development is the work of Parker [Ref. 15], which may be consulted for further details.

The development first begins with the definition of the triplet formation efficiency, ϕ_t , being the number of triplet molecules formed per quantum of exciting light absorbed. Assuming now that a system, illuminated with a beam of exciting light of constant intensity, is in a photochemically steady state. The rate of population of the lowest excited singlet state, S_1 , is found to equal the rate of light absorption, I_o , and the rate of formation of triplet molecules by crossing from S_1 is equal to $I_o\phi_t$.

Figure 4 illustrates the rates of the various processes by which the triplet is produced and consumed; these are represented in equation form as follows:

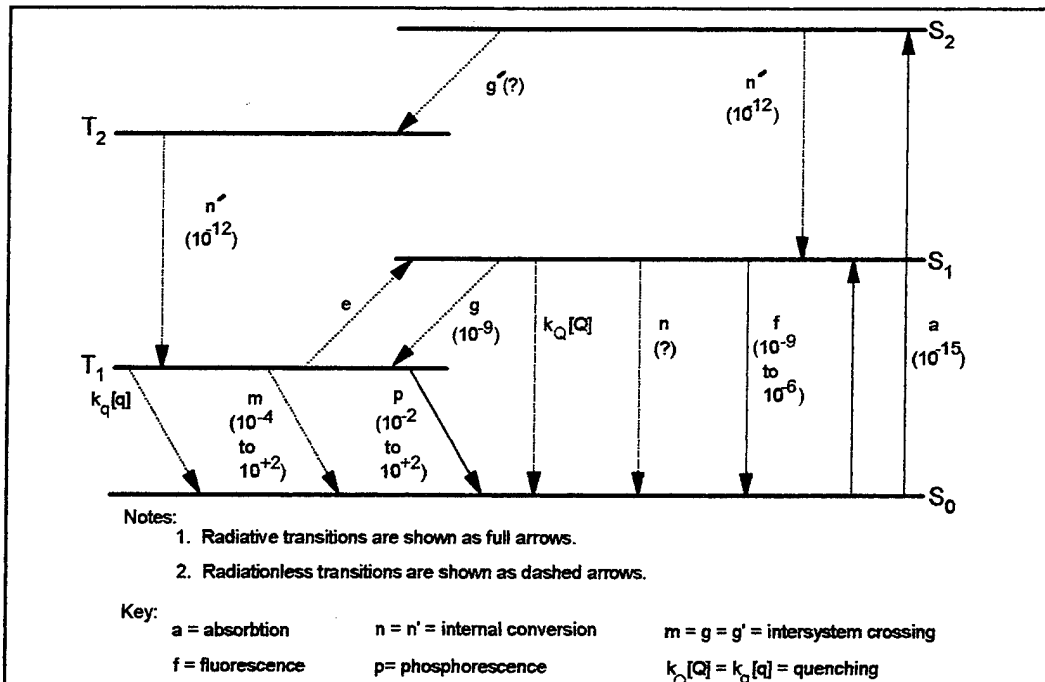


Figure 4. Summary of Transition Types and Associated Rates⁴



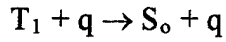
Rate = $I_a \phi_t$ (Triplet Production)



$k_p[T]$ (Phosphorescence)



$k_m[T]$ (Intersystem Crossing)



$k_q[T][q]$ (Triplet Quenching)



$k_e[T]$ (Intersystem Crossing)

The square bracketed $[q]$ and $[T]$ represent concentrations. $[q]$ represents the concentration of all quenching impurities in the system, $k_q[q]$ a composite pseudo first-order rate constant for impurity quenching, and $k_e[T]$ represents the rate of thermal activation of triplet molecules back to the excited singlet level [Ref. 15: p. 87].

⁴Figure 4 is found in Ref. 15, page 69, as Figure 23

[T] represents the concentration of excited triplet molecules when the steady state has been achieved. All processes so far considered in Figure 4, with the exception of light absorption, are first-order reactions having rate constants equal to the reciprocals of the lifetimes quoted.

Now consider, in addition to the previous statements and definitions made with respect to the steady state of the system, that the rate of production of excited triplet molecules (in state T_1) is just balanced by their rate of disappearance via the various processes discussed above. This can be expressed as

$$I_a \phi_t = (k_p + k_m + k_q[q] + k_e)[T] \quad (1)$$

Since the rate of emission of phosphorescence is $k_p[T]$, the phosphorescence efficiency ϕ_p is given by

$$\phi_p = k_p[T] / I_a \quad (2)$$

Equation (1) may be solved for I_a and substituted into equation (2) to arrive at

$$\phi_p = k_p \phi_t / (k_p + k_m + k_q[q] + k_e) \quad (3)$$

In the absence of quenching agents affecting the removal of triplet excitation energy, equation (3) gives, for the phosphorescence efficiency,

$$\phi_p^o = k_p \phi_t / (k_p + k_m + k_e) \quad (4)$$

Taking the ratio of equations (3) and (4):

$$\phi_p^o / \phi_p = 1 + k_q[q] / (k_p + k_m + k_e) \quad (5)$$

or,

$$\phi_p^o/\phi_p = 1 + K[q] \quad (6)$$

where

$$K = \tau_o k_q \text{ and } 1/\tau_o = (k_p + k_m + k_e) \quad (7)$$

Equation (6) is known as the Stern-Volmer equation for quenching, and the constant K as defined in equation (7) is referred to as the Stern-Volmer quenching constant.

For this particular application, the quenching impurity, [q], may be defined as

$$[q] = S P_{O_2} \quad (8)$$

where S is the solubility of oxygen in the system and P_{O_2} is the partial pressure of oxygen in equilibrium with it. This leads to the relation

$$\phi_p^o/\phi_p = 1 + K' P_{O_2} \quad (9)$$

Finally, by definition, the luminescence, I, is linearly proportional to the quantum yield (ϕ = photons emitted/photons absorbed) for a given quenching condition, (i.e., $I = I_{abs}\phi$), where I_{abs} is the excitation light intensity by the luminescent species. Thus

$$I_{max}/I = 1 + K' P_{O_2} \quad (10)$$

where I_{max} is the maximum possible value that occurs in the absence of a quencher.

1. Temperature Effects

The effect that temperature has on the efficiency of phosphorescence may lead to a decrease in the intensity by several orders of magnitude over the range of 77° K to room temperature. The effect results in the long lifetime of triplet states and the correspondingly greater susceptibility to impurity quenching and intersystem crossing [Ref. 15: p. 89].

The rate constants for each of the intramolecular processes depend on temperature, following the Arrhenius equation,

$$k = A e^{-E_a/R T},$$

where k is the rate constant, A is the pre-exponential factor, E_a is the activation energy, R is the gas constant, and T is the temperature in degrees Kelvin [Ref. 9: p. 20]. Hence, in equation (10), I , I_{max} , and K are all functions of temperature.

2. Aerodynamic Application

In order to apply the form of the Stern-Volmer relation presented in equation (10), it would be necessary to purge the vicinity of the surface of interest of all oxygen in order to determine I_{max} . In most cases of experimental work, this is impractical. A more convenient approach is to manipulate the governing equation so that determination of I_{max} becomes unnecessary.

Equation (10) is first modified by noting that the oxygen partial pressure, P_{O_2} , is related to the air pressure, P , by $P_{O_2} = X P$, where X is equal to the mole fraction of oxygen. Equation (10) then becomes:

$$I_{max}/I = 1 + K' X P \quad (11)$$

In the method used in the present work, two images are taken. In the "flow-on" case, the pressures are unknown. In the "flow-off" case, the pressure distribution is constant on the surface and equal to atmospheric pressure. These conditions are represented, respectively, as follows:

$$I_{max}/I = 1 + K' X P \quad (12)$$

and

$$I_{max}/I_o = 1 + K' X P_o \quad (13)$$

where the subscript "o" denotes the value for the flow-off conditions. Dividing equation (13) by equation (12),

$$I_o/I = (1 + K' X P)/(1 + K' X P_o) \quad (14)$$

Rearranging,

$$I_o/I = 1/(1 + K' X P_o) + [(K' X P_o)/(1 + K' X P_o)](P/P_o) \quad (15)$$

which gives

$$I_o/I = A + B (P/P_o) \quad (16)$$

where,

$$A = 1/(1 + K' X P_o) \text{ and } B = (K' X P_o)/(1 + K' X P_o) \quad (17)$$

A and B represent the coating sensitivity coefficients and are, in general, functions of temperature for both wind-on and wind-off conditions. In the absence of a temperature variation across the surface, A and B have the same value over the whole image. Notice that $A + B = 1$. This condition occurs only when the images of I and I_o are taken at the same temperature. If any temperature variation is present between the two images, a value other than one will result. [Ref. 1: p. 34] Techniques discussed in Section 3 will outline the procedures used for determining these coefficients.

III. EARLY DEVELOPMENT USING A FREE JET APPARATUS

A. APPARATUS AND FLAT PLATE ASSEMBLY

A sonic-jet nozzle system located in the Gas Dynamics Laboratory (Bldg. 216) at the Naval Postgraduate School was used in the initial experiments. A schematic of the facility is illustrated in Figure 5. A photograph of the jet nozzle is shown in Figure 6.

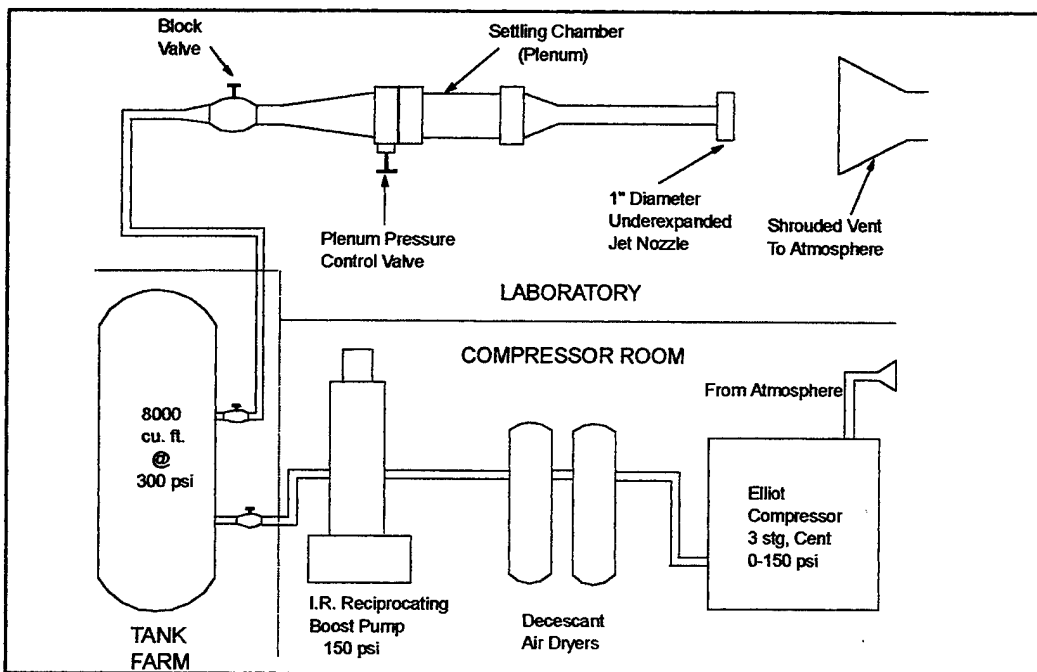


Figure 5. Schematic of the Underexpanded, Sonic Jet Nozzle and Supporting Facility

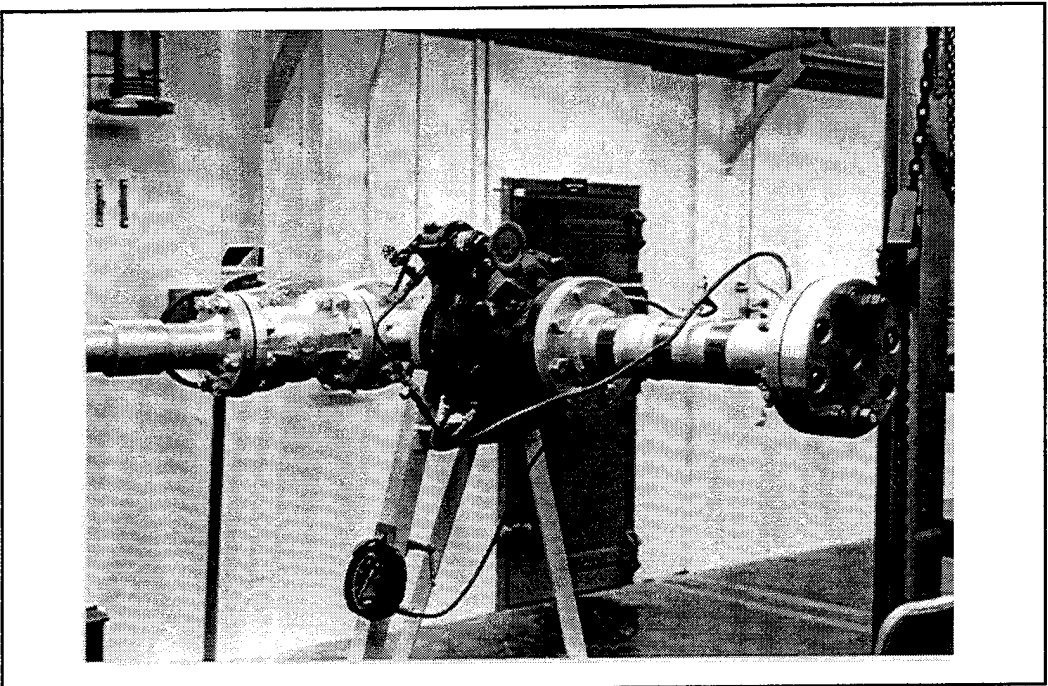


Figure 6. Underexpanded Jet Nozzle Apparatus

The flat plate used in the present work was a model designed and previously used for jet interaction studies in the supersonic wind tunnel. The plate was made of stainless steel with a leading edge diameter of 0.008 inches. Twelve of the existing pressure taps were chosen as close to the centerline of the plate as possible. Figure 7 shows a schematic of the surface of the plate showing the twelve taps relative to the centerline. The pre-arrangement of the taps, in addition to discovering two plugged ports, required that three offset taps be used to maintain near uniform spacing in the streamwise direction.

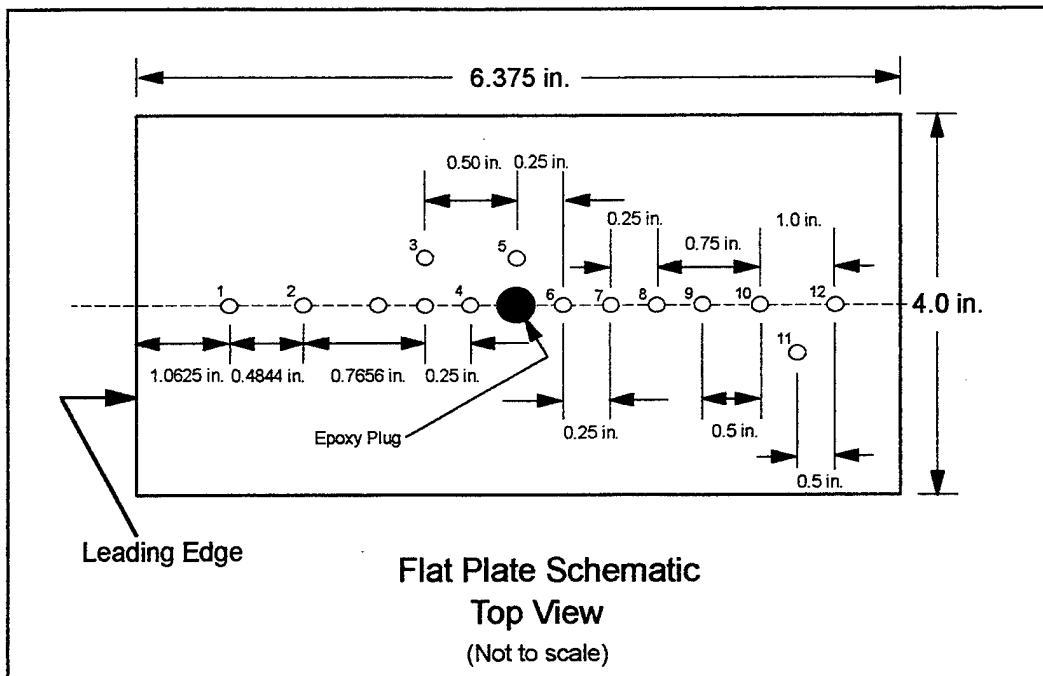


Figure 7. Schematic of the Pressure Port Arrangement on the Plate Surface

A simple bracket was made to mount the model so that the surface of the flat plate become a radial plane, effectively dividing the axi-symmetric jet in half. The bracket and model are shown in Figure 8 while Figure 9 illustrates this assembly mounted to the face of the jet. Plate washers were placed on the mounting bolts to create a 1/4 inch gap between the leading edge of the plate and nozzle face. This was necessary as it was found that the jet would not properly form if the plate were installed with its leading edge at the plane of the nozzle opening. Pneumatic pressure measurements were made using the Scanivalve ZOC system developed by Wendland [Ref. 17].

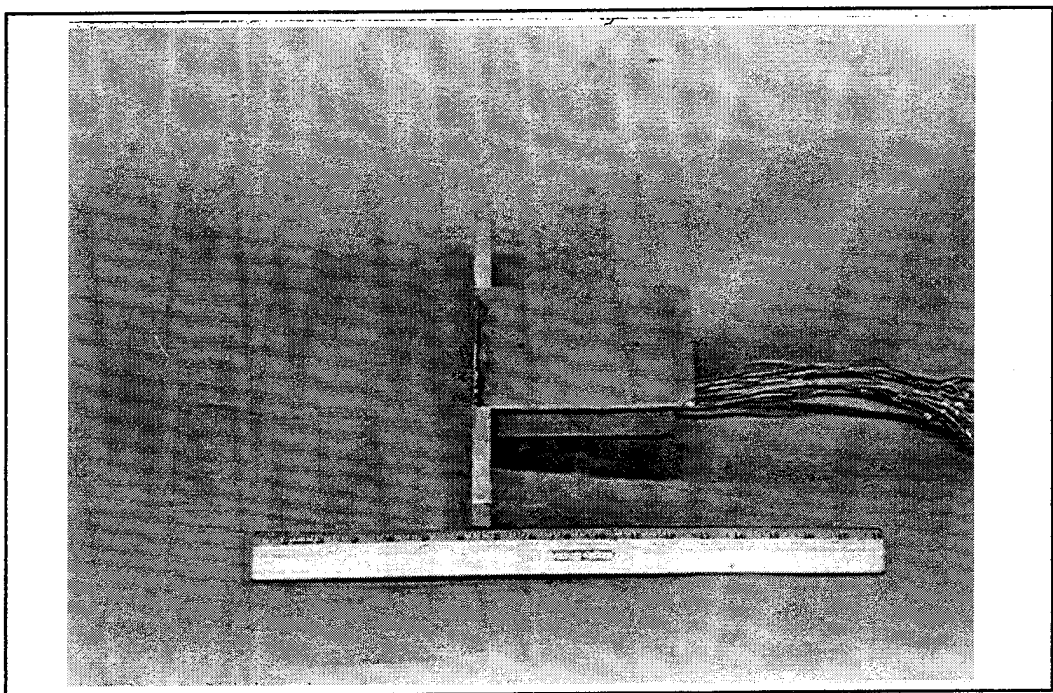


Figure 8. Bracket and Model Assembly

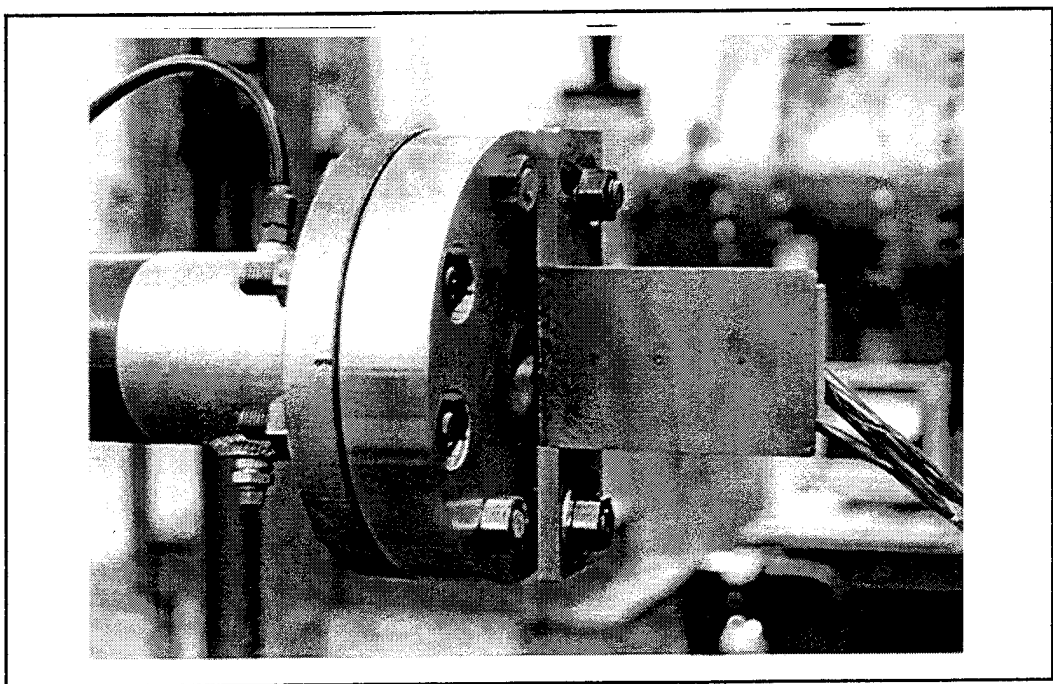


Figure 9. Bracket and Model Assembly Mounted to the Face of the Sonic Jet

1. Freestream Flow Field of the Underexpanded Sonic Jet

The mechanics of formation and structure of an underexpanded jet from a sonic nozzle have been studied in detail by Adamson and Nicholls [Ref. 18: p. 265]. A schematic of the structure is illustrated in Figure 10.

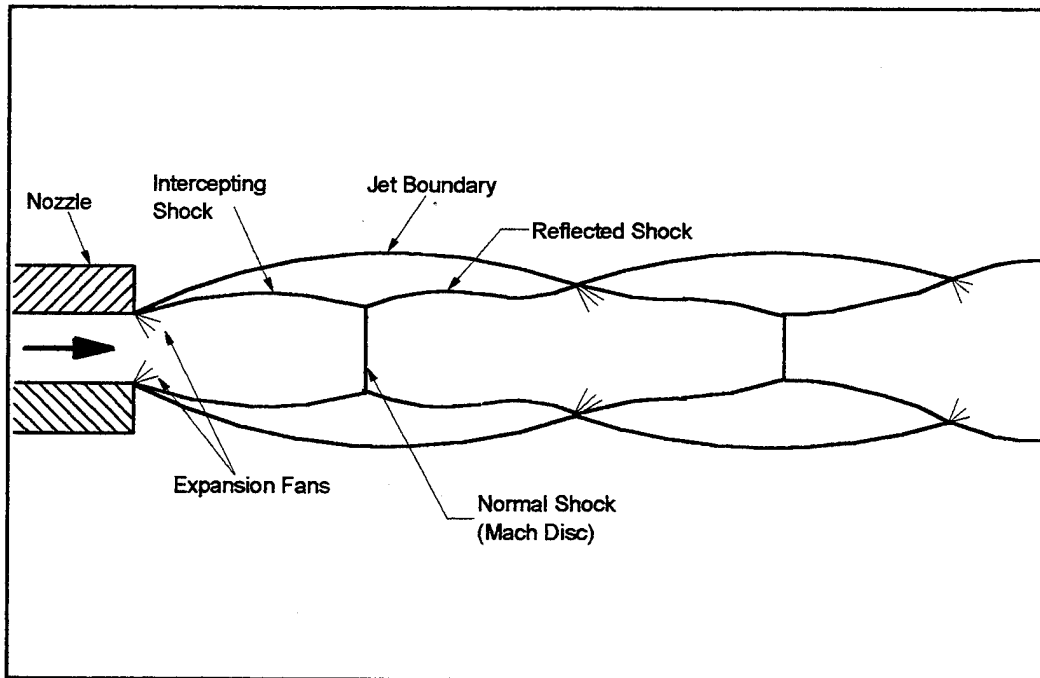


Figure 10. Sketch of Jet Structure Behind a Highly Underexpanded Nozzle⁵

The "Mach disc" within the free-jet offered an event that would produce a pressure discontinuity similar to that of the starting-shock structure in the supersonic wind tunnel, but without the visual restrictions imposed by thick test-section windows.

Using the schlieren technique, visualization studies of the flow field across the flat plate were recorded. The data acquired using the pressure-sensitive paint on the flat plate

⁵Figure 10 is found in Ref. 18, page 265, as Figure 1

could then be interpreted with reference to the flow structure. These studies began by observing the underexpanded jet without the flat plate mounted to the jet nozzle. This was done to provide a reference for changes in the flowfield as a result of the interaction with the plate. Since the jet structure was axi-symmetric, it was anticipated that, with the plate surface aligned along the centerline of the jet, the plate would simply isolate half of the jet structure. Figure 11 illustrates the jet structure without the flat plate installed at 65 psig plenum pressure. The flow proceeds from right to left.

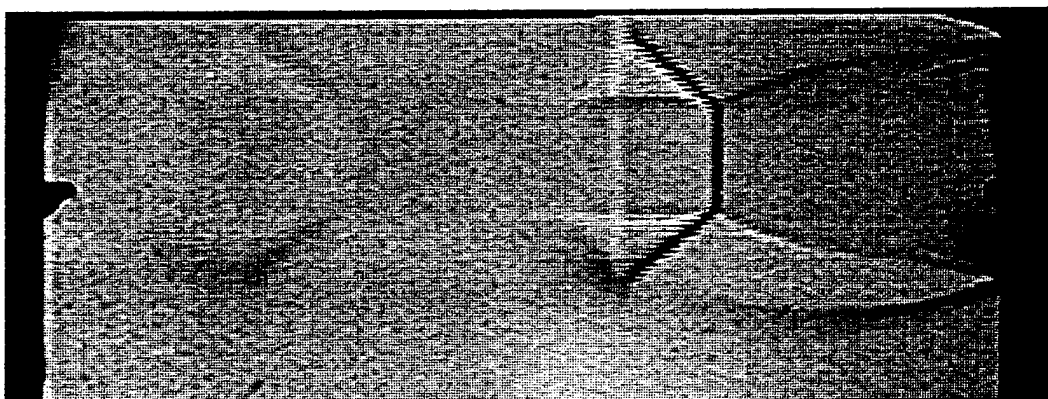


Figure 11. Underexpanded Free Jet at 65 psig Plenum Pressure

The flat plate was then bolted to the nozzle face and several runs were made at varying plenum pressures to record the shock structure. Three specific plenum pressures, 65, 80, and 90 psig were chosen as test points at which to compare pressure measurements with data using the luminescent paint, and the schlieren images of the flow field. The schlieren images of the three events and the corresponding pressure measurements from the orifices along the flat plate are illustrated in Figures 12, 13, and 14.

PRESSURE DISTRIBUTION ACROSS FLAT PLATE

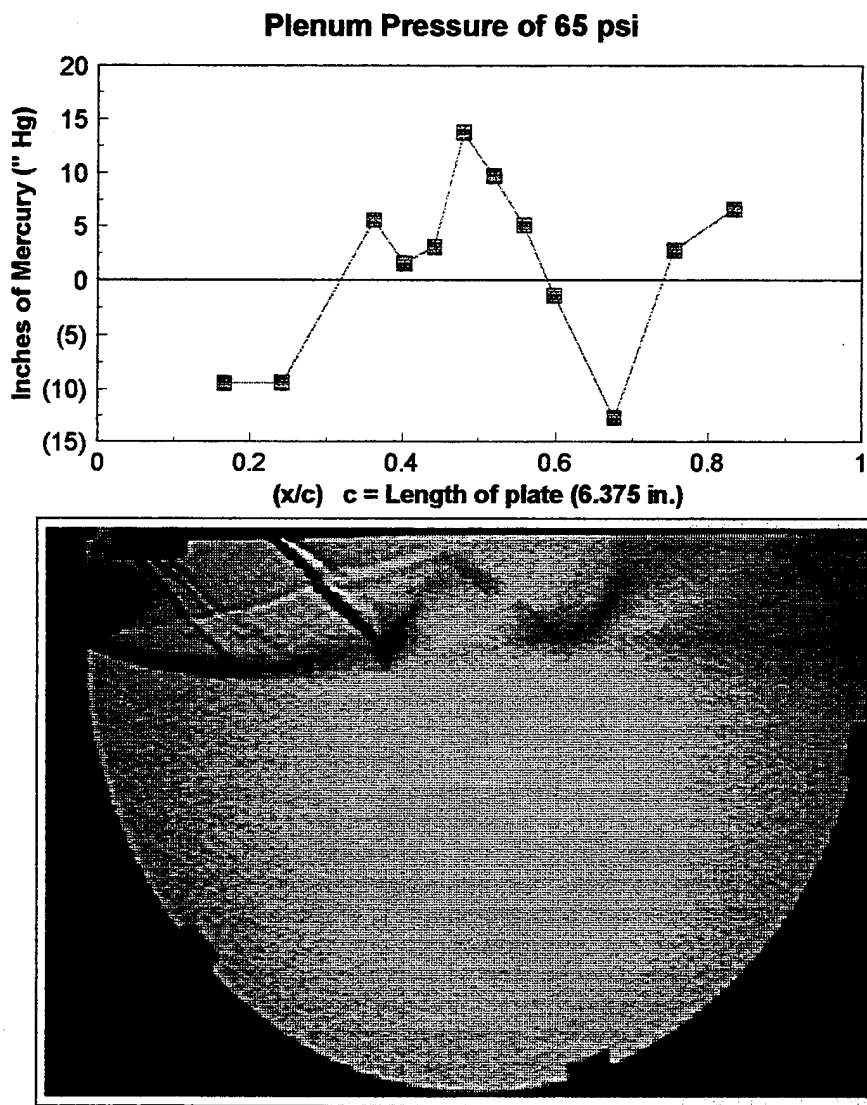


Figure 12. Flow Visualization and Pressure Distribution Across Flat Plate at 65 psig
(Flow is from left to right)

PRESSURE DISTRIBUTION ACROSS FLAT PLATE

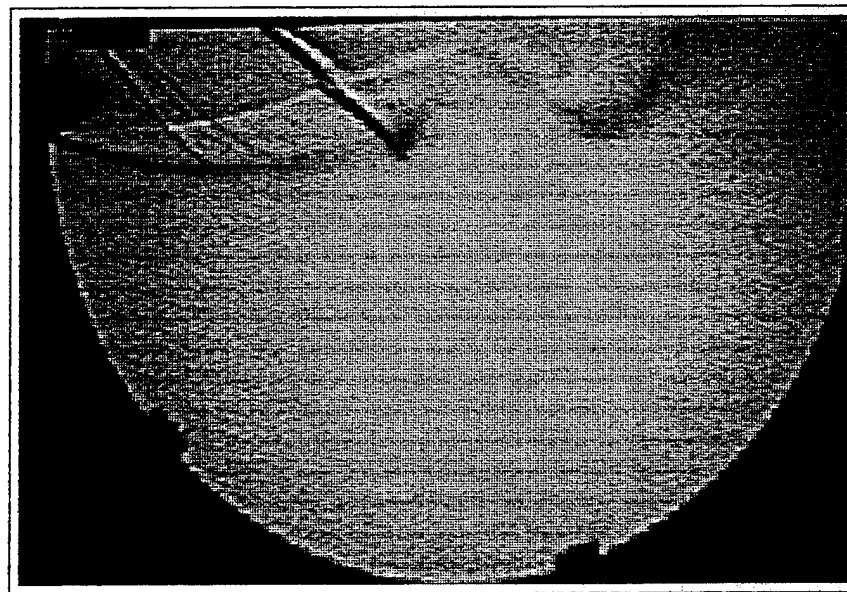
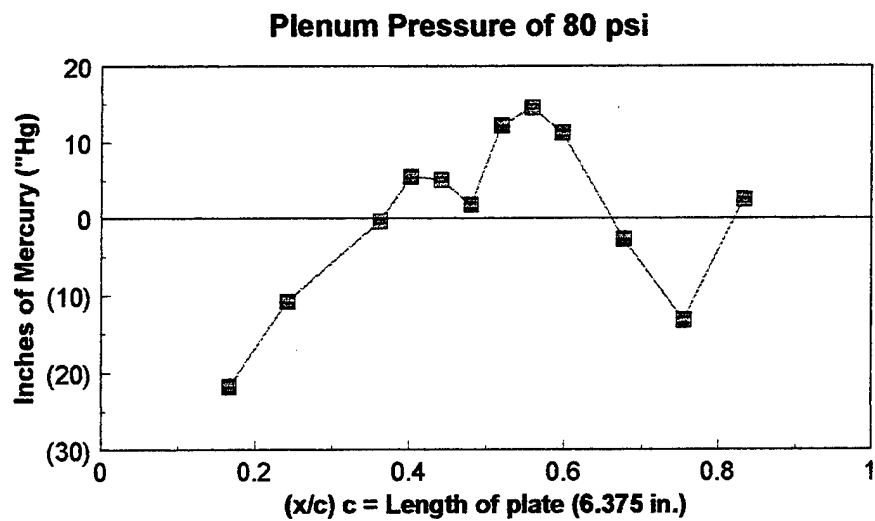


Figure 13. Flow Visualization and Pressure Distribution Across Flat Plate at 80 psig
(Flow is from left to right)

PRESSURE DISTRIBUTION ACROSS FLAT PLATE

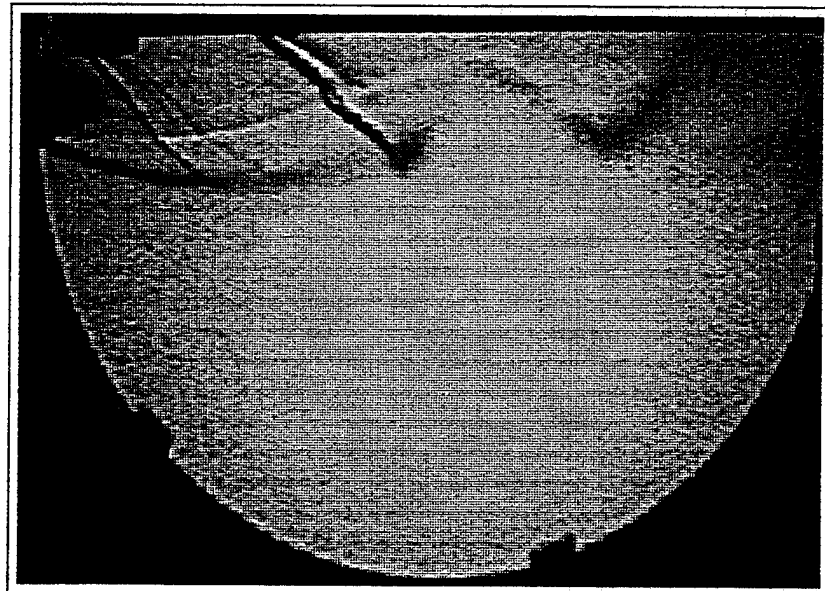
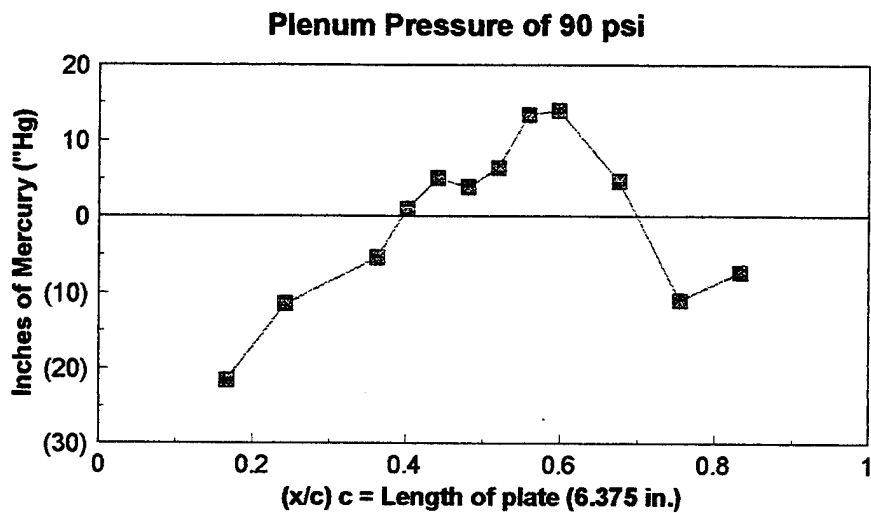


Figure 14. Flow Visualization and Pressure Distribution Across Flat Plate at 90 psig
(Flow is from left to right)

The images and the pressure measurement graphs have been aligned so that the pressure changes seen on the graphs correspond to the events occurring on the plate surface.

As can be discerned from the schlieren images in Figures 12, 13, and 14, two oblique shocks appear, a consequence of the plate being placed in the flow field. Figure 15 shows a comparison of the flow fields with and without the plate. The oblique shock emanating from the leading edge of the plate can be explained as being due to the underexpanded process the flow undergoes as it leaves the nozzle. The flow, as it exits

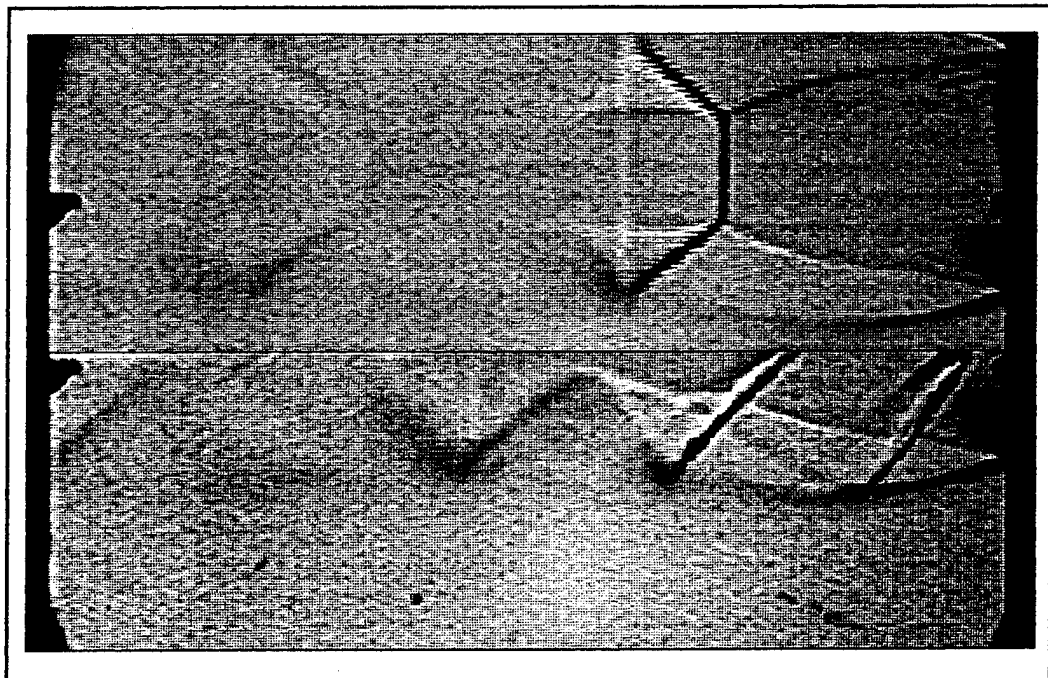


Figure 15. Flow Field Comparison Without (Top) and With (Bottom) the Flat Plate
the nozzle, is off-axis with respect to the centerline of the plate thus encountering the plate
at an incidence angle other than zero degrees. The flow in these images is from right to
left.

The second oblique shock's structure gives the perception that it extends from the surface of the plate to the jet boundary; however, closer examination of the two images in Figure 15 shows that the oblique shock actually merges with the reflected shock (see Figure 10) giving the erroneous illusion of a single entity. Of greater interest is the extent of the oblique shock to the point of total suppression of the normal shock. The sensitivity of the flow to the plate was much greater than first thought, and it was unclear what events were taking place to justify the magnitude of the oblique shock. Additional study seemed warranted.

a. Further Flow Field Studies

To visualize the flow, methanol was injected through the second pressure port in the plate surface. Several light fixtures were placed around the plate to better illuminate the injection area and to provide contrast between the background and flow field. A video recorder was used to record the events.

Figures 16 through 18 show the sequence of events from selected frames of the video at two different vantage points. In each set of images, the flow proceeds from left to right.

In Figure 16, the plenum pressure was steady at 30 psig -- the boundary layer up to this point remained attached. At 38 psig, Figure 17 shows initial indications of reversed flow at the center of the plate. In addition, 1/2 inch to the left of this point, a pooling of methanol formed. This behavior indicated the presence of a bubble in which a

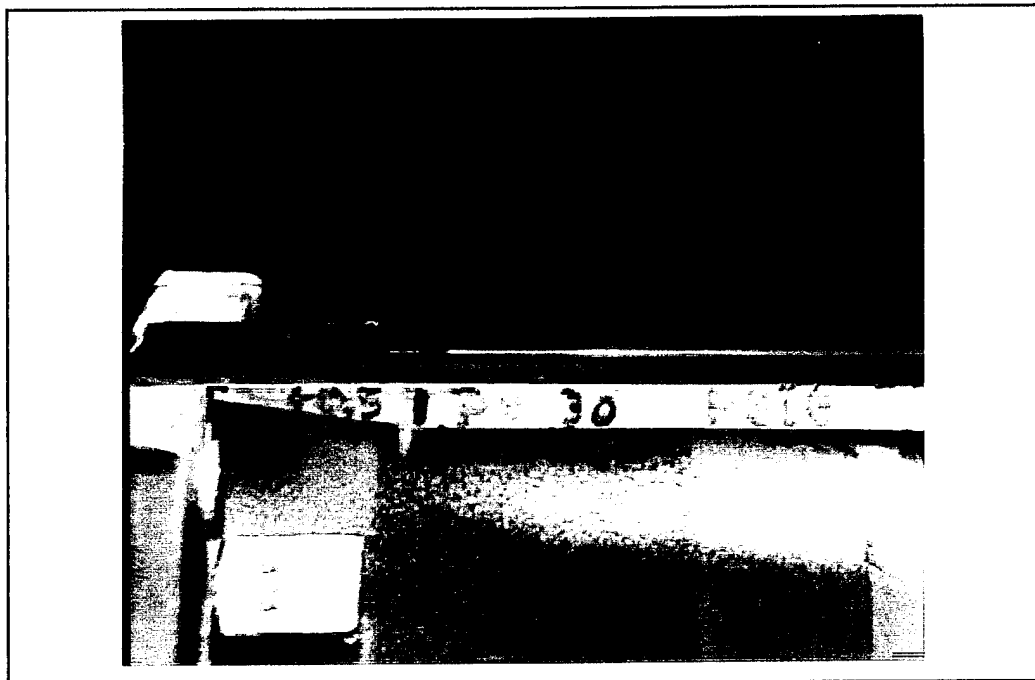


Figure 16a. Flow Visualization at 30 psig -- Cross Flow View

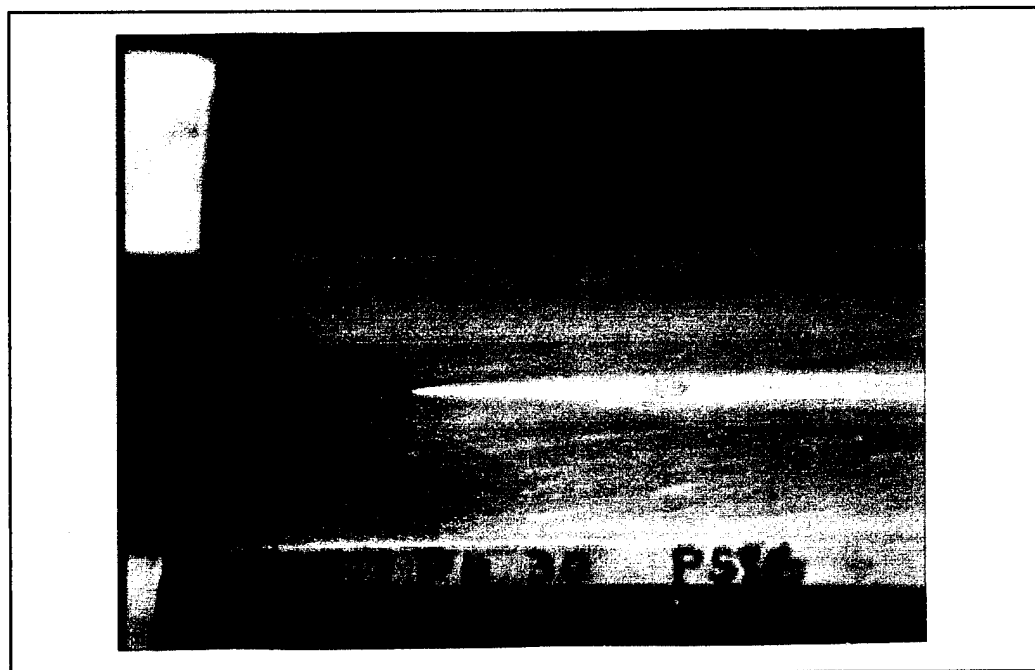


Figure 16b. Flow Visualization at 30 psig -- Acute View

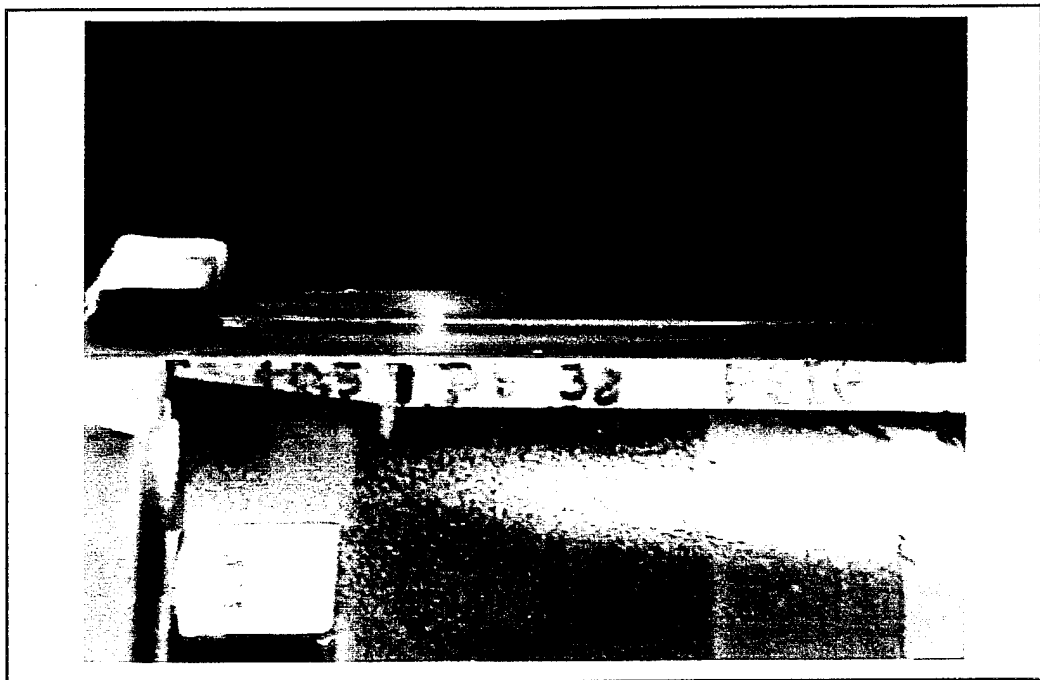


Figure 17a. Flow Visualization at 38 psig -- Cross Flow View

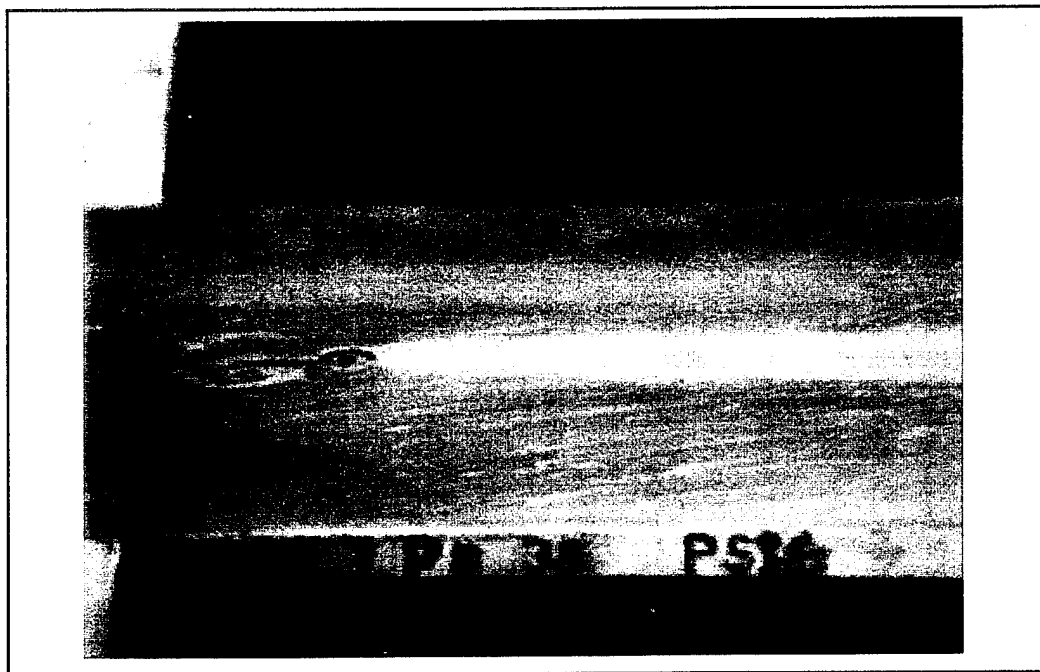


Figure 17b. Flow Visualization at 38 psig -- Acute View



Figure 18a. Flow Visualization at 65 psig -- Cross Flow View



Figure 18b. Flow Visualization at 65 psig -- Acute View

portion of the injected mass would be expected to stagnate near the separation point, as the flow re-circulated within the bubble's boundaries. This is more clearly shown in the schematic of Figure 19. With increasing plenum pressure, the separation and recirculation region of the flow field gradually moved downstream, eventually encompassing the injection port, and allowing the alcohol to more clearly define the boundary of what was indicated to be a separation bubble.

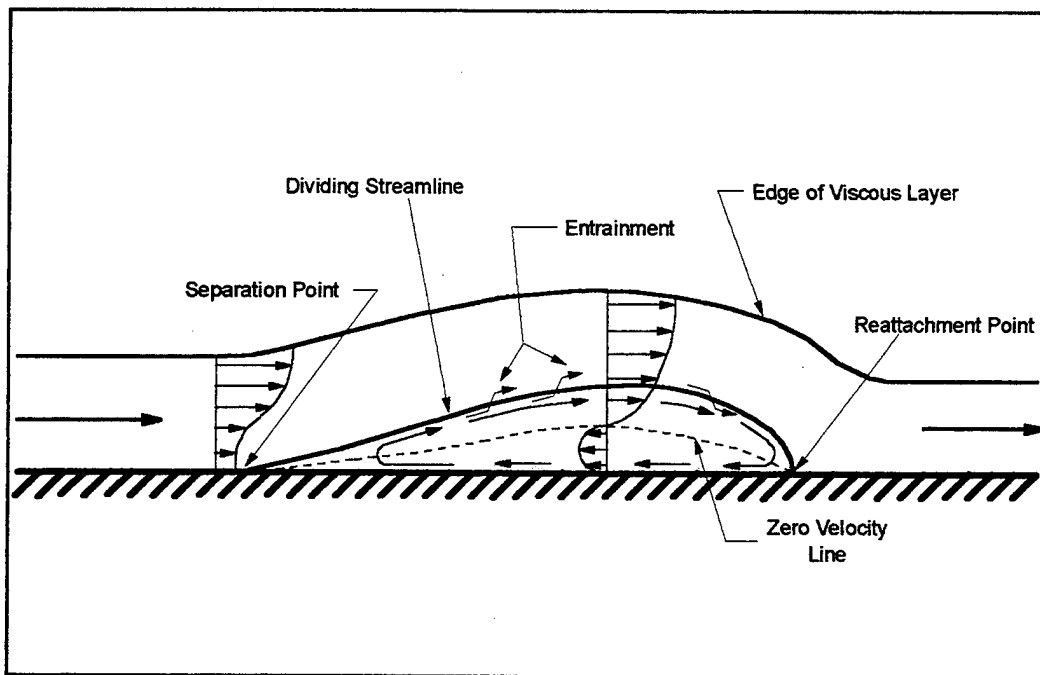


Figure 19. Details of Separation Bubble

To verify whether flow reattachment was in fact occurring downstream, a second injection port, port number 5, was rigged to concurrently admit methanol into the flow. Figures 20 through 23 show the sequence of images recorded in one such test.

Figure 20 shows that at 25 psig, attached flow was prevalent. At 40 psig, in Figure 21, the injectant at the first port (port number 2) indicated the presence of reversed

flow, while the injectant at the second port (port number 5) continued to indicate attached flow. The vortex patterns are an indication of the pressure gradients that exist within the bubble. In Figure 22, with the plenum pressure at 68 psig, the first sign of reversed flow is evident at the second injection port, while Figure 23 shows the port fully immersed in reversed flow at 75 psig.

The orientation of the plate relative to the centerline of the nozzle exit, and thus the centerline of the flow, was found to be 89.7 degrees. Since alignment could significantly influence the flow characteristics, the plate's inclination was changed to 90.3 degrees and the test runs were repeated. No dissimilarities between the results obtained at corresponding plenum pressures were noted.

The evidence of reversed flow and reattachment strongly suggested the presence of a closed separation bubble within the underexpanded jet when the plate was present. The apparent extent of the bubble, reaching 3/8 to 1/2 inch above the plate, is very surprising. However, it is consistent with the oblique shock in place of the normal shock. Further data are needed, such as impact probe measurements, in order to fully define the flow structure. For the present purpose, which was the investigation of pressure sensitive paint, this was not needed.

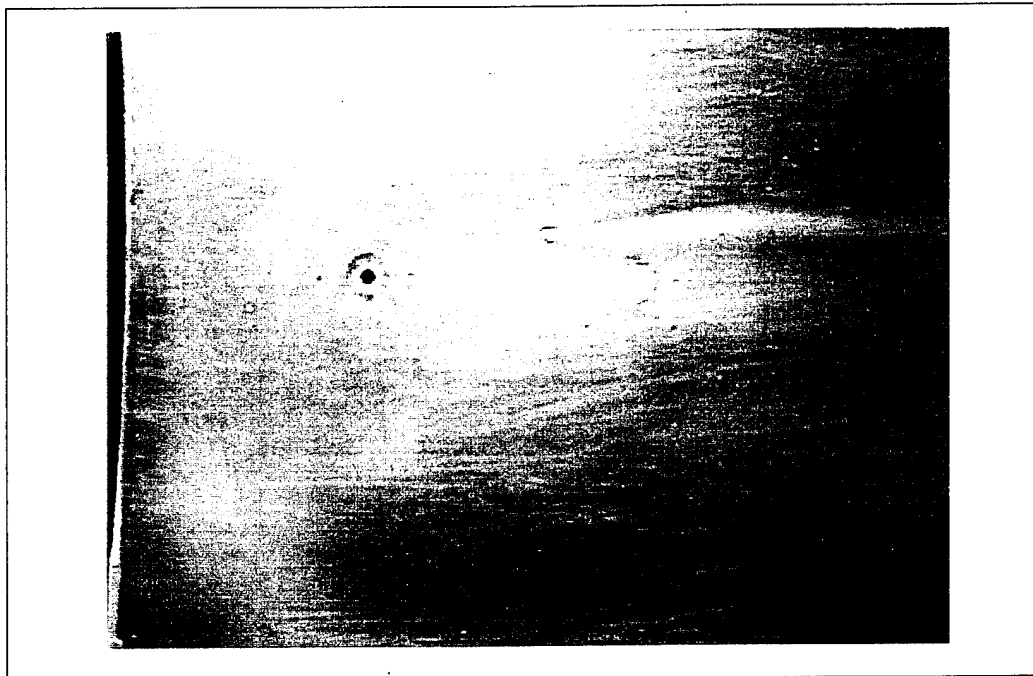


Figure 20. Flow Visualization at 25 psig

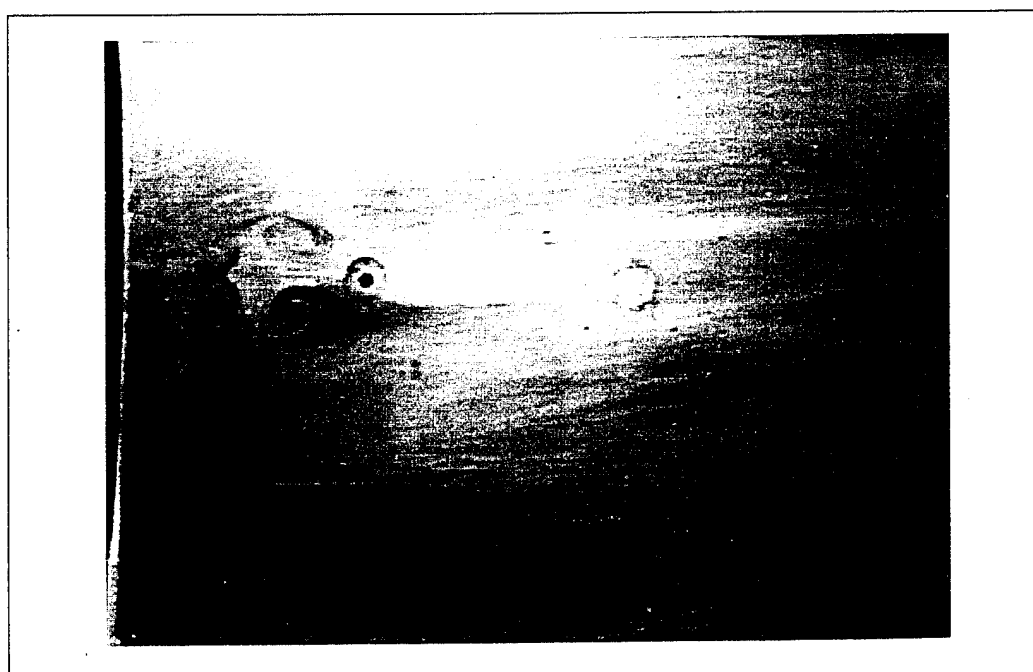


Figure 21. Flow Visualization at 40 psig

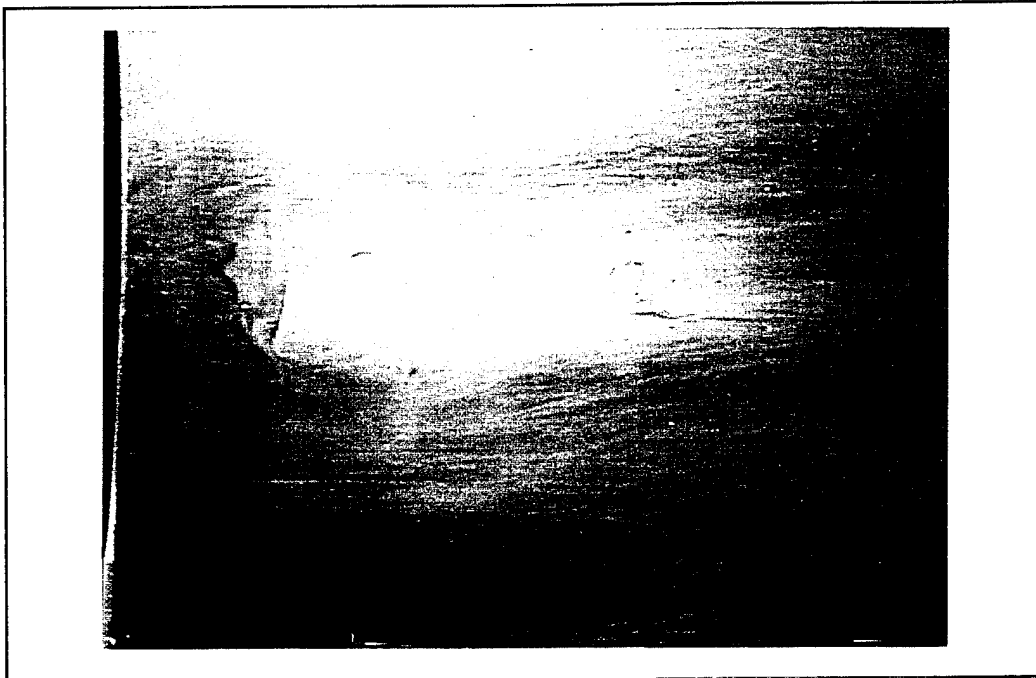


Figure 22. Flow Visualization at 68 psig

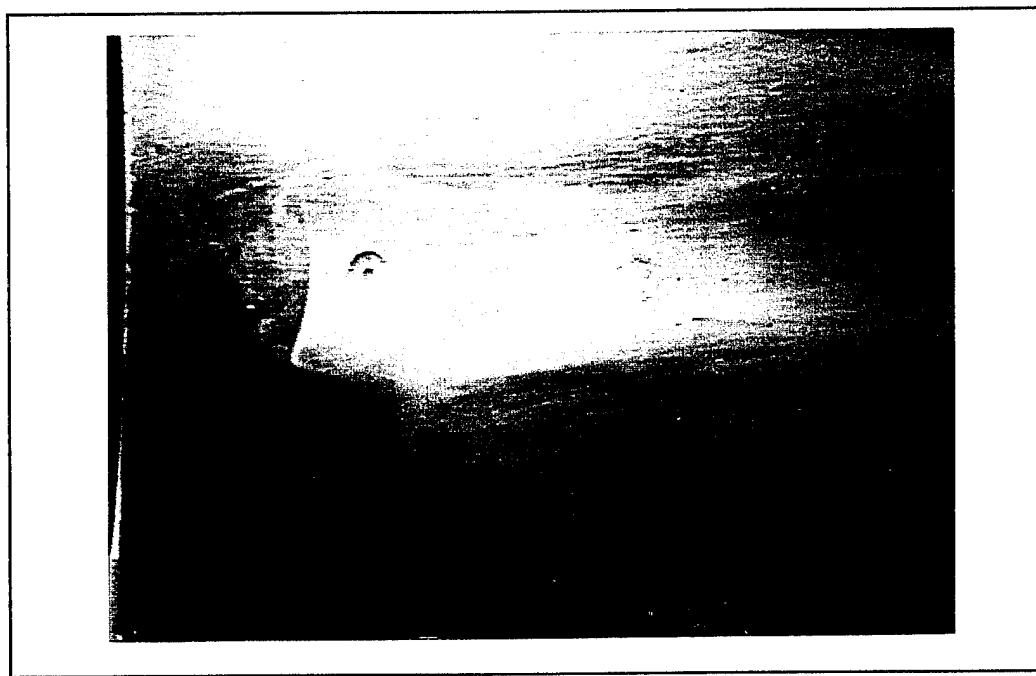


Figure 23. Flow Visualization at 75 psig

B. OPTICAL MEASUREMENT SYSTEM

The measurement system was composed of three main components: (1) the luminescence coating, (2) the illumination source, and (3) the luminescence detector and associated data processing hardware and software. Each component is discussed individually below. A schematic of the system used in conjunction with the free jet apparatus is illustrated in Figure 24.

1. Luminescence Coating

The luminescence coating used in the present work was developed by the Chemistry Department at the University of Washington and was provided, as a sample, by the NASA-Ames Research Center.

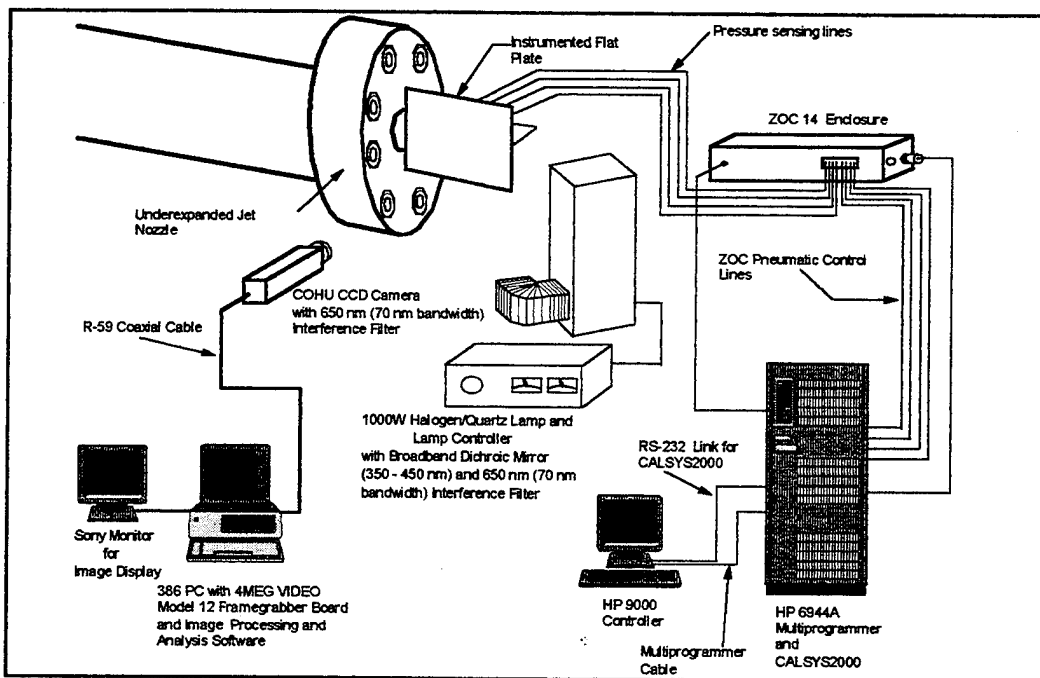


Figure 24. Schematic of Pressure Measurement System

The coating contained platinum octaethylporphyrin (PtOEP) as its active molecule. PtOEP has characteristics of high luminescent quantum yield (~90%), short triplet life (~100 micro seconds), and a high sensitivity to oxygen quenching [Ref. 1: p.35]. Figure 25 shows the excitation and emission spectra for the molecule. Excitation (absorption) peaks at 380 or 530 nm, whereas luminescence peaks at 650 nm. The coating mixture consisted of the active molecule dispersed in a Genesee GP-197 polymer-resin solution. The concentration was 0.1 gm of PtOEP per liter of polymer resin [Ref. 19]. When the mixture was applied to the surface, the solvent evaporated leaving a hard, thin film of PtOEP dissolved in an oxygen-permeable polymer [Ref. 9: p. 35]. Several undesirable characteristics associated with this coating are described in Appendix B.

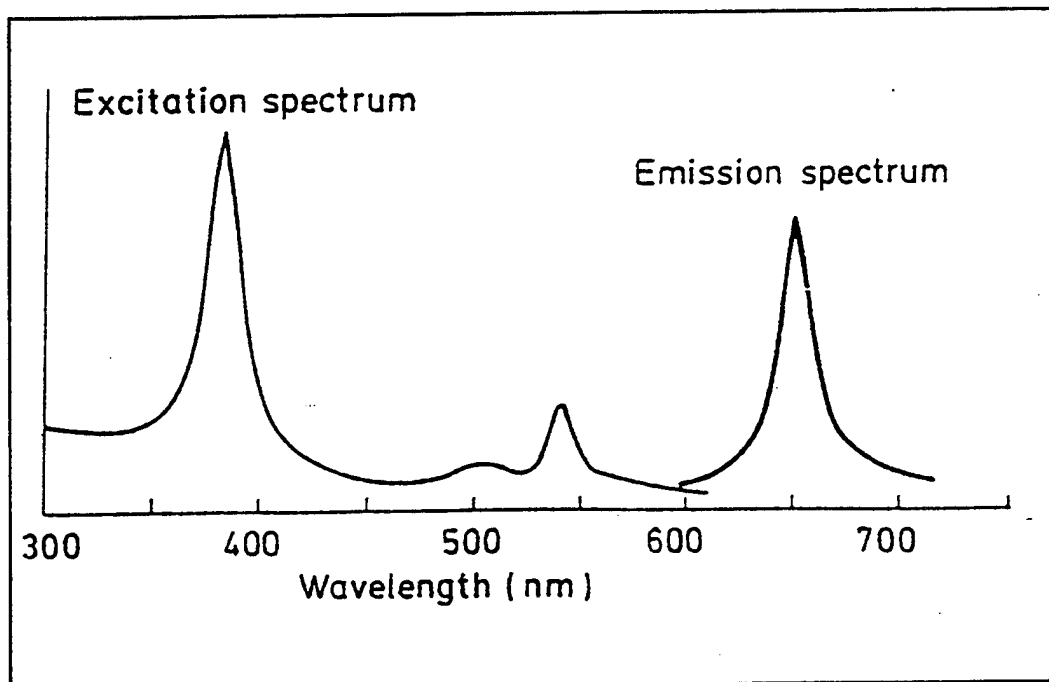


Figure 25. Excitation and Emission of Platinum Octaethylporphyrin

a. Reflective Backing

Before applying the luminescent coating to the surface, a white backing was first applied. A significant improvement in luminescence performance was thereby gained [Ref. 9: p. 32], allowing the camera to see a larger signal and an enhanced signal to noise ratio.

The particular type of white paint used for this backing was an important consideration. Kavandi [Ref. 9: p. 33] found that some paints tend to darken after long exposure to air and ultraviolet light. Krylon glossy-white spray paint (#1501) reportedly offered the greatest resistance to this effect and was therefore used in the current work.

2. Illumination Source

McDonnell-Douglas [Ref. 6: p. 3] considered several types of illumination sources to provide an adequate number of photons within the appropriate excitation wavelength of the paint. The results showed that tungsten-halogen incandescent sources were the most suitable in terms of compatibility and performance. Although the data in Figure 25 would suggest that arc lamps emit more energy in the excitation range of the coating, they also emit an EMF pulse that is damaging to CCD arrays. In addition, tungsten-halogen lamps are extremely stable, with minimum intensity fluctuations, and any such variations will directly effect the accuracy of the results. Consequently, an Oriel Corporation 1000 W quartz tungsten-halogen lamp, Model 66200, and the associated controller, Model 6405, were selected for the present measurement system.

Spatially-uniform illumination was also essential to reduce measurement errors. (According to McDonnell-Douglas [Ref. 6: p. 4], this is especially true when the surfaces are highly curved). Non-uniformity was found when the published procedures [Ref. 20: p.13] were followed to produce a collimated beam from the light source. The procedure resulted in generating a focused image of the filament in the lamp. However, by reversing the orientation of the barrel containing the lenses, a greater range of adjustment was achieved. Figure 26 illustrates this modification, which made it possible to produce a more uniform beam, although a slight degradation in spectral intensity was noted.

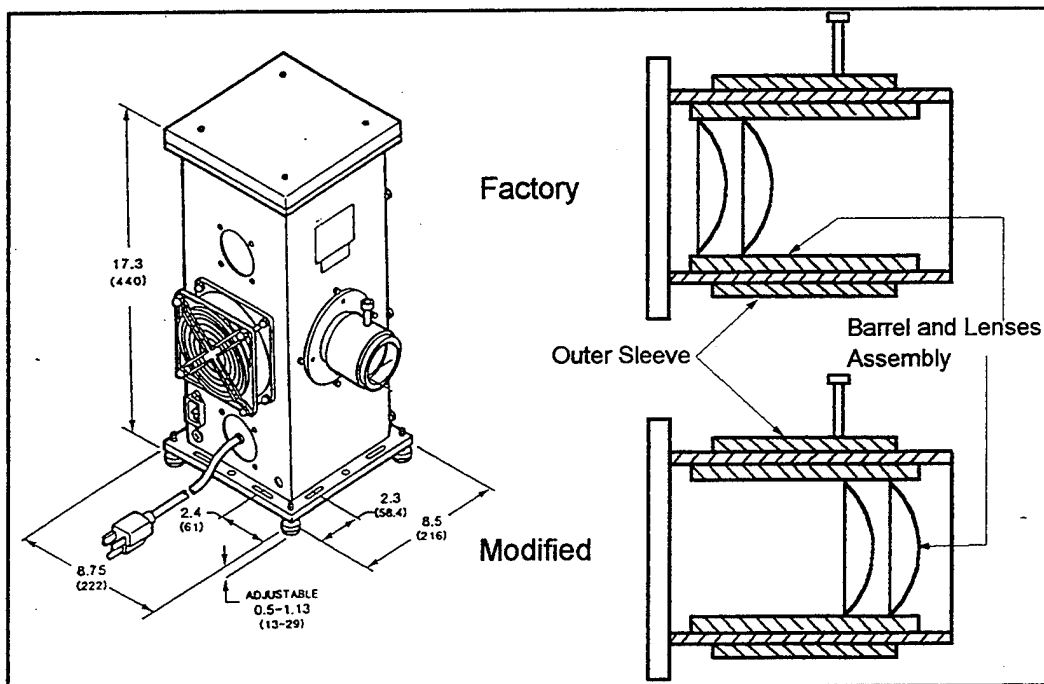


Figure 26. Modification of Focusing Assembly of the Light Source

a. Filters

The use of a broad-band light source mandated the use of filters to ensure that the appropriate wavelength for excitation of the luminescence was allowed to pass while blocking unwanted light. Unwanted light was that which would pass through the narrow-band filter that was installed on the camera.

As Figure 25 shows, there are two wavelengths at which excitation of the luminescent paint is optimum. Although either wavelength could have been used, the 380 nm wavelength was chosen because of its greater separation from the emission wavelength of 650 nm. This also had the advantage, as discussed in [Ref. 6: p. 5], of allowing a filter with a more gradual cutoff to be used which would allow more light energy to be utilized to excite the paint.

A combination of filters was used in the illumination system to isolate the 380 nm wavelength. The source beam first passed through a dichoric or cold mirror, Oriel Model 66228, which had a spectral range of 350 - 450 nm and a cut-off frequency of 550 nm [Cold mirrors are oriented at 45 degrees relative to the incoming beam from a source. The infrared wavelengths are transmitted undeviated, while the ultraviolet wavelengths are reflected through 90 degrees. This prevents the infrared from being reflected back to the source and overheating the system.]

The source light was then directed through an Oriel interference filter, Model 57521, having a bandwidth of 70 nm centered at 400 nm. The filters were installed in a 90

degree beam turner and mirror holder, Oriel Model 66246, which was fitted to the lamp housing.

Finally, the camera used to record the emitted luminescent energy from the paint had a 650 nm interference filter with a 70 nm bandwidth, Oriel Model 57610, mounted over its lens to block out all other frequencies.

3. Detection System

Luminescent data were acquired using a COHU Model 4910 high performance, monochrome, low-intensity CCD camera and transferred to a framegrabber board in a 80386 PC using an R-59 coaxial cable. The camera was fitted with a Cosmicar 16 mm, f/1.4 lens. To ensure the output signal would be linearly proportional to light intensity received, the camera was configured with the gamma set equal to one and the automatic gain control (AGC) disabled [Ref. 2: p. 3342]. The camera's spectral response, as shown in Figure 27, shows that its relative response at 650 nm is approximately 65%.

The camera produced a frame every 1/30 of a second and thus was limited to recording pressure fluctuations at rates less than 30 Hz. [A simple test to determine if the illumination system was bleeding over into the detection system was to illuminate an unpainted surface (i.e., no luminescent paint) and then direct the camera towards this surface to see if any spurious light was being detected. None should be present].

The analog output signal from the camera was initially digitized using an IDEC Supervision 16 framegrabber board residing in a 80386-based PC. The raw data were then reduced and analyzed using "Image Pro Plus" analysis and processing software.

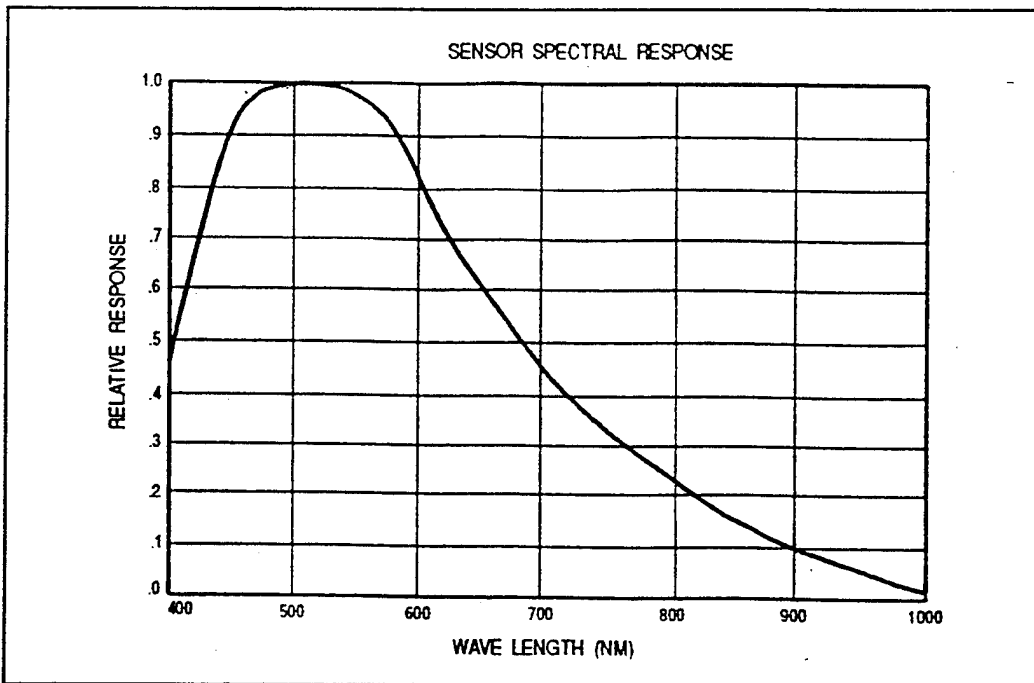


Figure 27. Spectral Response Curve for the COHU Camera Model 4910

However, this hardware/software combination was extremely limited in application resulting in long data acquisition periods and time-consuming data reduction. Because of the characteristic degradation of the luminescent coating, the accuracy of the data was questionable.

The initial hardware/software combination was replaced with a much more versatile Epix 4MEG Video Model 12 framegrabber board and software which included image analysis and processing programs. The spatial resolution of the framegrabber was operator adjustable, thus a balance between sampling resolution and the board's memory storage could be tailored to a given application. For the underexpanded-jet and flat-plate work, the spatial resolution was set to 752 x 480, the highest resolution setting. The gray-level resolution of the board was 8-bits.

C. EXPERIMENTAL PROGRAM

1. Flat Plate Preparation

The surface of the flat plate was cleaned with acetone, ensuring the removal of all oils and dirt. Fine wire was then inserted into each of the pressure ports to prevent paint from entering the holes. The white Krylon undercoating was then applied in a series of three to four thin coats, allowing four to five minutes between coats. Ten minutes after applying the last coat, the fine wires were removed from the ports. This was necessary to prevent the paint from drying on the wire. [Significant portions of the undercoating could be removed from around the pressure port when extracting a wire to which the paint had hardened]. At this point, the white undercoating was allowed to dry for one hour.

Prior to the application of the pressure-sensitive paint, the fine wires were re-inserted into the ports. The luminescent coating was then applied to the surface using a standard hobby airbrush. The nitrogen supply in the Gas Dynamics Laboratory was used as the pressure source for the airbrush (instead of shop air) as it offered a contaminant-free pressure source. With a properly adjusted airbrush and a good painting technique, continuous application of the luminescent coating to the surface could be achieved until the surface was "suitably" covered. Although Kavandi *et al* [Ref. 2:p. 3343] refers to normal coating thickness as being in the range of 5 to 15 micrometers, it was both impractical and unnecessary to measure the coatings to determine if the paint fell within these prescribed limits. The approach used in the present work was simply to observe when the pigment of the pressure-sensitive paint seemed insensitive to further application,

and that the texture of the surface appeared smooth. Several attempts were necessary to develop the technique and the judgement in applying the luminescent coating. Three to four minutes after the completion of the coating, the fine wire were removed. Once the model was installed for testing, sufficient time had elapsed for the coating to have properly cured. Note that it was important to avoid touching the painted surface at any time since body oils could adversely affect the behavior of the luminescent coating.

2. Experimental Procedure

Setting the video resolution for the framegrabber to the maximum (752 x 480) resulted in 11 frame buffers being available to store for image data. The controlling software for the framegrabber was capable of capturing a sequence of images, digitizing them, and storing each image of the sequence in consecutive image buffers, the number of buffers used in the sequence (from one up to the number of available buffers) being specified by the operator. Because of the limitation of collecting only 11 images for each execution of the sequence algorithm, and the fact that averaging one hundred images was desirable to obtain noise-free data, for each of the wind-on and wind-off conditions, ten runs were executed. (10 frame buffers vice 11 buffers were utilized). Since the underexpanded free jet was a steady and repeatable event, this method of collecting data was a feasible solution for the limited memory of the frame-grabber board.

The data for the wind-off condition was collected first. The flat plate was illuminated with the tungsten-halogen light source while the laboratory lights were turned off, preventing any spurious wavelengths from entering the camera and offsetting the

image data. A real-time image of the plate was displayed on the image monitor so that the camera output could be adjusted for the best quality picture using a combination of focus, manual gain, and lens iris. Manual gain was necessary because of the low light condition, but care had to be exercised because with an increase in gain there was an accompanying increase of noise introduced into the image. The shutter speed for the camera was set to off.

After the first sequence of images was captured and stored in the frame buffers, the light source was switched off to minimize the degradation to the paint. The light source was such that the line voltage applied to the lamp housing was adjustable; however, power was ultimately controlled with an on/off switch. Thus, the same illumination intensity was maintained each time the lamp was turned on.

The ten images were averaged together to form a single image. The single image was saved to a floppy disk. The light source was again switched on in preparation for the second sequence of images, allowing time for the luminescent coating to reach its maximum intensity. (This is referred to as the "induction period", which is explained in Appendix B). The second sequence of images was then captured and stored, and the tungsten-halogen lamp shut-off. The images were averaged to give a single image and again saved to floppy disk. This routine was executed until ten averaged images for the wind-off condition had been saved to floppy disk. Each sequence of capturing the data took less than one minute.

The procedure for obtaining images for the wind-on condition was similar. With the light source on and the plate properly illuminated, the underexpanded-jet apparatus was started. Once the desired pressure was set using the plenum control valve, and the pressure was stabilized, the imaging sequence was executed. When the software had completed its routine, the jet was shutdown and the light source turned off. The jet apparatus was equipped with a shutoff valve so that the jet could simply be turned on and off without disturbing the setting of the plenum control valve. This ensured repeatability of the event for each sequence of 10 images.

It is important to note that throughout these events, the camera and light source had to remain fixed, spatially, with respect to the plate. In addition, no adjustments of any kind could be made to the instruments or equipment. Any deviations would introduce errors into the results.

Conventional pressure data were obtained concurrently with the luminescent paint data using the CALSYS2000 data acquisition system [Ref. 17]. Twenty samples per port using a data collection rate of 33 Hz were obtained and averaged together. These pressure data would be used later in the calibration process. Ambient pressure and temperature were also recorded.

3. Image Data Reduction

a. Image Processing

Several image-processing techniques were used to manipulate the data in order to obtain the desired result. The techniques are described individually below.

Appendix C provides a summary of the steps used in operating the EPIX software for acquiring, processing, analyzing, and reducing the data.

Round-off error from the image processing routines was a concern. To ensure against loss of accuracy due to round-off error, the system hardware had to be capable of doing at least 16 bit arithmetic. The EPIX frame grabber board was capable of conducting 32-bit operations. When the image was processed, the 8-bit intensity values for each pixel in the image were first converted to 32 bit words. Once the processing was complete, the modified values of each pixel were converted back to an 8-bit format for display. If the mathematical operations were conducted with anything less than 16-bit precision, all significant digits would be truncated.

(1) Averaging. The emission of photons from any source is a random process following a Poisson distribution, and the number of photogenerated carries collected in a potential well of the camera array (see Appendix D for an explanation on the operation of a CCD camera) in time "t" is thus a random variable. The standard deviation of this random variable is referred to as photon (shot) noise. This noise is a fundamental limitation in all imaging applications since it is a property of light itself, not of the image sensor.

By averaging a sequence of images, the signal-to-noise ratio of the data has been found to be significantly improved. This process has the effect of reducing the scatter in the luminous intensity measurement [Ref. 6:p. 8]. McDonnell-Douglas [Ref. 6]

has found that as few as eight images averaged together showed a marked reduction of noise on the signal.

The reason for choosing one hundred images for each of the wind-on and wind-off conditions was the prior experience in the work conducted by NASA-Ames, the University of Washington, and McDonnell-Douglas. In each case, one hundred images was adopted in all work done to date.

The ten averaged images of the wind-off condition were loaded into ten frame buffers of the EPIX framegrabber board. As with the initial averaging of the raw image data, the ten buffers were averaged together to form a single image. This single image, a result of averaging one hundred "raw" images together, was then saved to floppy disk. The corresponding wind-on images were averaged in a similar manner, and the resultant image saved with its wind-off counterpart.

The procedure used in averaging the data in the present work was slightly different than used at NASA-Ames, the University of Washington, and McDonnell-Douglas. In those cases, one hundred images were collected and then averaged in one step. In the present work, ten averaged images were averaged to form the final image. Again, this is a result of the limited memory available on the frame grabber board. However, since each image has a random distribution of data associated with it, the averaging technique used will have little effect on the outcome of the result.

The significance of image averaging can be seen in Figures 28 through 30. In each figure, an image and a graphical distribution along a single line of pixel values in

the image is shown. Figure 28 shows a single raw image of the wind-on condition at 80 psig. Figure 29 shows the effect of averaging ten wind-on images together and Figure 30 shows one hundred images averaged together. In each figure, an image and a graphical distribution along a single line of pixel values in the image are shown.

(2) Dark Current. Appendix D details what dark current is and how it affects the storage of photogenerated carriers in the potential well of a photo-sensitive array element. The effect of the dark current on an image is that it produces an offset in which the zero incident light condition does not correspond to the zero grey level. To correct for this offset, a "dark" image was acquired and then subtracted from the wind-off and wind-on conditions.

To acquire a dark image, a lens cover was placed on the lens prohibiting any light from striking the CCD array, and then an image was acquired. One hundred images were taken and averaged as was done with the wind-on and wind-off conditions. A dark image was generated after each of the wind-on runs. Analysis of the dark current image showed that 1 to 2 grey levels were present, which were the levels subsequently subtracted from the wind-off and wind-on images.

(3) Registration. When a pixel-to-pixel comparison of two images of the same object field taken from the same sensor at different times is desired, it is necessary to spatially register the images to correct for relative translational shifts, rotational shifts, and geometrical distortions. In the general case, this is accomplished in the software

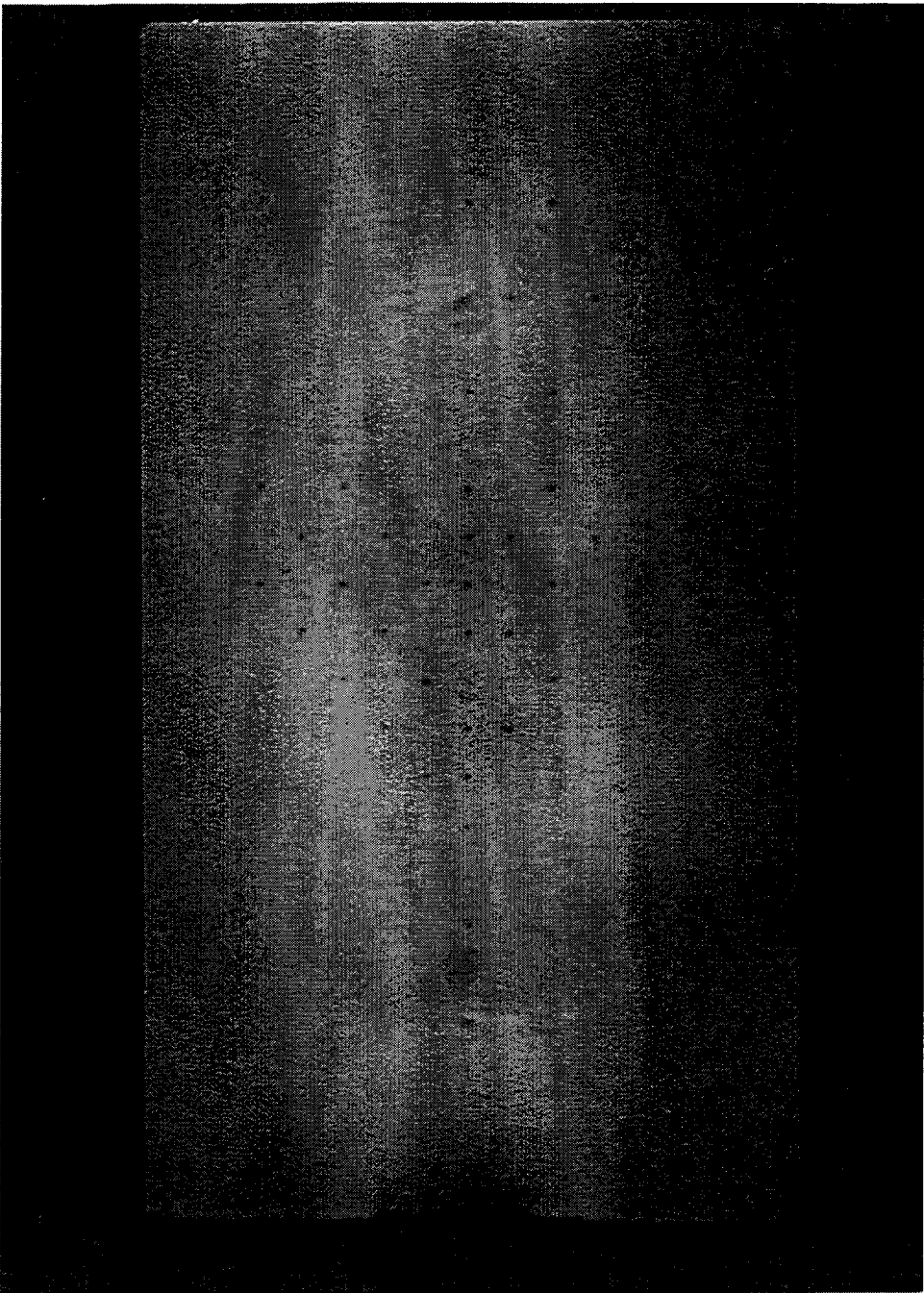


Figure 28a. Single Image of the Underexpanded Jet Across the Flat Plate at 80 psig

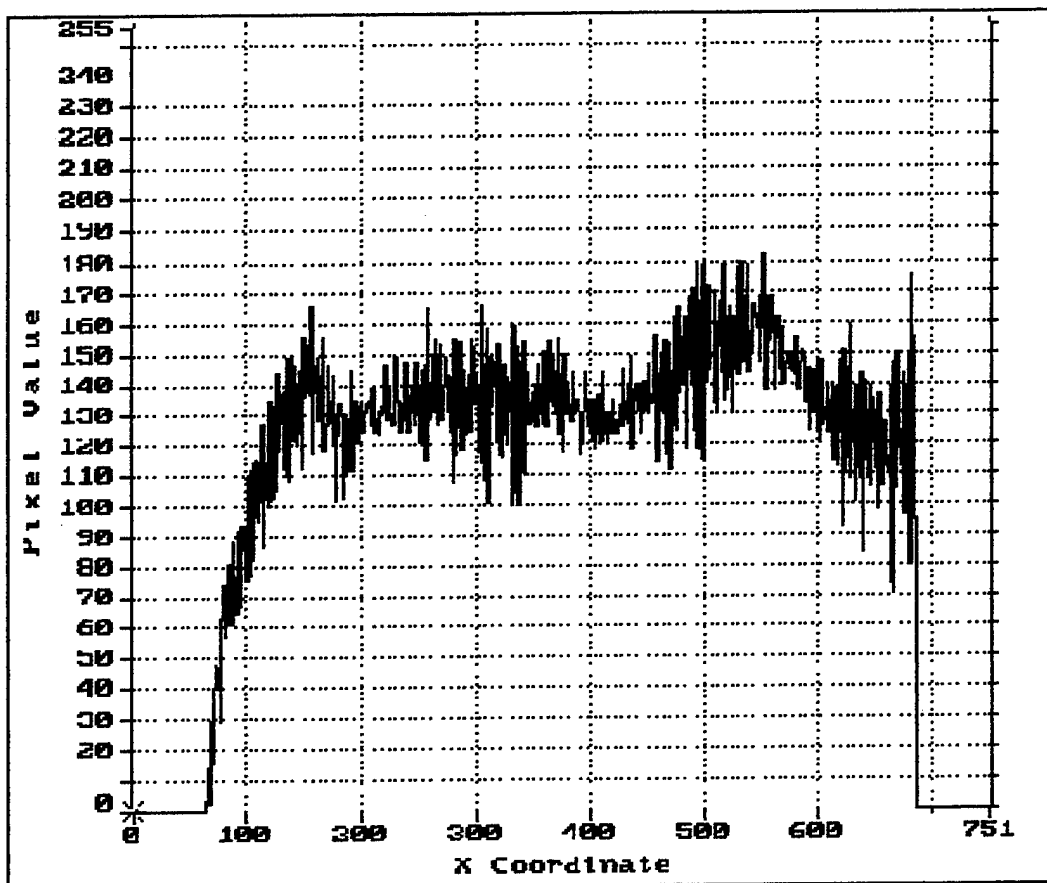


Figure 28b. Graphical Representation of a Single Line of Pixels of a Single Image

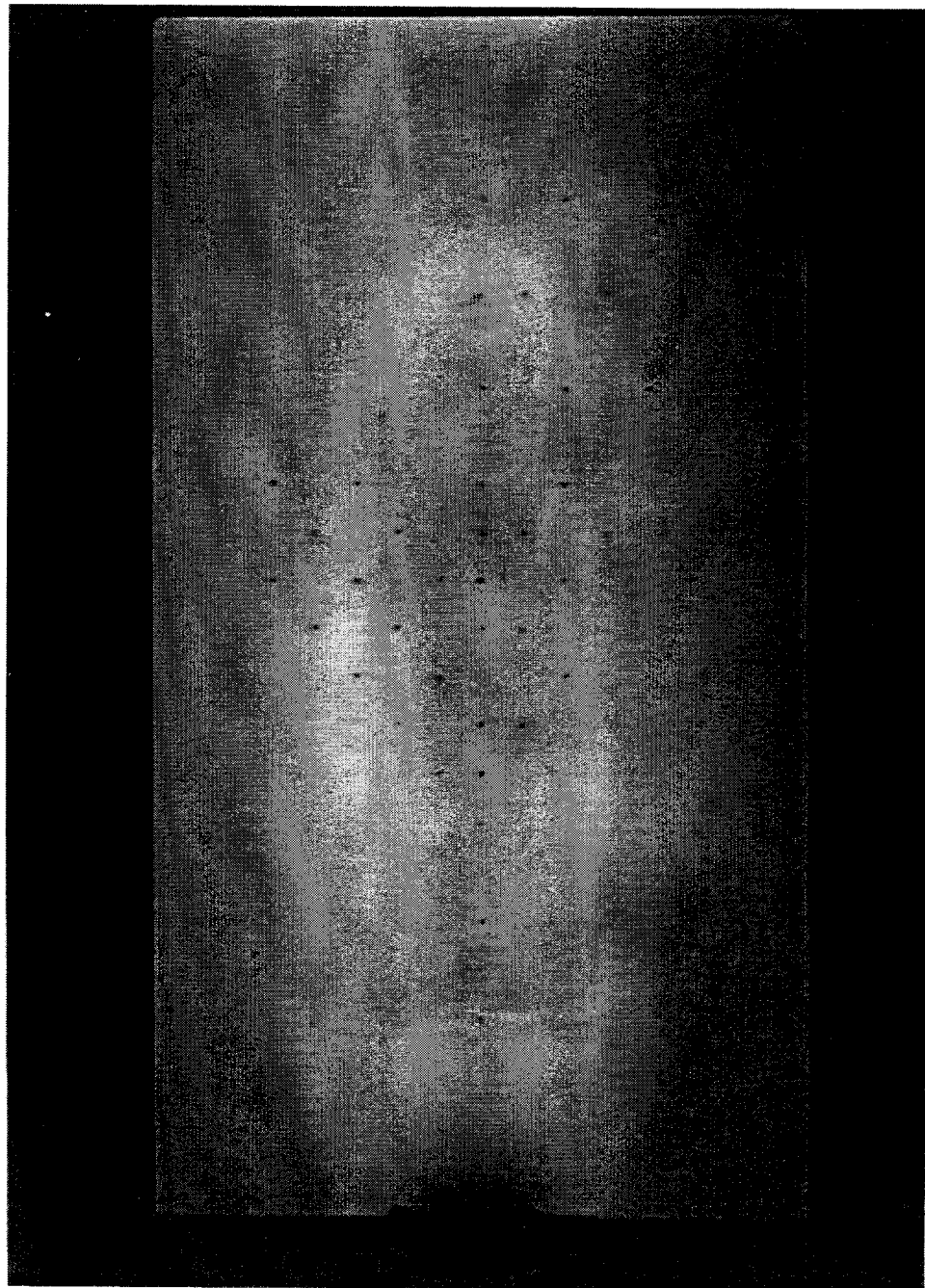


Figure 29a. Ten Averaged Images of the Underexpanded Jet Across the Flat Plate

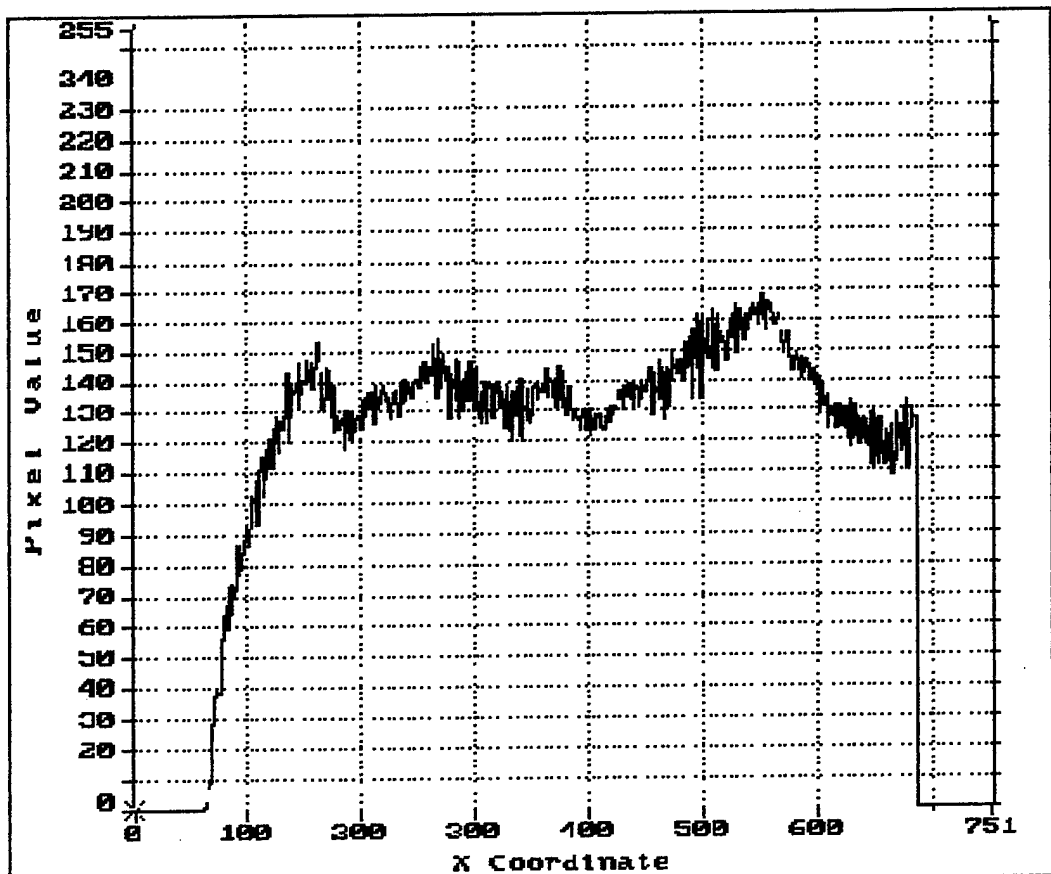


Figure 29b. Graphical Representation of a Single Line of Pixels of Ten Averaged Images

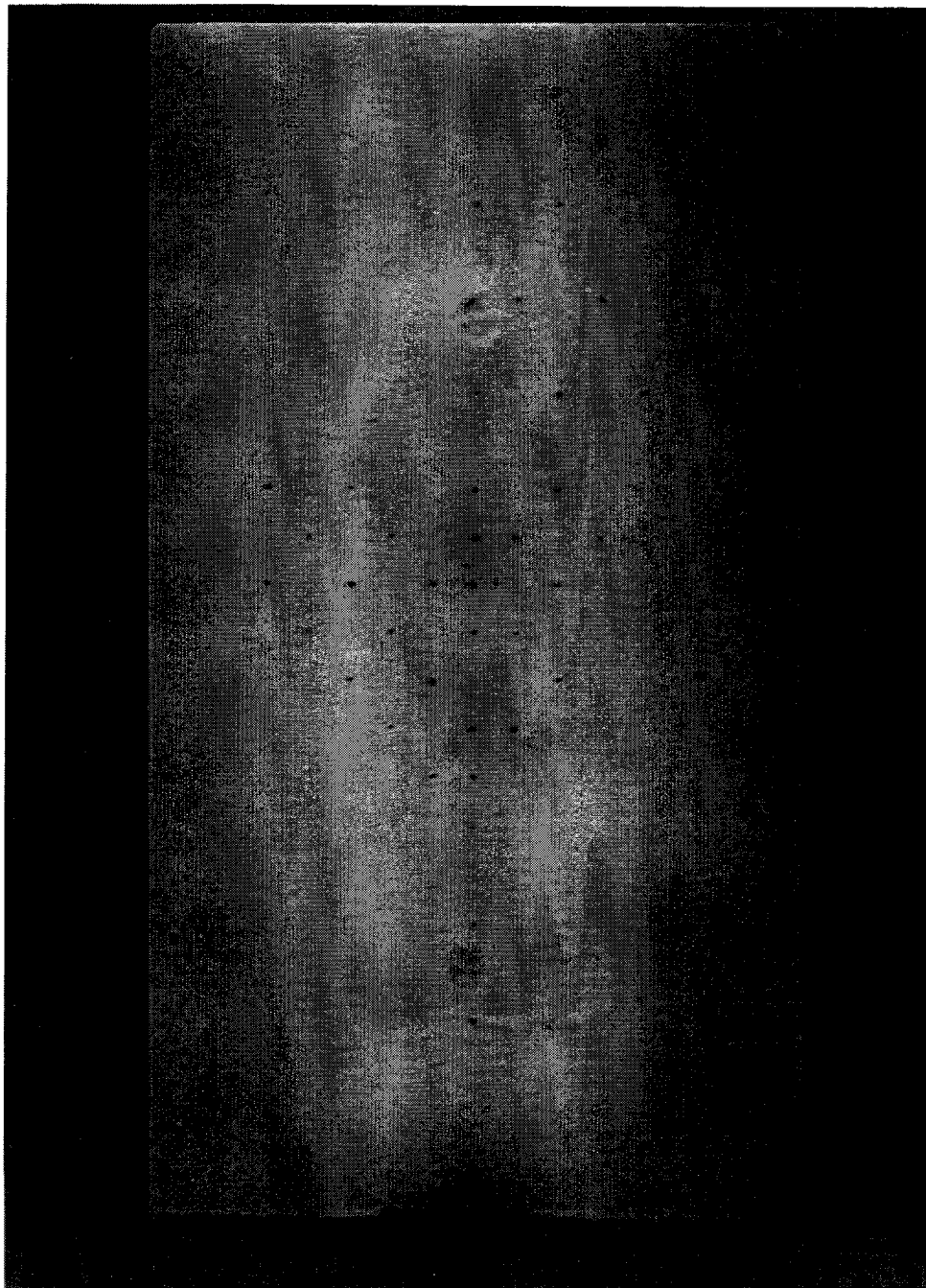


Figure 30a. One Hundred Averaged Images of the Underexpanded Jet /Flat Plate

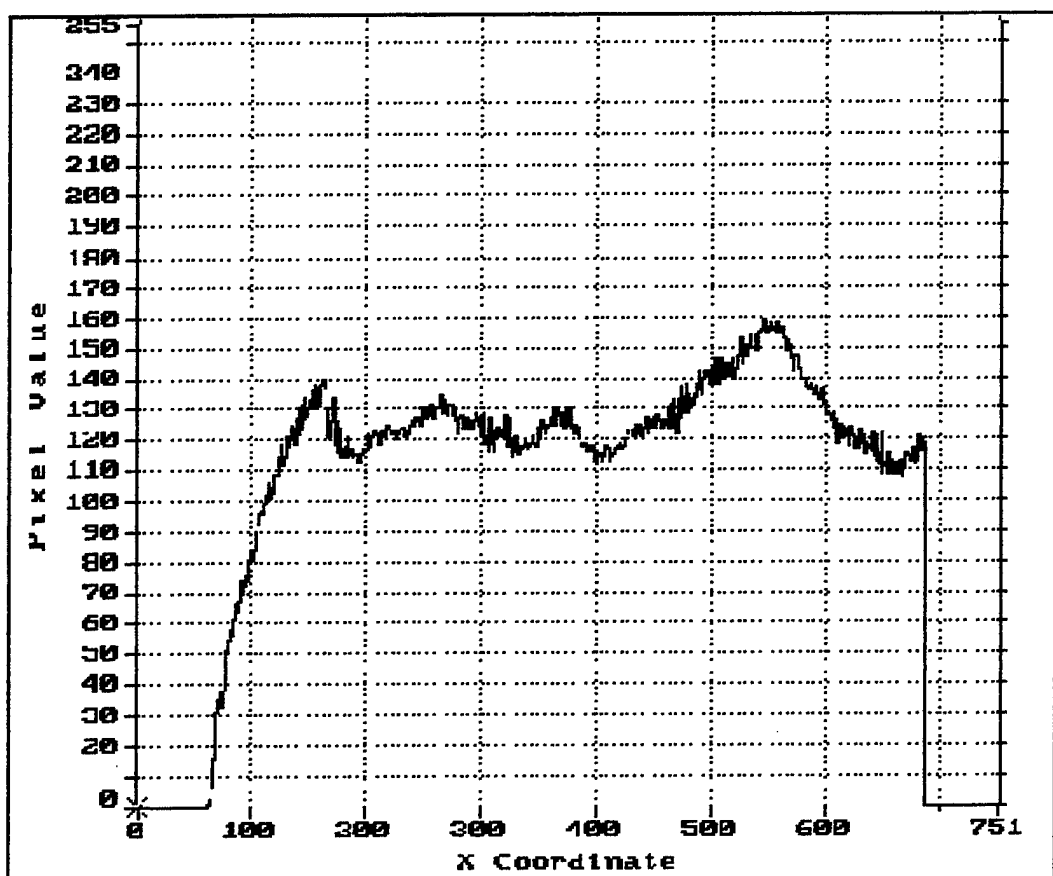


Figure 30b. Graphical Representation of a Single Line of Pixels of One Hundred Averaged images

using a pair of transformation equations relating the new coordinates to the old coordinates. An example set of transformation equations, termed the *affine projection*, are

$$x' = (a_{11}x + a_{12}y + a_{13})/(a_{31}x + a_{32}y + 1)$$

and

$$y' = (a_{21}x + a_{22}y + a_{23})/(a_{31}x + a_{32}y + 1)$$

where x, y are the old coordinates and x', y' are the new coordinates. The eight unknown coefficients in the two equations can be determined if the coordinates of four points, called control points, can be determined from each of the two images involved. [Ref. 21:p. 71]

In the jet/plate interaction experiment, the stiffness of the plate was expected to be sufficient to withstand the forces imposed on it by the jet so that any deformation that did occur would be insignificant, making registration unnecessary. However, comparison of the wind-on and wind-off images showed that the plate did experience a horizontal translation when the jet was on. It was found that the thrust produced by the jet caused a deformation in the structure supporting for jet apparatus. Thus, the jet apparatus and flat plate in combination experienced a displacement relative to the camera.

Examination of the wind-off and the corresponding wind-on images showed that for the 65 and 80 psig cases , the images had shifted one pixel width in the direction of the thrust, and two pixel widths for the 90 psig case. The image-registration algorithm in the EPIX software was found to be unsuitable for this correction. In

addition, the lack of "natural" features on the plate to serve as control points did not allow the use of the software. [When the object lacks such features and image registration is anticipated, artificial marks such as black circles can be distributed on to the surface. In the present case, registration was not expected to be needed, the plate was not so equipped.]

The registration between the wind-off and wind-on images was a relatively simple issue involving rigid body motion in one dimension. For this particular situation the images were aligned using the "Copy and Shift Image" function in the EPIX software which allowed an image to be shifted in its buffer up or down, left or right by an operator-specified number of pixels. The registration scheme was accomplished by first loading the wind-on and wind-off images into consecutive image buffers. The wind-on condition was considered the "warped" image and the wind-off image the "reference" image to which the warped image would be registered. A cursor overlay was simultaneously displayed on the image monitor with the wind-off image. The cursor was adjusted so that its horizontal character overlaid the pressure ports along the centerline of the plate while the vertical character of the cursor overlaid the pressure ports along the vertical centerline of the plate. The cursor remained fixed relative to the screen of the monitor; this served as a reference for comparison of object feature location when shifting between the wind-on and wind-off buffers. The wind-on image was then shifted relative to the vertical-cursor character until the vertical centerline pressure ports were overlaid by the vertical cursor character. When complete, the images were considered registered.

The accuracy of using this approach was judged to be similar to that of registration software since the registration software normally requires the operator to manually locate the control points in each image. In addition, since the body moved relative to the light source, consideration must be given to whether changes in brightness were due to the pressure variations, or were caused by the motion of the plate.

McClachlan *et al* [Ref. 22:p. 3] indicate that this is of greatest concern when model deflections and distortions are extreme. Since the flat plate motion consisted of rigid body translation, the magnitude of which was extremely small, this concern was considered to be insignificant.

(4) Ratioing. While the reason for ratioing the wind-off image with the wind-on image was to satisfy the Stern-Volmer relation and produce a pressure map, there were other benefits which arose from the procedure. In Figure 31 it is easy to discern the gross features of the pressure distribution in the wind-on image. The ratioing process had the effect of enhancing the finer detail in the image that would otherwise be too subtle for detection. [Ref. 7:p. 7]

Examination of the wind-off image in Figure 32 shows the evident brightness variations from point to point across the surface. This was due to a combination of differences in illumination, paint thickness variations, and features in the model itself. Figure 33 shows a three dimensional graphical representation of the wind-off intensity values across the surface of the plate. This illustrates the variations that exist across the plate. The result of ratioing was the elimination of these non-uniformities.

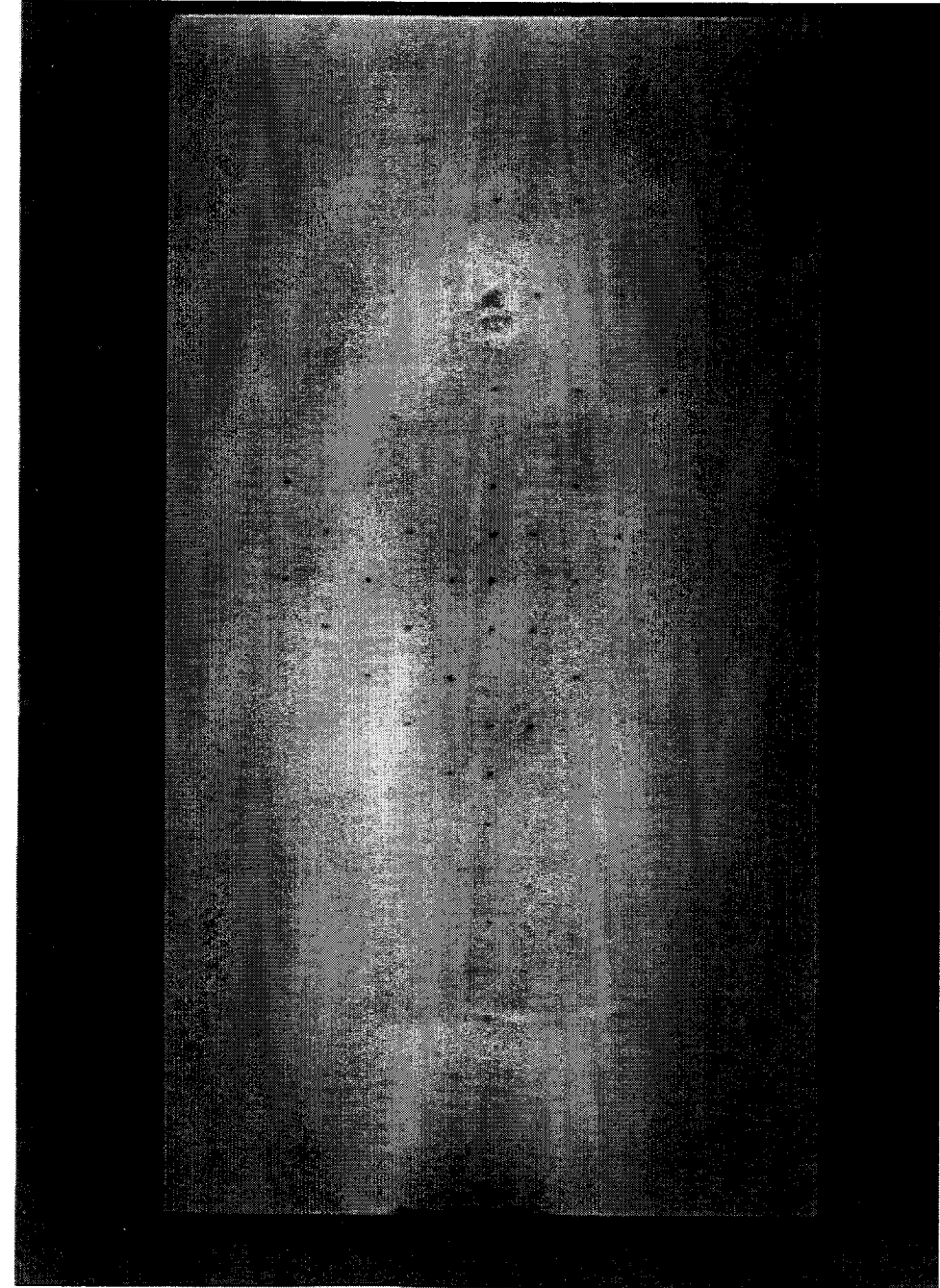


Figure 31. Wind-on Image of the Underexpanded Jet at 80 psig Across a Flat Plate

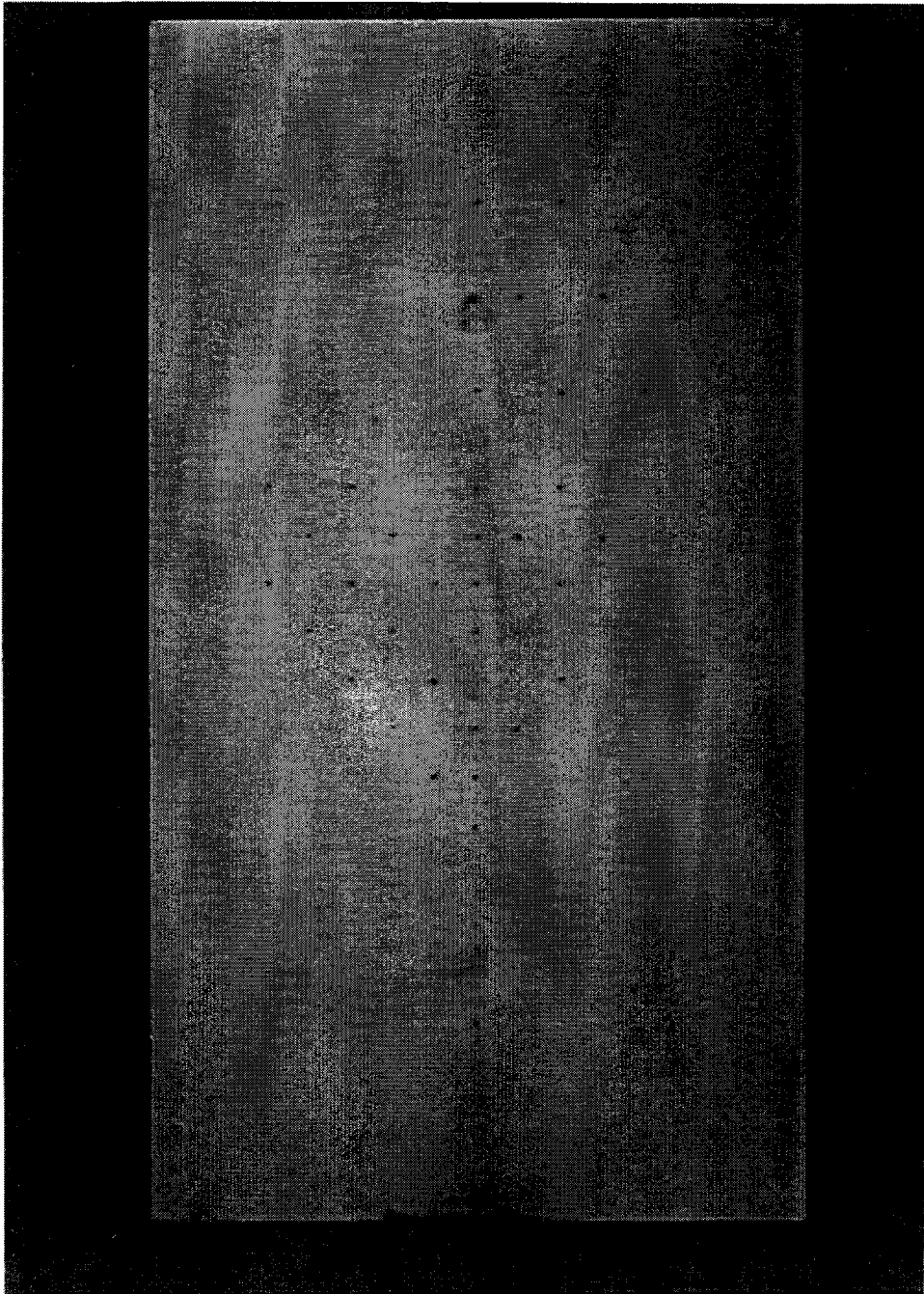


Figure 32. Wind-off Image for the 80 psig Condition

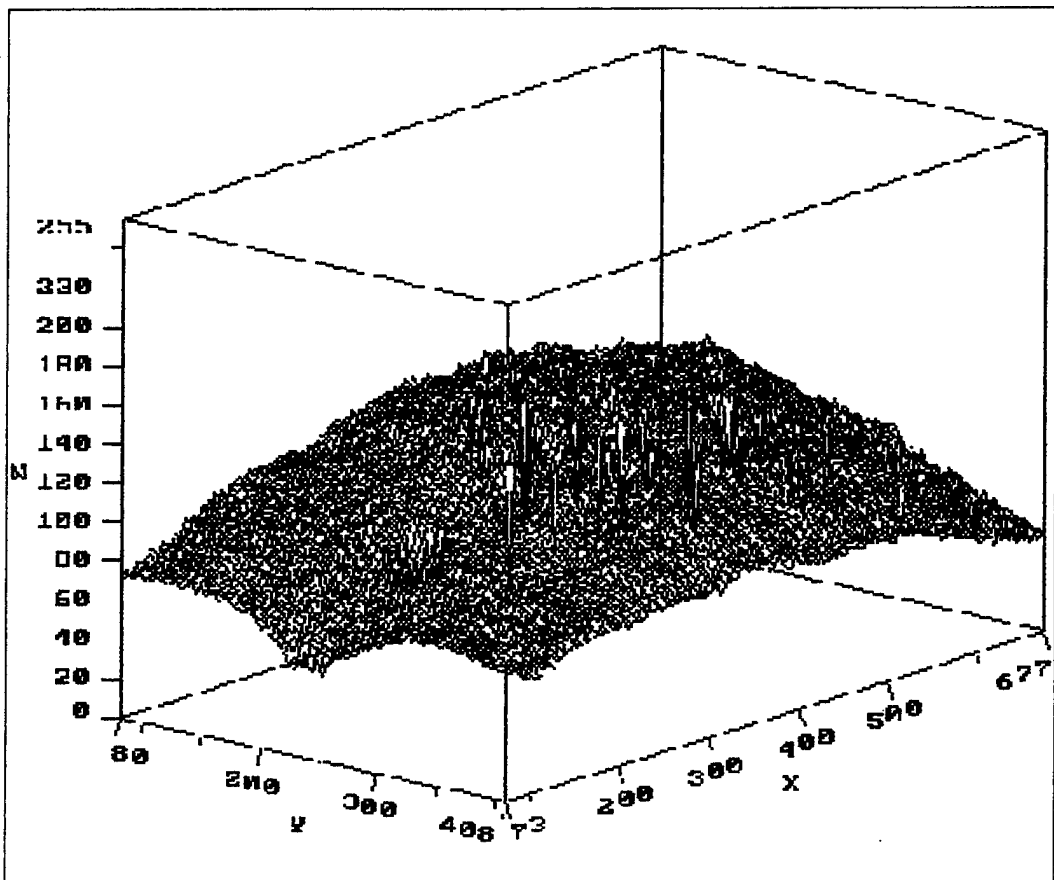


Figure 33. Three Dimensional Intensity Plot of the Wind-off Condition of the Plate

The "Ratio Image Operation" under the "Two Image Arithmetic" menu of the EPIX software formed the weighted ratio of corresponding pixels. The operation is mathematically expressed as

$$(c0 * \text{PixB} + c1) / (c2 * \text{PixA} + c3)$$

where the coefficients c_0 , c_1 , c_2 , and c_3 are modifiable. For the current work, PixA was designated the wind-on image while PixB , the wind-off image. In addition, the coefficient c_0 was assigned the value of 100 while the coefficients c_1 , c_2 , and c_3 were assigned the values 0, 1, 0 respectively. The reason for assigning c_0 the value of 100 was to scale the resultant ratioed intensity map such that differences of the grey values between neighboring pixels could be discerned.

Figure 34 illustrates the ratioed image for the underexpanded jet across the flat plate at 65 psig plenum pressure. The importance of proper registration of the wind-on and wind-off images prior to ratioing cannot be overstated. To illustrate the effect of improper registration, the images used to form the resultant image in Figure 34 were modified where the wind-on condition was shifted an additional five pixel widths in the direction of the thrust. The result of ratioing these two images is shown in Figure 35. A reduction in fine details, as compared to Figure 34, is clearly evident.

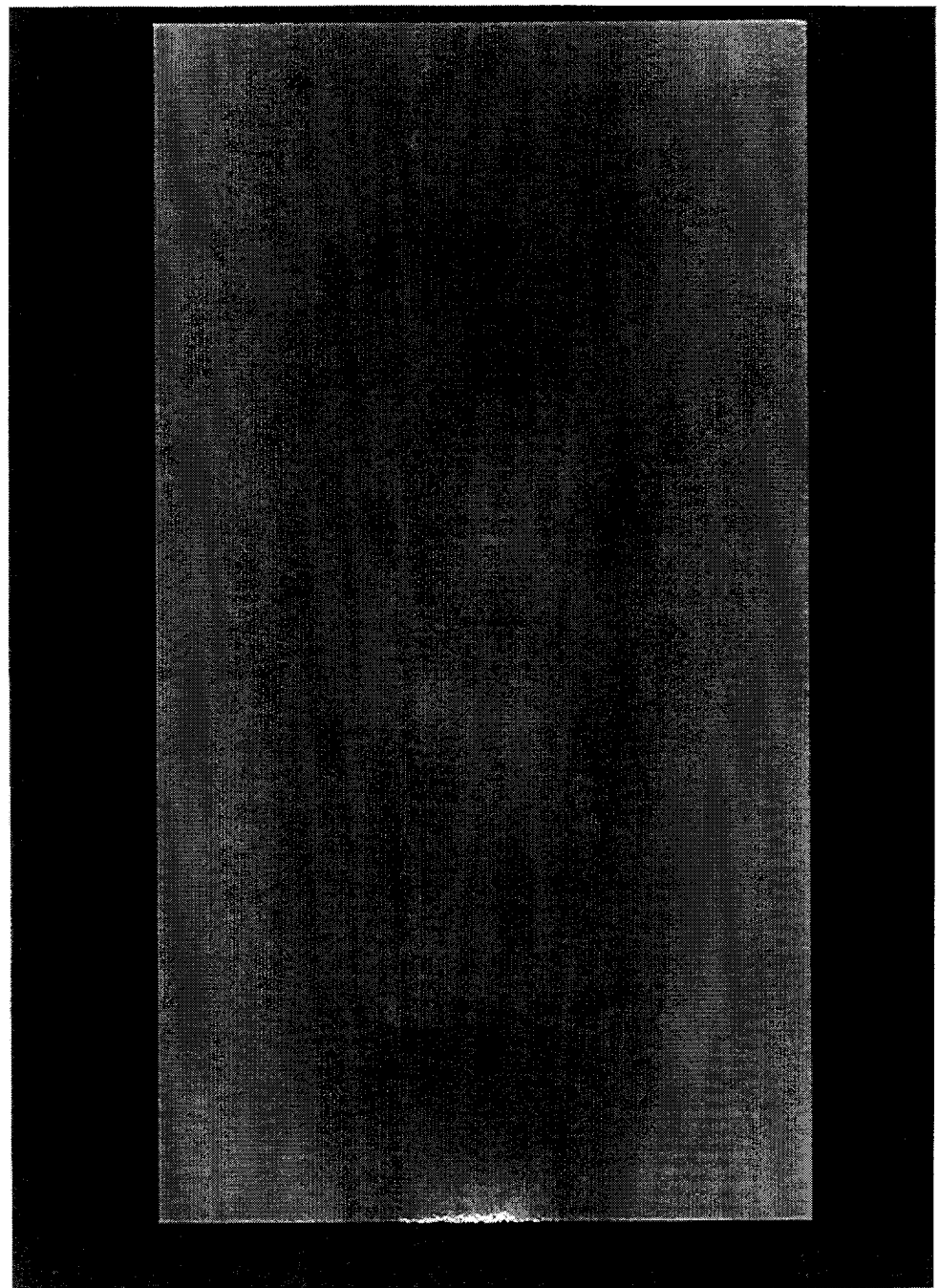


Figure 34. Ratioed Image of the Wind-off and Wind-on Images for the Flat Plate /Jet Interaction at 80 psig

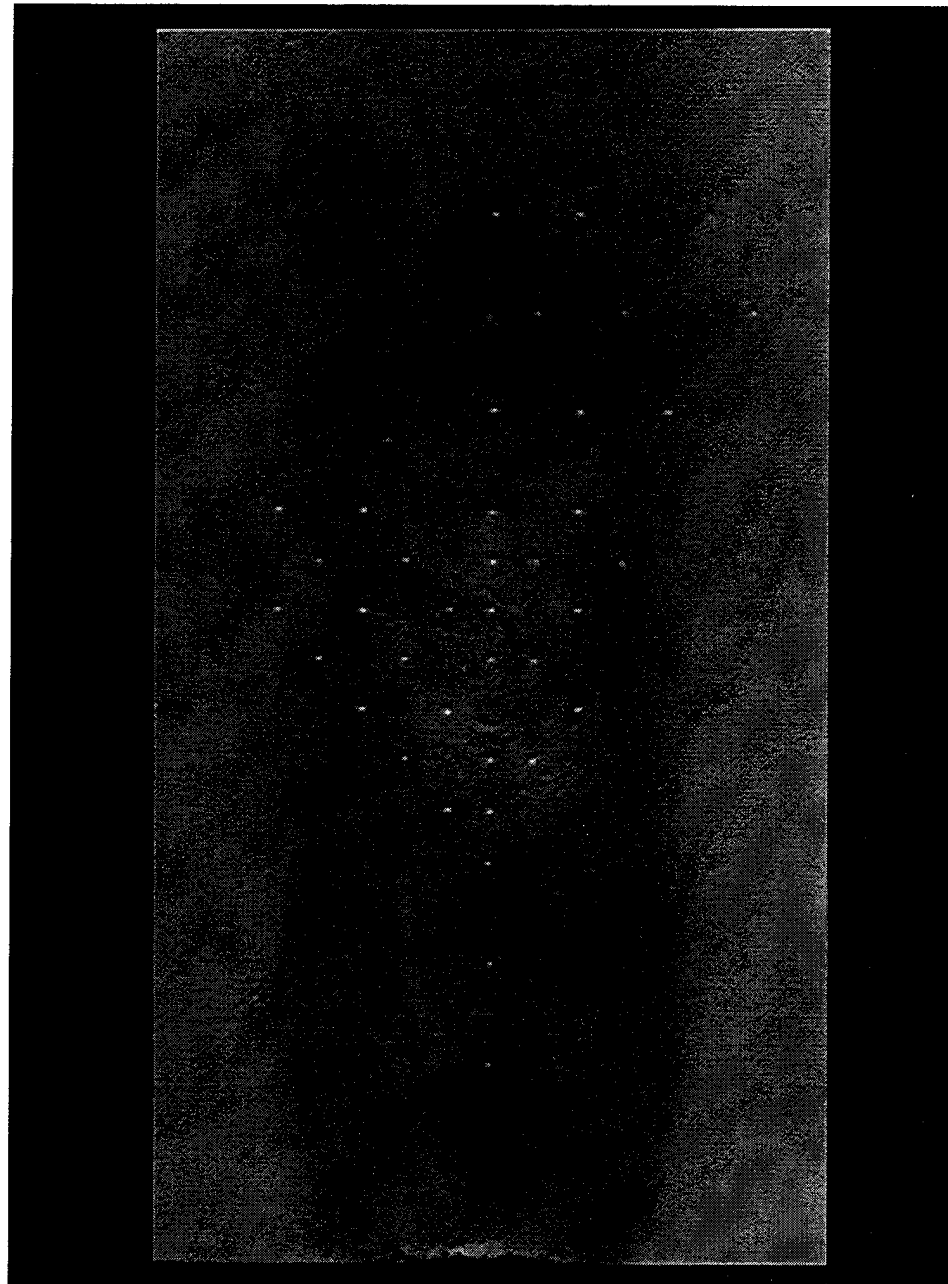


Figure 35. Result of a Ratioed Image Following Improper Registration Technique

b. Calibration

Two methods were available to calibrate the intensity ratio map, the intent of which was to obtain the sensitivity coefficients for the Stern-Volmer equation and establish the pressure map.

The first method, termed "*a prior*", involved calibrating a paint sample in a controlled pressure and temperature chamber. Using the data obtained from the chamber, and knowing the temperature of the model surface, the appropriate values for the Stern-Volmer coefficients could be found [Ref. 7:p. 7].

The second method, termed "*in situ*", which was the method employed in the present work, used the pressure obtained using a conventional pressure tap in the model surface and compared this with the intensity from the luminescent paint adjacent to the tap. Using data from a number of taps, the sensitivity coefficients were obtained by a least-squares linear fit. The coefficients A and B, being functions only of temperature, were good over that portion of the surface which was at the same temperature as the area containing the pressure taps. [Ref. 7:p. 10]

The approach used to produce pressure data from the ratioed image was similar to that used by Kavandi [Ref. 9:p. 94]. This entailed averaging the data from five adjacent rows of pixels near the pressure taps to produce a single row of data. (This, has the effect of averaging a total of five hundred images together.)

To do this, the ratioed image was loaded five times into consecutive frame buffers of the frame-grabber board. Each successive image was then vertically offset by

one pixel row with respect to the previous image, i.e., the first image remained unmodified, the second image was shifted one pixel row down in its frame buffer with respect to the first image, the third image shifted two pixel rows down with respect to the first image, etc. The five buffers were then averaged. Each row of pixels in the resultant image, with the exception of the first five and the last five rows of the image, was then an average of the corresponding row in each of the five images. A row of pixels close to the pressure taps was then selected to serve as calibration data. Figure 36 shows the data from the selected line of pixels for the flat plate in the underexpanded jet at 80 psig, prior to averaging with four adjacent lines of pixels. Figure 37 shows the data for the same line after the averaging procedure. [It is noted that the "spike" on the left side of the graph is due to paint that has separated from the leading edge of the plate]. From an examination of Figure 36 and Figure 37 it can be concluded that the five-row averaging procedure had the effect of reducing the noise level in the distribution with negligible effect on the distribution itself.

The calibration curves that resulted from plotting intensity values against the measured surface pressure at jet stagnation pressures of 65, 80 and 90 psig, are shown in Figures 38, 39 and 40, respectively. All data were obtained using the line of pixels and the line of pressure taps along the centerline of the jet. Two separate linear fits are shown in each of the figures. This was done when it was realized that the data were poorly represented by a single curve, and that large variations in temperature over the surface of the plate was the probable cause. It is possible that the groups of points which correlate

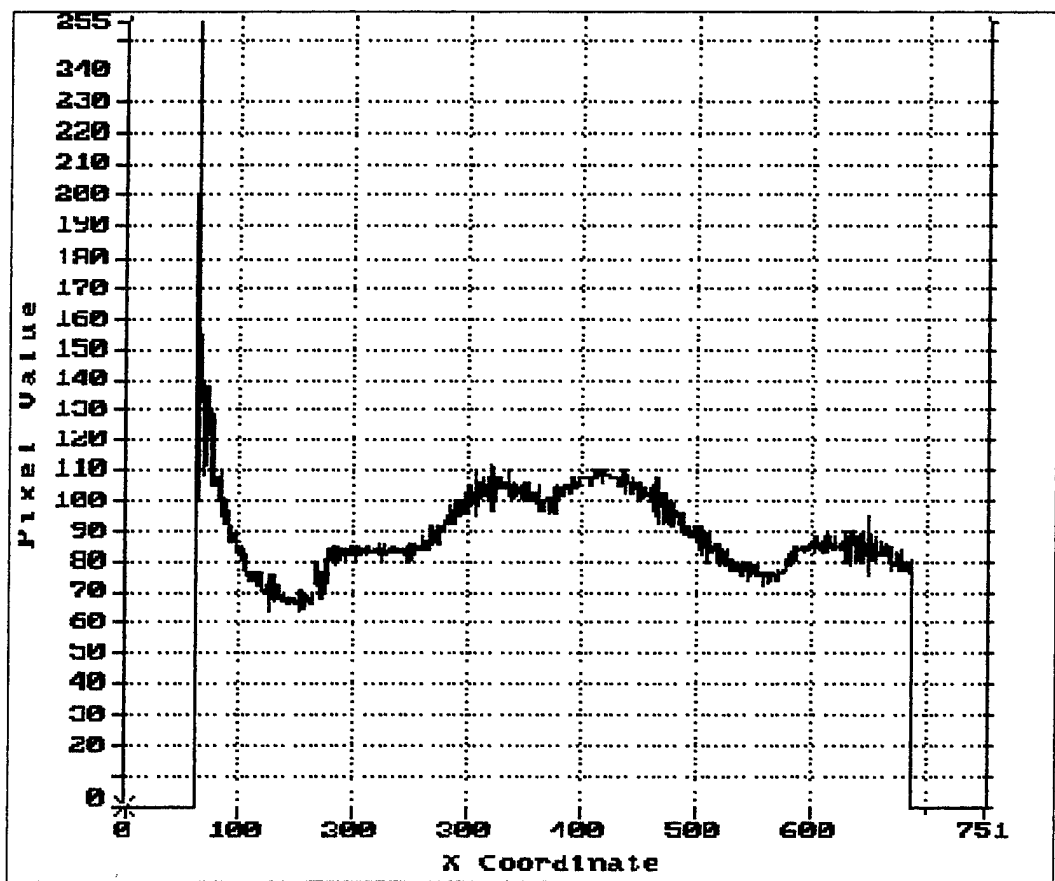


Figure 36. Calibration Line of Pixels for the 80 psig Case Prior to Spatial Averaging

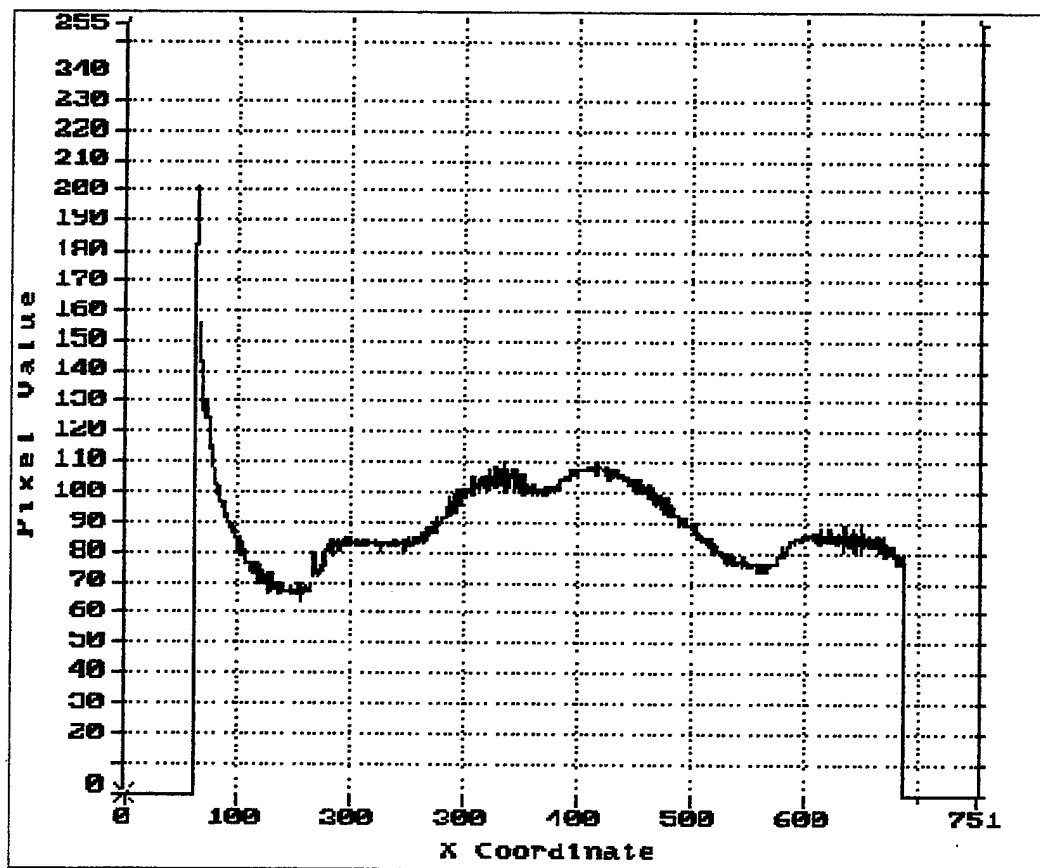


Figure 37. Calibration Line of Pixels for the 80 psig Case After Spatial Averaging

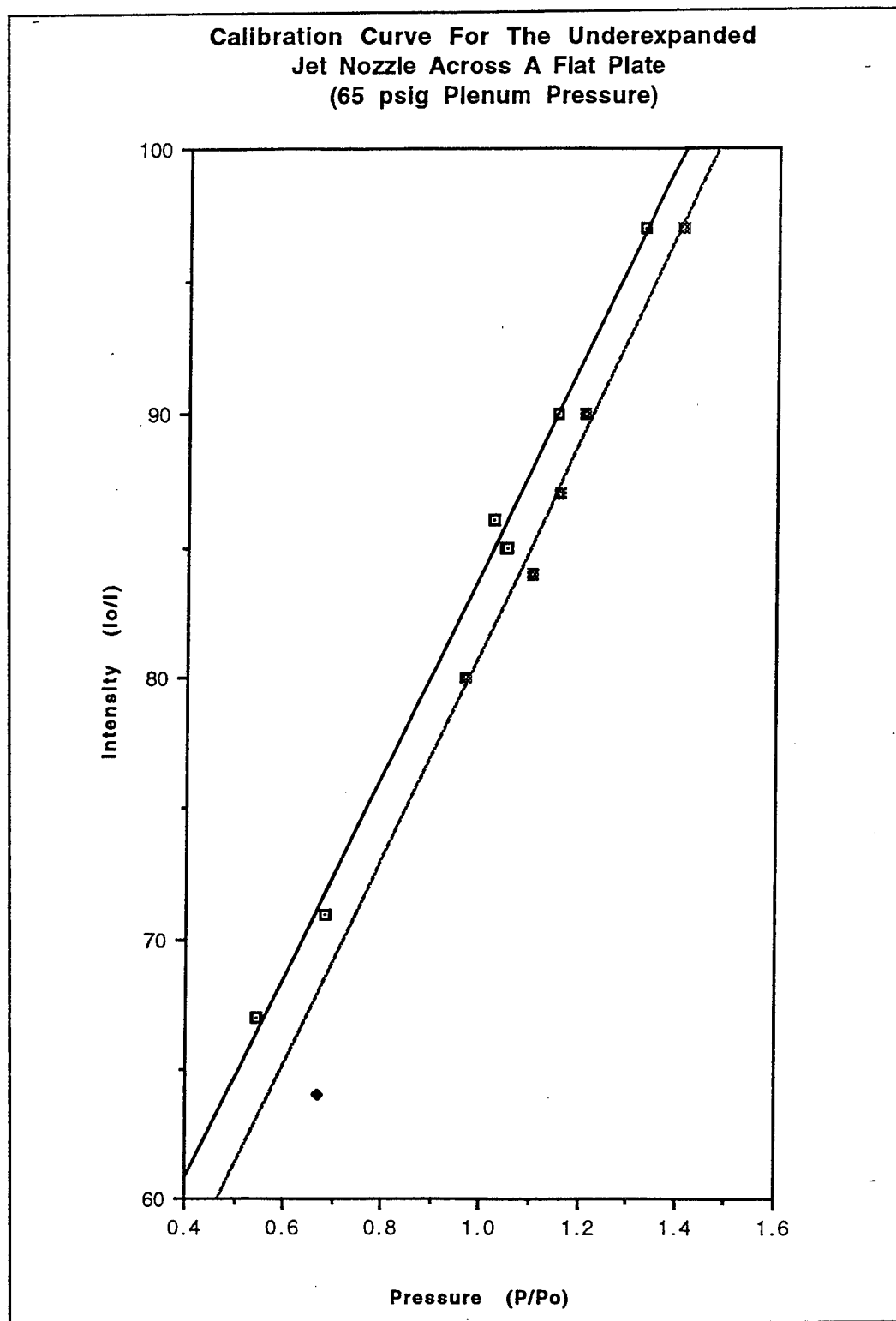


Figure 38. Calibration Curve for the Underexpanded Jet/Flat Plate at 65 psig

**Calibration Curve For The Underexpanded
Sonic Jet Across A Flat Plate
(80 psig Plenum Pressure)**

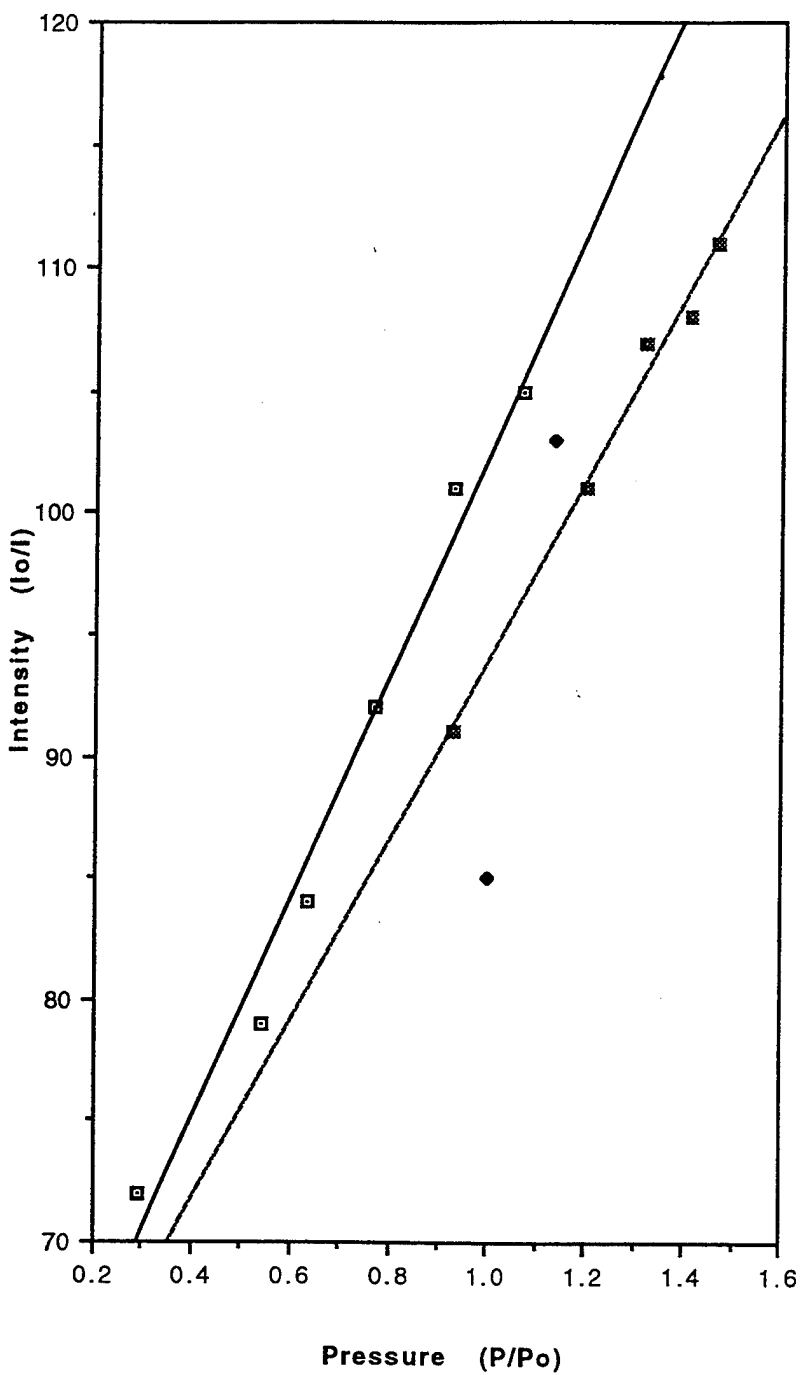


Figure 39. Calibration Curve for the Underexpanded Jet/Flat Plate at 80 psig

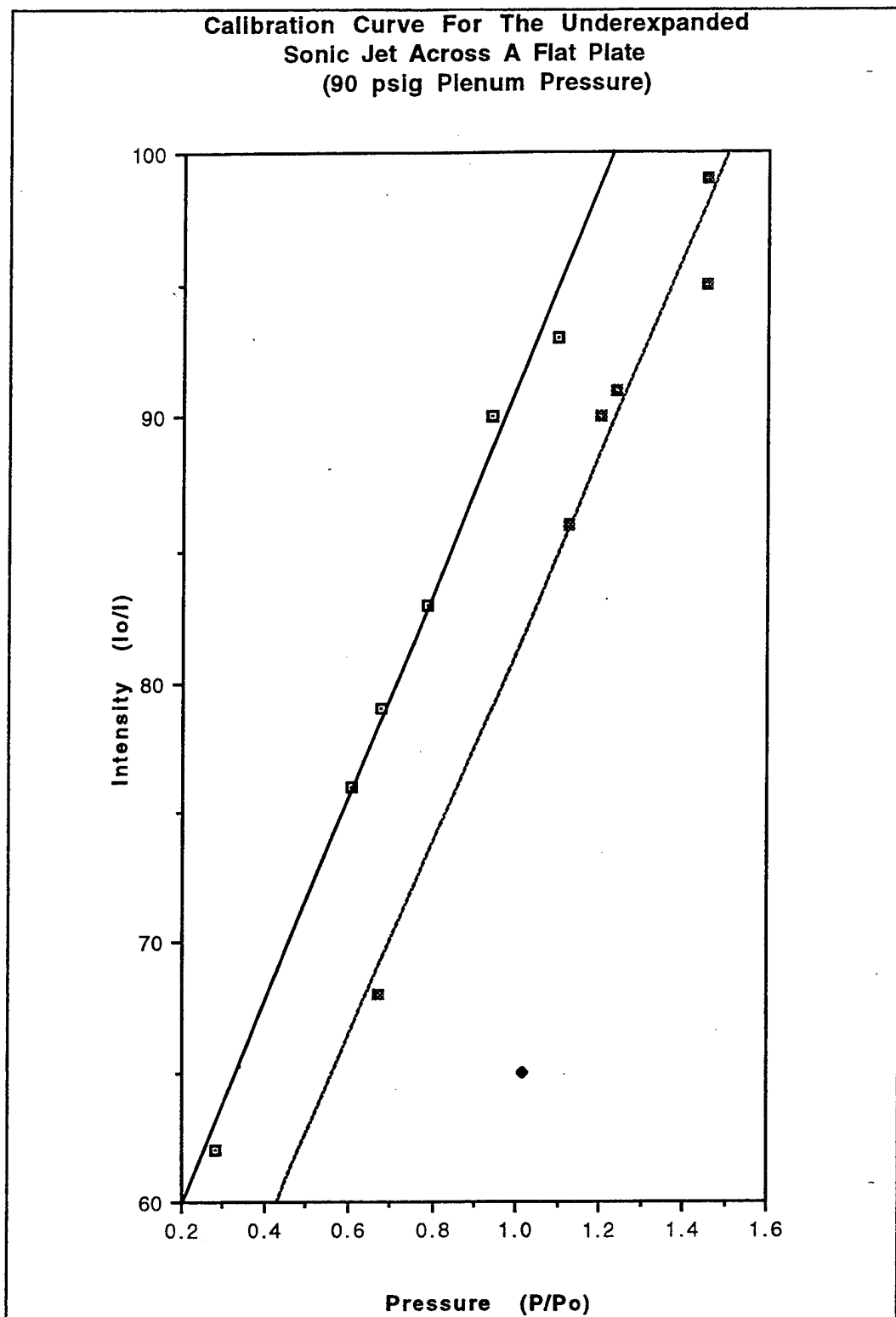


Figure 40. Calibration Curve for the Underexpanded Jet/Flat Plate at 90 psig

linearly are from regions of similar surface temperatures. However, the complexity of the flow over the plate surface, with a three-dimensional separation contained within it, makes the estimation of surface-temperature distribution very difficult. These results clearly indicate the need to measure surface temperature if *in-situ* calibration is to be used.

c. Field Pressure Map

Pseudo-coloring (or "false coloring") of a gray scale image was used to accentuate areas of an image that are not easily discerned by the eye. This was accomplished by providing an assignment of amounts of red, green and blue to a corresponding value of intensity in the gray-scale image. Through the use of look-up tables, the software allowed specification of linear ramps, logarithmic curves, polynomials, gamma correction, inversion and transposition in a pattern or sequence of a non-specific nature. For a gray-scale image the index value is synonymous with its intensity value. Reference 23 may be consulted for further information concerning the manipulation of lookup tables. The color map or sequence that was developed for the present work is shown in Figure 41. The constants A and B represent the minimum and maximum index values of the interval over which the color map was defined. All other index values were assigned the pixel value of zero in the color map. The minimum and maximum index values were found by conducting a histogram on the gray-scale image which gave a breakdown of the pixel intensity values and the frequency of occurrence in the image. The intensity values associated with the pressure-sensitive paint images are usually grouped in an interval between the 0 to 255 index value range.

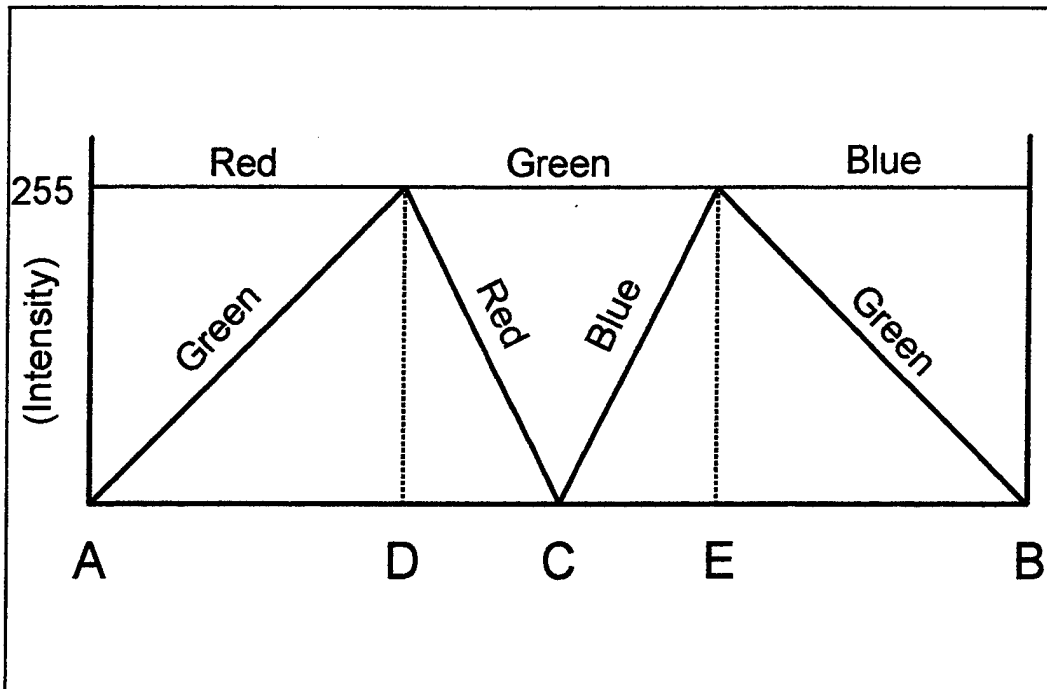


Figure 41. Graphical Representation of the Red, Green, and Blue Lookup Tables

The constant C represents the mid-point of this interval. The constants D and E were varied to obtain the desired bandwidth of the green lookup-table input which influenced the mid portion of the color spectrum.

The final pressure maps for the 65, 80, and 90 psig plenum conditions are given in Figures 42, 43, and 44 respectively. Although quantitative information is not available, the results in Figures 42, 43, and 44 show good qualitative agreement with their schlieren counterparts in Figures 12, 13, and 15 respectively.

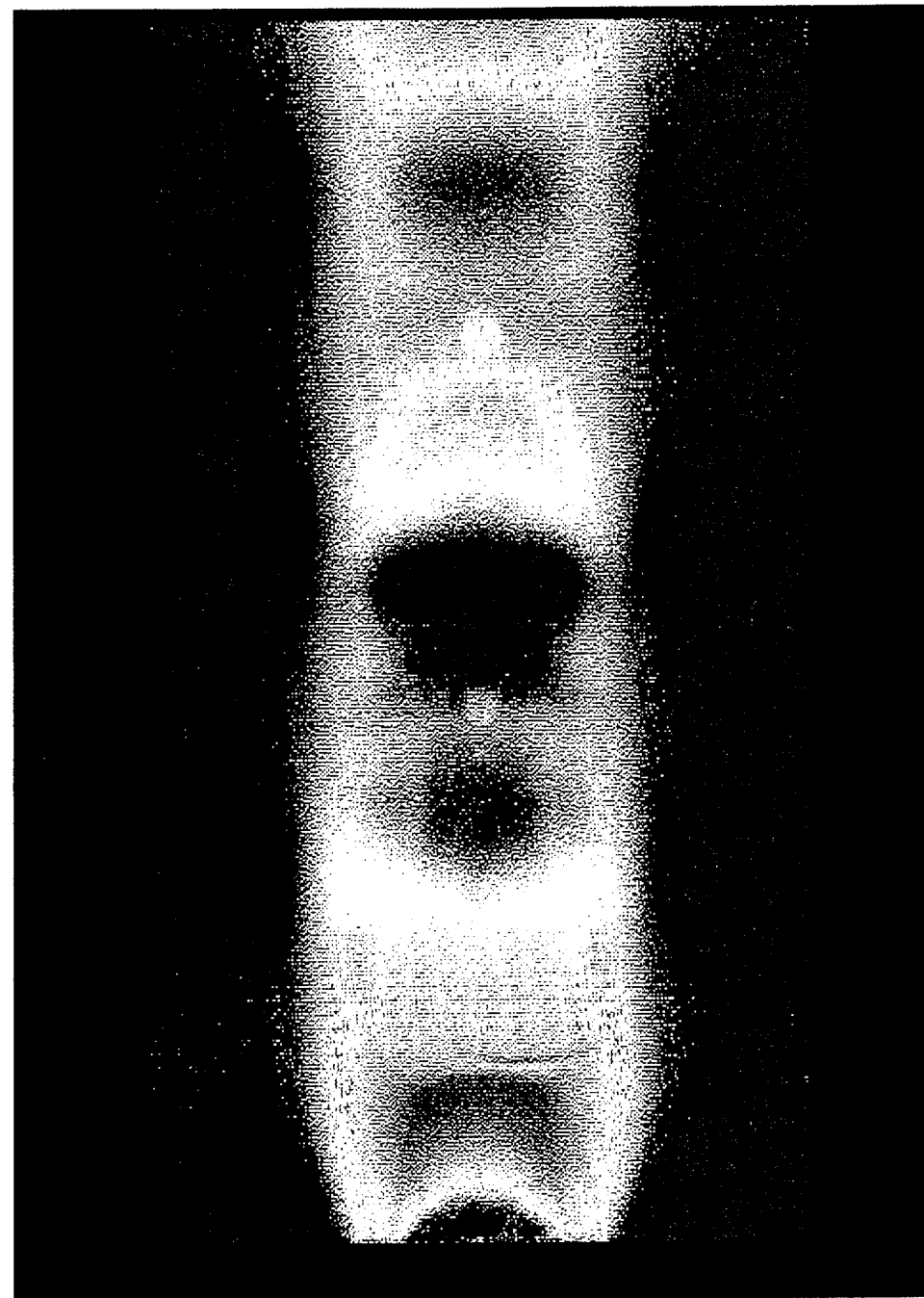


Figure 42. Pressure Map of the Underexpanded Jet at 65 psig Across a Flat Plate

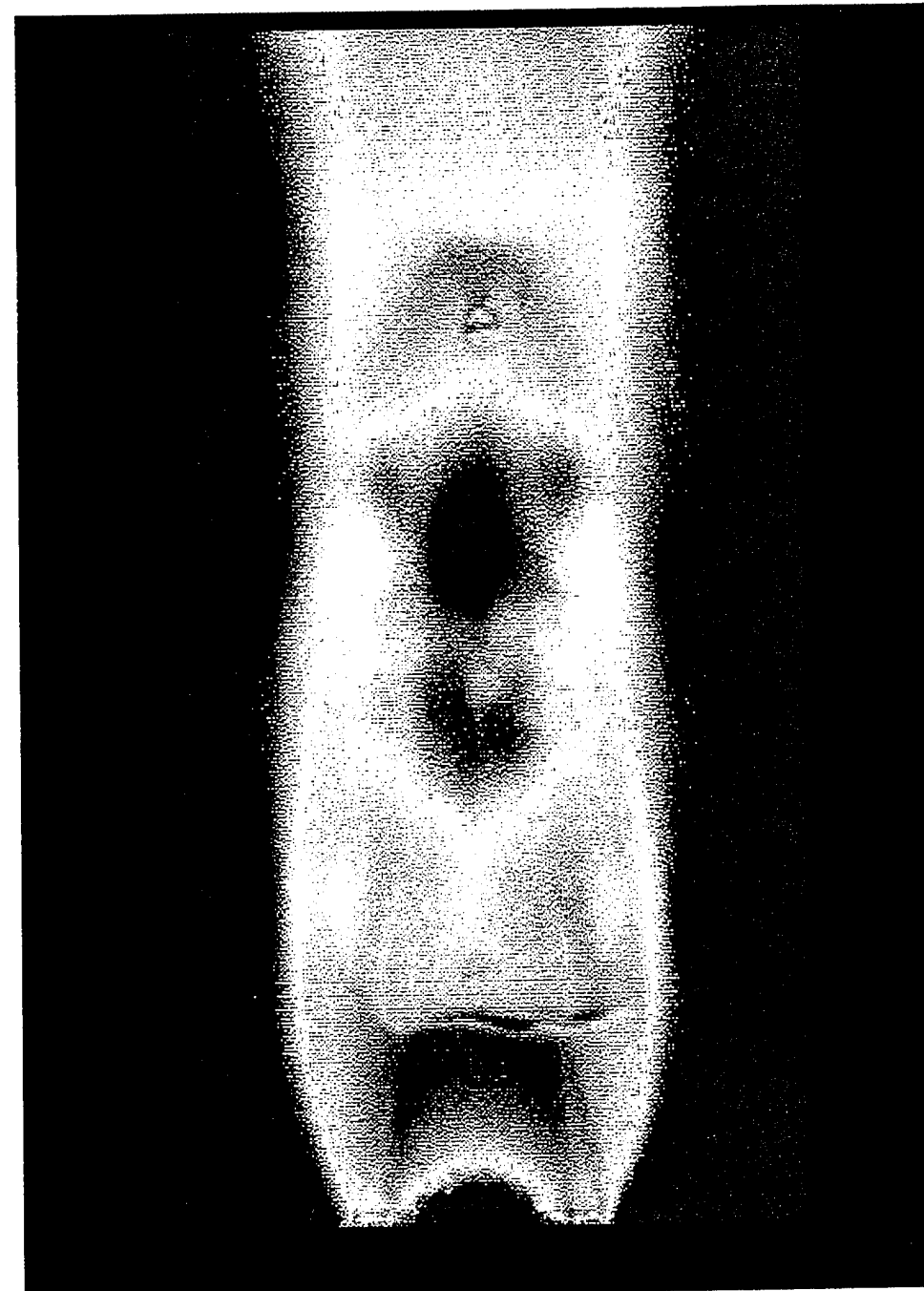


Figure 43. Pressure Map of the Underexpanded Jet at 80 psig Across a Flat Plate

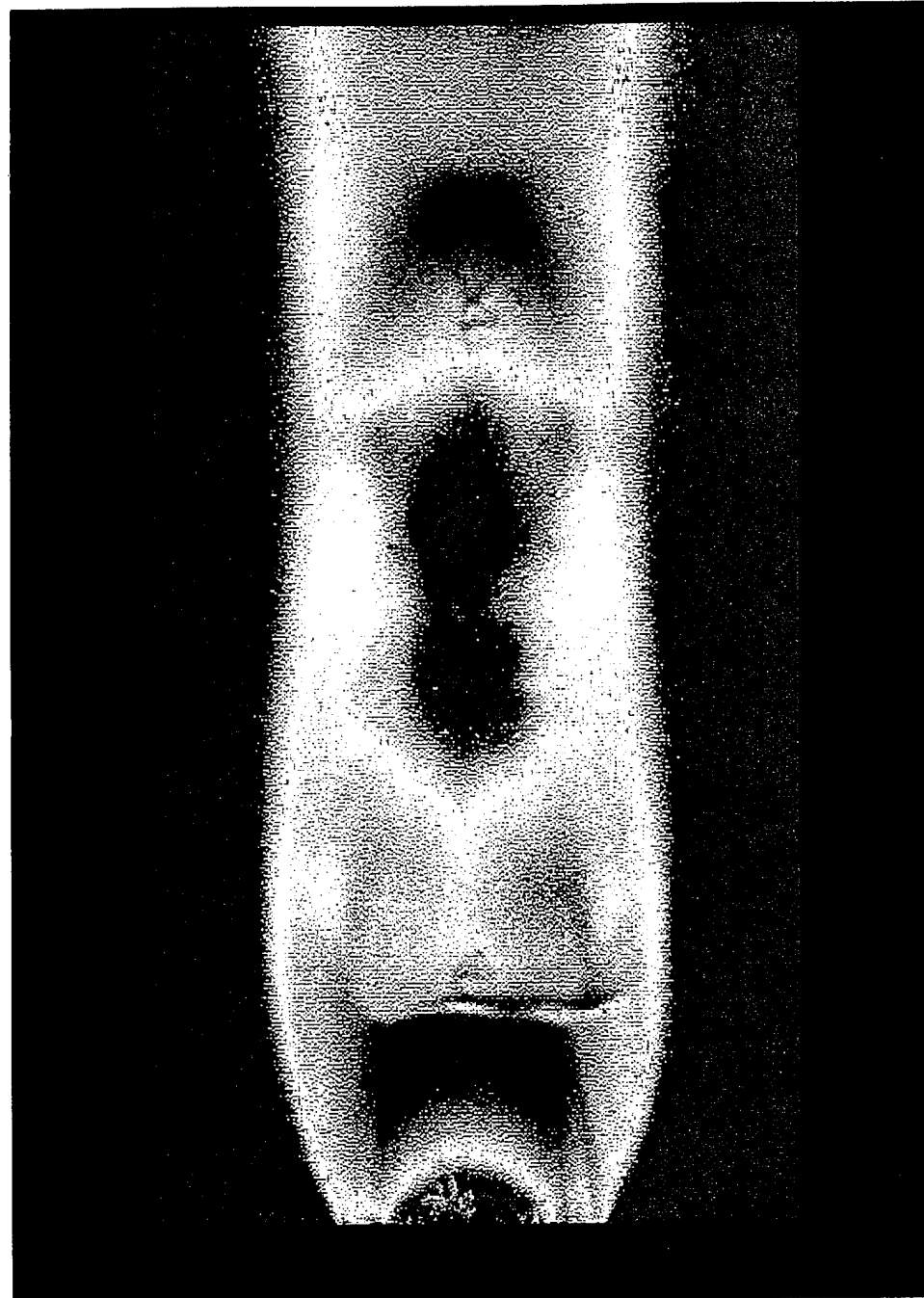


Figure 44. Pressure Map of the Underexpanded Jet at 90 psig Across a Flat Plate

IV. APPLICATION TO SHOCK-BOUNDARY LAYER INTERACTION IN A SUPersonic WIND TUNNEL

A. DESCRIPTION OF FACILITY

The supersonic wind tunnel, located in Bldg. 216 of the Gas Dynamics Laboratory [Bldg. 216] at the Naval Postgraduate School, was of the blow-down type. Supply air was produced by the same supporting facility as the underexpanded sonic jet apparatus. A schematic of the tunnel and supporting facility is shown in Figure 45 while Figure 46 shows a photograph of the wind tunnel.

Air to the tunnel, from a maximum pressure of 300 psi, was controlled by a pneumatic control valve. The control valve used a diaphragm actuator. Regulated instrument air from the supply system was routed to one side of the diaphragm and the controlled pressure, from a tap on the plenum, was connected to the other. This allowed precise control of the plenum pressure. A pressure gauge installed on the plenum provided pressure readout.

The plenum chamber was cylindrical with an internal diameter of approximately 20 inches. With the exception of a splash plate mounted perpendicular to the flow near the entrance of the chamber, the plenum was empty. The flow exited the chamber through a contraction and circular-to-rectangular transition section, into the convergent-divergent

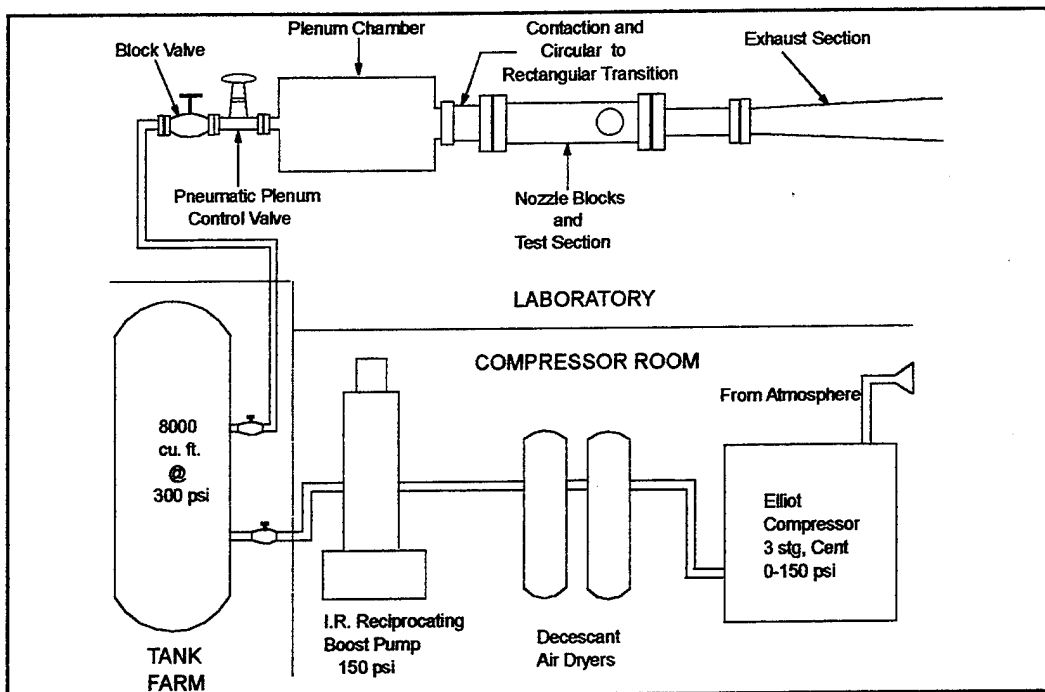


Figure 45. Schematic of the Supersonic Wind Tunnel and Supporting Facility

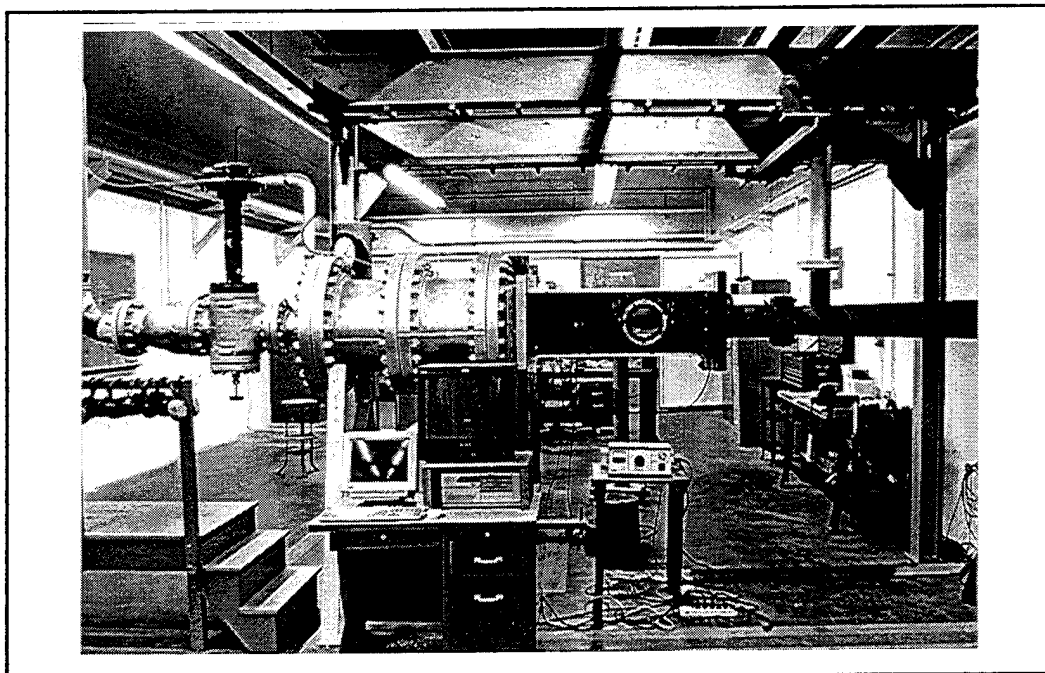


Figure 46. Supersonic Wind Tunnel Apparatus

nozzle. The nozzle and test section, shown schematically in Figure 47, were comprised of a set of two (interchangeable) aluminum blocks forming the contour and two flat plates forming the side walls and enclosing the constant-width section.

The test section was nominally four inches in width and four inches in height. Six-inch diameter circular glass windows on each side of the test section provided optical access. Two small gate valves were mounted on each of the side walls just downstream of the test section. They were used to allow "bleed" and thus control back pressure in order to position the "starting" normal shock in the test section. The flow exited the test section into an exhaust duct which vented to the atmosphere outside the building.

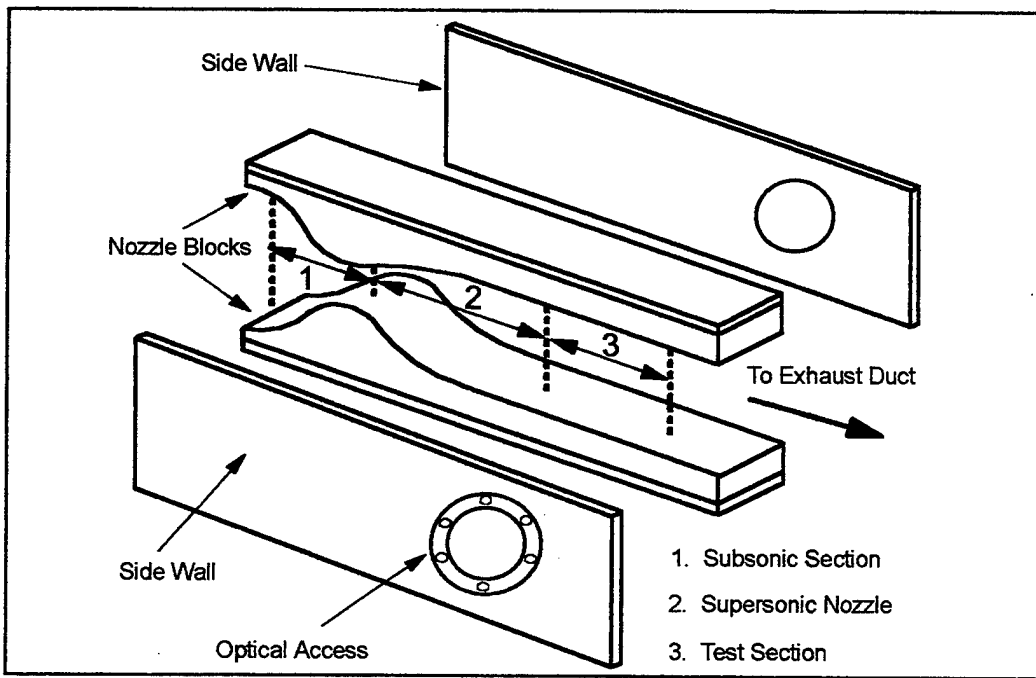


Figure 47. Nozzle Blocks and Test Section Exploded View

1. Nozzle Blocks

The interchangeable pairs of nozzle blocks were each designed to produce a specific Mach number in the test section. For the present study, two Mach numbers, 1.4 and 1.7, were used, since this was the range of Mach number of interest in the proposed study of control of shock-boundary layer interaction. A set of blocks for $M=1.4$ existed. However, it was necessary to design and manufacture a set of blocks to provide $M=1.7$. The program described in Appendix E was used to derive the contour for the $M=1.7$ nozzle. The new blocks were otherwise similar to the existing blocks and were manufactured to the original drawings using the new contour.

a. Performance Evaluation of the Mach 1.7 Nozzle Blocks

To evaluate the new nozzle blocks, several runs at varying plenum pressures were conducted. A series of pressure taps along one side of the tunnel allowed pressure data to be collected. The taps extended approximately four inches upstream of the nozzle throat and downstream to the entrance of the test section. A metal blank containing additional taps was installed in place of one of the test section windows to measure pressures through the test section. One tap downstream of the test section measured the pressure of the exiting flow.

The data acquired indicated that the normal shock associated with the nozzle starting process rapidly passed through the test section into the exhaust duct as soon as the operating pressure ratio decreased below the first critical condition. Unlike with the $M=1.4$ blocks, the bleed valves on the sides of the tunnel could not be used to position the

shock. It was realized that some form of blockage would have to be introduced into the passage at some point downstream of the test section in order to "set" the shock in the test section.

The mounting points for the gate valves, which were located three inches downstream of the test section and were aligned such that their centerlines coincided with each other, were adapted so that circular rods of varying diameter could be installed across the tunnel. A total of four rods was used. Operating the tunnel at 75 psi plenum pressure, the static pressure distribution was recorded for each configuration. The effect of rod diameter on shock position is clearly seen in Figure 48.

The 3/8 inch diameter rod was found to place the shock just prior to the test section. To position and control the shock precisely in the center of the test section, a means of bleeding off mass flow was developed. The solid rod was replaced by a 3/8 inch outside diameter tube. A series of 11/64 inch holes was drilled through the tube wall, in a line along its 4-inch length. The tube was then mounted between the gate valves with the holes aligned with the flow. This arrangement allowed a controlled mass flow to pass through the holes into the tube and out of the tunnel via the gate valves. The gate valves could be adjusted to vary the amount of outgoing mass, thus moving the shock to the desired position in the test section. A schematic of this arrangement is shown in Figure 49 while Figure 50 shows a photograph of the bleed-off tube mounted in the tunnel.

Pressure Distribution Along Tunnel Wall
Mach 1.7 (75 psi Plenum Pressure)

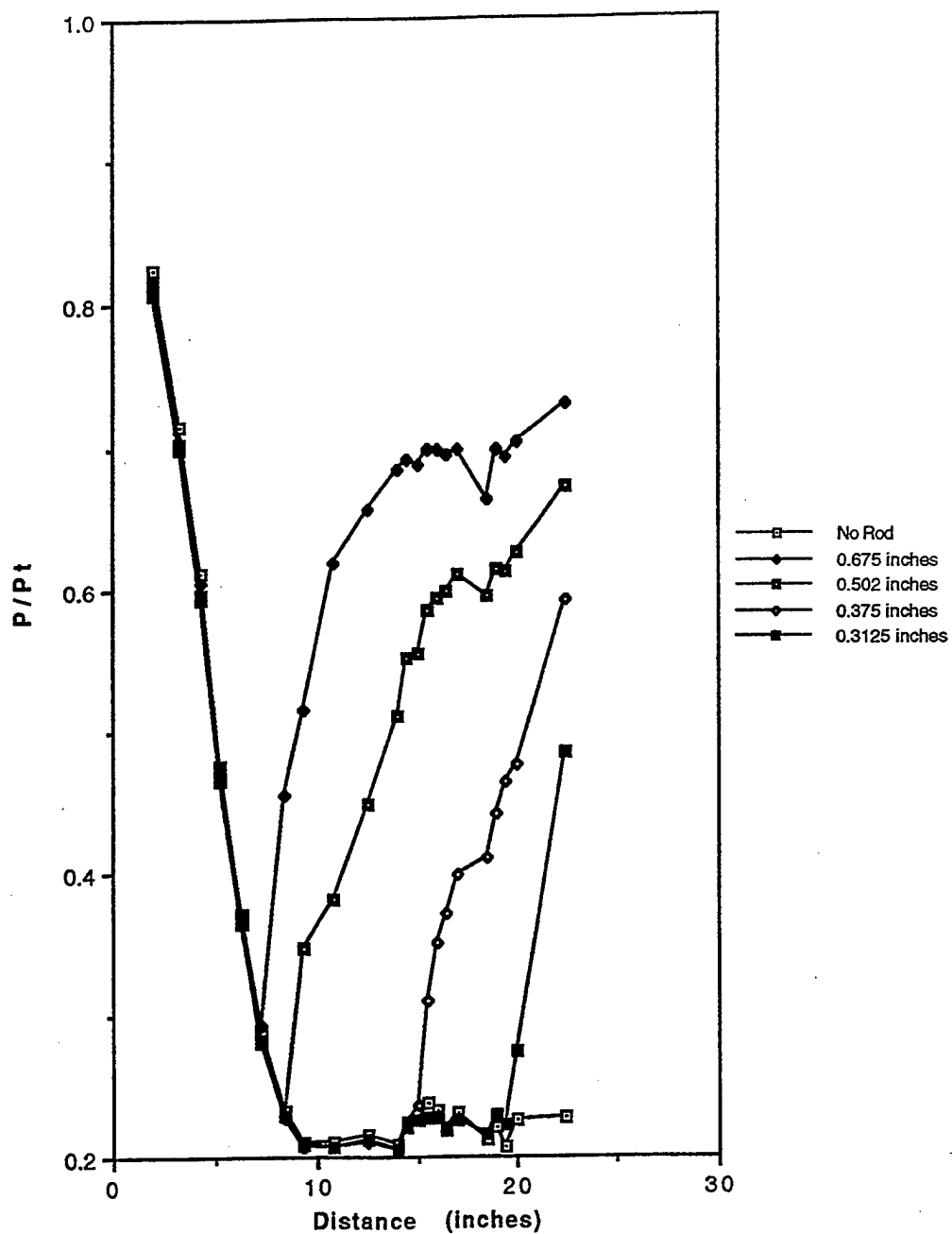


Figure 48. Tunnel Pressure Distributions as a Result of Varying Rod Diameters

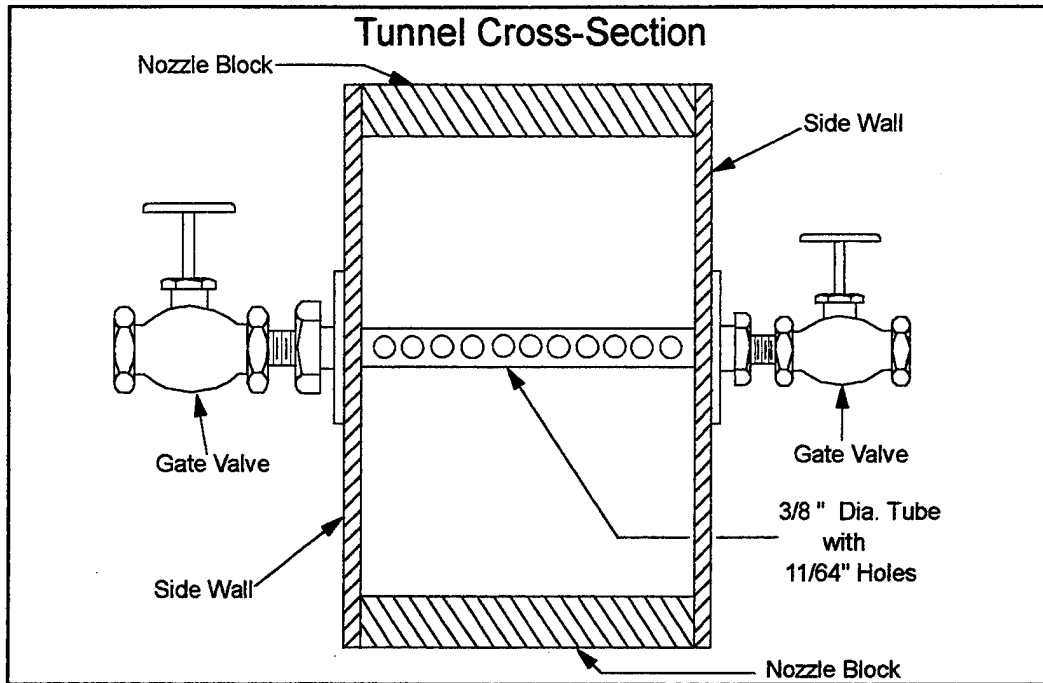


Figure 49. Cross-Sectional View of the Mass Bleed-Off System

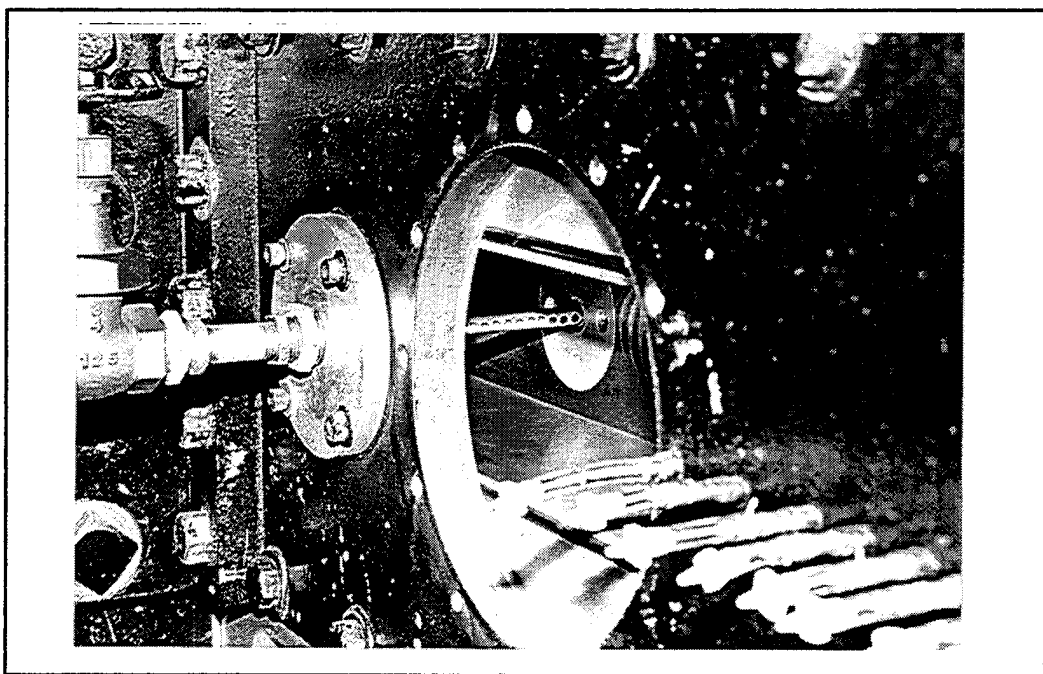


Figure 50. Mass Bleed-Off Tube Mounted in the Tunnel

B. INSTRUMENTATION

The metal blank, containing eleven pressure taps, and used as described above to measure the pressure distribution in the test section, was used as the model surface on which to observe the interaction between the starting normal shock and the nozzle boundary layer using pressure-sensitive paint. The metal blank was installed on one side of the test section and a six inch glass window was installed on the other. Concern for the spectral transmittance of the glass window led to an analysis of the glass for the range of 350 nm to 700 nm using a spectrometer. The results of the test, shown in Figure 51, indicated that the transmittance levels were satisfactory for the current work.

The optical measurement system was the same as was used for the underexpanded jet study described in chapter three. A schematic of the setup is shown in Figure 52.

C. EXPERIMENTAL PROCEDURE

It was found that the shock-boundary layer interaction in the test section was inherently unsteady. This precluded the use of the procedure outlined in chapter three for acquiring the wind-on data. That method required the event of interest to be steady and repeatable, thus enabling one hundred images to be taken over a series of ten runs. The approach taken for the unsteady process was simply to create as many image buffers as possible for a single sequence, and to execute this sequence in the shortest period of time.

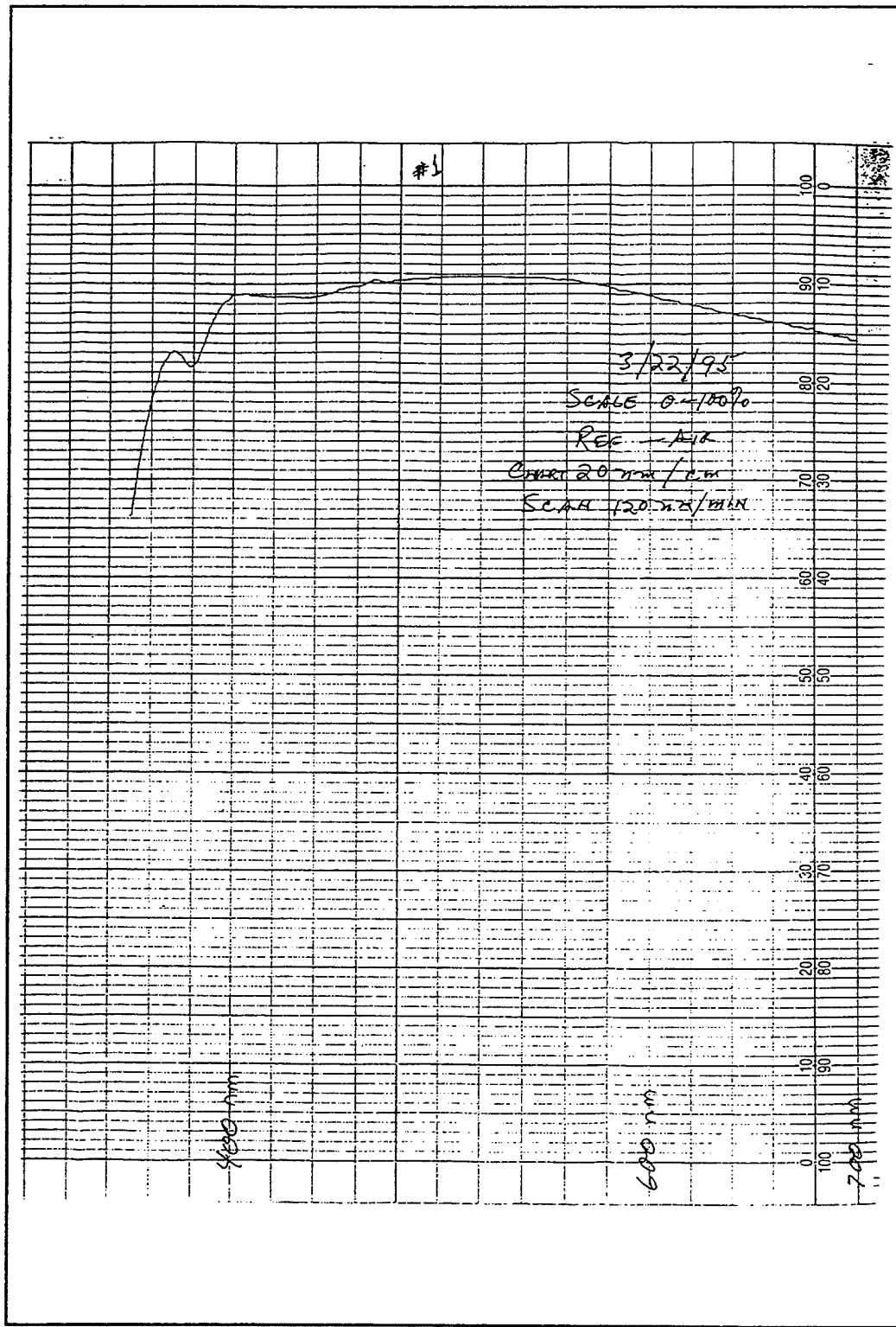


Figure 51. Spectrometer Results for the Optical Window

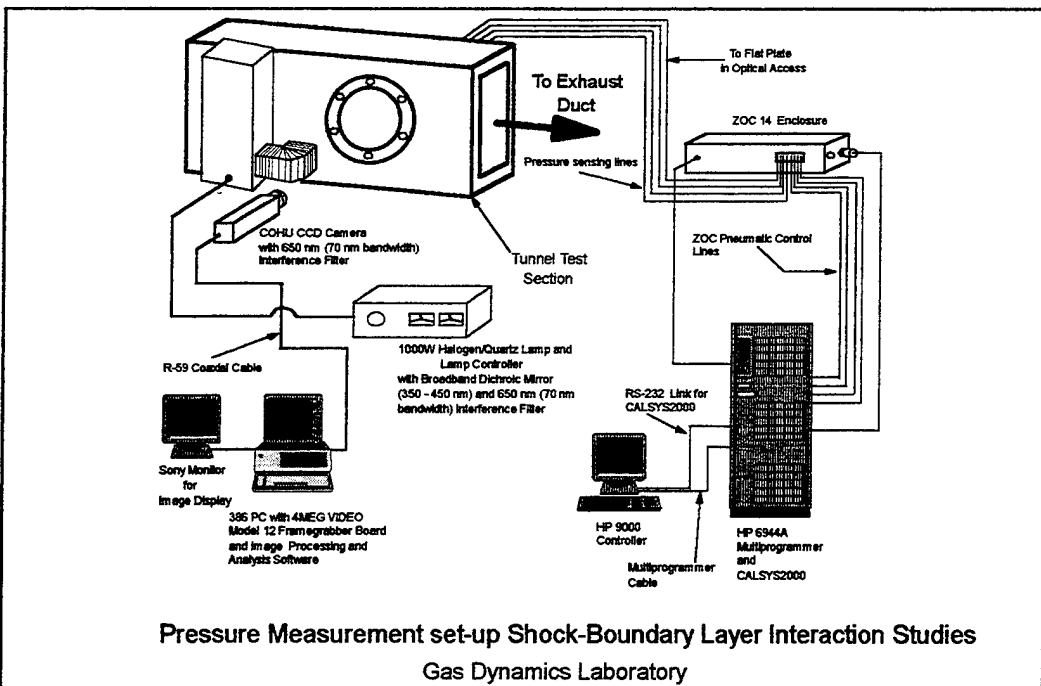


Figure 52. Instrumentation Setup for the Supersonic Wind Tunnel, Shock-Boundary Layer Experiment

The maximum number of image buffers that could be created for image capture was a function of video resolution. To maximize the number of available buffers it was necessary to minimize the video resolution. To accomplish this, the camera was focused on the test section so that the surface of the metal blank was clearly displayed on the video monitor. The video resolution was set at maximum (752 x 480) at this point. With the video resolution menu displayed on the computer screen, the parameters controlling the numbers of pixels and pixel lines were iteratively decreased until the camera's field of view shown on the video monitor exhibited only the test surface, the rest of the field of view being deleted. The resulting resolution was 600 pixels per line and 340 lines of video or 600 x 340 (assuming "Interlace: Use Distinct (2) Fields?" is active) which allowed 21 image buffers to be available for image capture. Since McDonnell-Douglas [Ref. 6:p. 8]

had shown that averaging data from as few as eight images significantly reduced the noise on the signal, it was concluded the 21 images would be sufficient.

The period required for a sequence to be completed was based on the time interval specified between consecutive samples, the shortest interval being 1/30 of a second. Since a video frame was generated every 1/30th of a second by the camera, the total time to execute a sequence containing 21 image buffers was 1.37 seconds.

The experiment began with the Mach 1.4 blocks installed in the tunnel. Using the shadowgraph technique, the normal shock was positioned in the test section by adjusting the backpressure through the gate valves, while the plenum pressure was set at 30 psi. When the valves were properly adjusted the tunnel was shut down, the metal window blank with pressure sensitive paint applied was installed, and the camera and illumination system were located eight inches away from the optical glass window. A real-time image of the test section was displayed on the image monitor, and the parameters to execute the desired sequence described above, were input into the computer. A cover was placed over the test section to prevent photodegradation of the paint, the light source was turned on and allowed to "ramp up" and stabilize. The wind tunnel was then started, the plenum pressure set at 30 psi, and the laboratory lights were turned off. The wind-on data were captured while pressure data were taken simultaneously using the CALSYS2000 data acquisition system. Twenty samples per port were taken at a sampling rate of 10,000 Hz. Three such runs were conducted. Between each run, wind-off and dark-current images were collected. Temperatures for the tunnel and the test plate were not available.

The Mach 1.7 nozzle blocks were then installed with the mass bleed-off system described earlier. With the plenum pressure set at 70 psi the shadowgraph was again used to position the normal shock. With the test plate installed, three runs were conducted in a similar manner to that described for the M=1.4 blocks. The data were post-processed using the techniques described in chapter three.

D. DISCUSSION AND RESULTS

The flow structure expected to be produced by the interaction between a normal shock and a turbulent boundary layer is shown schematically in Figure 53. The pressure-sensitive paint technique was to be used to measure the surface pressure through the interaction region. Previous work by Perretta [Ref. 24] involved a study of the flow across the shock structure shown in Figure 53, and the resulting separation, for the given M=1.4 tunnel configuration used in the present study.

For the M=1.4 case, the pressure map obtained is shown in Figure 54. It can be seen that the interaction was nearly two-dimensional. To illustrate the distribution of the pressure rise, a line of pixel intensity values taken along the plate is shown in Figure 55. The profile resembles those of Kooi [Ref. 25:p. 30-8] for turbulent boundary layer separation on a flat plate due to normal shock interaction. The steepest slope of the curve indicates the start of the interaction, according to Kooi's work. The separation point can be identified as that point in the curvature where either a discontinuity in the curvature

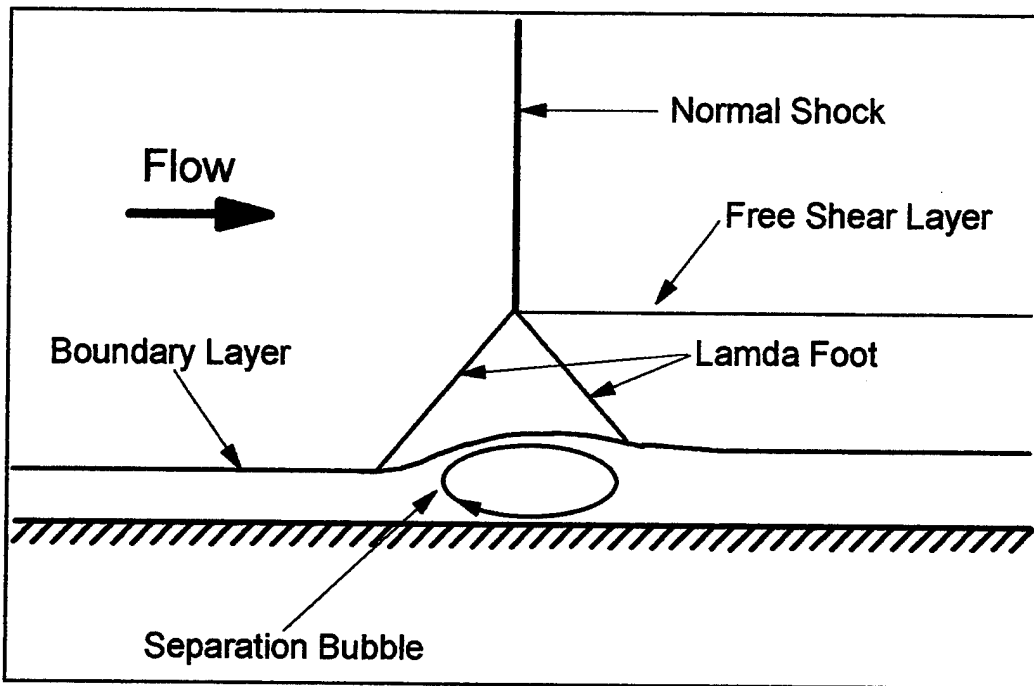


Figure 53. Schematic of the normal shock-boundary layer interaction

exists or the degree of change in curvature is much less compared to that of the start of the interaction, indicating a much slower rise in pressure. From the distribution of the intensity values, this point is difficult to determine. This can be attributed to oscillations of the normal shock, and the pressure-sensitive paint's poor dynamic response to these changes, causing an averaging effect and eliminating changes in curvature from the curve. Also, the time to execute the data collection sequence was much longer than the oscillation period of the shock, adding to the error in the results. The absence of a plateau in the intensity distribution suggests that the separation region was very short.

In the case of $M=1.7$, the determination of separation is more definite. The pressure map is shown in Figure 56 while the corresponding streamwise line of pixel-intensity

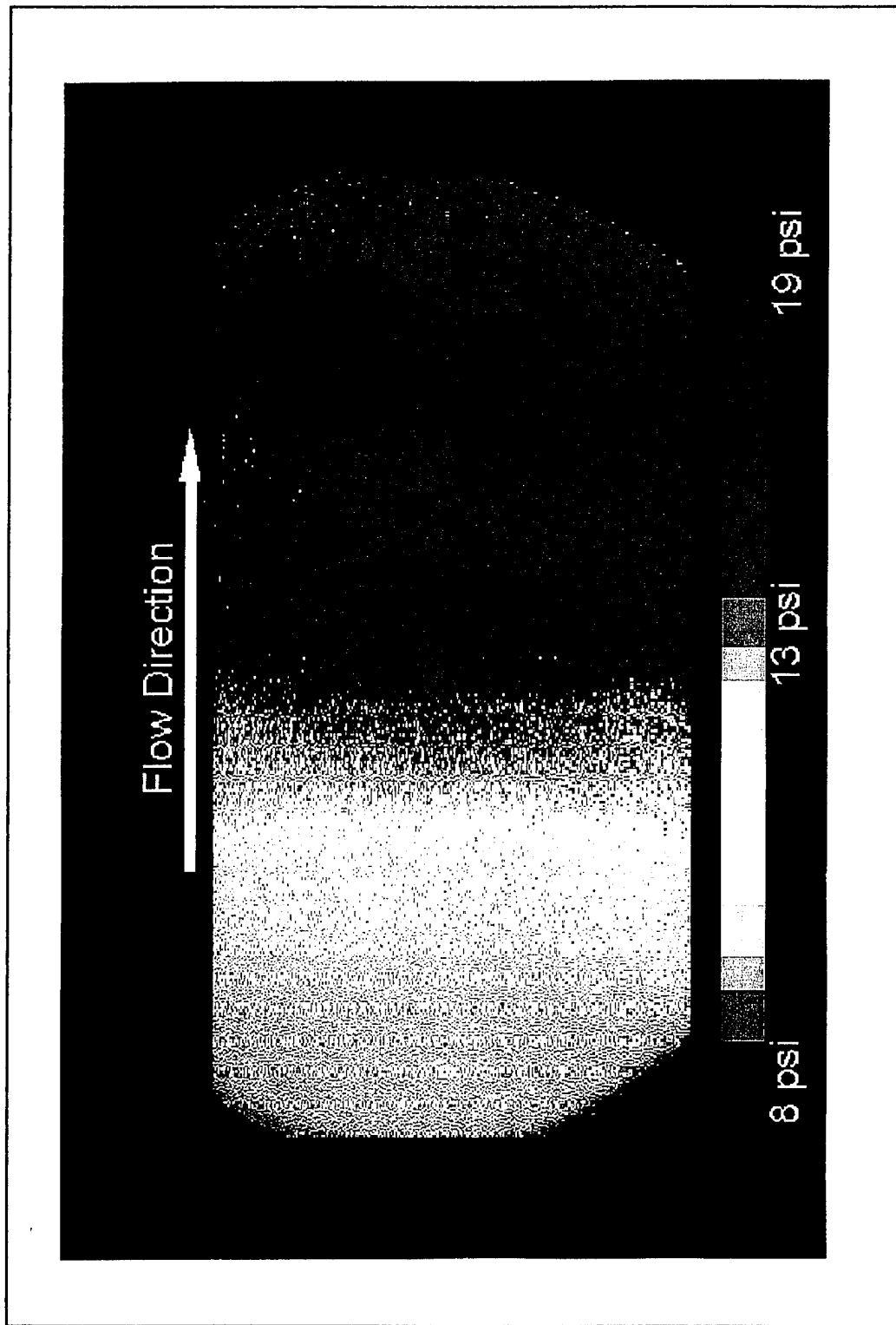


Figure 54. Mach 1.4 Pressure Map of the Shock-Boundary Layer Interaction

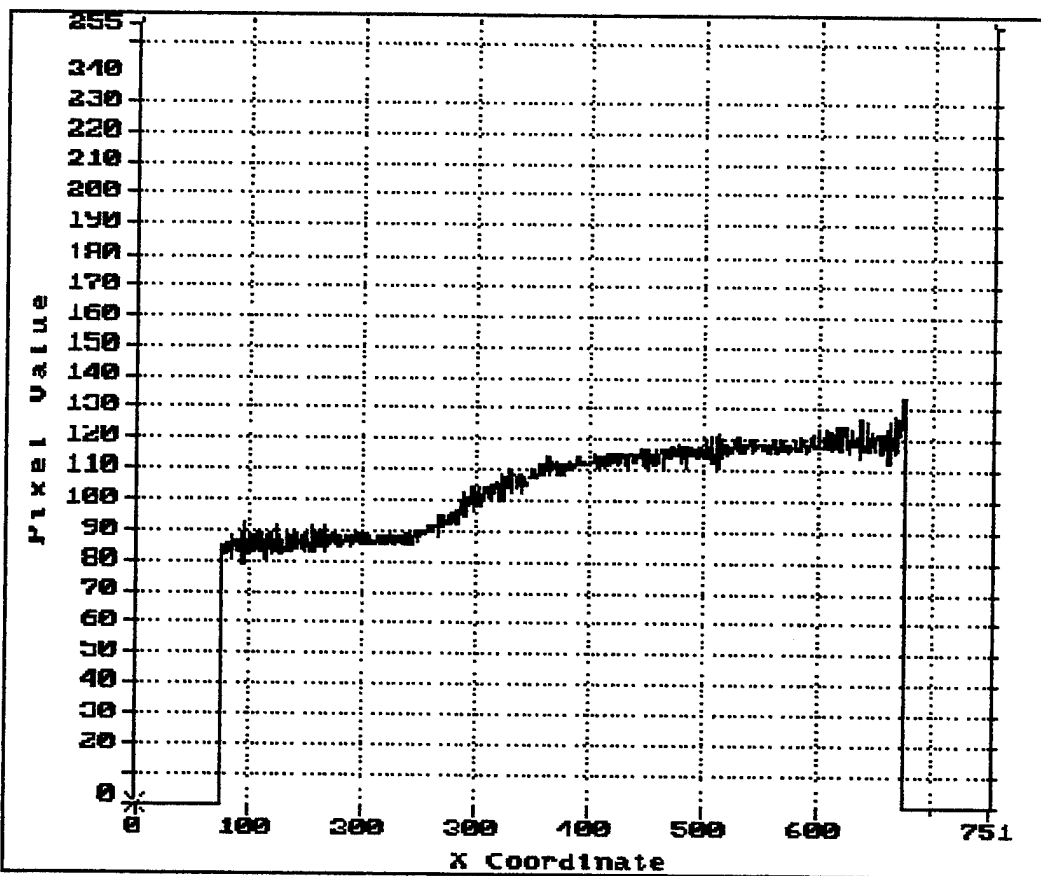


Figure 55. Graphical Representation of the Pressure Distribution of the Shock-Boundary Layer Interaction at Mach 1.4

values is displayed in Figure 57. The intensity curve here shows a definite plateau, a region of nearly constant pressure, which is an indication of an extended length of separation. This region corresponds to the area illustrated by the narrow green band in the pressure map of Figure 56.

The calibration curves for the $M=1.4$ and $M=1.7$ data are given in Figures 58 and 59 respectively. In contrast to the calibration curves developed for the underexpanded jet/flat plate data, areas of similar temperature are more easily identified in the shock-boundary layer experiment. The data points upstream and downstream of the normal shock have been linearly approximated separately since there was a near

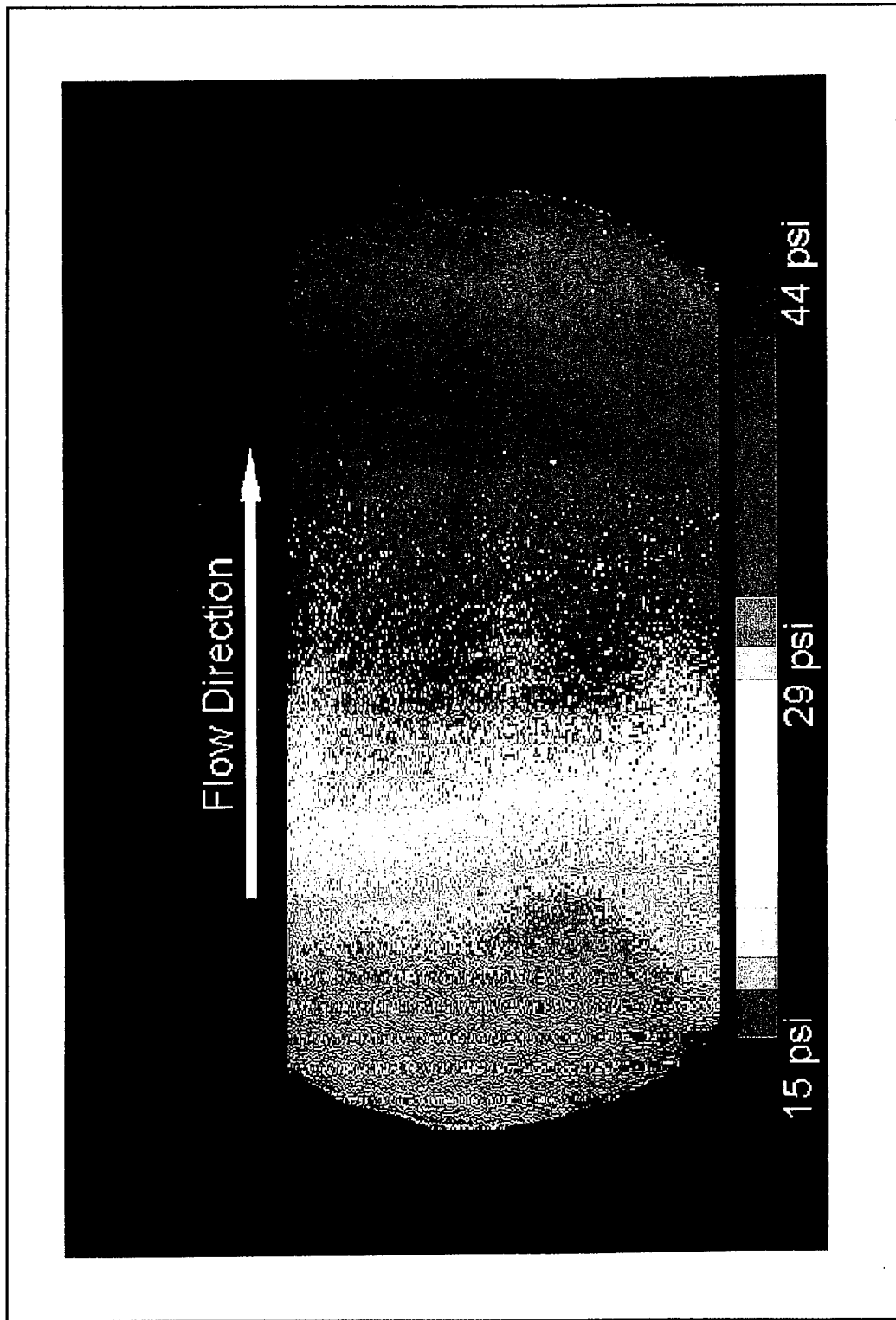


Figure 56. Mach 1.7 Pressure Map of the Shock-Boundary Layer Interaction

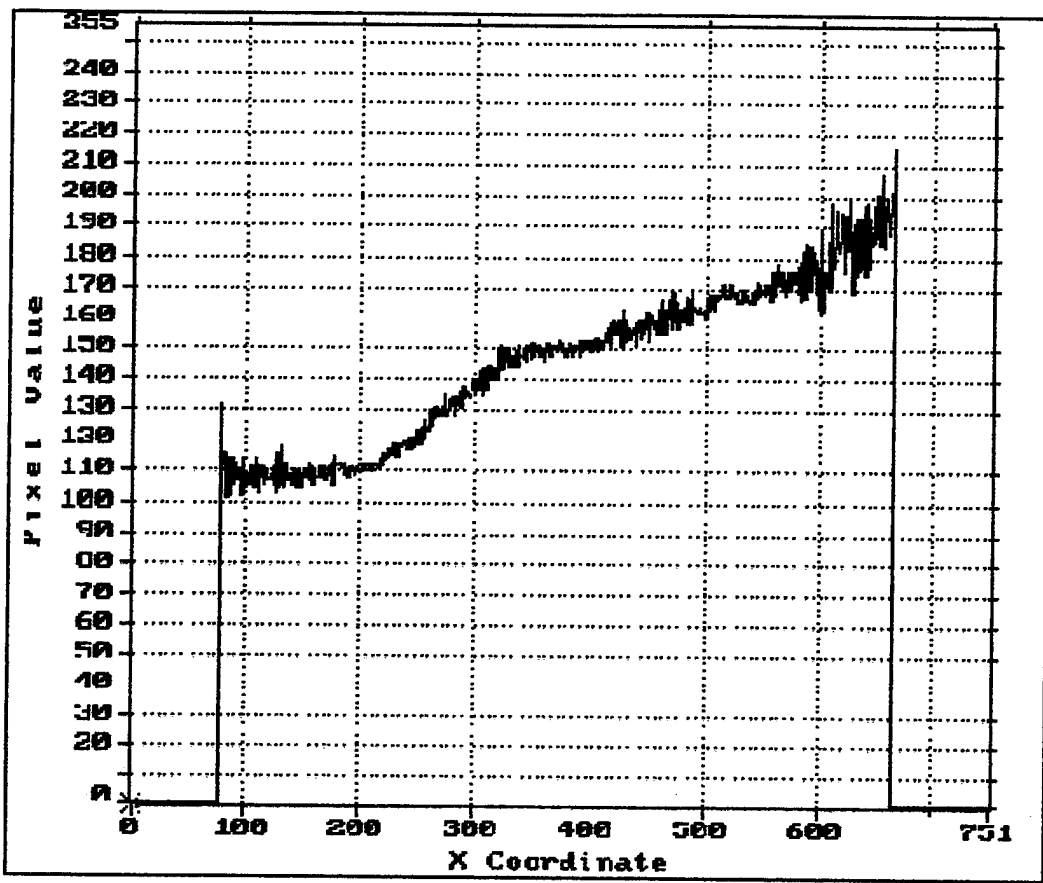


Figure 57. Graphical Representation of the Pressure Distribution of the Shock-Boundary Layer Interaction at Mach 1.7

discontinuity in temperature and heat transfer at the shock impingement location. There is seen to be a change in the sensitivity of the paint to pressure change which occurs at the shock. The paint is more sensitive downstream of the shock, which is consistent with the occurrence of higher temperature.

**Calibration Curve For The Shock-Boundary
Layer Interaction In The Supersonic Windtunnel
(Mach 1.4 -- 30 psig Plenum Pressure)**

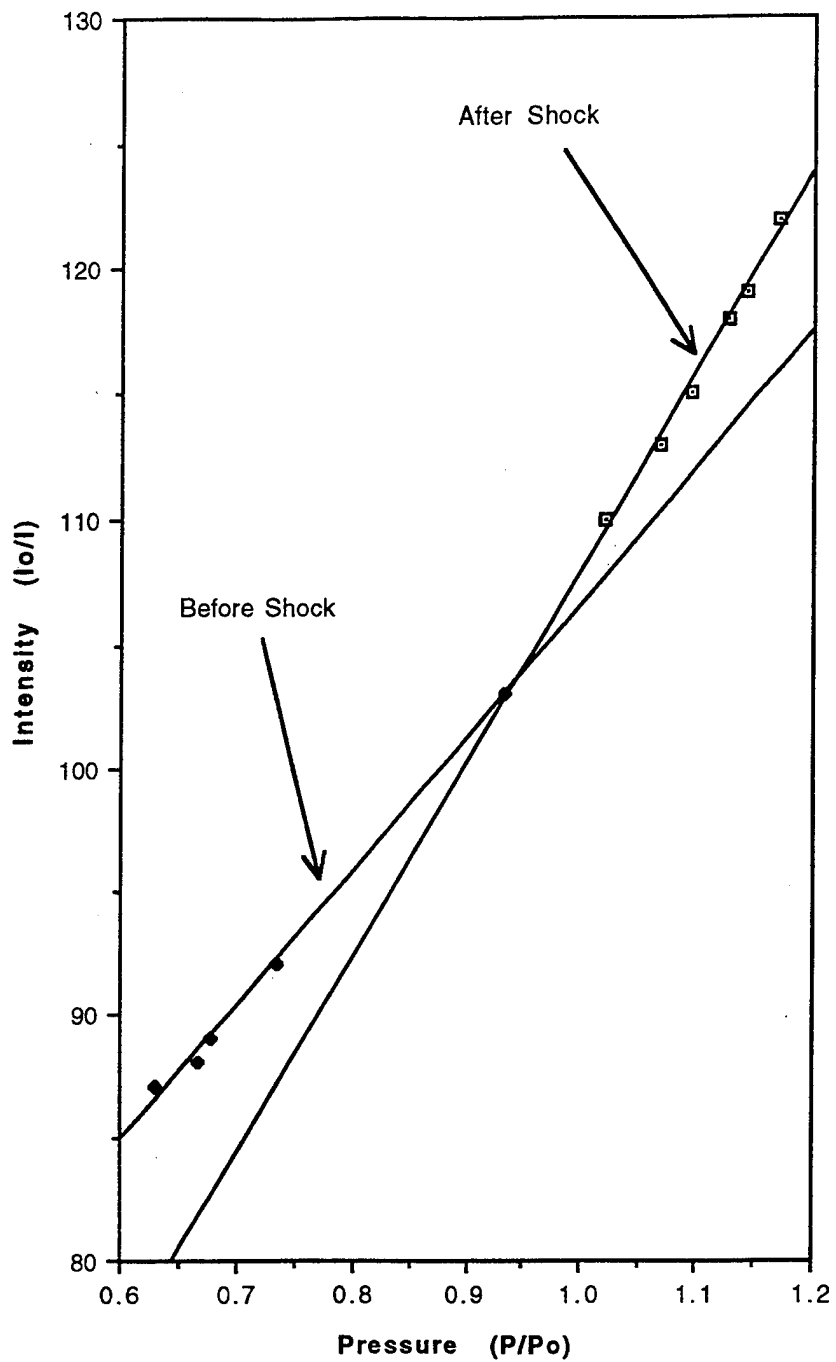


Figure 58. Calibration Curve for the Mach 1.4 Interaction

**Calibration Curve For The Shock-Boundary
Layer Interaction In The Supersonic Windtunnel
(Mach 1.7 -- 75 psig Plenum Pressure)**

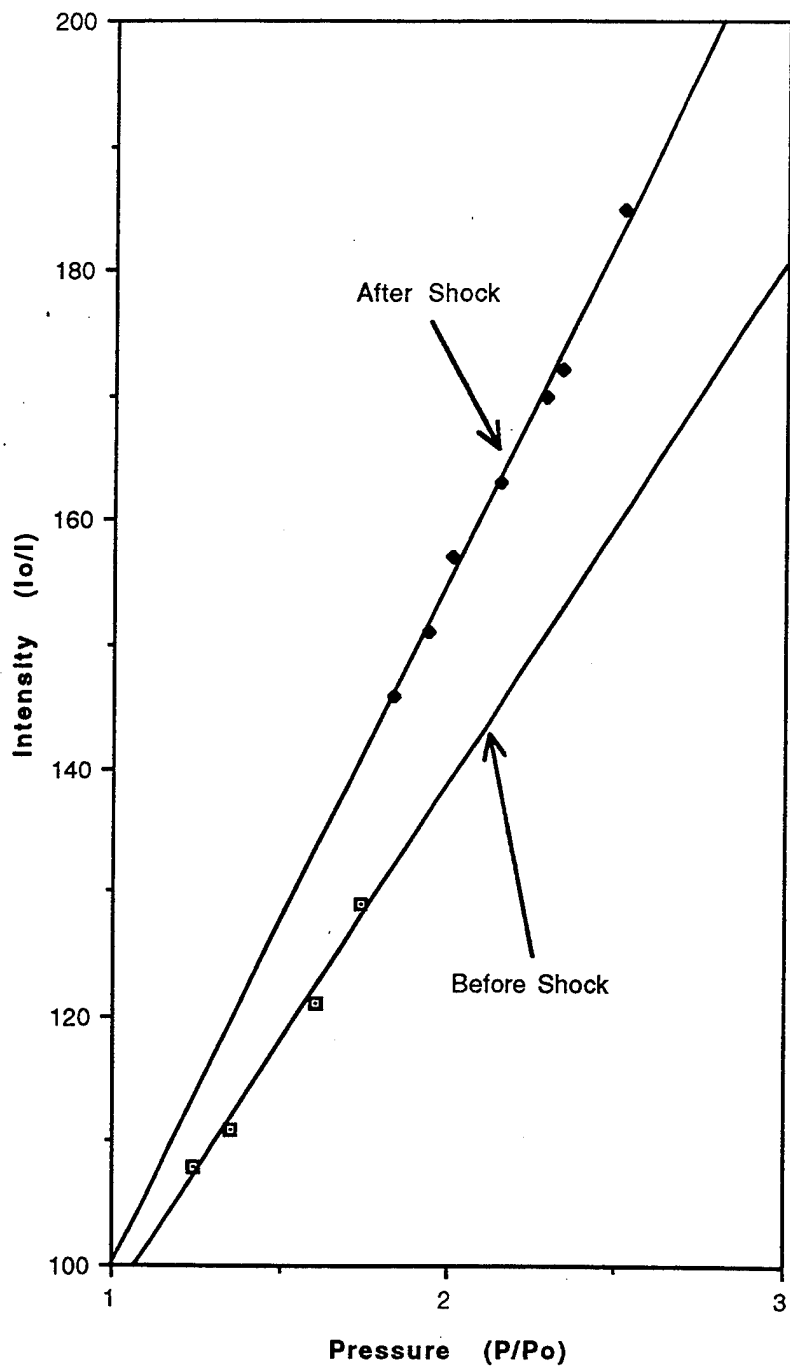


Figure 59. Calibration Curve for the Mach 1.7 Interaction

V. CONCLUSIONS AND RECOMMENDATIONS

The pressure-sensitive paint (PSP) technique offers a flexible and convenient method for measuring surface static pressures in aerodynamic testing. Its most significant feature is the non-intrusive manner in which it provides a mapping of a continuous pressure field over a surface. Because of its detailed spatial resolution (when compared to conventional pressure taps), a complete picture of the events occurring on the surface is available, including details not necessarily anticipated prior to testing. It appears to be highly suitable as a technique to use to validate results calculated using computational fluid dynamics (CFD). In the present study, pressure-sensitive paint was applied successfully in two experimental configurations involving shock-boundary layer interaction. The conclusions drawn from the present application are relevant to any first-time application of the technique.

The luminescent technique, although conceptionally simple, required learning. It was important to understand the entire process, including each of the components comprising the pressure measurement system (paint, optics, camera, software), the limitations of the system (particularly of the luminescent paint), and the interpretation of the measurements through calibration, before meaningful data were acquired. Several attempts to progress through the entire process were found to be necessary. Thus, the initial experimental arrangement (a flat plate immersed in an underexpanded jet) served well as a test bed for building experience before more complicated experimental geometries were attempted.

The components that comprised the current measurement system were adequate for initial experience, system development, and measurements. However, in order to make highly quantitative measurements routinely, some refinements are recommended. The camera and the digitizer combination are, by far, the most critical components in the PSP measurement system. The accuracy and precision of the measurements is highly dependent upon the dynamic range and signal-to-noise ratio of these components. The camera and digitizer used had a grey-scale resolution of eight bits giving a dynamic range of 256:1. Since many measurements, such as in shock-boundary layer interaction experiments, may generate changes in the luminescent intensity as little as two percent, it is crucial that the camera and digitizer be sensitive enough to these changes and to assign a gray-scale value that is appropriate for the given intensity level. Recommendations from NASA Ames Research Center and McDonnell Douglas have suggested a minimum of 14 bits for gray level resolution.

With a relatively low signal being detected, the signal-to-noise ratio at high light levels is limited by the photon shot noise. The accuracy of measurement is contingent upon the highest possible full-well potential of the CCD element, which requires a minimum generation of dark current. Active cooling of the CCD array would maximize the signal-to-noise ratio of the array. Such developments in CCD cameras can be expected [For example, Princeton Instruments Inc. currently offers a Penta Max camera that uses air circulation to cool its CCD array, which achieves -45 degrees Celsius]. Similarly,

system noise can be reduced by combining the digitizer with the camera, thereby reducing electrical noise, and then feeding the signal directly into a memory buffer in the computer.

The EPIX 4Meg Model 12 frame grabber and memory buffer and its associated software was limited in data collection. Since the board was limited to capturing only 11 images per sequence (assuming maximum resolution), the acquisition of one hundred images was far to slow to avoid inaccuracy of the results due to photodegradation of the paint. The EPIX 48Meg Model 12 frame grabber, for example, would provide the ability to capture up to 132 images per sequence. Not only would this reduce or eliminate the error associated with photodegradation, but image processing time would be significantly reduced. Data acquisition speed is mandatory in experiments in which the flow is not completely steady.

A similar issue concerns the present image-processing software. Designed for general applications, it is not the most efficient, or the most suitable, for the PSP applications. Although single-function algorithms such as registration software to spatially align two images together, to compensate for temperature sensitivity and apply the calibration to the data, and routines to pseudo-color the results must be written, consideration should be given to automating the entire process, from acquisition of the data to production of the calibrated pressure field map.

The temperature sensitivity of the paint and its effect on the results is a major concern if pressure measurements are to be made in the compressible flow regime. To accurately measure the pressures on a surface, it will be necessary to know the surface distribution of

temperature so that the calibration curves can be adjusted accordingly. Although temperature measurements could be made using thermocouples, this approach raises the same issues as those associated with using pressure taps to make pressure measurements. A possible solution is to use, concurrently, a high-performance infrared camera to record a high-resolution, continuous image of the temperature distribution on the surface. Since the results from infra-red cameras are produced using a digital process similar to that used in PSP, it is possible that the techniques could be combined to produce a temperature-compensated pressure map.

Finally, the applicability of the present technique to more complicated model configurations with more limited optical accessibility of the surface of interest, has yet to be attempted here. The combination of curved surfaces with significant temperature variations, and with limited optical access, will provide a significant challenge to the successful quantitative use of PSP.

APPENDIX A. RUSSELL-SANDERS COUPLING

Associated with the angular momentum of an electron is a magnetic moment. When the electron is placed in a magnetic field, the interaction of the field with the magnetic moment of the electron causes the angular-momentum vector to precess about the direction of the external field, much the same way a toy top precesses in a gravitational field. However, in contrast to the top, which can have an infinite number of momentum-vector orientations with respect to the field direction, the angular-momentum vectors of the electrons in an atom (or molecule) are allowed only certain orientations. The solutions of the Shrödinger equation dictate permitted orientations; not every orientation is allowed. The only allowed directions are those at which the components of the angular momentum along the direction defined by the magnetic field have certain quantized values. This behavior is called *space quantization*. [Ref. 10:p. 491]

Each orientation of the momentum vector with respect to the external field direction corresponds to a unique energy state. Since the angular motion of the electron is equivalent to an electromagnet, the energy of the interaction between the magnetic moment it possess and an external field can be expressed as $E = \mu H \cos \theta$, where H is the strength of the external field, θ is the angle between the field and momentum vector, and μ is the magnetic moment. [Ref. 26:p. 25]

Now consider what happens when a single unpaired electron is not in the presence of a magnetic field. Here, the orbital angular momentum of the electron creates the magnetic

field, defining a specific direction in space. Thus the angular momentum associated with the intrinsic spin of the electron is oriented with respect to this magnetic field. According to space quantization principles, the spin angular-momentum vector of the electron can have two orientations with respect to the direction defined by the magnetic field; this corresponds to the doublet line structure observed for the spectra of an atom, and is the basis for the spin quantum number (+1/2 and -1/2) assigned to the electron. [Ref. 26:p.27]

In an atom with several electrons, the orbits are usually oriented first with respect to each other, giving a resultant orbital magnetic moment. Similarly, there is a resultant spin moment which is oriented with respect to the resultant magnetic field due to the orbital motion. With space quantization, the resultant spin vector may have several orientations, each corresponding to a different energy level. Thus, the atom (or molecule) may have several energy levels for a single configuration. [Ref. 27:p. 79] These multiple energy levels for a single configuration of an atom (or molecule) is the basis for Russell-Sanders coupling which impacts the multiplicity of state that an atom or molecule can possess.

APPENDIX B. LUMINESCENCE COATING CHARACTERISTICS

The luminescent coating used in the present work possessed several undesirable characteristics of which the user must be aware if accurate results are to be obtained. A summary of these is presented below. For a more in-depth discussion, the reader may refer to the references mentioned.

A. TEMPERATURE SENSITIVITY

The photoluminescence process is temperature sensitive by nature. The coating used in the present work exhibited a non-linear response, and intensity decreased with increasing temperature. This response at a constant pressure is shown graphically in Figure B1. [Ref. 1:p36] The temperature dependence has a significant effect on the calibration curves of intensity vs. pressure. As is shown in Figure B2a, the variations in slope can be significant [Ref. 1:p. 62].

An interesting property displayed by the calibration curve for the coating is the condition where the coating-sensitivity coefficients add to unity (i.e. $A + B = 1$, in the Stern-Volmer equation). This occurs when the data taken for I and I_0 are taken at the same temperature. If this is not the case, the coefficients add to other than one, $A + B \neq 1$. The consequences are illustrated in Figure B2. In Figure B2(a) only the $23.7^\circ C$ curve exhibits the property that $A + B = 1$ while the 50 and $6^\circ C$ calibration curves were calculated with I and I_0 at different temperatures. In Figure B2(b), the 50 and $6^\circ C$

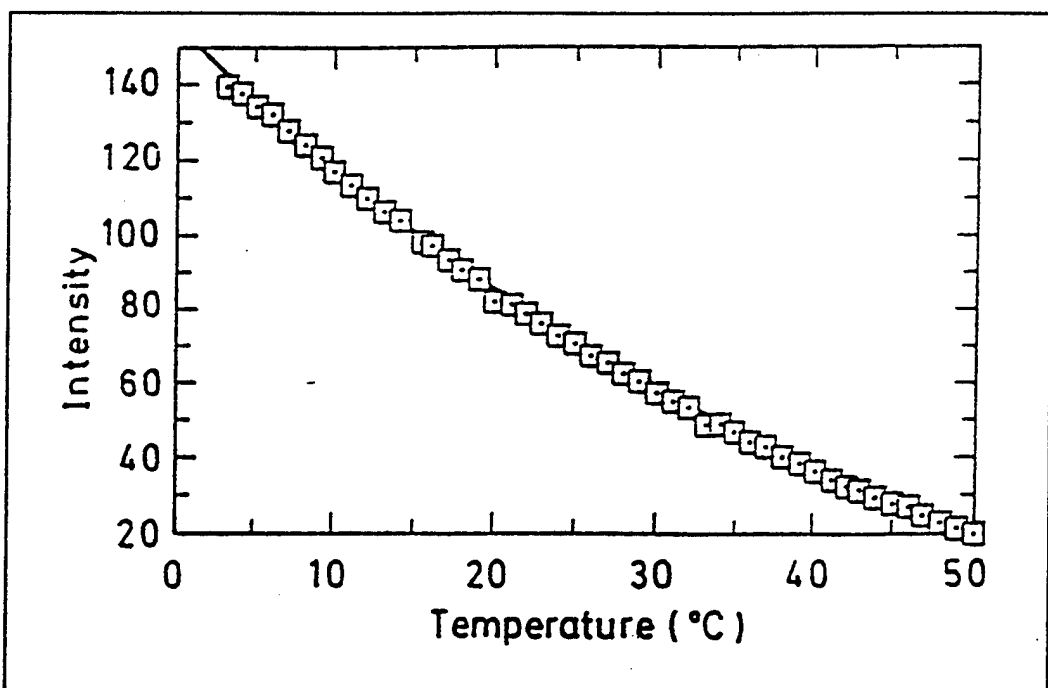


Figure B1. Luminescence Intensity as a Function of Temperature [From Ref. 1:p. 36]

calibration curves have been replotted using data for both I and I_0 obtained at similar temperatures. Clearly, the slope and zero intercept have been significantly altered. [Ref. 1:p.37]

B. PHOTODEGRADATION

When subjected to ultraviolet light, the luminescent coating undergoes photodegradation, resulting in a decrease of its response with time of exposure. A representative example of this is shown in Figure B3 where intensity is plotted as a function of time of exposure. In this case the coating lost 46% of its response after one hour of exposure. [Ref. 1:p. 36]

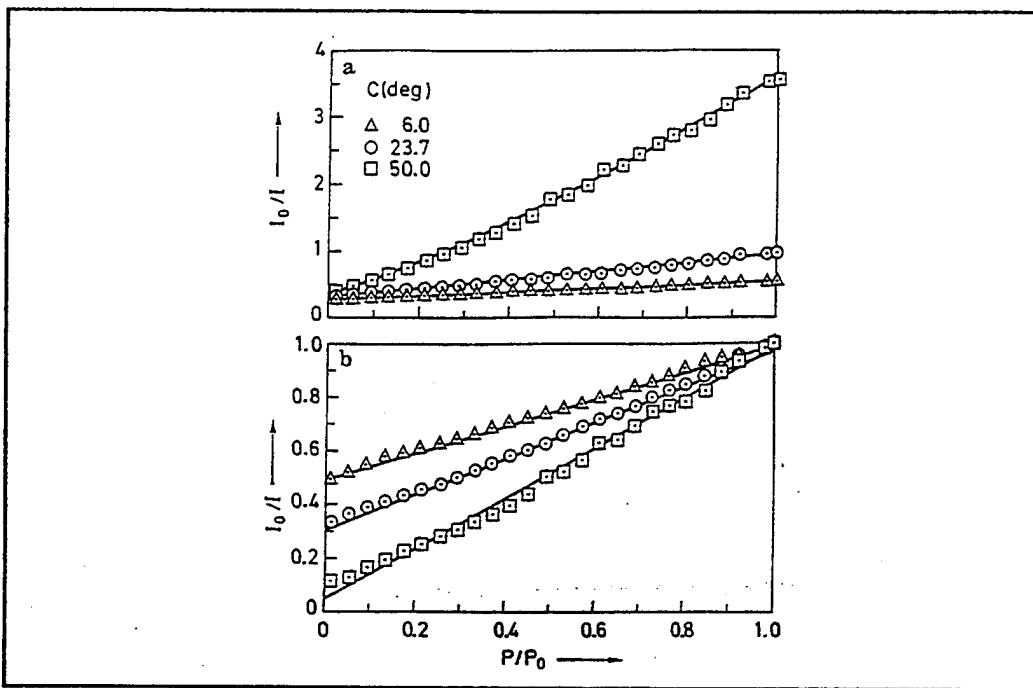


Figure B2. Effect of Temperature on Coating Calibration Curves [From Ref. 1p: 37]
(a). I_0/I for Curve Measured at 23.7°C
(b). I_0/I for Curve Taken at its Respective Temperature

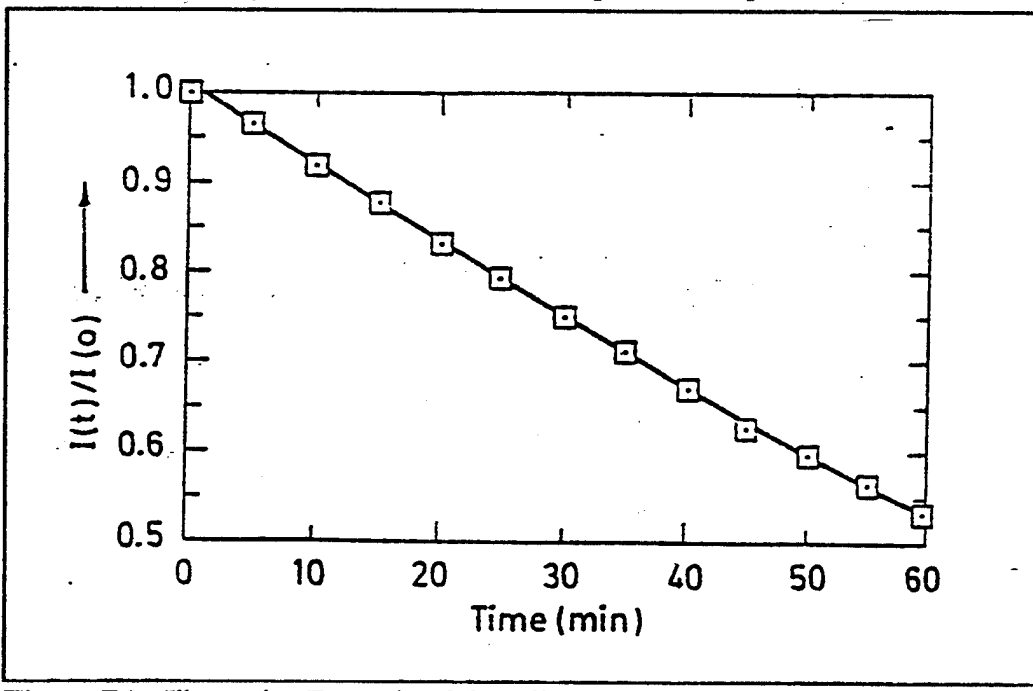


Figure B3. Illustrative Example of the Effect of Photodegradation on Response Time [From Ref. 1p:36]

C. TIME RESPONSE

The luminescent coating used in the present work has been found to exhibit a time response on the order of 1 second limiting measurements of pressure fluctuations to no greater than 1 Hz. [Ref. 8:p. 3]

This limitation is not a characteristic of the active molecule. In theory, the time response of the coating to pressure transients may be as fast as the decay of luminescence. For platinum octaethylporphyrin this is approximately 0.1 milliseconds. The problem lies with the polymer matrix in which the active molecule is embedded. By limiting the rate of oxygen diffusion, the polymer slows the optical response to surface pressure fluctuations. [Ref. 1:p. 41]

D. COATING THICKNESS / INDUCTION PERIOD

Kavandi [Ref. 9:p.86] has conducted tests to determine if film thickness has any effect on calibration results. Over the range of 5.5 micrometers to 17 micrometers, consistent with normal application, no significant variations were noted. However, a noticeable lag, or "induction period", existed between the time excitation light was turned on and the time that the detected luminescence reached maximum intensity. The period of maximum intensity was observed to be in the range of 30 to 45 seconds and it is therefore advisable to allow this period to elapse before taking data. A graph of absolute intensity as a function of time following exposure to the exciting light is shown in Figure B4. [Ref. 9:p.89]

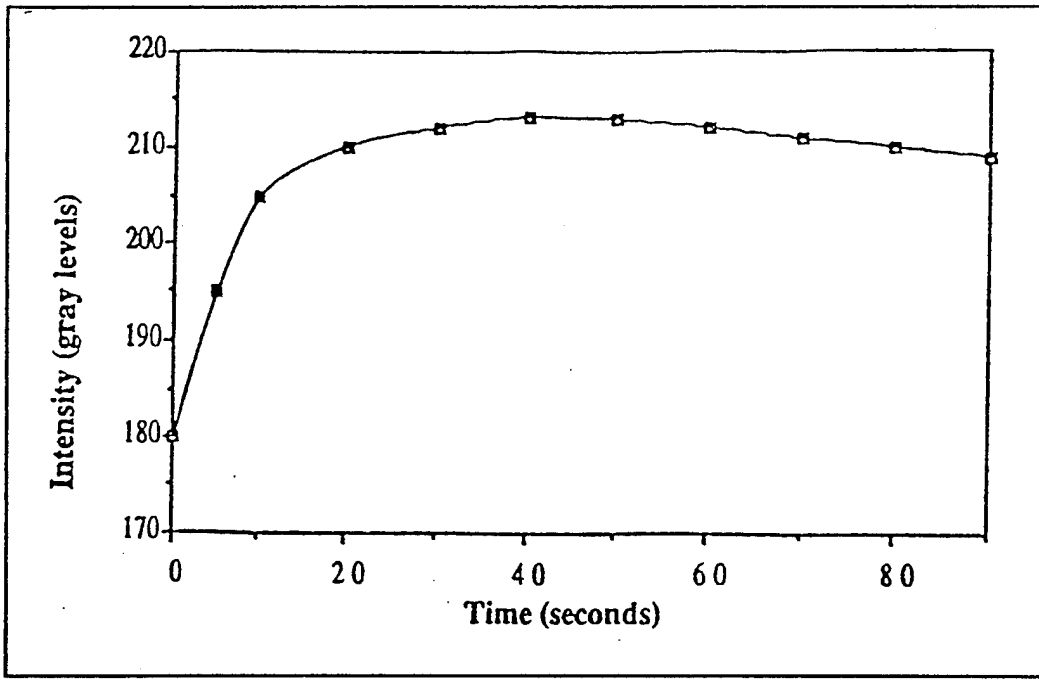


Figure B4. Induction Period of the Luminescent Coating with Thicknesses in Excess of 17 Micrometers [From Ref. 9:p. 89]

APPENDIX C. EPIX SOFTWARE SUMMARY

This appendix outlines the software steps used in acquiring, processing and reducing image data. All information discussed here may be found in [Ref. 23]. The appendix is intended to serve as a user guide but is not meant to be a substitute for the EPIX user's manual. The user's manual is vital to developing a sound understanding of the software in order to be able to use it to its fullest extent. The data acquisition and image processing system is set up such that the menus and commands are displayed on the computer monitor while the images are displayed on the Sony image monitor.

A. IMAGE DATA ACQUISITION

The main menu for the EPIX 4MIP-4MIPTOOL software is shown in Figure C1. Prior to data collection, the video resolution is set. Selecting "Video Resolution" from the main menu, the video resolution sub-menu will be displayed as in Figure C2. Check to insure that the "Interlace: Use Distinct (2) Fields ?" is set to "ON". The sampling resolution is considered next and it is application dependent. The sampling resolution sets the size of the video window displayed on the image monitor, allowing the selection of a smaller field of view. The maximum resolution is 752 pixels per line by 480 lines per frame or image (Two fields make up one frame; however the number of lines selected is based on each field, the maximum number being 240. For both fields to be active, the interlace function must be on). Upon setting the desired sampling resolution, the

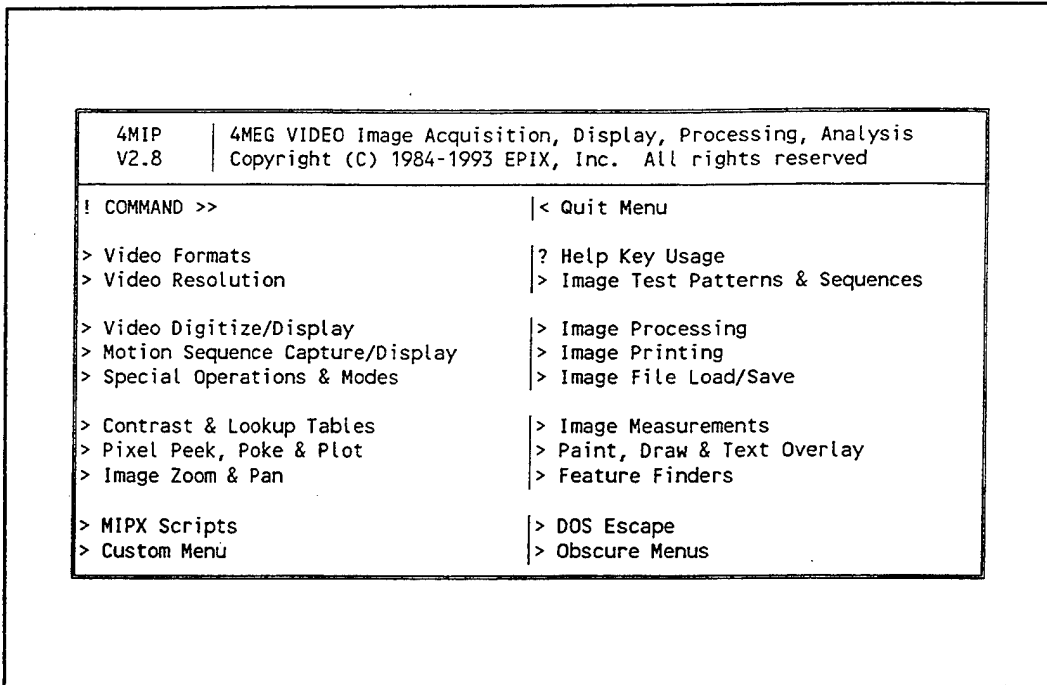


Figure C1. "Main Menu" for EPIX Interactive Image Analysis Software

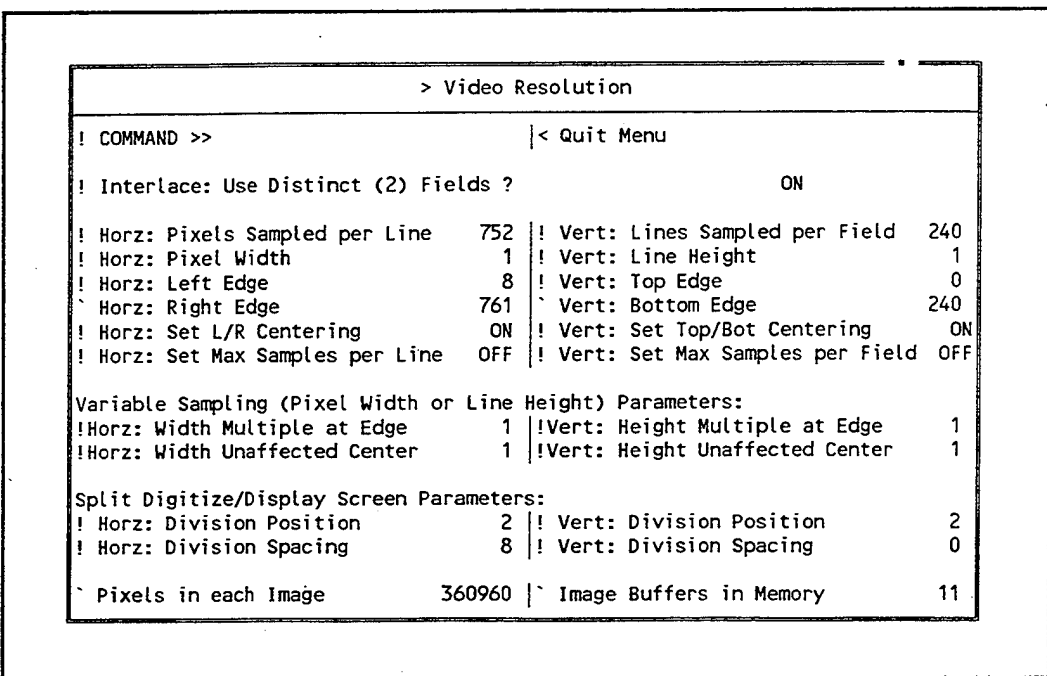


Figure C2. "Video Resolution" Sub-Menu

number of frame buffers available for capturing images is displayed in the lower right corner of the menu. For 752 x 480 resolution, 11 frame buffers are available. After setting the resolution, return to the main menu by selecting "Quit Menu".

From the main menu, select the "Video Digitize/Display"; this menu is shown in Figure C3. Select the function "Digitize", the result of which is a real-time video display of the camera's field of view. Adjustments to the camera can be performed, such as focus, gain, iris setting, etc., to achieve the desired image. When complete, return to the main menu; the real-time image will remain displayed on the monitor.

Next select the "Motion Sequence Capture/Display" sub-menu; this menu is illustrated in Figure C4. The first step here is to choose the length of the sequence, and which buffers are to be used, by selecting the sequence starting and ending buffers. For example,

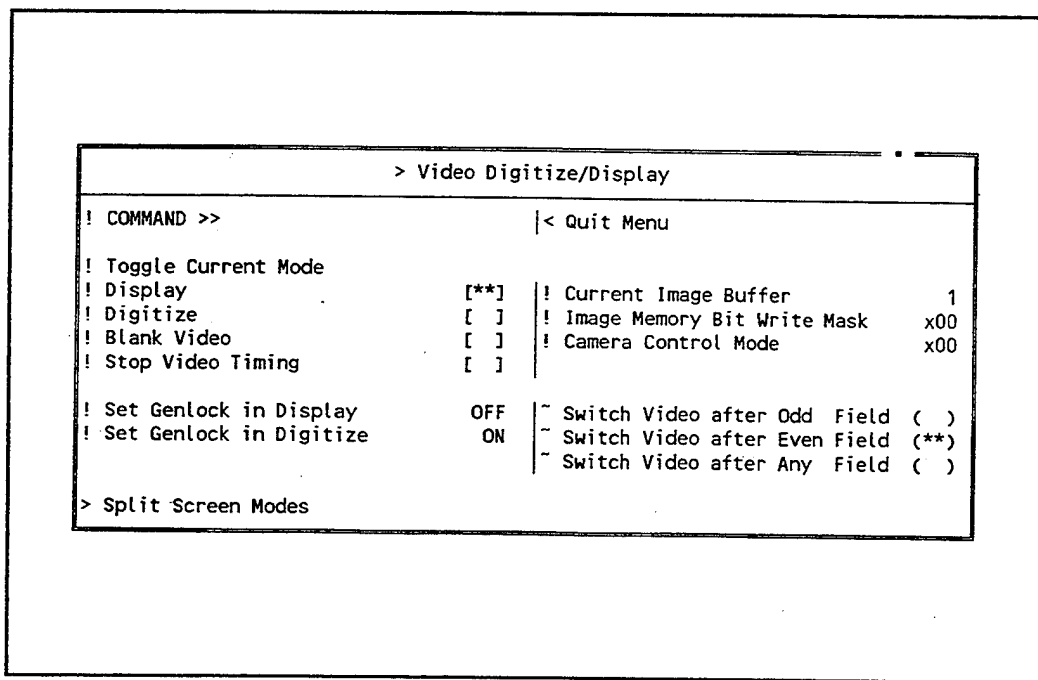


Figure C3. "Video Digitize/Display" Menu

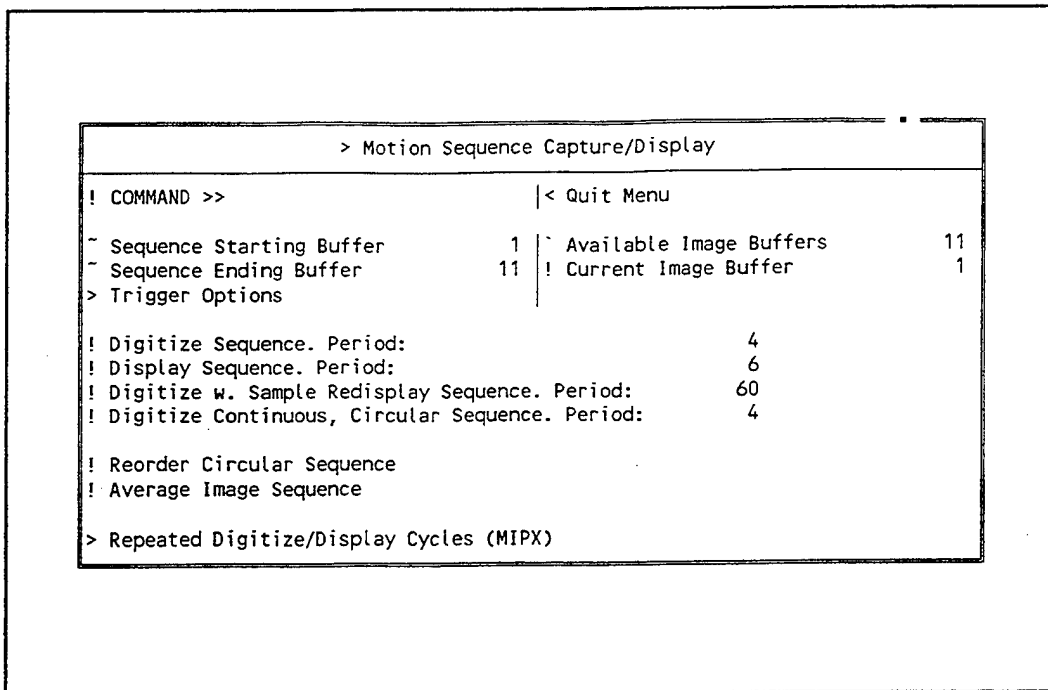


Figure C4. "Motion Sequence Capture/Display" Sub-Menu.

in the flat plate/jet interaction work only 10 of the 11 buffers were used; thus the starting buffer was set to 1 and the ending buffer to 10.

The time interval between consecutive samples is then set with the "Digitize Sequence. Period:" function. The period is based on units of video fields if the video is not interlaced (1/60 sec) or video frames if the video is interlaced (1/30 sec). The COHU camera was set internally to send an interlaced image to the frame-grabber board. Since the incoming signal to the board is interlaced, the software can be programmed using the interlace function to store either an image with both fields of the image (interlaced) or an image with a single field (non-interlaced). With the "Interlace: Use Distinct (2) Fields ?" set to active, the period will be based on units of frames. For the jet/plate interaction experiment collection, the period was set to the default value of 4 frame periods between each

captured image or $4/30 = 2/15$ of a second between each captured image. For the supersonic wind tunnel experiment the period was set to 1 or $1/30$ of a second between each captured image.

One note concerning this function; to enter the desired period, the mouse or arrow keys are first used to position the cursor on the function. The period is entered using the numeric keys, the program responding to the entry by "highlighting" it red. The entry is then entered into memory by either strobing the left mouse button or striking the "enter" key. This action, however, also starts the execution of the algorithm for sequence image capture. When complete, all designated buffers will contain a captured image. If the image buffer used to display the real-time image lies between the starting and ending sequence buffers, it too will contain a captured image. Therefore, until the desired event is being displayed on the monitor in the real-time format, the entry for the period should not be strobed or the above sequence of events will have to be repeated to redisplay the real time image. It is, of course, not necessary to display a real-time image to capture a sequence of images. By simply re-strobing the "Digitize Sequence. Period:" a new set of images is stored in the designated buffers. Displaying a real-time image of the desired event on the monitor is simply a matter of choice.

B. IMAGE PROCESSING

1. Averaging

The procedure outlined in Chapter III for data collection of the wind-on, wind-off, and dark-current conditions involved executing the above-described steps ten times, i.e., ten images per sequence, executing the motion-sequence algorithm ten times, for a total of one hundred images. After each sequence run, the images in the designated buffers were averaged together to form a single image. This was done by strobing the function "Average Image Sequence" in the "Motion Sequence Capture/Display" sub-menu. The averaged image is stored in the buffer designated as the starting sequence buffer.

The hard drive of the 80386 PC used in the present work contained software applications used in other research, which presented inadequate memory space for image-data storage. Therefore, all data was transferred from the frame-grabber board to floppy disk. The command to store data to disk is found in the main menu and is designated as "Image File Load/Save". From the resulting sub-menu, select the option "File Load/Save, Tiff Format w. AOI". The sub-menu for this option is brought up onto the computer screen. Position the cursor on the option, "Save Image to File. Name", and type "b: filename.tif". Striking the "enter" key will bring up the menu "Select IMAGE BUFFER and/or AREA OF INTEREST" to appear; select the option "Image Area Of Interest: Full Image". The image will then be sent to the floppy. "Full Image" refers to the image size that is set in the "Video Resolution" sub-menu; thus if the image resolution is set to 752 x 480, this will be the image size that is stored on the disk.

Once ten averaged images have been saved to disk, they can be loaded back into ten frame buffers on the frame-grabber board using "Image File Load/Save" function. Again, select "File Load/Save, Tiff Format w. AOI" and then position the cursor on "Load Image from File . Name:". Type "b:filename.tif" and strike "enter". In the "Select IMAGE BUFFER and/or AREA OF INTEREST" sub-menu, select "Image Area Of Interest: Full Image" and strike "enter". The image will be loaded into the current image buffer. The current image buffer is selected by simply toggling the Pg Up/Pg Dn keys.

With all ten averaged images loaded into the frame grabber, return to the main menu and select the "Motion Sequence Capture/Display" function. Insure the "Sequence Starting and Ending Buffers" reflect the sequence of buffers that the averaged images are stored in (See Figure C4). This complete, the images are averaged together using the "Average Image Sequence" option, the resultant image being stored in the buffer designated the sequence-starting buffer. This image represents either the wind-on and wind-off images that will eventually be ratioed or the averaged dark-current image that must first be subtracted from these two images. The three resultant images are again stored on floppy disk.

2. Subtraction

The averaged wind-on, wind-off, and dark-current images are loaded back into consecutive buffers of the frame-grabber board using the steps for loading files that were discussed above. From the main menu select "Image Processing", from which the image-processing sub-menu is displayed on the screen as in Figure C5. Choose the "Two Image

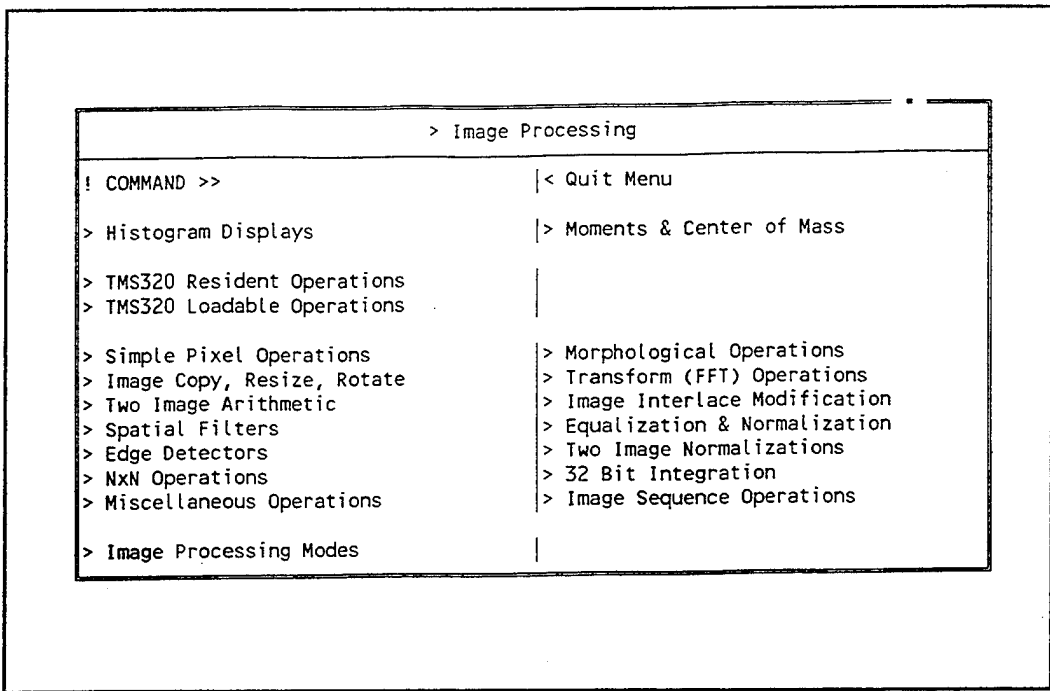


Figure C5. "Image Processing" Sub-Menu

"Arithmetic" option, which sub-sequently displays the options available for conducting operations involving two images, this menu being illustrated in Figure C6. Four subtraction options may be selected; the option "Abs(PixB - PixA)" was used in the present work, where the absolute value of an intensity value is taken if it is less than zero. When this function is selected, the "Select IMAGE BUFFER and/or AREA OF INTEREST" for PixA menu is displayed. Before selecting anything from this sub-menu, ensure that the current-image buffer that is being displayed on the image monitor is that containing the dark current image; this represents PixA. From the "Select IMAGE BUFFER and/or AREA OF INTEREST" menu, choose the option "Full Area of Interest: Full Image". When this step has been completed, the "Select IMAGE BUFFER and/or AREA OF INTEREST" for PixB is displayed. Here, ensure the current image buffer

```

> Two Image Arithmetic

! COMMAND >>                                |< Quit Menu

! Add Images:      PixB <- PixB + PixA MOD 256
! Add Images:      PixB <- Min(Pix + PixA, 255)
! Subtract Images: PixB <- 128+(PixB-PixA)/2
! Subtract Images: PixB <- PixB - PixA MOD 256
! Subtract Images: PixB <- Max(PixB - PixA, 0)
! Subtract Images: PixB <- Abs(PixB - PixA)
! AND Images:      PixB <- PixB & PixA
! Exclusive OR Images: PixB <- PixB o PixA
! Average Images:  PixB <- (PixA + PixB) / 2

! Product Images:  PixB <- (c0*PixA+c1) * (c2*PixB+c3) / c4
  ^Product Coefficient: c0      1   | ^Product Coefficient: c3      0
  ^Product Coefficient: c1      0   | ^Product Coefficient: c4     64
  ^Product Coefficient: c2      1

! Ratio Images:    PixB <- (c0 * PixB + c1) / (c2 * PixA + c3)
  ^Ratio Coefficient: c0      1   | ^Ratio Coefficient: c2      1
  ^Ratio Coefficient: c1      0   | ^Ratio Coefficient: c3      0

! Function on Images: PixB <- f(PixB, PixA). Expression:

! UnInsert Images: If (PixB ≈ PixA) PixB <- 0. Eps #:
! Insert Images: If (PixB == 0) then PixB <- PixA

```

Figure C6. "Two-Image Arithmetic" Sub-Menu

being displayed on the monitor is either the wind-on or wind-off image; this represents PixB. Again select "Full Area of Interest: Full Image" from the sub-menu. Execution will begin, the modified image residing in the frame buffer that originally contained PixB. Conduct this operation on both the wind-on and the wind-off images.

3. Registration

Registration of images will be unique to every application. As discussed in Chapter III, the registration procedure between the wind-on and wind-off images for the jet/flat plate interaction involved solid body motion, a relatively simple registration problem. Registration between images that involve more complex scenarios such as translational shifts, rotational shifts, and geometric distortions, will require more complicated software procedures than were used here.

If the extent of distortion between the images is simply solid body translation, then the following procedure can be used: Load the wind-on and wind-off images into consecutive buffers. From the main menu, select the "Pixel Peek, Poke & Plot" option; this sub-menu is shown in Figure C7. When this menu is displayed, the cursor will be overlaid on the image monitor, and can be controlled with the left button on the mouse is depressed. The cursor coordinates remain the same as the image buffer is changed, allowing examination of feature registration among image sequences. Thus using the wind-off image as the reference image, the vertical and horizontal characters of the cursor are aligned on a feature or control point that is distinctive in both images. By shifting back and forth between the buffers containing the images, using the Pg Up/Pg Dn keys and not disturbing the cursor location, an indication of the magnitude of distortion is obtained.

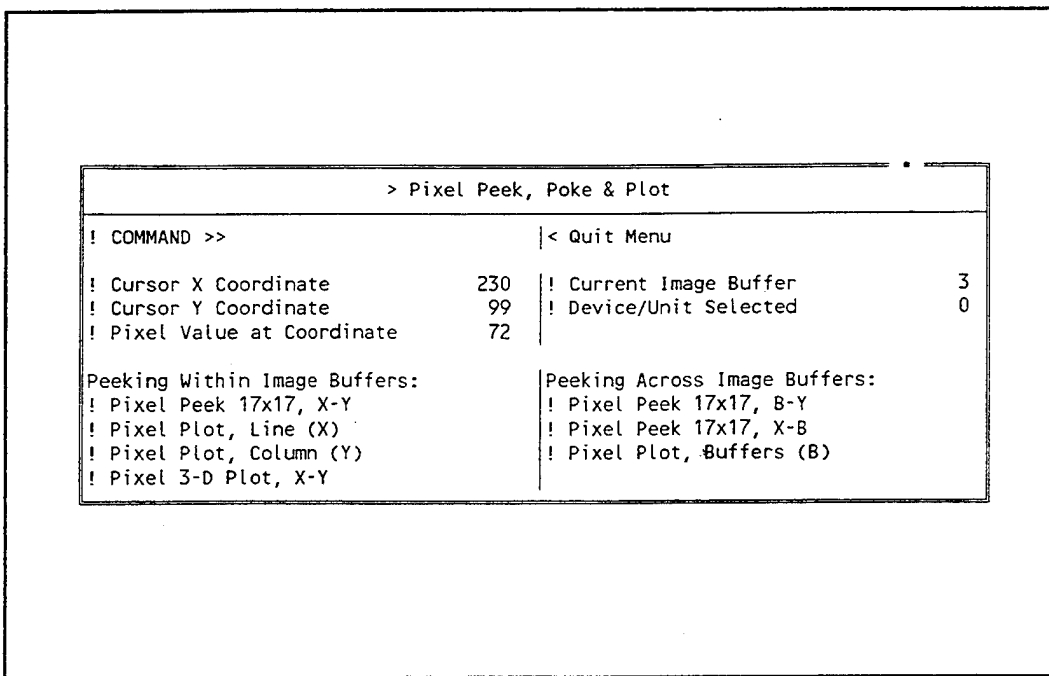


Figure C7. "Pixel Peek, Poke and Plot" Sub-Menu

Return to the main menu and select "Image Processing", followed by the option "Image Copy, Resize, Rotate"; this sub-menu is shown in Figure C8. The function "Copy & X,Y Shift" copies an image , shifting the image left or right and up or down in its buffer. The *Left(-X) Right(+X)* Shift parameter specifies the number of pixels the image is to be shifted left or right; the *Up(-Y) Down(+Y)* Shift parameter specifies the number of pixels the image is to be shifted up or down. When the parameters have been entered, strobe the "Copy & X,Y Shift" function using the left button of the mouse or the "enter" key. (Ensure that the wind-on image is in the current image buffer prior to this step). The "Select IMAGE BUFFER and/or AREA OF INTEREST" for image A menu will appear from which the "Image Area of Interest: Full Image" option is selected; when this is done the "Select IMAGE BUFFER and/or AREA OF INTEREST" will re-appear for image B

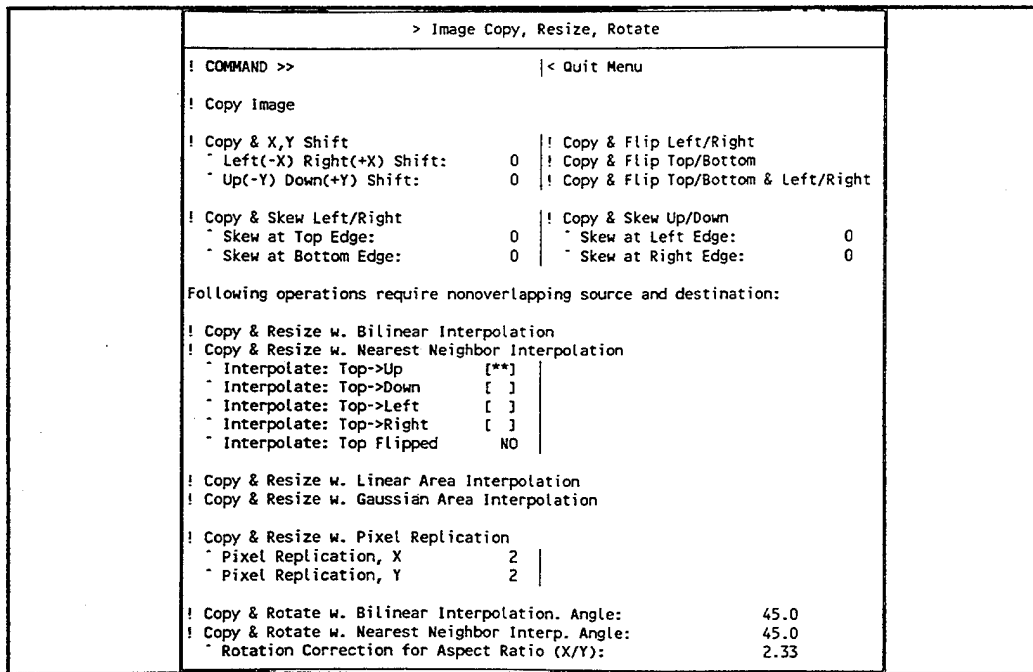


Figure C8. "Image, Copy, Resize, Rotate" Sub-Menu

where again the option "Image Area of Interest: Full Image" is chosen. When this selection is made the operation will then be executed. The current image buffer containing the wind-on image will be replaced with the modified wind-on image. Return to the "Pixel Peek, Poke & Plot" sub-menu and use the cursor to determine if the wind-on and wind-off images are properly registered. Several iterations may be necessary until the images are aligned.

4. Ratioing

With the images correctly registered, the ratioing process can now be executed, i.e., the wind-off may be divided by the wind-on images. Proceed to the "Two Image Arithmetic" sub-menu as previously done when the dark current image was subtracted from the wind-on and wind-off images. Under the "Ratio Images" option, set the ratio coefficients, that are used for "gain and offset", as follows: c0 = 100 (or 128), c1 = 0, c2 = 1, c3 = 0. Next strobe the "Ratio Images" function which will cause the "Select IMAGE BUFFER and/or AREA OF INTEREST" menu for PixA to be displayed. Ensure the current image buffer is displaying the wind-on image. Select "Image Area of Interest: Full Image". This will cause the "Select IMAGE BUFFER and/or AREA OF INTEREST" to be re-displayed for PixB. Now shift the buffer containing the wind-off image such that it becomes the current image buffer. Again select "Image Area of Interest: Full Image". The ratioing process will then commence replacing the image designated as PixB, i.e., the wind-off image, with the modified image.

5. Thresholding

A black background is usually added to the ratioed image to provide contrast and enhancement to the resultant image. From the main menu chose "Image Processing" and then the option "Simple Pixel Operations". Under the function "Threshold Pixel Values" set the values as follows:

- Threshold: Lowbound	0
- Threshold: Highbound	255
- Threshold: NewValue	0

Strobe the "Threshold Pixel Values" function with the left mouse button; the "Select IMAGE BUFFER and/or AREA OF INTEREST" menu will appear. The boundary shape of the painted surface depicted in the ratioed image will dictate which area of interest to select for this image processing operation, i.e., "Interactive Rectangular", "Interactive Elliptical", "Interactive Freehand", and "Interactive Polygon". The area of interest includes the area of the image that the painted surface does not occupy; for the flat plate, since the sides were parallel to the image axis, the "Interactive Rectangular Region" was selected as the region of interest. The area of the flat plate image not occupied by the plate was broken down to four areas of interest, that is, the area above the plate, below the plate, left of the plate, and to the right of the plate. Using the mouse with the right button depressed, these areas were outlined individually with the cursor. Once the areas had been outlined, the thresholding process was executed.

6. Pseudocoloring

To add false coloring or pseudocoloring to the gray-scale image, select the "Contrast & Lookup Tables" option from the main menu. This menu is illustrated in Figure C9. Each of the primary colors, red, green, and blue are set by selecting the "Numerically Set & Show" option for the individual colors. The option displays the sub-menu illustrated in Figure C10. Using the function "Set Partial Linear Ramp" any configuration of linear ramps may be constructed. A graphical display of the inputs can be shown on the computer screen by selecting the "Plot Table" option in the menu illustrated in Figure C10.

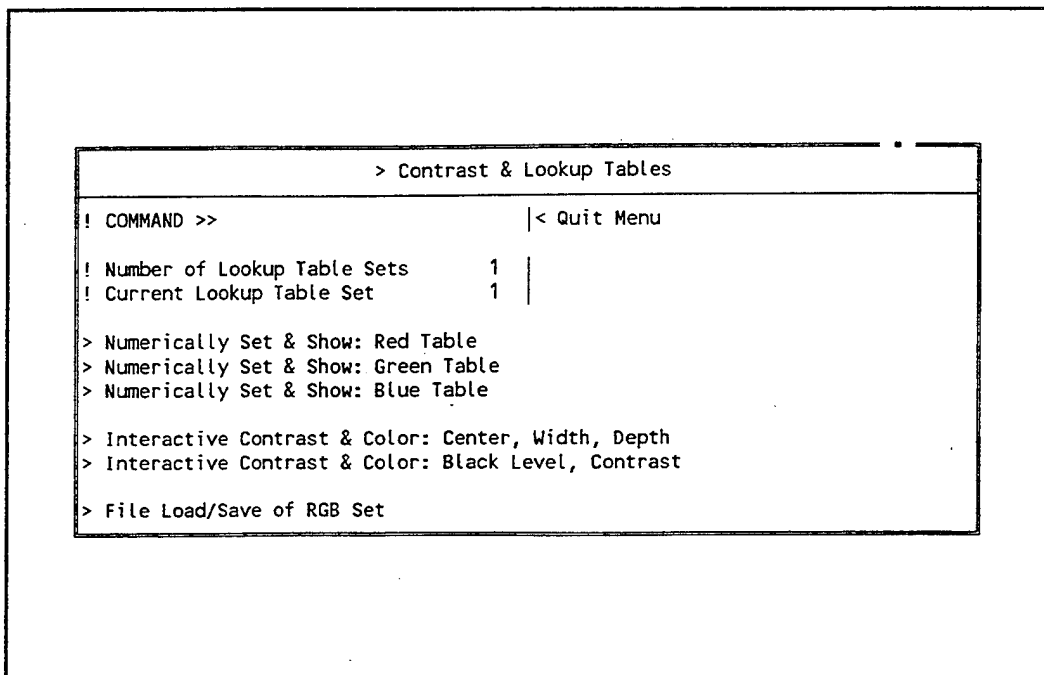


Figure C9. "Contrast & Lookup Table" Sub-Menu

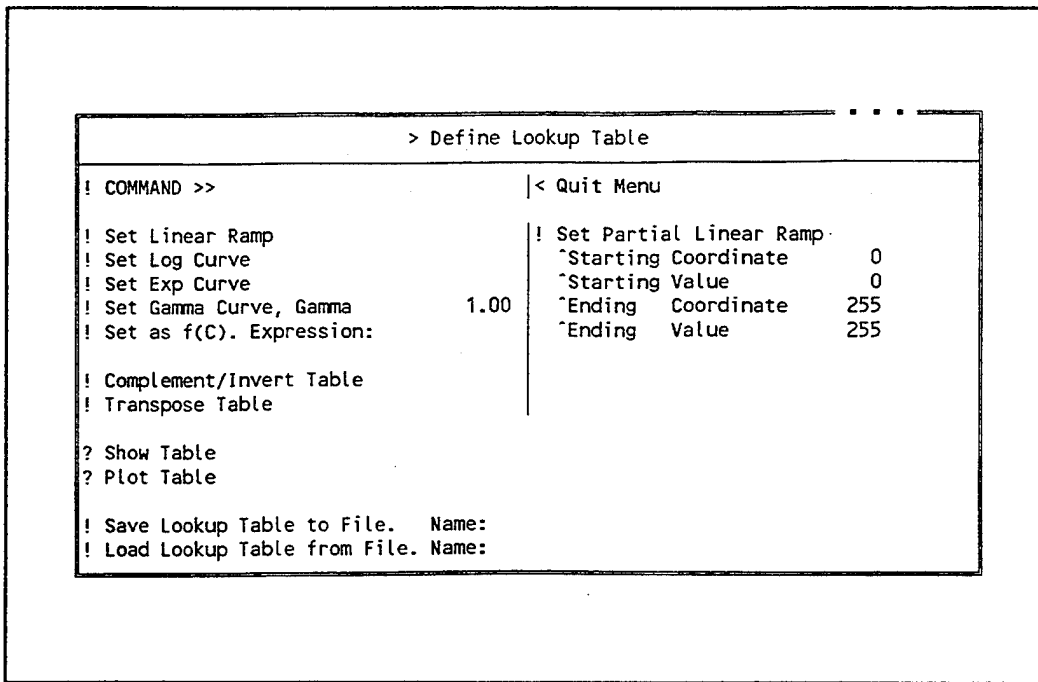


Figure C10. "Define Lookup Table" Sub-Menu

APPENDIX D. DARK CURRENT

Thermal generation of electrons or "dark-current" is a naturally-occurring consequence of using semiconductor devices for photo reception. To understand dark-current effects on pressure-sensitive paint measurements, it is necessary to review the operation of a charged-coupled device (CCD). A schematic illustration of a CCD is shown in Figure D1.

Consider a single CCD electrode in Figure D1. Absent the application of a bias to the gate electrode, a uniform distribution of holes or majority carriers exists in the p-type semiconductor. As a positive voltage is applied to the gate, the holes are repelled from the semiconductor immediately beneath the gate, forming a depletion layer or potential well. An increase in the voltage causes the depletion region to extend further down into the bulk semiconductor, causing an increasing positive potential known as a surface potential to exist at the semiconductor and insulator (oxide) interface. Eventually a gate bias is reached at which the surface potential becomes so positive that the minority carriers (in this case electrons) are attracted to the surface where they form an extremely thin but very dense inversion layer. [Ref. 28:p. 6]

In image-sensing applications of CCD's, the minority carriers are generated when photons entering the silicon substrate excite the valence electrons of the material into the "conduction band", becoming free electrons. The electrons are then collected under the

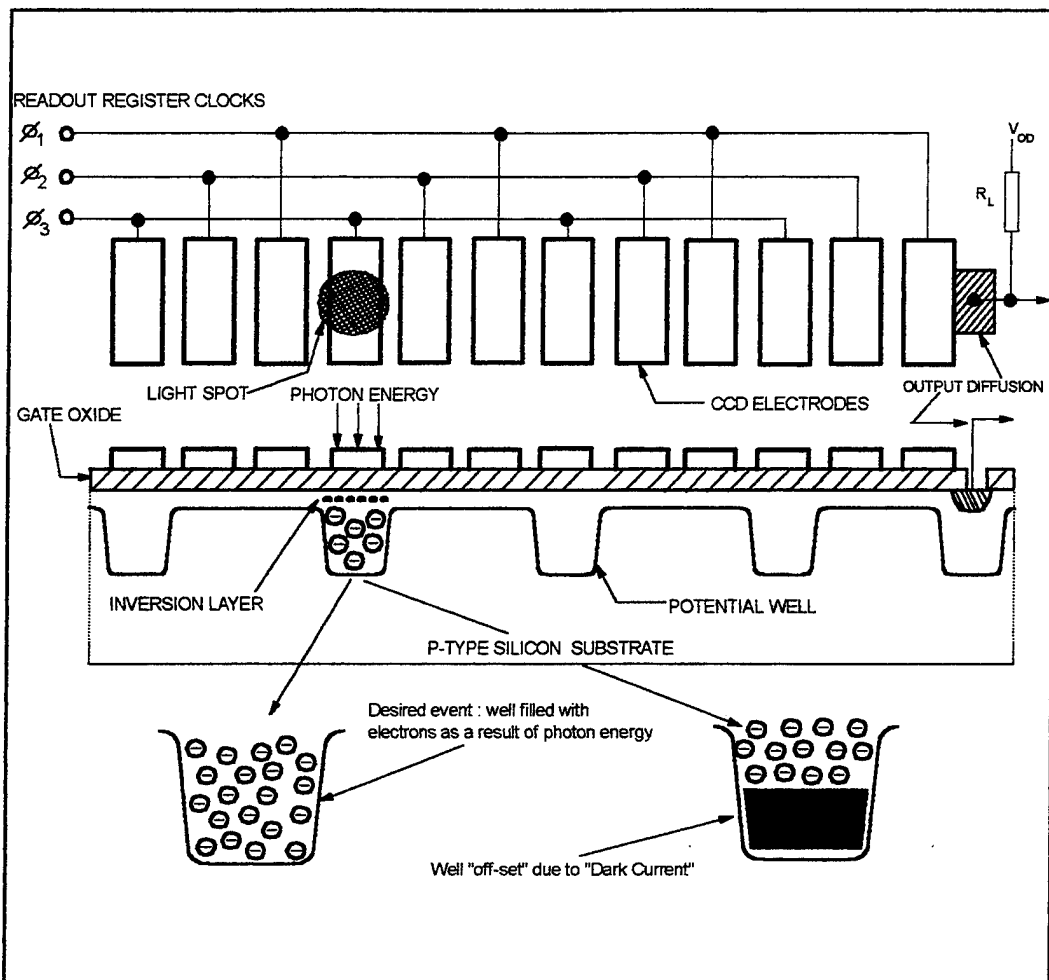


Figure D1. Representation of the Effect of Dark-Current on the Creation of Charge

electrode of the applied bias. The number of electrons under the electrode within a given period of time is proportional to the local light intensity.

In addition to the photoelectric effect described above, free electrons can also be produced by thermal energy, of which the rate of generation increases exponentially with temperature for a pure semiconductor. Thus, the presence of thermally generated minority carriers limits the maximum possible usefulness of the potential well by displacing optically generated carriers. This produces an "offset" in the measurement image such that the

zero-incident light level does not correspond to a zero gray-level pixel index. Thus, the dark image must be removed from the measurement images. To do this, a dark image is acquired by prohibiting any light from striking the CCD array and sampling an image. Several of these images are taken and time averaged together. This is necessary because dark current generation tends not to be uniform over a whole array. The resulting averaged dark current is then eliminated from the measurement images using image processing techniques discussed in Chapter III.

APPENDIX E. SUPERSONIC NOZZLE DESIGN PROGRAM

Software for the design of two-dimensional supersonic nozzles was acquired from the Naval Surface Warfare Center (NSWC), White Oak, Maryland. The software package is comprised of two programs; the first program is concerned with establishing the isentropic contour of the nozzle while the second corrects for the viscous effects of the fluid and adjusts the contour accordingly.

Support documentation for the software from a user's standpoint is not available. In addition, the early fortran code is not well structured, making it difficult to interpret the algorithm and follow its logic. It is difficult to recognize many of the variables, and there are no comment statements. However, enough information has been deduced such that the program may be operated effectively. The intention of this appendix is to document what is now known about the software.

Modifications have been made to the original software primarily involving the manner in which program input entries are made and data storage accomplished. Originally, the program was designed to access punch-card readers and magnetic-tape drives for data input and output management. Entries are now made directly to the program through interactive software in a format that is more flexible and user friendly. Output data are stored in a file structure compatible with hard drive systems. A listing of the modified software is given in Section C of Appendix E.

A. INVISCID CONTOUR SOFTWARE (Program char6)

The program "char6" generates the isentropic contour of the supersonic nozzle using the method of characteristics. Initiation of the program will depend on the filename assigned to the object code at the time of compiling and linking of the source code. Once started, the program first displays an introductory summary as shown in Figure E1. As indicated by these remarks, the storage of the output data is currently limited to the data for one run. A successive run will overwrite the data storage files from the previous run.

Entries made by the user through the interactive sequence of prompts for input data have been sub-divided into two categories; the first category identifies the "characteristic" lengths and nozzle type that will be used to define the configuration; the second specifies dimensions and flow characteristics to which the nozzle will be designed.

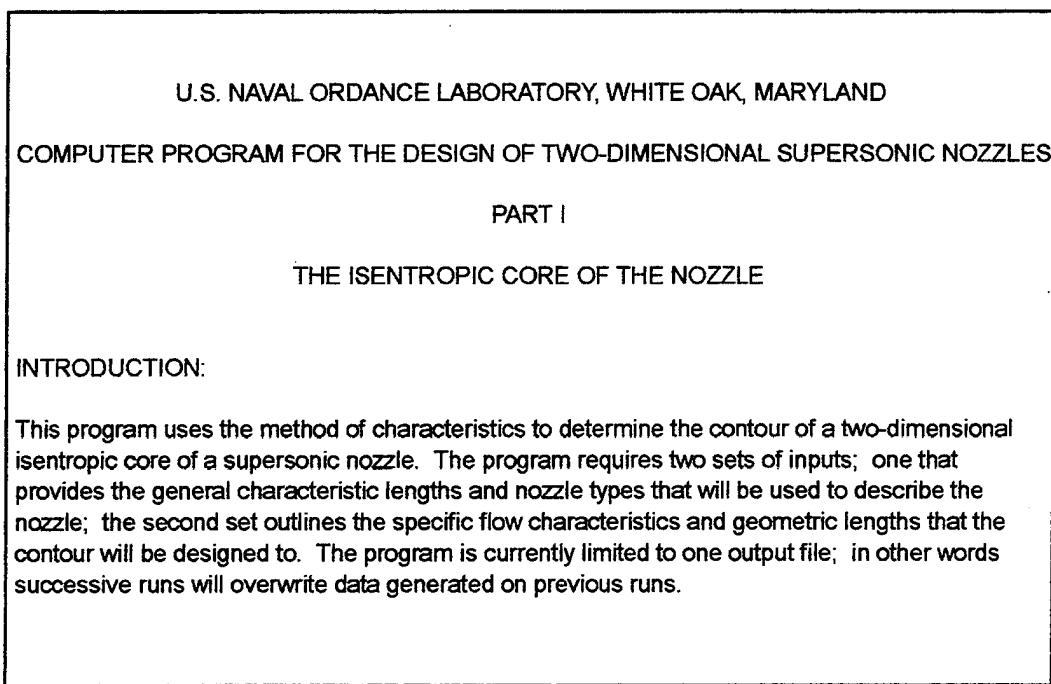


Figure E1. Illustrative Example of the Introductory Remarks for Program char6

1. Category 1: Characteristic Lengths and Nozzle Types

1. INPUT A DESCRIPTION OF THE PROJECT

Allows a short summary of the project to be recorded as part of the final output summary. The description is limited to 80 characters.

2. INDICATE TYPE OF NOZZLE, 1-SHORT, 2-REGULAR, 3-EXPONENTIAL

Provides the option of choosing a specific contour shape. The methodology the program uses to generate the contour begins by first determining the centerline Mach number distribution based on the choice of contour. The method of characteristics is then used in conjunction with the centerline distribution in determining contour geometry.

3. INDICATE THROAT OR EXIT HEIGHT TO BE READ, 1-EXIT, 2-THROAT

Irrespective which is used; the program calculates the option not selected using simple isentropic relations. Both heights are employed in the program in computing the contour.

4. INDICATE CHARACTERISTIC HORIZONTAL LENGTH TO BE READ, 1-EXIT LENGTH, 2-START OF TEST RHOMBUS

Refer to Figure E2 for clarification of the horizontal lengths discussed. The exit length is defined as the distance between the nozzle throat and the nozzle exit.

The characteristic network created by the method of characteristics is such that the last two characteristic lines in the grid complete the expansion process by turning the flow parallel to the centerline of the nozzle and thus expanding it to the desired test section Mach number. These two characteristic lines can also be thought of as forming half of an imaginary rhombus as shown in Figure E2. This is known as the test section rhombus. The distance between the nozzle throat and the intersection formed by the two characteristic lines defines the horizontal length referred to above.

5. INDICATE OUTPUT, 1-STEP-BY-STEP, 2-WALL POINTS ONLY

Generally, the approach used in applying the method of characteristics can be summarized in a three step process: Step 1 -- the determination of the characteristic lines in the xy space using

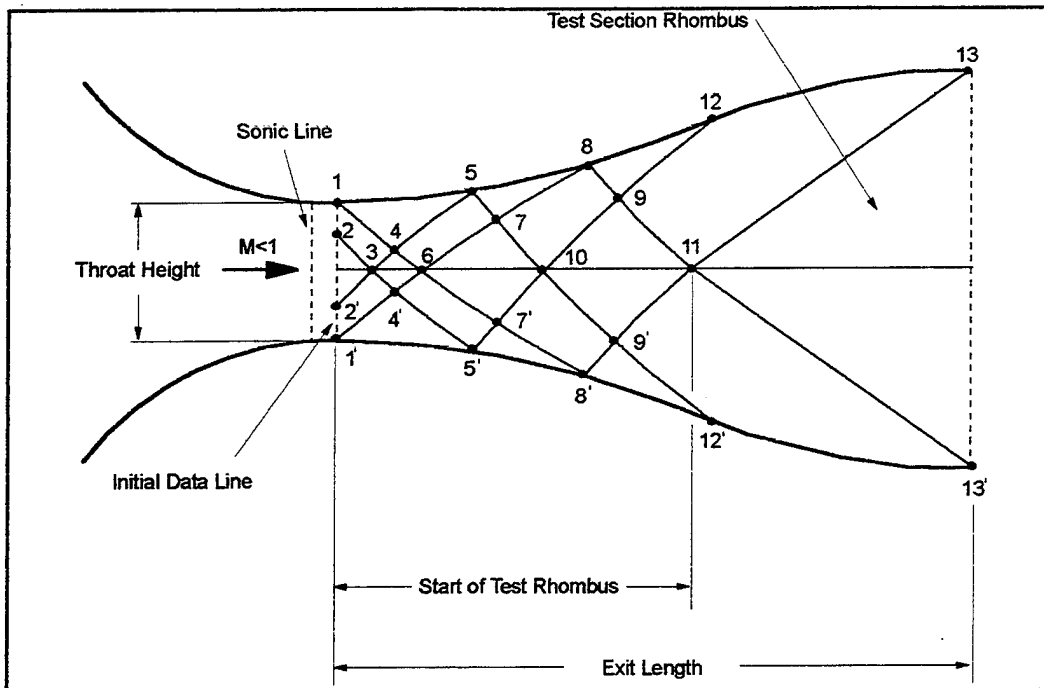


Figure E2. Schematic of Supersonic Nozzle Design by the Method of Characteristics

$$\left(\frac{dy}{dx}\right)_{\text{char}} = \tan(\theta \pm \mu)$$

where θ is the angle between the streamline of the flow and the horizontal and μ is the angle between the streamline and the characteristic line; Step 2 -- the determination of the compatibility equations

$$\begin{aligned} \theta + v(M) &= \text{const} = K_- && (\text{along the right characteristic}) \\ \theta - v(M) &= \text{const} = K_+ && (\text{along the left characteristic}) \end{aligned}$$

where again θ is the angle between the horizontal and the streamline, and, $v(M)$ is the Prandtl-Meyer function, the compatibility equations holding along the characteristics; Step 3 -- the solution of the compatibility equations point by point along the characteristics.

Note: The initial data line used in starting the computation of the method of characteristics in this program begins with the assumption that the sonic line at the throat is straight. A point ΔM downstream of the sonic line along the centerline Mach number distribution is chosen as the initial point for the characteristics procedure. With the combination of this initial point, the centerline distribution, and the radius of curvature at the throat, the method of characteristics is carried out in a marching fashion.

Choosing the option step-by-step will instruct the program to include in the final output all "steps" used in calculating the characteristic net, including local data pertaining to the nodal points comprising the turning angle, the x and y coordinates of the grid points and the Mach number. If in turn the option "wall points only" is exercised, the data associated with the grid points that decide the contour or wall geometry are included in the final output.

Once the last selection for the first category of inputs is chosen and the "enter" key is subsequently struck, the selections made are then displayed in the following format:

NOZZLE = SHORT (REGULAR, EXPONENTIAL)

HEIGHT TO BE READ = EXIT (THROAT)

LENGTH TO BE READ = LENGTH TO EXIT (LENGTH TO RHOMBUS)

OUTPUT FORMAT = STEP-BY-STEP (WALL POINTS)

The question, "Are input values correct?, 1-Yes, 2-No", follows immediately, allowing the opportunity to make changes to the inputs if necessary. Selecting "Yes" causes the following menu to be displayed:

INPUT VALUES TO BE CHANGED (1, 2, 3, 4):

1- TYPE OF NOZZLE: A. SHORT, B. REGULAR, C. EXPONENTIAL

2 - HEIGHT TO BE READ: A. EXIT, B. THROAT

3 - LENGTH TO BE READ: A. EXIT, B. TEST RHOMBUS

4 - TYPE OF OUTPUT: A. STEP-BY-STEP, B. WALL POINTS ONLY

By selecting a value from one to four a sub-menu of the descriptors to the right of the colon of the input chosen is listed. For example, selecting the value of 2 (Height to be read) from the above menu yields

1 - EXIT, 2 - THROAT

prompting a choice of height designation. After hitting the "enter" key, the program will again display the first-category input selections, showing the latest modifications. An opportunity to make additional alterations is also afforded when the question, "Any other changes?, 1-Yes, 2-No", immediately follows. Selection of "No" initiates the sequence of events for data input associated with the second category.

2. CATEGORY 2: NOZZLE FLOW AND GEOMETRY SPECIFICATIONS

Commencement of the sequence of prompts for the second category of inputs is denoted by the statements

**"THE NEXT SET OF INPUTS SPECIFY FLOW CHARACTERISTICS AND
SPECIFIC GEOMETRY DIMENSIONS FOR THE NOZZLE"**

******* PLEASE UTILIZE DECIMAL POINTS FOR THESE INPUTS *******

It is necessary to use decimal points when specifying numeric data; the program is formatted to read the input data in scientific notation, though numeric values may be entered into the program as real numbers. If a decimal point is not explicitly stated, the exponent field in the scientific notation format will reflect this with zeros, resulting in an ambiguous input. Thus, if the real number "14" is the desired input, it must be entered as "14."; this results in the scientific notation representation "0.14000E+02". If the number is entered as "14", the resulting representation will be "0.14000E+00".

The inputs for the second group are outlined as follows:

1. INPUT RATIO OF SPECIFIC HEATS

Self-explanatory.

2. INPUT TEST SECTION MACH NUMBER

The Mach number of the uniform flow that is required at the exit plane of the nozzle.

3. INPUT EXIT LENGTH (INCHES) OR INPUT BEGINNING OF TEST RHOMBUS (INCHES)

The choice made in the first category of inputs concerning the horizontal length will dictate which prompt will be displayed. Refer to Figure E2.

4. INPUT HALF HEIGHT OF EXIT (INCHES) OR INPUT HALF HEIGHT OF THROAT (INCHES)

Again dependent on the selection made in the first category of inputs with reference to the height to be read.

5. INPUT RADIUS OF CURVATURE AT THROAT (INCHES)

Self-explanatory.

6. INPUT MULTIPLICATIVE FACTOR FOR "X" INCREMENT

Influences the spacing between consecutive contour points. A range between 1.0 (representing 150 points to describe the contour) to 0.5 (representing 400 points) is available.

Note: Generation of the cubic centerline Mach number distribution, which is associated with the regular nozzle contour, is dependent upon the result of a "feasibility expression" involving the second category values input by the user. If the outcome of the expression does not fall into a pre-determined interval, the program halts execution and displays the message,

***** CUBIC CENTERLINE MACH NO. DISTRIBUTION IS
NOT APPROPRIATE FOR INPUT GIVEN *****

At this point, the program must be re-initialized and the process of re-entering the input started over. One of the input values, gamma, test section Mach number, exit length or length to test rhombus, exit or throat height, or the radius of curvature, or a combination thereof

must be changed such that the compatibility requirements set forth by the feasibility expression are satisfied.

When the data for the multiplicative factor has been entered and the "enter" key struck the second category of inputs are displayed in the following fashion:

```
GAMMA = 0.14000E+01  
SMT = 0.17000E+01  
XEXXT = 0.11500E+02  
YTHEX = 0.19500E+01  
RCT = 0.11500E+01  
DELMUL = 0.70000E+00  
ARE INPUT VALUES CORRECT ?, 1 - YES, 2 - NO
```

where

GAMMA = Ratio of specific heats
SMT = Test section Mach number
XEXXT = Exit length or length to the beginning of test
 rhombus depending on the choice in first category
 of inputs
YTHEX = Half height of exit or half height of throat depending
 on the choice in the first category of inputs
DELMUL = Multiplicative factor for "x" increment

As in the first category of inputs, the option to make changes to the input data is available. When changes are desired a listing of the input descriptors is displayed:

```
INPUT VALUE TO BE CHANGED: 1 - GAMMA, 2 - SMT,  
3 - XEXXT, 4 - YTHEX, 5 - RCT, 6 - DELMUL
```

A selection will exhibit a directive prompting the user to input the new value. For example, choosing gamma (1) results in,

```
INPUT NEW VALUE FOR GAMMA
```

Fulfilling this and subsequently striking the "enter" key causes the second category of inputs to be re-displayed showing the recent modifications. Additional changes may also be conducted at this point if necessary.

If the second category of inputs have been reviewed with satisfaction, the program will begin calculation of the isentropic contour at this point. Conclusion of the routine is indicated by the remarks,

**OUTPUT ISENTROPIC DATA FOR NOZZLE CONTOUR
STORED IN FILENAME "outpt1"**

**DATA FROM THIS FILE TO BE USED IN THE VISCOUS
PROGRAM "nbl6.f" IS STORED IN FILENAME "outpt2"**

The file "outpt1" contains a systematic breakdown of the data calculated by the program which are then available to the user for review. A complete explanation and an example of the format are presented in the following section. The file "outpt2" contains the data that are to be utilized in the program "nbl6" and are in a format that is convenient for file processing.

3. "outpt1" EXAMPLE AND DESCRIPTION

Figure E3 shows the format in an example of the file "outpt1". It has been sub-divided into it's major components and labeled for reference below.

1. Introductory Header - Self-explanatory.
2. Descriptive Comments - Refers to the comments made in the first category of inputs when prompted by the program for a description of the project.
3. User Inputs - Encompasses all the inputs into the program made by the user. The input identifiers associated with the first category of inputs are defined as follows:

INDSR = Nozzle Type

INDYTH = Characteristic Height (Throat or Exit)

indxte = Characteristic Length (Exit or Test Rhombus)

INDOUT = Output Mode (Step-by-Step or Wall Points)

U.S. NAVAL ORDANCE LABORATORY, WHITE OAK, MARYLAND

COMPUTER PROGRAM FOR THE DESIGN OF TWO-DIMENSIONAL SUPERSONIC NOZZLES

PART I

THE ISENTROPIC CORE OF THE NOZZLE

1.7 MACH NOZZLE

INPUT DATA

CARD NO. 1	INDSR = 2 INDYTH = 1 INDEXTE = 1 INDOUT = 1 INDCAL = 0 INDTAP = 0 INCDRD = 0
CARD NO. 2	GAMMA = 0.14000E+01 SMT = 0.17000E+01 XEXT = 0.11500E+02 YTHEX = 0.19800E+01 RCT = 0.11500E+02 DELMUL = 0.70000E+00

NOZZLE PARAMETERS

MACH NO.	YTH	YEXIT	XEXIT	XT
0.17000E+01	0.14803E+01	0.19800E+01	0.11500E+02	0.87780E+01
	RCT	B		
	0.11500E+02	0.35425E+00		

CENTERLINE MACH NUMBER DISTRIBUTION USING CUBIC EQUATION

N	X	MACH NO.
1	0.534600E-03	0.100010E+01
2	0.732600E-03	0.100014E+01
3	0.930600E-03	0.100017E+01

CHARACTERISTICS MANIPULATION (*INTERPOLATED WALL VALUES)

N	K	X(INCHES)	Y(INCHES)	MACH NO.	STREAM ANGLE
2	3	0.629684E-03	0.6428261E-02	0.000000E+00	0.136713E-04
3	2	0.828632E-03	0.5607560E-02	0.000000E+00	0.156680E-04
3	3	0.718964E-03	0.1198140E-01	0.000000E+00	0.293399E-04

FINAL OUTPUT TO PART I, ISENTROPIC CORE CONTOUR

I	X(INCHES)	Y(INCHES)	CL MACH NO.	WALL MACH NO.	WALL ANGLE	RAD OF CURV (IN)
1	0.435619E+00	0.149273E+01	0.107887E+01	0.114198E+01	0.220395E+01	0.000000E+00
2	0.462758E+00	0.149380E+01	0.108359E+01	0.114598E+01	0.228777E+01	0.188330E+02
3	0.490391E+00	0.149492E+01	0.108838E+01	0.115003E+01	0.237073E+01	0.193154E+02

Figure E3. Example Showing the Format of File "outpt1"

INDCAL, INDTAP, and INDCRD are no longer user-accessible. These variables were used in the original software and controlled the medium to be used to record the output data, i.e., magnetic tape or punch cards. The variables have been "hardwired" in order to accommodate the current software modifications for data output management.

The input descriptors for the second category of inputs have been previously defined.

4. Nozzle Parameters - These include, in addition to those dimensions supplied by the user, the "related" values calculated by the program using isentropic relationships or simple geometric relations. Thus, given the input of the throat height the program calculates the exit height ,or, given the horizontal length from the throat to the exit plane the program calculates the length from the throat to the test rhombus. The parameters are defined as,

Mach No. = Nozzle exit Mach number

YTH = Half height of nozzle throat

YEXIT = Half height of nozzle exit

XEXIT = Length between nozzle throat and exit

XT = Length between nozzle throat and test rhombus

RCT = Radius of curvature at throat

* B = Indicates result of "Feasibility Expression"

* Note: The result of the feasibility expression, to determine if the cubic centerline Mach number distribution may be calculated with the given nozzle dimensional inputs, must fall in the interval $-2.0 < B < 1.0$.

5. Centerline Mach Number Distribution - Denotes the centerline location (relative to the throat) and corresponding Mach number. The function used to generate the distribution, i.e., cubic, exponential, etc., is dependent upon the choice of nozzle type (regular, exponential, short).
6. Method of Characteristic Results - Describes the characteristic manipulation used to generate the wall values along the contour.

N = Characteristic line (From left to right)

L = Nodal points along characteristic line

X (inches) = X-coordinate of nodal point

Y (inches) = Y-coordinate of nodal point

Mach No. = Local Mach number at nodal point

Stream angle = Local velocity angle at nodal point with
respect to the horizontal

7. Contour Output - Final output of the isentropic core.

X(INCHES) = X - coordinate of isentropic core

Y(INCHES) = Y - coordinate of isentropic core

CL MACH NO. = Centerline Mach number

WALL MACH NO. = Mach number along contoured wall

WALL ANGLE = Wall angle relative to centerline

RAD. OF CURV. (IN) = Radius of curvature

B. MODIFICATION FOR VISCOUS EFFECTS (Program nbl6)

The program "nbl6" modifies the contour of the nozzle to account for the boundary layer formation. Originally, this software considered the boundary layer effects along the contour of the nozzle only and neglected the effects that would be caused with the addition of side walls. To compensate for this deficiency in correcting for boundary layer displacement, the approach used by Demo [Ref. 29: p. 24] was employed. The assumption is made that the displacement thickness is the same on both contoured and side walls. The viscous displacement effects on all surfaces are then summed together and evenly distributed between the two contour surfaces only, as illustrated in Figure E4.

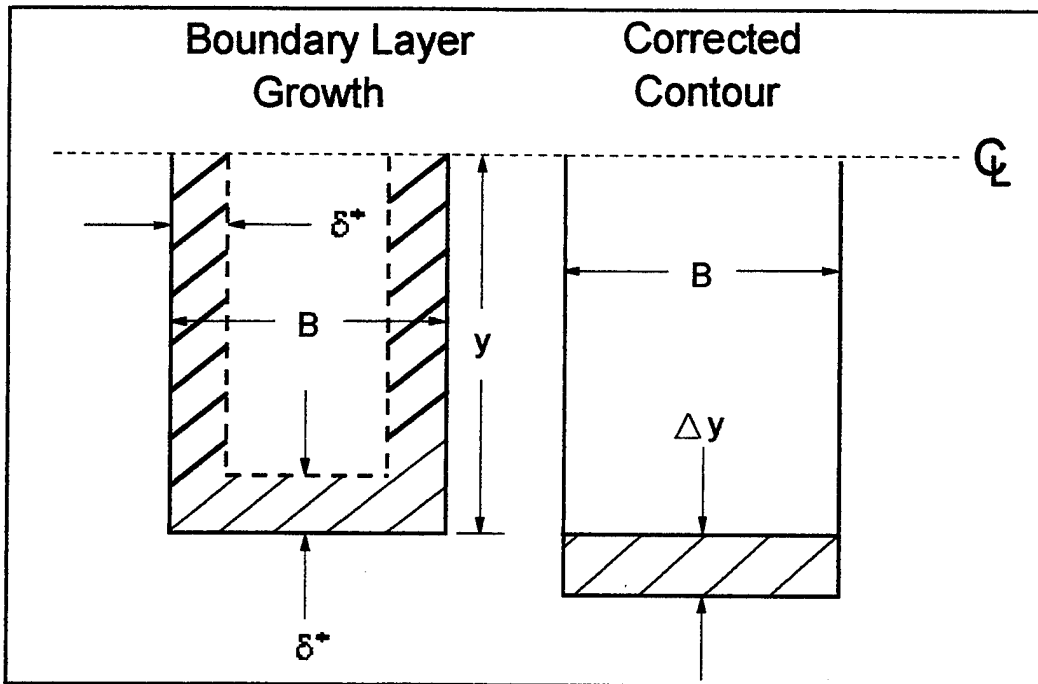


Figure E4. Nozzle Wall Correction for Boundary Layer

Thus, the total displacement area of the entire nozzle cross-section is compensated by modifying only the contoured walls, allowing the side walls to remain flat and parallel. The displacement required to the inviscid contour was calculated using the expression

$$\Delta y = \frac{2y\delta^* + (B - 2\delta^*)\delta^*}{B} \quad (E1)$$

where δ^* = displacement thickness, B = nozzle width, and y = half height of the contour. This equation has been incorporated into the software. The final output, discussed later, was modified to reflect this change.

The data-output management structure, as before, is limited to storing data for one run. A successive run will overwrite the data stored from the preceding run.

Input into the program is supplied by both the output from "char6" (i.e., file outpt2) and the user using an interactive presentation similar to that discussed above for the

inviscid contour. The first category of inputs consists of a series of functional mode selections concerned with the thermal and velocity boundary layer behavior. The second category is comprised of numerical input prompts for flow conditions and nozzle dimensions.

1. CATEGORY 1: FUNCTIONAL MODES

The functional modes establish the desired profile behavior that the velocity and thermal boundary layers will undergo while traversing the length of the nozzle. The modes are outlined below.

- 1. INDICATE WHERE THE BOUNDARY LAYER CALCULATION WILL TAKE PLACE, 1. ALONG CENTERLINE ONLY, 2. ALONG THE WALL ONLY, 3. BOTH THE CENTERLINE AND THE WALL**

Specifying the first option results in the message,

```
*****  
*      CENTERLINE PARAMETER INPUT DATA      *  
*****
```

indicating that all input into the program from this point will pertain to the effects of the boundary layer along the nozzle centerline. Selection of the second option displays

```
*****  
*      WALL PARAMETER INPUT DATA      *  
*****
```

indicating further inputs will apply to the effects of the boundary layer along the nozzle contoured walls. Option three effectively causes the program to run twice, once for the effects along the centerline followed by a run associated with the boundary layer effects along the contoured walls. The final output for option three is consolidated as a single output vice individual outputs for each run.

2. INDICATE BOUNDARY LAYER MODE BEGINNING AT NOZZLE THROAT, 1. STRICTLY LAMINAR, 2. STRICTLY TURBULENT, 3. LAMINAR-TRANSITION-TURBULENT

Self-explanatory.

3. INDICATE WALL TEMPERATURE FOR NOZZLE, 1. CONSTANT TEMPERATURE, 2. ADIABATIC WALL, 3. TEMPERATURE DISTRIBUTION ALONG NOZZLE TO BE INPUT BY PROGRAM USER

Wall temperature is assumed only along the contour of the nozzle. Since the boundary layer displacement thickness for the entire cross-section of the nozzle is a function of the displacement thickness generated along the contour, it can be thought of that the temperature distribution exists both on the contour and side walls.

4. INDICATE THE CHARACTERISTIC PARAMETER ON WHICH TRANSITION WILL BE BASED, 1. REYNOLDS NUMBER, 2. "X" DISTANCE FROM THE THROAT

The transition mode only becomes active if the laminar-transition-turbulent selection of the boundary layer mode is chosen. The point of transition from laminar flow to turbulent flow may be based upon a horizontal distance "x" relative to the nozzle throat and along the centerline or a Reynolds number in which the momentum thickness of the boundary layer is used as the characteristic length

The last entry made for the mode options is followed by a listing of the selections to verify the settings:

B.L. MODE = LAMINAR (TURBULENT, LAM-TRANS-TURB)

WALL TEMP. MODE = CONSTANT (ADIABATIC, USER DEFINED)

*TRANSITION PARAMETER = REYNOLDS NUMBER ("X" DISTANCE)

B.L. CALCULATION = CENTERLINE ONLY (WALL ONLY, BOTH CENTERLINE AND WALL)

"ARE INPUT VALUES CORRECT?, 1-YES, 2-NO

*Note: Displayed only if B.L. Mode = Lam-Trans-Turb

If a mode is incorrectly set or a change is desired, "no" is subsequently chosen, resulting in a modification menu:

INPUT VALUE TO BE CHANGED (1,2,3,4):

1. B.L. MODE: A. LAMINAR, B. TURBULENT, C. LAM-TRANS-TURB
2. WALL TEMP. MODE: A. CONSTANT, B. ADIABATIC, C. USER DEFINED
3. B.L. CALCULATION: A. CENTERLINE, B. WALL, C. CENTERLINE AND WALL
- *4. TRANSITION: A. REYNOLDS NUMBER, B. "X" TRANSITION

*Note: selection of the transition mode with the B.L. Mode set other than B.L. Mode = Lam-Trans-Turb will result in the message, "Transition parameter not required for inputs given".

The mode to be modified is selected from the menu list, which in turn causes a sub-listing of the options to which the mode may be set to be displayed. For example, if the boundary layer mode is to be changed, its selection from the modification menu would be followed by,

1. LAMINAR, 2. TURBULENT, 3. LAM-TRANS-TURB

A choice of one of the available options sets the mode and then causes a re-display of all the modes and their current status;

B.L. MODE = LAMINAR

WALL TEMP. MODE = CONSTANT

TRANSITION PARAMETER = REYNOLDS NUMBER

B.L. CALCULATION = WALL ONLY

"ANY OTHER CHANGES?, 1-YES, 2-NO"

Other modifications may be done at this point in a sequence similar to that discussed above. If no other changes are required or if the modes initially set were correct, the series of prompts for the second category of inputs will be initiated.

2. CATEGORY 2: FLOW CONDITIONS AND NOZZLE DIMENSIONS

The second category of inputs includes the numerical data associated with the flow conditions, and additional dimensions of the nozzle, which will be made clear below. The onset of the second set of inputs is denoted by the message

*** * * PLEASE UTILIZE DECIMAL POINTS FOR THE FOLLOWING INPUTS * * ***

followed by the first prompt for information. Decimal points are necessary for the numeric inputs for the reasoning previously explained.

Most of the input prompts are self-explanatory and require no elaboration. Those prompts requiring explanation or having relevant comments will be summarized following the prompt.

1. INPUT REYNOLDS NUMBER FOR TRANSITION

(Reynolds number based on momentum thickness of boundary layer)

Displayed only if the boundary layer mode is set to B.L. Mode = Lam-Trans-Turb and the transition indication mode set to Transition Parameter = Reynolds Number.

2. INPUT TRANSITION DISTANCE FROM THE THROAT IN FEET

Displayed only if the boundary layer mode is set to B.L. Mode = Lam-Trans-Turb and the transition indication mode is set to Transition Parameter = "X" Distance From Throat.

3. INPUT MOMENTUM THICKNESS OF BOUNDARY LAYER AT THE THROAT IN FEET

A value of 1.0E-5 feet is suggested.

4. INPUT STAGNATION PRESSURE IN LBS/IN²

5. INPUT TOTAL TEMPERATURE OF SUPPLY MEDIUM IN DEGREES R

6. INPUT TEMPERATURE OF THE WALL IN DEGREES R

Displayed only if the wall temperature indication mode is set to Wall Temp. Mode = Constant.

7. INPUT THE EXTENSION LENGTH OF NOZZLE PAST THE EXIT IN INCHES AS DEFINED FOR THE ISENTROPIC CORE

The nozzle contour may be extended past the exit plane of the nozzle, as defined by "char6", if, for instance, a test section is to be added. Assumes uniform duct flow.

8. INPUT INCREMENT OF "X" IN INCHES FOR EXTENSION LENGTH TO INTERPOLATE CONTOUR OF NOZZLE

Establishes the horizontal distance between consecutive points that describe the contour of the extension length.

9. INPUT WIDTH OF NOZZLE

10. INPUT RATIO OF SPECIFIC HEATS

11. INPUT EXPONENT FOR VISCOSITY-TEMPERATURE RELATION

For air, this is (ω) 0.76.

12. INPUT MOLECULAR WEIGHT OF GAS SUPPLY (AIR = 28.97)

13. INPUT SPECIFIC HEAT OF GAS IN BTU/LB-DEG-R (AIR = 0.24)

14. INPUT PRANDTL NUMBER FOR GAS (AIR = 0.72)

Following the conclusion of the last prompt, a listing of all the input descriptors and the values assigned to them is displayed:

```
*REYNOLDS NUMBER = 0.50000E-02
*"X" TRANSITION = 0.60000E+01
MOMENTUM THICKNESS = 0.10000E-04
STAGNATION PRESSURE = 0.47500E+02
STAGNATION TEMPERATURE = 0.68000E+02
**WALL TEMPERATURE = 0.72000E+02
EXTENSION LENGTH PAST NOZZLE EXIT = 0.12000E+02
INCREMENT "X" FOR EXTENSION = 0.65000E+00
WIDTH OF NOZZLE = 0.40000E+01
GAMMA = 0.14000E+01
VISCOSITY-TEMP. EXPONENT = 0.76000E+00
MOLECULAR WEIGHT OF GAS = 0.28970E+02
SPECIFIC HEAT = 0.24000E+00
PRANDTL NUMBER = 0.72000E+00
```

"ARE INPUTS CORRECT?, 1-YES, 2-NO"

*Note: Displayed only if boundary layer mode is set to B.L.
Mode = 3 and the transition indication mode is set to
either Transition Parameter = Reynolds Number or
Transition Parameter = "X" Distance from Throat

**Note: Displayed only if the wall temperature indication
mode is set to Wall Temp. Mode = Constant

If the option is exercised to change any of the input values, the user will be presented with
the following menu:

INPUT VALUE TO BE CHANGED (1,2,3,4,5,6,7,8,9,10,11,12,13):

1. TRANSITION PARAMETER
2. MOMENTUM THICKNESS AT THROAT
3. STAGNATION PRESSURE
4. TOTAL TEMPERATURE
5. WALL TEMPERATURE

6. EXTENSION LENGTH OF NOZZLE
7. "X" INCREMENT FOR EXTENSION LENGTH
8. WIDTH OF NOZZLE
9. RATIO OF SPECIFIC HEATS
10. VISCOSITY-TEMPERATURE EXPONENT
11. MOLECULAR WEIGHT OF GAS
12. SPECIFIC HEAT (C_p) FOR GAS
13. PRANDTL NUMBER

Selection from the menu generates a prompt for the new information to be input for the chosen descriptor. Upon entering the new value and striking the "enter" or "return" key, the list containing the input descriptors and their assigned values will be re-displayed exhibiting the latest changes and soliciting further modifications.

If at this point no other changes are desired and if the wall temperature indication mode is set to an option other than Wall Temp. Mode = Temperature Distribution Input By User, the program will proceed to calculate the modified contour according to the inputs given. If the user has elected to enter a defined temperature distribution along the nozzle contour, the following sequence of prompts can be expected:

INDICATE THE NUMBER OF TEMPERATURE POINTS
TO BE ENTERED. THREE OR MORE POINTS ARE
REQUIRED OR PROGRAM WILL TERMINATE THE DATA
OUTPUT PRIOR TO COMPLETION.

INPUT THE "X" LOCATION FOR POINT NUMBER _____
RELATIVE TO THE THROAT

INPUT TEMPERATURE IN DEGREES R FOR POINT
NUMBER _____

The second and third statement are repeated until the number of points designated in the first statement have been entered. When the last point is entered, the program proceeds in

its calculation of the modified contour. Completion of the routine is denoted by the message,

PROGRAM RUN COMPLETE. OUTPUT DATA
TRANSFERRED TO FILE "outpt3"

3. FILE "outpt3" FORMAT DESCRIPTION

Figure E5 illustrates an example of the format used for the output file "outpt3". Again it, as before, has been sub-divided into its major components and labeled as follows:

1. Functional Modes

***INDINP = 2**

***INDPRG = 1**

INDMO = 2 (Boundary Layer Mode) where 1 = Laminar,
2 = Turbulent, 3 = Lam-Trans-Turb

INDTW = 1 (Wall Temperature Mode) where 1 = Constant Temp.,
2 = Adiabatic, 3 = User Defined Distribution

INDTR = 1 (Transition Indication Mode) where 1 = Transition at
Reynolds Number, 2 = Transition at "X" Length

***INDCF = 1**

***INDOUT = 0**

***Note:** Indicates values are hardwired into the program and
are no longer user accessible

**** INPUT DATA ****

CARD 1

INDINP =	2
INDPRG=	1
INDMO =	2
INDTW =	1
INDTR =	0
INDWC =	3
INDCF =	1
INDOUT =	0

CARD 2

TRCON =	0.000000E+00
THZERO =	0.100000E-04
PO =	0.728000E+02
TO =	0.820000E+03
TWALL =	0.530000E+03
XTEND =	0.265000E+02
DL =	0.625000E+01

CARD 3

GAMMA =	0.140000E+01
OMEGA =	0.760000E+00
WATE =	0.280000E+02
CP =	0.240000E+00
PR =	0.720000E+00
XINC =	0.000000E+00

* WALL DATA *

X(IN)	Y(IN)	M
0.318238E+00	0.142340E+01	0.111979E+01
0.333082E+00	0.142388E+01	0.112352E+01
0.348089E+00	0.142434E+01	0.112726E+01

*** OUTPUT CODE ***

X(IN)	S(IN)	Y(IN)	M	REL(1/FT)	RETH	PE/PO
UE(FT/SEC)	MUE(PSEC/FT2)	RHO E(PSEC2/FT4)	TE(R)	TW(R)	TAD(R)	TE/TO
DELTA(IN)	THETA(IN)	DELSTAR(IN)	H	TW/TO	TW/TAD	TAD/TO
DPDS(P/FT2)	DMDS(1/FT)	DUDS(1/SEC)	DTHDS	TAUWAL(P/FT2)	CF	BETATH
Q(BTU/FT2/SEC)	HA(BTU/FT2SECR)	N				

POINT NO. 1

0.283755E+02	0.263687E+02	0.189600E+01	0.170000E+01	0.120507E+08	0.300775E+05	0.202593E+00
0.189944E+04	0.374381E-06	0.237520E-02	0.519645E+03	0.530000E+03	0.788847E-03	0.633714E+00
0.349474E+00	0.300135E-01	0.540088E-01	0.180251E+01	0.846341E+00	0.671866E+00	0.962009E+00
0.000000E+00	0.000000E+00	0.000000E+00	0.100080E-02	0.857629E+01	0.200095E-02	0.000000E+00
0.112397E+02	0.434220E-01	0.753040E+01				
0.307368E+02						

POINT NO. 2

0.284380E+02	0.264612E+02	0.189600E+01	0.170000E+01	0.120507E+08	0.301403E+05	0.202593E+00
0.189944E+04	0.374381E-06	0.237520E-02	0.519645E+03	0.530000E+03	0.788847E+03	0.633714E+00
0.349255E+00	0.300761E-01	0.542106E-01	0.180245E+01	0.846341E+00	0.671866E+00	0.962009E+00
0.000000E+00	0.000000E+00	0.000000E+00	0.100047E-02	0.857346E+01	0.200095E-02	0.000000E+00
0.112397E+02	0.434220E-01	0.753225E+00				
0.307953E+02						

* WALL RESULTS *

X(INCHES)	DELSTAR(INCHES)	YCORE+DELSTAR	MWALL	DELTAY	YCORE+DELTAY
0.318238E+00	0.197801E-03	0.142360E+01	0.111979E+01	0.338726E-03	0.142374E+01
0.333082E+00	0.280479E-03	0.142414E+01	0.112352E+01	0.480121E-03	0.142434E+01
0.348089E+00	0.353288E-03	0.142470E+01	0.112726E+01	0.604827E-03	0.142495E+01

```

graph TD
    A["**** INPUT DATA ****"] --> B["CARD 1"]
    A --> C["CARD 2"]
    A --> D["CARD 3"]
    B --> E["FUNCTIONAL MODES"]
    C --> F["FLOW CONDITIONS AND NOZZLE DIMENSIONS"]
    D --> G["INPUT DATA"]
    E --> H["OUTPUT CODE"]
    F --> I["OUTPUT CODE"]
    G --> J["OUTPUT CODE"]
    H --> K["FINAL RESULTS"]
    I --> L["FINAL RESULTS"]
    J --> M["FINAL RESULTS"]

```

Figure E5. Example Showing the Format of File "outpt3"

2. Flow Conditions and Nozzle Dimensions

TRCON = 0.000000E+00	(Reynolds number value or "x" length depending on the option set in the Transition Indication Mode)
THZERO = 0.100000E-04	(Momentum thickness at nozzle throat)
PO = 0.726000E+02	(Stagnation pressure)
TO = 0.820000E+03	(Stagnation temperature)
TWALL = 0.520000E+03	(Wall temperature when INDTW = 1)
XTEND = 0.265000E+02	(Extension length past nozzle exit plane)
DL = 0.625000E-01	(Increment in "x" of extension length)
GAMMA = 0.140000E+01	(Ratio of specific heats)
OMEGA = 0.76000E+00	(Viscosity-Temperature exponent)
WATE = 0.290000E+02	(Molecular weight of gas)
CP = 0.240000E+00	(Specific heat of gas)
PR = 0.720000E+00	(Prandtl number)
XINC = 0.000000E+00	(Not applicable; hardwired value)

3. Input Data from "outpt2" - Data generated from the inviscid contour software "char6".
4. Output Code - Constitutes the flow properties along the contour of the nozzle calculated by "nbl6" for each set of coordinates that define the nozzle contour.

X (IN)	x - coordinate of contour point
S (IN)	Contour length
Y (IN)	y - coordinate of contour point
M	Mach number along contour
REL (1/FT)	$REL = (\rho U_E)/\mu$
RETH	Reynolds Number; $RETH = (REL)(\Theta)$

PE/PO	Static Pressure / Total Pressure
UE(FT/SEC)	Velocity
MUE (PSEC/FT2)	Absolute Viscosity (μ)
RHOE (PSEC2/FT4)	Density (ρ)
TE (R)	Static Temperature
TW (R)	Wall Temperature
TAD (R)	Adiabatic Wall Temperature
TE/TO	Static Temperature / Total Temperature
DELTA (IN)	Boundary Layer Thickness (δ)
THETA (IN)	Momentum Thickness (θ)
DELSTAR (IN)	Boundary Layer Displacement (δ^*)
H	Form Factor ($H = \delta^*/\theta$)
TW/TO	Wall Temperature / Total Temperature
TW/TAD	Wall Temperature / Adiabatic Wall Temperature
TAD/TO	Adiabatic Wall Temperature / Total Temperature
DPDS (P/FT2)	Change in pressure with respect to surface distance
DMDS (1/FT)	Change in Mach number with respect to surface distance
DUDS (1/SEC)	Change in velocity with respect to surface distance
DTHDS	Change in momentum thickness with respect to surface distance
TAUWAL (P/FT2)	Wall shear stress (τ_w)
CF	Friction Coefficient
Q (BTU/FT2/SEC)	Local rate of heat transfer
HA (BTU/FT2-SEC-R)	Convection heat transfer coefficient

5. Final Results - Modified contour output as calculated by "nbl6"

X (INCHES)	x - coordinate of modified contour
DELSTAR (INCHES)	Boundary layer displacement thickness
YCORE+DELSTAR	Modified contour accounting for boundary layer growth on contoured wall only
MWALL	Mach number at the wall
DELTAY	Modified displacement thickness as determined by the equation modeled by Demo [Ref. 28: p.24].

YCORE+DELTAY

Modified contour accounting for the
boundary layer effects contributed by the
side walls

C. PROGRAM LISTINGS

Listings are given as follows:

1. Program "char6"
2. Program "nbl6"

Program "char6"

卷之三

Page 1

BRIEF REPORTS

```

903 WRITE(*,35) LENGTH
35 FORMAT(IX,'//',INDICATE CHARACTERISTIC HORIZONTAL LENGTH TO BE'
      ', READ 1-EXIT LENGTH, //',2-START OF TEST RHOMBUS,')
      READ(*,16) TYPITH
      FORMATT(16) TYPITH
      IF (TYPITH .NE. '1' .AND. TYPITH .NE. '2') THEN
        GO TO 903
      END IF
      IF (TYPITH .GE. 'A' .AND. TYPITH .LE. 'Z') THEN
        GO TO 903
      END IF

904 WRITE(*,37) LENGTH
37 FORMAT(IX,'//',INDICATE OUTPUT, 1-STEP-BY-STEP,
      1-2-HALF POINTS ONLY)
      READ(*,38) TYPOUT
      FORMATT(38) TYPOUT
      IF (TYPOUT .NE. '1' .AND. TYPOUT .NE. '2') THEN
        GO TO 904
      END IF
      IF (TYPOUT .GE. 'A' .AND. TYPOUT .LE. 'Z') THEN
        GO TO 904
      END IF

DISPLAY INPUT RESULTS

      IF (TYPNOZ .EQ. '1') THEN
        WRITE(*,11) NOZZLE
        11 FORMAT(IX,'1',NOZZLE = ',TYPE1
          FORMAT(1X,'1',NOZZLE = ',TYPE1
          ELSE IF (TYPNOZ .EQ. '2') THEN
            WRITE(*,12) NOZZLE
            12 FORMAT(IX,'2',NOZZLE = ',TYPE2
            ELSE
              WRITE(*,1662) NOZZLE = ',TYPE3
              FORMAT(1X,'2',NOZZLE = ',TYPE3
            END IF

```

```

IF (TYPINGT *EQ. '1') THEN
  WRITE(*,1053) HEIGHT TO BE READ =
  1063 FORMAT(1X,/,A20,A4)
ELSE
  WRITE(*,1064) HEIGHT TO BE READ =
  1064 FORMAT(1X,/,A20,A6)
END IF

IF (TYPINGT *EQ. '1') THEN
  WRITE(*,1065) LENGTH TO BE READ =
  1065 FORMAT(1X,/,A20,A4)
ELSE
  WRITE(*,1066) LENGTH TO BE READ =
  1066 FORMAT(1X,/,A20,A17)
END IF

IF (TYPINGT *EQ. '1') THEN
  WRITE(*,1067) OUTPUT FORMAT =
  1067 FORMAT(1X,/,A16,A12)
ELSE
  WRITE(*,1068) OUTPUT FORMAT =
  1068 FORMAT(1X,/,A16,A11)
END IF

```

C C C CHANGES TO INPUT IF NECESSARY

Program "char6" (cont.)

<pre> JUL 11 1996 16:04:49 char6.f Page 5 ELSE IF (TYPNO2 .EQ. '2') THEN WRITE(*,1011) NOZZLE = ,TYPE2 ELSE WRITE(*,1012) NOZZLE = ,TYPE3 FORMAT(IX//,A9,A7) END IF 1073 IF (TYPHGT .EQ. '1') THEN WRITE(*,1073) HEIGHT TO BE READ = ,HGT1 FORMAT(IX//,A20,A4) ELSE WRITE(*,1074) HEIGHT TO BE READ = ,HGT2 FORMAT(IX//,A20,A6) END IF 1074 IF (TYPLTH .EQ. '1') THEN WRITE(*,1075) LENGTH TO BE READ = ,LGTH1 FORMAT(IX//,A20,A4) ELSE WRITE(*,1076) LENGTH TO BE READ = ,LGTH2 FORMAT(IX//,A20,A17) END IF 1075 IF (TYPOUT .EQ. '1') THEN WRITE(*,1077) OUTPUT FORMAT = ,OUTPT1 FORMAT(IX//,A16,A12) ELSE WRITE(*,1078) OUTPUT FORMAT = ,OUTPT2 FORMAT(IX//,A16,A11) END IF 1076 WRITE(*,910) FORMAT(IX//,'ANY OTHER CHANGES?, 1-YES, 2-NO') FORMAT(IX//,A16,A11) 1077 910 FORMAT(IX//,A16,A11) READ(*,911) INDSR IF (INOUT .NE. 1 .AND. INOUT .NE. 2) THEN GO TO 1020 END IF IF (INOUT .EQ. 1) THEN GO TO 1030 END IF END IF END IF </pre>	<pre> C CONVERSION TO INTEGER FORMAT C IF (TYPNO2 .EQ. '1') THEN INDTH=1 ELSE IF (TYPNO2 .EQ. '2') THEN INDTH=2 END IF IF (TYPLTH .EQ. '1') THEN INDATE=1 ELSE INDATE=2 END IF IF (TYPHGT .EQ. '1') THEN INDYTH=1 ELSE INDYTH=2 END IF IF (TYPOUT .EQ. '1') THEN INDOUT=1 ELSE INDOUT=2 END IF </pre>
<pre> 1071 WRITE(*,1011) NOZZLE = ,TYPE2 1072 FORMAT(IX//,A9,A7) 1073 IF (TYPHGT .EQ. '1') THEN WRITE(*,1073) HEIGHT TO BE READ = ,HGT1 FORMAT(IX//,A20,A4) ELSE WRITE(*,1074) HEIGHT TO BE READ = ,HGT2 FORMAT(IX//,A20,A6) END IF 1074 IF (TYPLTH .EQ. '1') THEN WRITE(*,1075) LENGTH TO BE READ = ,LGTH1 FORMAT(IX//,A20,A4) ELSE WRITE(*,1076) LENGTH TO BE READ = ,LGTH2 FORMAT(IX//,A20,A17) END IF 1075 IF (TYPOUT .EQ. '1') THEN WRITE(*,1077) OUTPUT FORMAT = ,OUTPT1 FORMAT(IX//,A16,A12) ELSE WRITE(*,1078) OUTPUT FORMAT = ,OUTPT2 FORMAT(IX//,A16,A11) END IF 1076 WRITE(*,910) FORMAT(IX//,'ANY OTHER CHANGES?, 1-YES, 2-NO') FORMAT(IX//,A16,A11) READ(*,911) INDSR IF (INOUT .NE. 1 .AND. INOUT .NE. 2) THEN GO TO 1020 END IF IF (INOUT .EQ. 1) THEN GO TO 1030 END IF END IF END IF </pre>	<pre> C NOZZLE FLOW CHARACTERISTICS AND SPECIFIC GEOMETRY INPUTS C WRITE(*,21) 21 FORMAT(IX//,'THE NEXT SET OF INPUTS SPECIFY FLOW 1, CHARACTERISTICS AND SPECIFIC //,18/, GEOMETRY DIMENSIONS' 2, FOR THE NOZZLE') WRITE(*,22) 22 FORMAT(IX//,'8X, ***** PLEASE UTILIZE DECIMAL POINTS FOR THESE 1, INPUTS *****') ERROR=0 500 WRITE(*,51) 51 FORMAT(IX//,'INPUT RATIO OF SPECIFIC HEATS') READ(*,52,STAT=ERROR) GAMMA 52 FORMAT(E10.5) IF (ERROR .GT. 0) THEN GO TO 500 END IF ERROR=0 505 WRITE(*,53) 53 FORMAT(IX//,'INPUT TEST SECTION MACH NUMBER') READ(*,54,STAT=ERROR) SMT 54 FORMAT(E10.5) IF (ERROR .GT. 0) THEN GO TO 505 END IF IF (INDATE .EQ. 1) THEN ERROR=0 510 WRITE(*,55) 55 FORMAT(IX//,'INPUT EXIT LENGTH (INCHES)') READ(*,56,STAT=ERROR) XEXT 56 FORMAT(E10.5) IF (ERROR .GT. 0) THEN GO TO 515 END IF ELSE ERROR=0 515 WRITE(*,57) 57 FORMAT(IX//,'INPUT BEGINNING OF TEST RHOMBUS (INCHES)') READ(*,58,STAT=ERROR) XEXT 58 FORMAT(IX//,'INPUT HALF HEIGHT OF EXIT (INCHES)') READ(*,59,STAT=ERROR) YTHEX 59 FORMAT(IX//,'INPUT HALF HEIGHT OF THROAT (INCHES)') 61 FORMAT(E10.5) IF (ERROR .GT. 0) THEN GO TO 520 END IF END IF IF (INDYTH .EQ. 1) THEN ERROR=0 520 WRITE(*,59) 59 FORMAT(IX//,'INPUT HALF HEIGHT OF THROAT (INCHES)') READ(*,61,STAT=ERROR) YTHEX 61 FORMAT(E10.5) IF (ERROR .GT. 0) THEN GO TO 520 END IF ELSE ERROR=0 525 WRITE(*,62) 62 FORMAT(IX//,'INPUT HALF HEIGHT OF THROAT (INCHES)') READ(*,63,STAT=ERROR) YTHEX 63 FORMAT(E10.5) END IF </pre>

Program "char6" (cont.)

```

Page 8
 108 116449 charge 1

      550      WRITE(*,81)
      551      FORMAT(1X,'//',INPUT NEW VALUE FOR XEXT')
      552      READ(*,102,IOSTAT=ERROR) XEXT
      553      FORMAT(10.5)
      554      IF (ERROR .GT. 0) THEN
      555          END IF
      556          GO TO 550
      557      END IF

      558      IF (INCHG .EQ. 4) THEN
      559          ERROR=0
      560          WRITE(*,83)
      561          FORMAT(1X,'//',INPUT NEW VALUE FOR YTHEX')
      562          READ(*,104,IOSTAT=ERROR) YTHEX
      563          FORMAT(10.5)
      564          IF (ERROR .GT. 0) THEN
      565              END IF
      566              GO TO 555
      567      END IF

      568      IF (INCHG .EQ. 5) THEN
      569          ERROR=0
      570          WRITE(*,86)
      571          FORMAT(1X,'//',INPUT NEW VALUE FOR RCT')
      572          READ(*,107,IOSTAT=ERROR) RCT
      573          FORMAT(10.5)
      574          IF (ERROR .GT. 0) THEN
      575              END IF
      576              GO TO 560
      577      END IF

      578      IF (INCHG .EQ. 6) THEN
      579          ERROR=0
      580          WRITE(*,88)
      581          FORMAT(1X,'//',INPUT NEW VALUE FOR DELMUL')
      582          READ(*,109,IOSTAT=ERROR) DELMUL
      583          FORMAT(10.5)
      584          IF (ERROR .GT. 0) THEN
      585              END IF
      586              GO TO 565
      587      END IF

      588      IF (INCHG .EQ. 96) THEN
      589          GAMMA = 'GAMMA'
      590          SMT = 'SMT'
      591          XEXT = 'XEXT'
      592          YTHEX = 'YTHEX'
      593          RCT = 'RCT'
      594          DELMUL = 'DELMUL'
      595          INNEXT = 'INNEXT'
      596          INNXKT = 'INNXKT'
      597          NE = 'NE'
      598          1YES = '1-YES'
      599          2NO = '2-NO'
      600          1INNKT = '1-INNKT'
      601          2INNKT = '2-INNKT'
      602          1INEXT = '1-INEXT'
      603          2INEXT = '2-INEXT'
      604          1INNXKT = '1-INNXKT'
      605          2INNXKT = '2-INNXKT'
      606          1NE = '1-NE'
      607          2NE = '2-NE'
      608          11YES = '1-1YES'
      609          21NO = '2-1NO'
      610          12YES = '1-2YES'
      611          22NO = '2-2NO'
      612          11INNKT = '1-1INNKT'
      613          21INNKT = '2-1INNKT'
      614          12INNKT = '1-2INNKT'
      615          22INNKT = '2-2INNKT'
      616          11INEXT = '1-1INEXT'
      617          21INEXT = '2-1INEXT'
      618          12INEXT = '1-2INEXT'
      619          22INEXT = '2-2INEXT'
      620          11INNXKT = '1-1INNXKT'
      621          21INNXKT = '2-1INNXKT'
      622          12INNXKT = '1-2INNXKT'
      623          22INNXKT = '2-2INNXKT'
      624          11NE = '1-1NE'
      625          21NE = '2-1NE'
      626          12NE = '1-2NE'
      627          22NE = '2-2NE'
      628          111YES = '1-1-1YES'
      629          211NO = '2-1-1NO'
      630          121YES = '1-2-1YES'
      631          221NO = '2-2-1NO'
      632          112YES = '1-1-2YES'
      633          212NO = '2-1-2NO'
      634          122YES = '1-2-2YES'
      635          222NO = '2-2-2NO'
      636          111INNKT = '1-1-1INNKT'
      637          211INNKT = '2-1-1INNKT'
      638          121INNKT = '1-2-1INNKT'
      639          221INNKT = '2-2-1INNKT'
      640          111INEXT = '1-1-1INEXT'
      641          211INEXT = '2-1-1INEXT'
      642          121INEXT = '1-2-1INEXT'
      643          221INEXT = '2-2-1INEXT'
      644          111INNXKT = '1-1-1INNXKT'
      645          211INNXKT = '2-1-1INNXKT'
      646          121INNXKT = '1-2-1INNXKT'
      647          221INNXKT = '2-2-1INNXKT'
      648          111NE = '1-1-1NE'
      649          211NE = '2-1-1NE'
      650          121NE = '1-2-1NE'
      651          221NE = '2-2-1NE'
      652          112INNKT = '1-1-2INNKT'
      653          212INNKT = '2-1-2INNKT'
      654          122INNKT = '1-2-2INNKT'
      655          222INNKT = '2-2-2INNKT'
      656          112INEXT = '1-1-2INEXT'
      657          212INEXT = '2-1-2INEXT'
      658          122INEXT = '1-2-2INEXT'
      659          222INEXT = '2-2-2INEXT'
      660          112INNXKT = '1-1-2INNXKT'
      661          212INNXKT = '2-1-2INNXKT'
      662          122INNXKT = '1-2-2INNXKT'
      663          222INNXKT = '2-2-2INNXKT'
      664          112NE = '1-1-2NE'
      665          212NE = '2-1-2NE'
      666          122NE = '1-2-2NE'
      667          222NE = '2-2-2NE'
      668          1111YES = '1-1-1-1YES'
      669          2111NO = '2-1-1-1NO'
      670          1211YES = '1-2-1-1YES'
      671          2211NO = '2-2-1-1NO'
      672          1121YES = '1-1-2-1YES'
      673          2121NO = '2-1-2-1NO'
      674          1221YES = '1-2-2-1YES'
      675          2221NO = '2-2-2-1NO'
      676          1112YES = '1-1-1-2YES'
      677          2112NO = '2-1-1-2NO'
      678          1212YES = '1-2-1-2YES'
      679          2212NO = '2-2-1-2NO'
      680          1122YES = '1-1-2-2YES'
      681          2122NO = '2-1-2-2NO'
      682          1222YES = '1-2-2-2YES'
      683          2222NO = '2-2-2-2NO'
      684          1111INNKT = '1-1-1-1INNKT'
      685          2111INNKT = '2-1-1-1INNKT'
      686          1211INNKT = '1-2-1-1INNKT'
      687          2211INNKT = '2-2-1-1INNKT'
      688          1112INNKT = '1-1-1-2INNKT'
      689          2112INNKT = '2-1-1-2INNKT'
      690          1212INNKT = '1-2-1-2INNKT'
      691          2212INNKT = '2-2-1-2INNKT'
      692          1121INNKT = '1-1-2-1INNKT'
      693          2121INNKT = '2-1-2-1INNKT'
      694          1221INNKT = '1-2-2-1INNKT'
      695          2221INNKT = '2-2-2-1INNKT'
      696          1122INNKT = '1-1-2-2INNKT'
      697          2122INNKT = '2-1-2-2INNKT'
      698          1222INNKT = '1-2-2-2INNKT'
      699          2222INNKT = '2-2-2-2INNKT'
      700          1111INEXT = '1-1-1-1INEXT'
      701          2111INEXT = '2-1-1-1INEXT'
      702          1211INEXT = '1-2-1-1INEXT'
      703          2211INEXT = '2-2-1-1INEXT'
      704          1112INEXT = '1-1-1-2INEXT'
      705          2112INEXT = '2-1-1-2INEXT'
      706          1212INEXT = '1-2-1-2INEXT'
      707          2212INEXT = '2-2-1-2INEXT'
      708          1121INEXT = '1-1-2-1INEXT'
      709          2121INEXT = '2-1-2-1INEXT'
      710          1221INEXT = '1-2-2-1INEXT'
      711          2221INEXT = '2-2-2-1INEXT'
      712          1122INEXT = '1-1-2-2INEXT'
      713          2122INEXT = '2-1-2-2INEXT'
      714          1222INEXT = '1-2-2-2INEXT'
      715          2222INEXT = '2-2-2-2INEXT'
      716          1111INNXKT = '1-1-1-1INNXKT'
      717          2111INNXKT = '2-1-1-1INNXKT'
      718          1211INNXKT = '1-2-1-1INNXKT'
      719          2211INNXKT = '2-2-1-1INNXKT'
      720          1112INNXKT = '1-1-1-2INNXKT'
      721          2112INNXKT = '2-1-1-2INNXKT'
      722          1212INNXKT = '1-2-1-2INNXKT'
      723          2212INNXKT = '2-2-1-2INNXKT'
      724          1121INNXKT = '1-1-2-1INNXKT'
      725          2121INNXKT = '2-1-2-1INNXKT'
      726          1221INNXKT = '1-2-2-1INNXKT'
      727          2221INNXKT = '2-2-2-1INNXKT'
      728          1122INNXKT = '1-1-2-2INNXKT'
      729          2122INNXKT = '2-1-2-2INNXKT'
      730          1222INNXKT = '1-2-2-2INNXKT'
      731          2222INNXKT = '2-2-2-2INNXKT'
      732          1111NE = '1-1-1-1NE'
      733          2111NE = '2-1-1-1NE'
      734          1211NE = '1-2-1-1NE'
      735          2211NE = '2-2-1-1NE'
      736          1112NE = '1-1-1-2NE'
      737          2112NE = '2-1-1-2NE'
      738          1212NE = '1-2-1-2NE'
      739          2212NE = '2-2-1-2NE'
      740          1121NE = '1-1-2-1NE'
      741          2121NE = '2-1-2-1NE'
      742          1221NE = '1-2-2-1NE'
      743          2221NE = '2-2-2-1NE'
      744          1122NE = '1-1-2-2NE'
      745          2122NE = '2-1-2-2NE'
      746          1222NE = '1-2-2-2NE'
      747          2222NE = '2-2-2-2NE'
      748          11111YES = '1-1-1-1-1YES'
      749          21111NO = '2-1-1-1-1NO'
      750          12111YES = '1-2-1-1-1YES'
      751          22111NO = '2-2-1-1-1NO'
      752          11211YES = '1-1-2-1-1YES'
      753          21211NO = '2-1-2-1-1NO'
      754          12211YES = '1-2-2-1-1YES'
      755          22211NO = '2-2-2-1-1NO'
      756          11121YES = '1-1-1-2-1YES'
      757          21121NO = '2-1-1-2-1NO'
      758          12121YES = '1-2-1-2-1NO'
      759          22121NO = '2-2-1-2-1NO'
      760          11221YES = '1-1-2-2-1YES'
      761          21221NO = '2-1-2-2-1NO'
      762          12221YES = '1-2-2-2-1NO'
      763          22221NO = '2-2-2-2-1NO'
      764          11112YES = '1-1-1-1-2YES'
      765          21112NO = '2-1-1-1-2NO'
      766          12112YES = '1-2-1-1-2YES'
      767          22112NO = '2-2-1-1-2NO'
      768          11212YES = '1-1-2-1-2YES'
      769          21212NO = '2-1-2-1-2NO'
      770          12212YES = '1-2-2-1-2NO'
      771          22212NO = '2-2-2-1-2NO'
      772          11122YES = '1-1-1-2-2YES'
      773          21122NO = '2-1-1-2-2NO'
      774          12122YES = '1-2-1-2-2NO'
      775          22122NO = '2-2-1-2-2NO'
      776          11222YES = '1-1-2-2-2YES'
      777          21222NO = '2-1-2-2-2NO'
      778          12222YES = '1-2-2-2-2NO'
      779          22222NO = '2-2-2-2-2NO'
      780          11111INNKT = '1-1-1-1-1INNKT'
      781          21111INNKT = '2-1-1-1-1INNKT'
      782          12111INNKT = '1-2-1-1-1INNKT'
      783          22111INNKT = '2-2-1-1-1INNKT'
      784          11121INNKT = '1-1-1-2-1INNKT'
      785          21121INNKT = '2-1-1-2-1INNKT'
      786          12121INNKT = '1-2-1-2-1INNKT'
      787          22121INNKT = '2-2-1-2-1INNKT'
      788          11212INNKT = '1-1-2-1-2INNKT'
      789          21212INNKT = '2-1-2-1-2INNKT'
      790          12212INNKT = '1-2-2-1-2INNKT'
      791          22212INNKT = '2-2-2-1-2INNKT'
      792          11122INNKT = '1-1-1-2-2INNKT'
      793          21122INNKT = '2-1-1-2-2INNKT'
      794          12122INNKT = '1-2-1-2-2INNKT'
      795          22122INNKT = '2-2-1-2-2INNKT'
      796          11222INNKT = '1-1-2-2-2INNKT'
      797          21222INNKT = '2-1-2-2-2INNKT'
      798          12222INNKT = '1-2-2-2-2INNKT'
      799          22222INNKT = '2-2-2-2-2INNKT'
      800          11111INEXT = '1-1-1-1-1INEXT'
      801          21111INEXT = '2-1-1-1-1INEXT'
      802          12111INEXT = '1-2-1-1-1INEXT'
      803          22111INEXT = '2-2-1-1-1INEXT'
      804          11121INEXT = '1-1-1-2-1INEXT'
      805          21121INEXT = '2-1-1-2-1INEXT'
      806          12121INEXT = '1-2-1-2-1INEXT'
      807          22121INEXT = '2-2-1-2-1INEXT'
      808          11212INEXT = '1-1-2-1-2INEXT'
      809          21212INEXT = '2-1-2-1-2INEXT'
      810          12212INEXT = '1-2-2-1-2INEXT'
      811          22212INEXT = '2-2-2-1-2INEXT'
      812          11122INEXT = '1-1-1-2-2INEXT'
      813          21122INEXT = '2-1-1-2-2INEXT'
      814          12122INEXT = '1-2-1-2-2INEXT'
      815          22122INEXT = '2-2-1-2-2INEXT'
      816          11222INEXT = '1-1-2-2-2INEXT'
      817          21222INEXT = '2-1-2-2-2INEXT'
      818          12222INEXT = '1-2-2-2-2INEXT'
      819          22222INEXT = '2-2-2-2-2INEXT'
      820          11111INNXKT = '1-1-1-1-1INNXKT'
      821          21111INNXKT = '2-1-1-1-1INNXKT'
      822          12111INNXKT = '1-2-1-1-1INNXKT'
      823          22111INNXKT = '2-2-1-1-1INNXKT'
      824          11121INNXKT = '1-1-1-2-1INNXKT'
      825          21121INNXKT = '2-1-1-2-1INNXKT'
      826          12121INNXKT = '1-2-1-2-1INNXKT'
      827          22121INNXKT = '2-2-1-2-1INNXKT'
      828          11212INNXKT = '1-1-2-1-2INNXKT'
      829          21212INNXKT = '2-1-2-1-2INNXKT'
      830          12212INNXKT = '1-2-2-1-2INNXKT'
      831          22212INNXKT = '2-2-2-1-2INNXKT'
      832          11122INNXKT = '1-1-1-2-2INNXKT'
      833          21122INNXKT = '2-1-1-2-2INNXKT'
      834          12122INNXKT = '1-2-1-2-2INNXKT'
      835          22122INNXKT = '2-2-1-2-2INNXKT'
      836          11222INNXKT = '1-1-2-2-2INNXKT'
      837          21222INNXKT = '2-1-2-2-2INNXKT'
      838          12222INNXKT = '1-2-2-2-2INNXKT'
      839          22222INNXKT = '2-2-2-2-2INNXKT'
      840          11111NE = '1-1-1-1-1NE'
      841          21111NE = '2-1-1-1-1NE'
      842          12111NE = '1-2-1-1-1NE'
      843          22111NE = '2-2-1-1-1NE'
      844          11121NE = '1-1-1-2-1NE'
      845          21121NE = '2-1-1-2-1NE'
      846          12121NE = '1-2-1-2-1NE'
      847          22121NE = '2-2-1-2-1NE'
      848          11212NE = '1-1-2-1-2NE'
      849          21212NE = '2-1-2-1-2NE'
      850          12212NE = '1-2-2-1-2NE'
      851          22212NE = '2-2-2-1-2NE'
      852          11122NE = '1-1-1-2-2NE'
      853          21122NE = '2-1-1-2-2NE'
      854          12122NE = '1-2-1-2-2NE'
      855          22122NE = '2-2-1-2-2NE'
      856          11222NE = '1-1-2-2-2NE'
      857          21222NE = '2-1-2-2-2NE'
      858          12222NE = '1-2-2-2-2NE'
      859          22222NE = '2-2-2-2-2NE'
      860          111111YES = '1-1-1-1-1-1YES'
      861          211111NO = '2-1-1-1-1-1NO'
      862          121111YES = '1-2-1-1-1-1YES'
      863          221111NO = '2-2-1-1-1-1NO'
      864          111211YES = '1-1-1-2-1-1YES'
      865          211211NO = '2-1-1-2-1-1NO'
      866          121211YES = '1-2-1-2-1-1YES'
      867          221211NO = '2-2-1-2-1-1NO'
      868          112121YES = '1-1-2-1-2-1YES'
      869          212121NO = '2-1-2-1-2-1NO'
      870          122121YES = '1-2-2-1-2-1NO'
      871          222121NO = '2-2-2-1-2-1NO'
      872          111221YES = '1-1-1-2-2-1YES'
      873          211221NO = '2-1-1-2-2-1NO'
      874          121221YES = '1-2-1-2-2-1NO'
      875          221221NO = '2-2-1-2-2-1NO'
      876          112221YES = '1-1-2-2-2-1YES'
      877          212221NO = '2-1-2-2-2-1NO'
      878          122221YES = '1-2-2-2-2-1NO'
      879          222221NO = '2-2-2-2-2-1NO'
      880          111111INNKT = '1-1-1-1-1-1INNKT'
      881          211111INNKT = '2-1-1-1-1-1INNKT'
      882          121111INNKT = '1-2-1-1-1-1INNKT'
      883          221111INNKT = '2-2-1-1-1-1INNKT'
      884          111211INNKT = '1-1-1-2-1-1INNKT'
      885          211211INNKT = '2-1-1-2-1-1INNKT'
      886          121211INNKT = '1-2-1-2-1-1INNKT'
      887          221211INNKT = '2-2-1-2-1-1INNKT'
      888          112121INNKT = '1-1-2-1-2-1INNKT'
      889          212121INNKT = '2-1-2-1-2-1INNKT'
      890          122121INNKT = '1-2-2-1-2-1INNKT'
      891          222121INNKT = '2-2-2-1-2-1INNKT'
      892          111221INNKT = '1-1-1-2-2-1INNKT'
      893          211221INNKT = '2-1-1-2-2-1INNKT'
      894          121221INNKT = '1-2-1-2-2-1INNKT'
      895          221221INNKT = '2-2-1-2-2-1INNKT'
      896          112221INNKT = '1-1-2-2-2-1INNKT'
      897          212221INNKT = '2-1-2-2-2-1INNKT'
      898          122221INNKT = '1-2-2-2-2-1INNKT'
      899          222221INNKT = '2-2-2-2-2-1INNKT'
      900          111111INEXT = '1-1-1-1-1-1INEXT'
      901          211111INEXT = '2-1-1-1-1-1INEXT'
      902          121111INEXT = '1-2-1-1-1-1INEXT'
      903          221111INEXT = '2-2-1-1-1-1INEXT'
      904          111211INEXT = '1-1-1-2-1-1INEXT'
      905          211211INEXT = '2-1-1-2-1-1INEXT'
      906          121211INEXT = '1-2-1-2-1-1INEXT'
      907          221211INEXT = '2-2-1-2-1-1INEXT'
      908          112121INEXT = '1-1-2-1-2-1INEXT'
      909          212121INEXT = '2-1-2-1-2-1INEXT'
      910          122121INEXT = '1-2-2-1-2-1INEXT'
      911          222121INEXT = '2-2-2-1-2-1INEXT'
      912          111221INEXT = '1-1-1-2-2-1INEXT'
      913          211221INEXT = '2-1-1-2-2-1INEXT'
      914          121221INEXT = '1-2-1-2-2-1INEXT'
      915          221221INEXT = '2-2-1-2-2-1INEXT'
      916          112221INEXT = '1-1-2-2-2-1INEXT'
      917          212221INEXT = '2-1-2-2-2-1INEXT'
      918          122221INEXT = '1-2-2-2-2-1INEXT'
      919          222221INEXT = '2-2-2-2-2-1INEXT'
      920          111111INNXKT = '1-1-1-1-1-1INNXKT'
      921          211111INNXKT = '2-1-1-1-1-1INNXKT'
      922          121111INNXKT = '1-2-1-1-1-1INNXKT'
      923          221111INNXKT = '2-2-1-1-1-1INNXKT'
      924          111211INNXKT = '1-1-1-2-1-1INNXKT'
      925          211211INNXKT = '2-1-1-2-1-1INNXKT'
      926          121211INNXKT = '1-2-1-2-1-1INNXKT'
      927          221211INNXKT = '2-2-1-2-1-1INNXKT'
      928          112121INNXKT = '1-1-2-1-2-1INNXKT'
      929          212121INNXKT = '2-1-2-1-2-1INNXKT'
      930          122121INNXKT = '1-2-2-1-2-1INNXKT'
      931          222121INNXKT = '2-2-2-1-2-1INNXKT'
      932          111221INNXKT = '1-1-1-2-2-1INNXKT'
      933          211221INNXKT = '2-1-1-2-2-1INNXKT'
      934          121221INNXKT = '1-2-1-2-2-1INNXKT'
      935          221221INNXKT = '2-2-1-2-2-1INNXKT'
      936          112221INNXKT = '1-1-2-2-2-1INNXKT'
      937          212221INNXKT = '2-1-2-2-2-1INNXKT'
      938          122221INNXKT = '1-2-2-2-2-1INNXKT'
      939          222221INNXKT = '2-2-2-2-2-1INNXKT'
      940          111111NE = '1-1-1-1-1-1NE'
      941          211111NE = '2-1-1-1-1-1NE'
      942          121111NE = '1-2-1-1-1-1NE'
      943          221111NE = '2-2-1-1-1-1NE'
      944          111211NE = '1-1-1-2-1-1NE'
      945          211211NE = '2-1-1-2-1-1NE'
      946          121211NE = '1-2-1-2-1-1NE'
      947          221211NE = '2-2-1-2-1-1NE'
      948          112121NE = '1-1-2-1-2-1NE'
      949          212121NE = '2-1-2-1-2-1NE'
      950          122121NE = '1-2-2-1-2-1NE'
      951          222121NE = '2-2-2-1-2-1NE'
      952          111221NE = '1-1-1-2-2-1NE'
      953          211221NE = '2-1-1-2-2-1NE'
      954          121221NE = '1-2-1-2-2-1NE'
      955          221221NE = '2-2-1-2-2-1NE'
      956          112221NE = '1-1-2-2-2-1NE'
      957          212221NE = '2-1-2-2-2-1NE'
      958          122221NE = '1-2-2-2-2-1NE'
      959          222221NE = '2-2-2-2-2-1NE'
      960          1111111YES = '1-1-1-1-1-1-1YES'
      961          2111111NO = '2-1-1-1-1-1-1NO'
      962          1211111YES = '1-2-1-1-1-1-1YES'
      963          2211111NO = '2-2-1-1-1-1-1NO'
      964          1112111YES = '1-1-1-2-1-1-1YES'
      965          2112111NO = '2-1-1-2-1-1-1NO'
      966          1212111YES = '1-2-1-2-1-1-1YES'
      967          2212111NO = '2-2-1-2-1-1-1NO'
      968          1121211YES = '1-1-2-1-2-1-1YES'
      969          2121211NO = '2-1-2-1-2-1-1NO'
      970          1221211YES = '1-2-2-1-2-1-1YES'
      971          2221211NO = '2-2-2-1-2-1-1NO'
      972          1112211YES = '1-1-1-2-2-1-1YES'
      973          2112211NO = '2-1-1-2-2-1-1NO'
      974          1212211YES = '1-2-1-2-2-1-1YES'
      975          2212211NO = '2-2-1-2-2-1-1NO'
      976          1122211YES = '1-1-2-2-2-1-1YES'
      977          2122211NO = '2-1-2-2-2-1-1NO'
      978          1222211YES = '1-2-2-2-2-1-1YES'
      979          2222211NO = '2-2-2-2-2-1-1NO'
      980          1111111INNKT = '1-1-1-1-1-1INNKT'
      981          2111111INNKT = '2-1-1-1-1-1INNKT'
      982          1211111INNKT = '1-2-1-1-1-1INNKT'
      983          2211111INNKT = '2-2-1-1-1-1INNKT'
      984          1112111INNKT = '1-1-1-2-1-1INNKT'
      985          2112111INNKT = '2-1-1-2-1-1INNKT'
      986          1212111INNKT = '1-2-1-2-1-1INNKT'
      987          2212111INNKT = '2-2-1-2-1-1INNKT'
      988          1121211INNKT = '1-1-2-1-2-1INNKT'
      989          2121211INNKT = '2-1-2-1-2-1INNKT'
      990          1221211INNKT = '1-2-2-1-2-1INNKT'
      991          2221211INNKT = '2-2-2-1-2-1INNKT'
      992          1112211INNKT = '1-1-1-2-2-1INNKT'
      993          2112211INNKT = '2-1-1-2-2-1INNKT'
      994          1212211INNKT = '1-2-1-2-2-1INNKT'
      995          2212211INNKT = '2-2-1-2-2-1INNKT'
      996          1122211INNKT = '1-1-2-2-2-1INNKT'
      997          2122211INNKT = '2-1-2-2-2-1INNKT'
      998          1222211INNKT = '1-2-2-2-2-1INNKT'
      999          2222211INNKT = '2-2-2-2-2-1INNKT'
      1000         1111111INEXT = '1-1-1-1-1-1INEXT'
      1001         2111111INEXT = '2-1-1-1-1-1INEXT'
      1002         1211111INEXT = '1-2-1-1-1-1INEXT'
      1003         2211111INEXT = '2-2-1-1-1-1INEXT'
      1004         1112111INEXT = '1-1-1-2-1-1INEXT'
      1005         2112111INEXT = '2-1-1-2-1-1INEXT'
      1006         1212111INEXT = '1-2-1-2-1-1INEXT'
      1007         2212111INEXT = '2-2-1-2-1-1INEXT'
      1008         1121211INEXT = '1-1-2-1-2-1INEXT'
      1009         2121211INEXT = '2-1-2-1-2-1INEXT'
      1010         1221211INEXT = '1-2-2-1-2-1INEXT'
      1011         2221211INEXT = '2-2-2-1-2-1INEXT'
      1012         1112211INEXT = '1-1-1-2-2-1INEXT'
      1013         2112211INEXT = '2-1-1-2-2-1INEXT'
      1014         1212211INEXT = '1-2-1-2-2-1INEXT'
      1015         2212211INEXT = '2-2-1-2-2-1INEXT'
      1016         1122211INEXT = '1-1-2-2-2-1INEXT'
      1017         2122211INEXT = '2-1-2-2-2-1INEXT'
      1018         1222211INEXT = '1-2-2-2-2-1INEXT'
      1019         2222211INEXT = '2-2-2-2-2-1INEXT'
      1020         1111111INNXKT = '1-1-1-1-1-1INNX
```

```

PAGE 7
JUL 11 1996 18:04:38   chapter6.f

      IF (ERROR .GT. 0) THEN
        GO TO 525
      END IF

      ERROR=0
      520 WRITE(*, 64)
      64 FORMAT(1X //, 'INPUT RADIUS OF CURVATURE AT THROAT (INCHES) ')
      READ(*, 66, IOSTAT=ERROR) RCT
      66 FORMAT(6I0, 5)
      IF (ERROR .GT. 0) THEN
        GO TO 530
      END IF

      ERROR=0
      525 WRITE(*, 67)
      67 FORMAT(1X //, 'INPUT MULTIPLICATIVE FACTOR FOR X INCREMENT'
      1, 1.0-150.0, P5.0, 5.00 P5.0)
      READ(*, 68, IOSTAT=ERROR) DELMUL
      68 FORMAT(1I0, 5)
      IF (ERROR .GT. 0) THEN
        GO TO 525
      END IF

      C DISPLAY INPUT RESULTS
      WRITE(*, 71) 'GAMMA = ', GAMMA, 'SHT = ', SHT, 'SEXT = ', REXT,
      71 'THIX = ', THIX, 'RCT = ', RCT, 'DELMUL = ', DELMUL
      71 FORMAT(1X, 7I1, A9, E10.5, 7I5, 1X, A9, E10.5, 1I)

      C CHANGE INPUT VALUES IF NECESSARY
      800 WRITE(*, 72)
      72 FORMAT(1X //, 'ARE INPUT VALUES CORRECT, 1-YES, 2-NO')
      73 FORMAT(1I1)
      IF (INANS .NE. 1 .AND. INANS .NE. 2) THEN
        GO TO 800
      END IF

      IF (INANS .EQ. 2) THEN
        WRITE(*, 74)
        74 FORMAT(1X //, 'INPUT VALUE TO BE CHANGED: 1-GAMMA, 2-SHT, '
        1, '3-THIX, 4-RCT, 5-RCT, 6-DELMUL')
        READ(*, 75, IOSTAT=ERROR) IRCHG
        75 FORMAT(1I1)
        IF (IRCHG .EQ. 1) THEN
          WRITE(*, 76)
          76 FORMAT(1X //, 'INPUT NEW VALUE FOR GAMMA')
          READ(*, 77, IOSTAT=ERROR) GRMMA
          77 FORMAT(1I0, 5)
          IF (GRMMA .GT. 0) THEN
            GO TO 540
          END IF
        END IF
        IF (INCHG .EQ. 2) THEN
          WRITE(*, 78)
          78 FORMAT(1X //, 'INPUT NEW VALUE FOR SHT')
          READ(*, 79, IOSTAT=ERROR) SHT
          79 FORMAT(1I0, 5)
          IF (SHT .GT. 0) THEN
            GO TO 545
          END IF
        END IF
      END IF
      IF (INCHG .EQ. 3) THEN

```

JUL 11 1968 10:04:49

Page 9

Char6.f

IOT: 1998.1610479 Char6.f Page 10

```

1      SX, INDSR = ',112,/34X, INDWTH = ',112,/
2      134X, 'INDEXE = ',112,/34X, INDOU = ',112,/
3      83X, 'INDTR = ',112,/34X, INDCRD = ',112,/
4      52X, 'CRD = ',112,/34X, GARRA = '(ML(N)-XT)*TANA
5      SM(2,KAPPA)=SNT
6      A(2,KAPPA)=TANA
7      T(2,KAPPA)=0.
8      THE(2,KAPPA)=0.
9      ETA(2,KAPPA)=TANA*X(2,KAPPA)
10     IF(LASTN.GT.N) GO TO 490
11     KAPPA*KAPPA+1
12     DO 700 K=KAPPA, N
13     KO=K
14     X(2,KAPPA)=X(1,K-1)+WU*ATAN(1./((WU*A(1,K-1))*
15     ATAN(1./A(1,K-1)))
16     Y(2,KAPPA)=Y(1,K-1)+WU*ATAN(1./((WU*A(2,K-1))*
17     ATAN(1./A(2,K-1)))
18     THE(2,K)=THE(1,K-1)
19     T(2,K)=T(1,K-1)
20     SM(2,K)=SNT*THE(2,K)/COS(1./K)
21     CALL ACOM(A(1,K-1),A(2,K-1),WU,WU,THEL,THEF,EPSC,LOLTA,A(2,K))
22     TAB=(A(1,K-1)*T(2,K))/A(2,K)
23     AA=A(1,K-1)/A(2,K)
24     TA=A(1,K-1)*T(2,K)/A(2,K)
25     AA=A(1,K-1)/A(2,K)
26     SM(2,K)=SM(2,K)*SNT*(A(2,K-1)/A(2,K))
27     SM(2,K)=SM(2,K-1)*SM(2,K)/A(2,K)
28     CALL TAB(AB)/A(1,K-1)*TAB(AB)
29     DAT=ITAB(AB)/(1.-TAB(AB))
30     X(2,K)=Y(1,K-1)-Y(1,K-1)*CAT(X(2,K-1)-DAT*X(1,K-1)) / (CAT-DAT)
31     Y(2,K)=Y(1,K-1)-Y(1,K-1)*CAT(X(2,K-1)-CAT(X(2,K-1),X(2,K-1)))
32     CALL TS(GP,GT,SPAT,GP,GT,SPAT,GP,X(2,K),X(2,K),X(2,K-1),X(2,K),X(2,K-1),Y(2,K),
33     Y(1,K-1),SM(2,K-1),SM(2,K),ETA(2,K),ETA(2,K))
34     KIT=1
35     KIP=2
36     IF (INDOOR.EQ.2) GO TO 650
37     XXXXX=N
38     YTH=THEX*ETAW
39     YTH=THEX*ETAW
40     IF (INDETE.EQ.1) GO TO 65
41     XT=EXXT
42     XEXT=XT*EXXT*SORISMT*SMT-1.0
43     GO TO 70
44     YEXT=THEX*ETAW
45     XEXT=EXXT
46     XT=EXXT*EXXT*SORISMT*SMT-1.0
47     DO 80 B=1,600
48     SM(1)=1.00000
49     YH(1)=ETAW
50     CONTINUE
51     GO TO 100,85,98,INDSR
52     B=XT/2.0/SMT-1.0*SORISMT*BCT/YTH-2.0
53     IF(B.GT.-2.AND.B.LT.1.0) GO TO 95
54     WHITE(1,6,90)=B
55     90 FORMAT(1X,'//,19X,'*** CUBIC CENTERLINE MACH NO. DISTRIBUTION //,
56     12X,TIS NOT APPROPRIATE FOR INPUT GIVEN, B =',E12.6)
57     1200 FORMAT(1X,'*** CUBIC CENTERLINE MACH NO. DISTRIBUTION IS NOT',
58     1, APPROPRIATE FOR INPUT //1X, 'GIVEN')
59     GO TO 95
60     95 CALL REG(XL,SML,XCOR,SMT,YTH,EXITXT,XT,RCT,B,LASTN,NEND,GAMMA,XEXIT
61     1,ETAN,DELNU1)
62     GO TO 110
63     98 CALL XIO(XL,SML,XCOR,SMT,YTH,EXITXT,XT,RCT,B,LASTN,NEND,GAMMA,XEXIT
64     1,ETAN,DELNU1)
65     GO TO 110
66     100 CALL SIO(XL,SML,XCOR,SMT,YTH,EXITXT,XT,RCT,B,LASTN,NEND,GAMMA,XEXIT
67     1,ETAN,DELNU1)
68     110 ASSIGN 740 TO MU
69     KAPP=2
70     NEND=END-1
71     Y(2,1)=0.0
72     THE(2,1)=0.0
73     T(2,1)=0.0
74     ETA(2,1)=0.0
75     WATT(16,111)=0.0
76     111 FORMAT(1X,'//,10X,'CHARACTERISTICS MANIPULATION',
77     1,*'INTERPOLATED WALL VALUES', //,5X,'4X',6X,'X(INCHES)'
78     2,5X,'Y(INCHES)',7X,'MACH NO.',5X,'STREAM ANGLE',/)

    IF(LASTN.LE.N) GO TO 370
    SM(2,1)=SML(N)
    X(2,1)=XL(N)
    A(2,1)=XL(N)
    IF(N.GT.1) SORT(SML(N)**2-1.)
    IF(N.GT.1) GO TO 470

```

Program "char6" (cont.)

Program "char6" (cont.)

Program "char6" (cont.)

JUL 11 1996 16:04:49

JF113961B0449 char6.f Page 15	<pre> IMPLICIT DOUBLE PRECISION (A-H,O-Z) DIFF(XI,XJ)=XI-XJ DIVAYF(R,S,XI,XJ)=DIFF(R,S)/DIFF(XI,XJ) DIVBF(R,S,T,XI,XJ,XK)=DIVAYF(DIVAYF(R,S,XI,XJ),DIVAYF(S,T,XJ,XK), XI,XK) IF (K .EQ. 2) GO TO 10 TER=(R*DIFF(EM,XI)*(DIVAYF(R,S,XI,XJ)*DIFF(EM,XJ)*DIVBF(R,S,T,X 11,XJ,XK)) GO TO 15 TER=(EXM-XJ)*R/(XI-XJ) 15 RETURN END SUBROUTINE ATE(GA,GB,SMAB,GB,THETA,ETAI,X2,X1,Y2,Y1,SM1,SM2,ETA2) IMPLICIT DOUBLE PRECISION (A-H,O-Z) PQF(FM)=FM/(GA/(Z*GB*FM**2))**CD X2X1=X2-X1 Y2Y1=Y2-Y1 SM1=.5*(1./SM1+.1./SM2) ETA2=ETAI+.5*(PQF(SM1)*PQF(SM2))+SNA*SQRT(X2X1*X2X1+Y2Y1*Y2Y1) RETURN END SUBROUTINE SETK(XW,NO,XL,SM1,NEND) IMPLICIT DOUBLE PRECISION (A-H,O-Z) DIMENSION XW(600),XL(600),SM1(600),SMN(600) DO 70 J=1,600 IF (XL(J),GE,XW(NO)) GO TO 71 CONTINUE 71 K=J+1 KEND=NEND-3 DO 40 I=NO,NEND 5 IF (XW(I) .LE. XL(K)) GO TO 10 K=K+1 GO TO 5 10 IF (K .LE. KEND) GO TO 20 GO TO 30 20 CALL LAGINT(XW(K-2),SM1(K-2),5,XW(I),SMN(I),DYO) GO TO 40 30 CALL LAGINT(XW(K-4),SM1(K-4),5,XW(I),SMN(I),DYO) 40 CONTINUE DO 60 J=NO,NEND XL(J)=XW(J) SM1(J)=SMN(J) 60 CONTINUE RETURN END SUBROUTINE LAGINT(X,Y,NPTS,XX,YY,DY) IMPLICIT DOUBLE PRECISION (A-H,O-Z) DIMENSION X(11),Y(11) YY=0. DY=0. DO 40 I=1,NPTS C1=1. DO 10 J=1,NPTS I=(I-J+11)%11 C1=C1*(XX-X(J)) C2=C2*(X(11)-X(J)) 10 CONTINUE SUM=0. DO 30 J=1,NPTS I=(I-J+11)%11 C3=1. DO 20 K=1,NPTS I=(I-K+11)%11 C1=C1*(XX-X(K)) C2=C2*(X(11)-X(K)) 20 CONTINUE SUM=SUM+C3 30 CONTINUE C1=(I-1)/C2 I=I+1 C1=C1*DY 40 CONTINUE </pre>
--	--

JUL 1 1996 16:03:07

Page 1

nbl6.f

Page 2

PROGRAM NBL6
 Modified by: LT Douglas L. Setwright
 March 1994

PROGRAM INPUTS:

INDM-BOUNDARY LAYER MODE: 1. STRICTLY LAMINAR, 2. STRICTLY TURBULENT, 3. LAM-TRANS-WALL, 4. CONSTANT-WALL, 2. ADIA WALL TEMP, INDM-WALL TEMP INDICATION: 1. CONSTANT, 2. TRANSITION INPUT BY USER, 3. TEMPERATURE DISTRIBUTION INPUT BY USER, 4. TRANSITION INDICATION (IF INDM=3): 1. TRANS AT RETHETA VALUE GIVEN IN TRCON, 2. TRANS AT X GIVEN IN TRCON, INDIC- INDICATE BOUNDARY LAYER CALCULATION: 1. CALCULATE CENTERLINE ONLY, 2. CALCULATE WALL ONLY, 3. CALCULATE BOTH

TRCON-TRANSITION CONSTANT EQUAL TO RETHETA (REYNOLDS NUMBER BASED ON THE MOMENTUM THICKNESS OF THE BOUNDARY LAYER) OR XTTRANS (HORIZONTAL DISTANCE RELATIVE TO THE THROAT) DEPENDING ON INDR.

THZERO-THETA (MOMENTUM THICKNESS) AT THROAT IN FEET (USUALLY 1.0E-5)

PO-SPIGATION PRESSURE IN LB/SIN² TO-SUPPLY TEMP IN DEGREES R IF INDR=1 TWALL-WALL TEMP IN DEGREES R IF INDR=1 XTEND-EXTENSION LENGTH OF NOZZLE WALL PAST EXIT AS DEFINED BY THE ISENTROPIC CORE LENGTH (ASSUMES UNIFORM DUCT FLOW) DL-INCREMENT IN X FROM ISENTROPIC EXIT TO EXTENSION LENGTH IN INCHES

B-WIDTH OF NOZZLE

GAMMA-RATIO OF SPECIFIC HEATS OMEGA-EXPONENT IN VISCOSITY-TEMP RELATION (AIR=0.76)

HATE-MOLECULAR WT OF GAS (AIR=29)

CP-SPECIFIC HEAT OF GAS IN BTU/LB-DEG R (AIR=0.24) OR LEAVE BLANK AND LET PROGRAM PICK VALUES

PR-PRANDTL NUMBER (AIR=0.72)

** IFINDTH=3:
 NUM-NUMBER OF WALL TEMP INPUT CARDS (THREE OR MORE POINTS ARE REQUIRED OR PROGRAM WILL TERMINATE DATA OUTPUT PRIOR TO COMPLETING RUN)
 XXX-DISTANCE FROM THROAT IN INCHES
 THW-WALL TEMPS. (DEGREES R) CORRESPONDING TO XXX

IMPLICIT DOUBLE PRECISION (A-H, O-Z)
 DIMENSION X(1000), YX(1000), YM(1000), HALFA(16), XT(16), XTLN(16), ITW(1000), S(1000), PPOV(1000), DMDS(1000), FMT(100), YSV(1000), 2DLS(1000), YS(1000), DELY(1000), YY(1000), YCDY(1000)
 CHARACTER 8, FMT
 REAL B
 COMMON CFOV2, CFOV2L, DELR, DELT, DELT, DELT, DHEAT, DTDS,
 1, DUDS, EN, ENBAR, ENTRB, H, HINC, OLDT, REL, RETH, RHED, THETA,
 2TAHAL, THAR, THET2, THOLD, TLTE, ULUS, TRCON, THERO, TO, TWALL,
 3GAMA, 3MECA, WATE, CP, GRHE, SW, A, BI, R2, C2, A3, B3, GRHE, TAD,
 4TADTE, RTTE, QUAY, TETO, UP, GRHE, HA, OPDS, DL, XINC, X(16), YY(1000),
 5EME(1000), HALFA(16), XT(16), XTLN(16), TM(1000), S(1000), PPOV(1000),
 6DMDS(1000), FMT(100), YY(1000), YCDY(1000),
 7INDM, INDR, INDMC, MAX, MIN, LINDE, MOUNT, LAP, NN, INDFE, INDMO, INDMU,
 OPEN UNIT=17, FILE="contpt2", STATUS="UNKNOWN", INDPNG, B,
 OPEN UNIT=26, FILE="contpt3", STATUS="UNKNOWN",
 HALF A(1) = .01351623

Program "nbl6"
 Page 1
 nbl6.f
 Page 2
 16JUL1996 16:03:07

```

      11 HALF A(2) = .031126762
      12 HALF A(3) = .041529256
      13 HALF A(4) = .062314485
      14 HALF A(5) = .074791995
      15 HALF A(6) = .084578260
      16 HALF A(7) = .093301710
      17 HALF A(8) = .094753035
      18 HALF A(9) = .0959935
      19 HALF A(10) = .0961816
      20 HALF A(11) = .0962916
      21 HALF A(12) = .0963456
      22 HALF A(13) = .0963816
      23 HALF A(14) = .0964156
      24 HALF A(15) = .0964496
      25 HALF A(16) = .0964836
      26 XT(1) = .005199315
      27 XT(2) = .0071249
      28 XT(3) = .0071844
      29 XT(4) = .0072299
      30 XT(5) = .007269188
      31 XT(6) = .007299161
      32 XT(7) = .007328152
      33 XT(8) = .007358142
      34 XT(9) = .007388132
      35 XT(10) = .007418122
      36 XT(11) = .007448112
      37 XT(12) = .007478102
      38 XT(13) = .007508102
      39 XT(14) = .007538102
      40 XT(15) = .007568102
      41 XT(16) = .007598102
      42 XTLN(1) = .577506256
      43 XTLN(2) = .582493761
      44 XTLN(3) = .587487266
      45 XTLN(4) = .592480339
      46 XTLN(5) = .597473292
      47 XTLN(6) = .602466159
      48 XTLN(7) = .607459024
      49 XTLN(8) = .612451891
      50 XTLN(9) = .617444758
      51 XTLN(10) = .622437625
      52 XTLN(11) = .627430492
      53 XTLN(12) = .632423259
      54 XTLN(13) = .637416026
      55 XTLN(14) = .642408793
      56 XTLN(15) = .647401471
      57 XTLN(16) = .652404149
      C INTRODUCTION TO PROGRAM
      C
      WRITE(*,120)
      120 FORMAT(1X,'//',1X,'//',1X,'//',1X,'//',1X,'//',1X,'//',1X,
     1' U.S. NAVAL ORDNANCE LABORATORY', WHITE,
     2' 11, OAK, MARYLAND, //', 'SA', 'COMPUTER PROGRAM FOR THE DESIGN', ON,
     3' 2. A TWO-DIMENSIONAL SUPERSONIC NOZZLE', //', 'PART II', //', '15X',
     3' ISENTROPIC CORE CONTOUR MODIFIED FOR VISCOUS EFFECTS', )
      125 FORMAT(1X,'/','Introduction', //', 'This program models the ', //,
     2' isentropic contour from Part I to take into account //', 'the ', //,
     2' effects of the boundary layer. The program has been modified to ', //,
     3' take //', 'into account both the boundary layer for the side ', //,
     4' plate as well //', 'as the contour of the nozzle.', //)
      PRINT*
      PRINT*
      PRINT*
      PRINT*
      PAUSE
      XINC=0.0
      INDF1=1
      INDRG2=2
  
```

Program "nbl6" (cont.)

```

Page 4

JUN 11 1996 16:08:07          Job 61

250 H=2.7477951*DONOPO(N)*PO*EME(N)/SQRT((TE))*CFOV2
260 DHAT=H*(TDR-TMN(N))
261 T=TM(N) EQ. MTN(GO TO 265)
265 TMRAFE=FCFOV2*RHOE*(US/2)
267 DELTA=HTHETA
268 DELTA=(N-DELTAN)
269 CALL OUT
270 T(FIN,0,1) GO TO 288
271 QSUM=QSUM+(DHEAT+DH1)/2.+(S(N)-S(N-1))
272 DH1=DHEAT
273 WRITE(26,289) QSUM
274 FORMAT(15X,E15.6)
275 F1(FINDMO,1.E-12)GO TO 1642
276 CALL IPO
277 1642 OOLDTH=PTIDS
278 1643 THDR=THETA
279 1644 THTR=EQ.3) GO TO 180
280 CONTINUE
281 N=NMAX
282 IF(LFLAP,EO,1) GO TO 380
283 IF(LFLAP,EO,2) GO TO 410
284 WRITE(26,400)
285 400 FORMAT(1X,19,100,'//',55X,'* WALL RESULTS *//',9X,'N',8X,
1'X INCHES,',6X,'DELSTAR INCHES,',4X,'0.0 DELSTAR',11X,
2'MICL',11X,'DELTA',12X,'CORE+DELSTAR',9X,
245 DO 416 17-MIN,MAX
246 YSAV(IT)=0.0
247 CONTINUE
248 GO TO 450
249 WRITE(26,420)
250 420 FORMAT(1X,19,100,'//',60X,'* CENTERLINE RESULTS *//',9X,'N',8X,
1'X INCHES,',6X,'DELSTAR INCHES,',4X,'0.0 DELSTAR',11X,
2'MICL',11X,'DELTA',12X,'CORE+DELSTAR',9X,
251 DO 430 IAMIN,MAX
252 X(IAM)=X(MIN)
253 Y(IAM)=Y(MIN)
254 Y(YIA)=Y(YIA)+12.
255 Y(YIA)=Y(YIA)+12.
256 Y(YIA)=Y(YIA)+12.
257 DELTAS(IA)=DELTAS(IA)+12.
258 DELTAS(IA)=12*(YIA)*DELTAS(IA)+(B-2.*DELTAS(IA))*DELTAS(IA)/B
259 Y(ZCDYI)(IA)=Y(SAV)(IA)+DELY(IA)
260 Y(ZCDYI)(IA)=Y(SAV)(IA)+DELY(IA)
261 Y(YAV)(IA)=Y(YIA)+YY(IA)
262 Y(YAV)(IA)=Y(SAV)(IA)+YY(IA)
263 Y(YAV)(IA)=Y(SAV)(IA)+YY(IA)
264 CONTINUE
265 WRITE(26,440)((IA,X(IA),DELTAS(IA),YY(IA),EME(IA),DELY(IA),
266 Y(IA)),IA=MIN,MAX)
267 440 FORMAT(15X,15,6I18.6)
268 IF (INDC-JO,3,3) AND LAP-EQ. 1) GO TO 10
269 IF (INDC-JO,3) GO TO 600
270 490 WRITE(26,500)
271 500 FORMAT(1X,19,100,'//',45X,'* WALL AND CENTERLINE RESULTS COMBINED *',
1'//',35X,N',35X,X INCHES')
272 510 WRITE(26,510)((16,X(16),YSAV(16),YCDDLY(16),YCORE*(21*DLSSAR),AX,YCORE*(21*',
273 511 XINC),16-MIN,MAX)
274 600 IF (XINC,EO,0,0) GO TO 9
275 WRITE(26,630)(PM1,I=1,10)
276 630 FORMAT(1X,10A8,'//',T22,'Y',//,
277 511 1T22-X,T22-Y,/,/
278 512 DO 539 I=2,500
279 MINC=1-1
280 S1=I-S1(-1)*XINC
281 IF(S1,GT,X(MAX)) GO TO 489
282 489 MINX=MIN+1
283 DO 600 I=MIN,MAX
284 YS(1)=YS(1)+YY(I)
285 IF (INDC,NE,3) YS(1)=YY(I)
286 CONTINUE
287 CALL SCKT(XMIN,X,VS,MINC)
288 WRITE(26,610)((1,S1),VS,1,1,F=2,MTNC)

```

Program "nbl6" (cont.)

Program "nbl6" (cont.)

Page 8

NOTE:

```

100  FORMAT(IX,/, 'WALL TEMP. MODE = CONSTANT')
    IF (INDMO .EQ. '2') THEN
        WRITE(*,105)
    FORMAT(IX,/, 'WALL TEMP. MODE = ADIABATIC')
    ELSE IF (INDMO .EQ. '3') THEN
        WRITE(*,110)
    FORMAT(IX,/, 'WALL TEMP. MODE = USER DEFINED DISTRIBUTION')
110  END IF

    IF (INDMO .EQ. '3') THEN
        IF (INDR .EQ. '1') THEN
            WRITE(*,115)
        FORMAT(IX,/, 'TRANSITION PARAMETER = REYNOLDS NUMBER')
        ELSE IF (INDR .EQ. '2') THEN
            WRITE(*,120)
        FORMAT(IX,/, 'TRANSITION PARAMETER = "X" DISTANCE FROM'
120          ' THROAT')
        1      END IF
    END IF

    IF (INDIC .EQ. '1') THEN
        WRITE(*,125)
        FORMAT(IX,/, 'B.L. CALCULATION = CENTERLINE ONLY')
    ELSE IF (INDIC .EQ. '2') THEN
        WRITE(*,130)
        FORMAT(IX,/, 'B.L. CALCULATION = WALL ONLY')
    ELSE IF (INDIC .EQ. '3') THEN
        WRITE(*,135)
        FORMAT(IX,/, 'B.L. CALCULATION = BOTH WALL AND CENTERLINE')
    END IF

C   CHANGES TO KEYBOARD INPUTS
C

    IF (COUNT .EQ. 0) THEN
150    WRITE(*,140)
        FORMAT(IX,/, 'ARE INPUT VALUES CORRECT? 1-YES, 2-NO')
    READ(*,145,INRSP)
    FORMAT(IX,/, INRSP)
    1      INPUT *1,
        IF (INRSP .NE. '1' .AND. INRSP .NE. '2') THEN
            GO TO 150
        ELSE IF (INRSP .GE. 'A' .AND. INRSP .LE. 'Z' .OR. INRSP
1           .GE. '1' .AND. INRSP .LE. '/') THEN
            GO TO 150
        END IF

    END IF

    IF (COUNT .EQ. 0) THEN
165    WRITE(*,155)
        FORMAT(IX,/, 'ANY OTHER CHANGES? 1-YES, 2-NO')
    READ(*,160,INOUT)
    FORMAT(IX,/, INOUT)
    1      INRSP = 2,
        IF (INOUT .NE. '1' .AND. INOUT .NE. '2') THEN
            GO TO 165
        ELSE IF (INOUT .GE. 'A' .AND. INOUT .LE. 'Z' .OR. INOUT
1           .GE. '1' .AND. INOUT .LE. '/') THEN
            GO TO 165
        END IF

    END IF

    IF (INSP .EQ. '2' .AND. INOUT .EQ. '1') THEN
180    WRITE(*,170)
        FORMAT(IX,/, 'INPUT VALUE TO BE CHANGED (1,2,3,4): // , / , '
1           '1, B.L. MODE: A: LAMINAR, B: TURBULENT, C: LAM-TRANS-TURB,
1           '2, / , 3, X2, WALL TEMP. MODE: A: CONSTANT, B: ADIABATIC, C: USER,
3           'DEFINITION: / , 3, B.L. CALCULATION: A: CENTERLINE, B: '

```

```

Page 7
16111996110507
nblast

29 WRITE(*,30)
30 FORMAT(1A$,' //,' ,1$,' INDICATE BOUNDARY LAYER MODE BEGINNING AT NOZZLE',
1$,' 1. /THROAT',1$,' 2. STRICTLY LAMINAR',1$,' 3. / 2. STRICTLY TURBULENT',
2$,' 2/3X.',3$,' LAMINAR-TRANSITION-TURBULENT')
35 READ(*,35) INDMO
35 FORMAT(1A$)

IF (INDMO .NE. '1' .AND. INDMO .NE. '2' .AND. INDMO .NE. '3') THEN
GO TO 29
ELSE IF (INDMO .GE. 'A' .AND. INDMO .LE. 'Z' .OR. INDMO
1$,.GE.,.SP.,.AND. INDMO .LE.,/) THEN
GO TO 29
END IF

40 WRITE(*,45)
45 FORMAT(1X,$,' INDICATE WALL TEMPERATURE FOR NOZZLE',/,' 1X,
1$,' CONSTANT TEMPERATURE',/,' 3X,$,' 2. ADIABATIC WALL',/,' 1X,
2$,' 3. TEMPERATURE DISTRIBUTION ALONG NOZZLE TO BE INPUT BY',
3$,' PROGRAM USER')
READ(*,50) INDTW
50 FORMAT(1A$)

IF (INDTW .NE. '1' .AND. INDTW .NE. '2' .AND. INDTW .NE. '3') THEN
GO TO 40
ELSE IF (INDTW .GE. 'A' .AND. INDTW .LE. 'Z' .OR. INDTW
1$,.GE.,.SP.,.AND. INDTW .LE.,/) THEN
GO TO 40
END IF

55 IF (INDMO .EQ. '3') THEN
WRITE(*,60)
60 FORMAT(1X,$,' INDICATE THE CHARACTERISTIC PARAMETER THAT'
1$,' THE FLOW WILL BE BASED',/,' 3X,$,' 1. REYNOLDS NUMBER',
2$,' 2. / 3X.',2$,' DISTANCE FROM THE THROAT')
READ(*,65) INDR
FORMAT(1A$)

65 IF (INDR .NE. '1' .AND. INDR .NE. '2') THEN
GO TO 55
ELSE IF (INDR .GE. 'A' .AND. INDR .LE. 'Z' .OR. INDR
1$,.GE.,.SP.,.AND. INDR .LE.,/) THEN
GO TO 55
END IF

IF (INDMO .EQ. '3') THEN
GO TO 224
END IF

C C DISPLAY/RE-DISPLAY KEYBOARD INPUT RESULTS

224 COUNT=0
225 IF (INDMO .EQ. '1') THEN
WRITE(*,85)
85 FORMAT(1X,$,' //,' ,1$,' B.L. MODE = LAMINAR')
ELSE IF (INDMO .EQ. '2') THEN
WRITE(*,90)
90 FORMAT(1X,$,' //,' ,1$,' B.L. MODE = TURBULENT')
ELSE IF (INDMO .EQ. '3') THEN
WRITE(*,95)
95 FORMAT(1X,$,' //,' ,1$,' B.L. MODE = LAM.-TRANS.-TURB.')
END IF

IF (INDTW .EQ. '1') THEN
WRITE(*,100)

```

Program "nbl6" (cont.)

```

14-1 1998-03-03 06:11 Page 16

      IF (ERROR .GT. 0) THEN
        GO TO 231
      END IF
      ELSE IF (INDTR.EQ. '2') THEN
        WRITE(*,45)
        FORMAT(IX,'//',INPUT MOMENTUM THICKNESS OF BOUNDARY LAYER AT'
1, THE THROAT IN FEET //, '(USUALLY = 1.0E-5 FEET')
        READ(*,250,IOSTAT=ERROR) TRCON
        FORMAT(E10.3)
        IF (ERROR .GT. 0) THEN
          GO TO 241
        END IF
      END IF
      ERROR=0
      251 WRITE(*,255)
      255 FORMAT(IX,'//',INPUT STAGNATION PRESSURE IN LBS./IN2')
      1, READ(*,270,IOSTAT=ERROR) P0
      260 FORMAT(E10.3)
      IF (ERROR .GT. 0) THEN
        GO TO 251
      END IF
      ERROR=0
      261 WRITE(*,265)
      265 FORMAT(IX,'//',INPUT TOTAL TEMPERATURE OF SUPPLY MEDIUM IN'
1, DEGREES R)
      READ(*,280,IOSTAT=ERROR) T0
      270 FORMAT(E10.3)
      IF (ERROR .GT. 0) THEN
        GO TO 261
      END IF
      ERROR=0
      271 WRITE(*,275)
      275 FORMAT(IX,'//',INPUT TEMPERATURE OF THE WALL IN DEGREES R')
      1, READ(*,285,IOSTAT=ERROR) TWALL
      280 FORMAT(E10.3)
      IF (ERROR .GT. 0) THEN
        GO TO 271
      END IF
      END IF
      281 IF (INDTH.EQ. '1') THEN
        ERROR=0
        WRITE(*,285)
        FORMAT(IX,'//',INPUT LENGTH OF NOZZLE PAST THE EXIT')
        1, READ(*,290,IOSTAT=ERROR) XEND
        290 FORMAT(E10.3)
        IF (ERROR .GT. 0) THEN
          GO TO 281
        END IF
        END IF
        ERROR=0
        291 WRITE(*,295)
        295 FORMAT(IX,'//',INPUT INCHES FOR 'X' IN INCHES FOR'
1, 'X', 'INCHES FOR 'X', DEFINING THE ISENTROPIC CORE')
        1, READ(*,300,IOSTAT=ERROR) XEND
        300 FORMAT(E10.3)
        IF (ERROR .GT. 0) THEN
          GO TO 291
        END IF
        END IF
        ERROR=0
        301 WRITE(*,305)
        305 FORMAT(IX,'//',INPUT INCREMENT OF "X" IN INCHES FOR'
1, 'X', EXTENSION LENGTH TO INTERPOLATE //, CONTOUR OF NOZZLE')
        1, READ(*,310,IOSTAT=ERROR) DL
        310 FORMAT(E10.3)
        IF (ERROR .GT. 0) THEN

```

Program "nbl6" (cont.)

JUN 19 1980 164307 P-9912
 161

```

END IF

      WRITE(*,315) 'MOMENTUM THICKNESS = ',THZERO
375 FORMAT(1X,'/3X,A21,E10.3)
      WRITE(*,380) 'STAGNATION PRESSURE = ',PO
380 FORMAT(1X,'/3X,A22,E10.3)
      WRITE(*,385) 'STAGNATION TEMPERATURE = ',T0
385 FORMAT(1X,'/3X,A25,E10.3)

      IF (INDW .EQ. '1') THEN
        WRITE(*,390) 'WALL TEMPERATURE = ',TWALL
      END IF
      FORMAT(1X,'/3X,A19,E10.3)

      WRITE(*,391) 'EXTENSION LENGTH PAST NOZZLE EXIT= ',XTEND
391 FORMAT(1X,'/3X,A5,E10.3)

      WRITE(*,395) 'INCREMENET "Y" FOR EXTENSION = ',DI,
395 FORMAT(1X,'/3X,A10,E10.3)

      WRITE(*,400) 'WIDTH OF NOZZLE = ',B
400 FORMAT(1X,'/3X,A18,E10.3)

      WRITE(*,405) 'GAMMA = ',GAMMA
405 FORMAT(1X,'/3X,A8,E10.3)

      WRITE(*,410) 'VISCOOSITY-TEMP. EXPONENT = ',OMEGA
410 FORMAT(1X,'/3X,A21,E10.3)

      WRITE(*,415) 'MOLECULAR WEIGHT OF GAS = ',MATE
415 FORMAT(1X,'/3X,A26,E10.3)

      WRITE(*,420) 'SPECIFIC HEAT (CP) = ',CP
420 FORMAT(1X,'/3X,A21,E10.3)

      WRITE(*,425) 'FRANDIL NUMBER = ',PR
425 FORMAT(1X,'/3X,A1,E10.3)

      IF (INVALID('EQ.1')) THEN
        WRITE(*,431)
431 1       FORMAT(1X,'//,*****INPUT NOT NECESSARY FOR DATA,
         1   PREVIOUSLY GIVEN*****')
      END IF

C           CHANGES TO INPUT
C
      INVALID=0
      IF (COUNT1 .EQ. 0) THEN
445       WRITE(*,435)
435       FORMAT(1X,'//, ARE INPUTS CORRECT?, 1-YES, 2-NO')
        READ(*,440) INANS
440       FORMAT(1X)
        INDIR(A1)=1
        IF (INANS .NE. '1' .AND. INANS .NE. '2') THEN
          GO TO 445
        ELSE IF (INANS .GE. 'A' .AND. INANS .LE. 'Z') THEN
          GO TO 445
        END IF
      END IF

      IF (COUNT1 .GT. 0) THEN
460       WRITE(*,450)
450       FORMAT(1X,'//, ANY OTHER CHANGES?, 1-YES, 2-NO')
        READ(*,455) INDIR
455       FORMAT(1X)
        INANS = ''
        IF (INDIR .NE. '1' .AND. INDIR .NE. '2') THEN

```

```

Page 11          Page 11

JUL 11 1990 60307      1066.1

      GO TO 301
    END IF

    ERROR=0
311  WRITE(*,315)
315  FORMAT(1X,'//',1INPUT WIDTH OF NOZZLE IN INCHES (ASSUMING'
1CONSTANT WIDTH)',1
      READ(*,330,IOSTAT=ERROR) B
320  FORMAT(E10.3)
      IF (ERROR .GT. 0) THEN
        GO TO 311
      END IF

      ERROR=0
321  WRITE(*,325)
325  FORMAT(1X,'//',1INPUT EXPONENT FOR VISCOSITY-TEMPERATURE RELATION'
1,1
      READ(*,330,IOSTAT=ERROR) GAMMA
330  FORMAT(E10.3)
      IF (ERROR .GT. 0) THEN
        GO TO 321
      END IF

      ERROR=0
331  WRITE(*,335)
335  FORMAT(1X,'//',1INPUT EXPONENT FOR VISCOSITY-TEMPERATURE RELATION'
1,1
      READ(*,340,IOSTAT=ERROR) OMEGA
340  FORMAT(E10.3)
      IF (ERROR .GT. 0) THEN
        GO TO 331
      END IF

      ERROR=0
341  WRITE(*,345)
345  FORMAT(1X,'//',1INPUT MOLECULAR WEIGHT OF GAS SUPPLY (AIR = 28.97)')
      READ(*,350,IOSTAT=ERROR) WATE
350  FORMAT(E10.3)
      IF (ERROR .GT. 0) THEN
        GO TO 341
      END IF

      ERROR=0
351  WRITE(*,355)
355  FORMAT(1X,'//',1INPUT SPECIFIC HEAT OF GAS IN BTU/LB-DEG-R (AIR =
1,0.4)
      READ(*,356,IOSTAT=ERROR) CP
356  FORMAT(E10.3)
      IF (ERROR .GT. 0) THEN
        GO TO 351
      END IF

      ERROR=0
351  WRITE(*,355)
355  FORMAT(1X,'//',1INPUT PRANDTL NUMBER FOR GAS (AIR = 0.72))
      READ(*,358,IOSTAT=ERROR) PR
358  FORMAT(E10.3)
      IF (ERROR .GT. 0) THEN
        GO TO 356
      END IF

      C DISPLAY/RE-DISPLAY INPUTS
      C
635  COUNT=0
      IF (INDMO .EQ. '3') THEN
        IF (INDTR .EQ. '1') THEN
          WRITE(*,365) 'REYNOLDS NUMBER = ',TRCON
          FORMAT(*,365)
          FORMAT(1X,3X,A18,10)
        ELSE IF (INDTR .EQ. '2') THEN
          WRITE(*,370) 'TRANSITION = ',TRCON
          FORMAT(*,370)
          FORMAT(1X,3X,A17,B10,3)
      END IF

```

Program "nbl6" (cont.)

```

00111986160307    nbl6.f          Page 13
      GO TO 460
      ELSE IF (INDIR .EQ. 'A' .AND. INDIR .LE. 'Z') THEN
      GO TO 460
      END IF
      IF (INTRANS .EQ.'2' .AND. INDIR .EQ. '1') THEN
1150      WRITE(*,13) //, 'INPUT VALUE TO BE CHANGED (1,2,3,4,5,6,7,8,9,
      10,11,12,13)', 'TRANSITION PARAMETER', '/X', XN
      12      MOUNTAIN, TWOAGES, AT THROAT', '/X', 1, 'TRANSITION',
      13      'PRESSURE', '/X', 4, 'TOTAL TEMPERATURE', '/X', 5, 'STAGNATION',
      14      'TEMPERATURE', '/X', 7, 'EXTENSION LENGTH OF NOZZLE', '/X', 3X,
      15      'X'INCREMENT FOR EXTENSION LENGTH', '/X', 8, 'WIDTH',
      16      'OF NOZZLE', '/X', 9, 'RATIO OF SPECIFIC HEATS', '/X', 10,
      17      'VISCOSITY', '/X', 11, 'SPECIFIC HEAT EXPONENT', '/X', 12, 'MOLECULAR WEIGHT',
      18      'OF GAS', '/X', 12. SPECIFIC HEAT (CP) FOR GAS', '/X', 13,
      19      'PRANDTL NUMBER',
      READ(14,10) INCHG
      FORMAT(12) 10
      IF (INCHG .EQ. '1') THEN
        IF (INRD .EQ. '3') THEN
          ERROR=0
          IF (INDR .EQ. '1') THEN
            WRITE(*,415)
            FORMAT(1X,'//', INPUT NEW REYNOLDS NUMBER')
            READ(*,480,IOSTAT=ERROR) TRCON
            FORMAT(E10.3)
            IF (ERROR .GT. 0) THEN
              GO TO 471
            END IF
            ELSE IF (INDTR .EQ. '2') THEN
              WRITE(*,485)
              FORMAT(1X,'//', INPUT NEW "X" TRANSITION'
              'DISTANCE (INCHES)')
              READ(*,490,IOSTAT=ERROR) TRCON
              FORMAT(E10.3)
              IF (ERROR .GT. 0) THEN
                GO TO 481
              END IF
            ELSE IF (INDTR .EQ. '2') THEN
              WRITE(*,495)
              FORMAT(1X,'//', INPUT NEW VALUE OF MOMENTUM THICKNESS',
              'AT THROAT (FEET)')
              READ(*,505,IOSTAT=ERROR) THZERO
              FORMAT(E10.3)
              IF (ERROR .GT. 0) THEN
                WRITE(*,510)
                FORMAT(1X,'//', INPUT NEW STAGNATION PRESSURE (lb/in2)
                PO)
                FORMAT(E10.3)
                IF (ERROR .GT. 0) THEN
                  GO TO 499
                END IF
              ELSE IF (INCHG .EQ. '3') THEN
                ERROR=0
                IF (INRD .EQ. '3') THEN
                  WRITE(*,515)
                  FORMAT(1X,'//', INPUT NEW TOTAL TEMPERATURE (DEGREES RI')
                  READ(*,520,IOSTAT=ERROR) TOT
                  FORMAT(E10.3)
                  IF (ERROR .GT. 0) THEN
                    GO TO 519
                  END IF
                ELSE IF (INCHG .EQ. '4') THEN
                  ERROR=0
                  WRITE(*,520)
                  FORMAT(1X,'//', INPUT NEW MOLECULAR WEIGHT)
                  READ(*,525,IOSTAT=ERROR) TO
                  FORMAT(E10.3)
                  IF (ERROR .GT. 0) THEN
                    GO TO 519
                  END IF
                ELSE IF (INCHG .EQ. '5') THEN
                  INVALID=1
                  END IF
                ELSE IF (INCHG .EQ. '2') THEN
                  ERROR=0
                  WRITE(*,530)
                  FORMAT(1X,'//', INPUT NEW RATIO OF SPECIFIC HEATS')
                  READ(*,535,IOSTAT=ERROR) GAMMA
                  FORMAT(E10.3)
                  IF (ERROR .GT. 0) THEN
                    GO TO 571
                  END IF
                ELSE IF (INCHG .EQ. '9') THEN
                  ERROR=0
                  WRITE(*,545)
                  FORMAT(1X,'//', INPUT NEW EXTENSION LENGTH (INCHES))
                  READ(*,550,IOSTAT=ERROR) XTEND
                  FORMAT(E10.3)
                  IF (ERROR .GT. 0) THEN
                    GO TO 541
                  END IF
                ELSE IF (INCHG .EQ. '6') THEN
                  ERROR=0
                  WRITE(*,555)
                  FORMAT(1X,'//', INPUT NEW "X" INCREMENT (INCHES))
                  READ(*,560,IOSTAT=ERROR) DL
                  FORMAT(E10.3)
                  IF (ERROR .GT. 0) THEN
                    GO TO 551
                  END IF
                ELSE IF (INCHG .EQ. '7') THEN
                  ERROR=0
                  WRITE(*,565)
                  FORMAT(1X,'//', INPUT NEW WIDTH OF NOZZLE (INCHES))
                  READ(*,570,IOSTAT=ERROR) B
                  FORMAT(E10.3)
                  IF (ERROR .GT. 0) THEN
                    GO TO 561
                  END IF
                ELSE IF (INCHG .EQ. '8') THEN
                  ERROR=0
                  WRITE(*,575)
                  FORMAT(1X,'//', INPUT NEW RATIO OF VISCOSITY-TEMP. EXPONENT)
                  READ(*,580,IOSTAT=ERROR) OMEGA
                  FORMAT(E10.3)
                  IF (ERROR .GT. 0) THEN
                    GO TO 571
                  END IF
                ELSE IF (INCHG .EQ. '10') THEN
                  ERROR=0
                  WRITE(*,595)
                  FORMAT(1X,'//', INPUT NEW MOLECULAR WEIGHT)
                  READ(*,600,IOSTAT=ERROR) WATE
                  FORMAT(E10.3)
                  IF (ERROR .GT. 0) THEN
                    GO TO 591
                  END IF
                ELSE IF (INCHG .EQ. '11') THEN
                  ERROR=0
                  WRITE(*,605)
                  FORMAT(1X,'//', INPUT NEW SPECIFIC HEAT (CP - BTU/lb-°),

```

```

      11      Page 14
      12      nbl6.f          Page 14
      13      IF (INDW .EQ. '1') THEN
        ERROR=0
        WRITE(*,330) //, 'INPUT NEW WALL TEMPERATURE',
        FORMAT(1X,'//', DEGREES RI')
        READ(*,335,IOSTAT=ERROR) TWALL
        FORMAT(E10.3)
        IF (ERROR .GT. 0) THEN
          GO TO 529
        END IF
      ELSE
        WRITE(*,540)
        FORMAT(1X,'//', INPUT NOT NECESSARY FOR DATA'
        'PREVIOUSLY GIVEN')
        END IF
      ELSE IF (INCHG .EQ. '6') THEN
        ERROR=0
        WRITE(*,545)
        FORMAT(1X,'//', INPUT NEW EXTENSION LENGTH (INCHES))
        READ(*,550,IOSTAT=ERROR) XTEND
        FORMAT(E10.3)
        IF (ERROR .GT. 0) THEN
          GO TO 541
        END IF
      ELSE IF (INCHG .EQ. '7') THEN
        ERROR=0
        WRITE(*,555)
        FORMAT(1X,'//', INPUT NEW "X" INCREMENT (INCHES))
        READ(*,560,IOSTAT=ERROR) DL
        FORMAT(E10.3)
        IF (ERROR .GT. 0) THEN
          GO TO 551
        END IF
      ELSE IF (INCHG .EQ. '8') THEN
        ERROR=0
        WRITE(*,565)
        FORMAT(1X,'//', INPUT NEW WIDTH OF NOZZLE (INCHES))
        READ(*,570,IOSTAT=ERROR) B
        FORMAT(E10.3)
        IF (ERROR .GT. 0) THEN
          GO TO 561
        END IF
      ELSE IF (INCHG .EQ. '9') THEN
        ERROR=0
        WRITE(*,575)
        FORMAT(1X,'//', INPUT NEW RATIO OF VISCOSITY-TEMP. EXPONENT)
        READ(*,580,IOSTAT=ERROR) OMEGA
        FORMAT(E10.3)
        IF (ERROR .GT. 0) THEN
          GO TO 571
        END IF
      ELSE IF (INCHG .EQ. '10') THEN
        ERROR=0
        WRITE(*,595)
        FORMAT(1X,'//', INPUT NEW MOLECULAR WEIGHT)
        READ(*,600,IOSTAT=ERROR) WATE
        FORMAT(E10.3)
        IF (ERROR .GT. 0) THEN
          GO TO 591
        END IF
      ELSE IF (INCHG .EQ. '11') THEN
        ERROR=0
        WRITE(*,605)
        FORMAT(1X,'//', INPUT NEW SPECIFIC HEAT (CP - BTU/lb-°),

```

Program "nbl6" (cont.)

<pre> 1 *DEG-R') READ(*,610,IOSTAT=ERROR) CP FORMAT(610,3) IF (ERROR .GT. 0) THEN GO TO 601 END IF ELSE IF (INCHG .EQ. '13') THEN ERROR=0 WRITE(*,615) FORMAT(1X,'/ / / INPUT NEW PRANDTL NUMBER') READ(*,620,IOSTAT=ERROR) PR FORMAT(620,1) IF (ERROR .GT. 0) THEN GO TO 611 END IF COUNT1=COUNT1+1 GO TO 635 END IF </pre>	<pre> C CONVERSION TO INTEGRAL FORMAT C IF (INDH0 .EQ. '1') THEN INDH0=1 ELSE IF (INDH0 .EQ. '2') THEN INDH0=2 ELSE IF (INDH0 .EQ. '3') THEN INDH0=3 END IF IF (INDTH .EQ. '1') THEN INDTH=1 ELSE IF (INDTH .EQ. '2') THEN INDTH=2 ELSE IF (INDTH .EQ. '3') THEN INDTH=3 END IF IF (INDHC .EQ. '1') THEN INDHC=1 ELSE IF (INDHC .EQ. '2') THEN INDHC=2 ELSE IF (INDHC .EQ. '3') THEN INDHC=3 END IF IF (INDTR .EQ. '1') THEN INDTR=1 ELSE IF (INDTR .EQ. '2') THEN INDTR=2 END IF IF (INDR .EQ. '1') THEN INDR=1 ELSE IF (INDR .EQ. '2') THEN INDR=2 END IF IF (INDP .EQ. '1') THEN INDP=1 ELSE IF (INDP .EQ. '2') THEN INDP=2 END IF C END OF KEY BOARD INPUTS </pre>	<pre> IF (XEND.LE.X(MAX)) GO TO 640 DO 645 I=1,MAX I=I+1 X(I)=X(I)+600 GO TO 650 X(N)=X(N)+1 Y(N)=Y(N)+1 YS(N)=YS(N)+1 ENDS(N)=ENDS(N)+1 IIS(N)=IIS(N)+1 ENES(N)=ENES(N)+1 IIX(N)=IIX(N)+1 YW(N)=YW(N)+1 MAXT=MAXT+1 GO TO (710,710,655), INDP </pre>
<pre> 610 FORMAT(1X,10,I3) IF (ERROR .GT. 0) THEN GO TO 601 END IF ELSE IF (INCHG .EQ. '13') THEN ERROR=0 WRITE(*,615) FORMAT(1X,'/ / / INPUT NEW PRANDTL NUMBER') READ(*,620,IOSTAT=ERROR) PR FORMAT(620,1) IF (ERROR .GT. 0) THEN GO TO 611 END IF COUNT1=COUNT1+1 GO TO 635 END IF </pre>	<pre> C CONVERSION TO INTEGRAL FORMAT C IF (INDH0 .EQ. '1') THEN INDH0=1 ELSE IF (INDH0 .EQ. '2') THEN INDH0=2 ELSE IF (INDH0 .EQ. '3') THEN INDH0=3 END IF IF (INDTH .EQ. '1') THEN INDTH=1 ELSE IF (INDTH .EQ. '2') THEN INDTH=2 ELSE IF (INDTH .EQ. '3') THEN INDTH=3 END IF IF (INDHC .EQ. '1') THEN INDHC=1 ELSE IF (INDHC .EQ. '2') THEN INDHC=2 ELSE IF (INDHC .EQ. '3') THEN INDHC=3 END IF IF (INDTR .EQ. '1') THEN INDTR=1 ELSE IF (INDTR .EQ. '2') THEN INDTR=2 END IF IF (INDR .EQ. '1') THEN INDR=1 ELSE IF (INDR .EQ. '2') THEN INDR=2 END IF IF (INDP .EQ. '1') THEN INDP=1 ELSE IF (INDP .EQ. '2') THEN INDP=2 END IF C END OF KEY BOARD INPUTS </pre>	<pre> IF (XEND.LE.X(MAX)) GO TO 640 DO 645 I=1,MAX I=I+1 X(I)=X(I)+600 GO TO 650 X(N)=X(N)+1 Y(N)=Y(N)+1 YS(N)=YS(N)+1 ENDS(N)=ENDS(N)+1 IIS(N)=IIS(N)+1 ENES(N)=ENES(N)+1 IIX(N)=IIX(N)+1 YW(N)=YW(N)+1 MAXT=MAXT+1 GO TO (710,710,655), INDP </pre>
<pre> IF (XEND.LE.X(MAX)) GO TO 640 DO 645 I=1,MAX I=I+1 X(I)=X(I)+600 GO TO 650 X(N)=X(N)+1 Y(N)=Y(N)+1 YS(N)=YS(N)+1 ENDS(N)=ENDS(N)+1 IIS(N)=IIS(N)+1 ENES(N)=ENES(N)+1 IIX(N)=IIX(N)+1 YW(N)=YW(N)+1 MAXT=MAXT+1 GO TO (710,710,655), INDP </pre>	<pre> IF (XEND.LE.X(MAX)) GO TO 640 DO 645 I=1,MAX I=I+1 X(I)=X(I)+600 GO TO 650 X(N)=X(N)+1 Y(N)=Y(N)+1 YS(N)=YS(N)+1 ENDS(N)=ENDS(N)+1 IIS(N)=IIS(N)+1 ENES(N)=ENES(N)+1 IIX(N)=IIX(N)+1 YW(N)=YW(N)+1 MAXT=MAXT+1 GO TO (710,710,655), INDP </pre>	<pre> IF (XEND.LE.X(MAX)) GO TO 640 DO 645 I=1,MAX I=I+1 X(I)=X(I)+600 GO TO 650 X(N)=X(N)+1 Y(N)=Y(N)+1 YS(N)=YS(N)+1 ENDS(N)=ENDS(N)+1 IIS(N)=IIS(N)+1 ENES(N)=ENES(N)+1 IIX(N)=IIX(N)+1 YW(N)=YW(N)+1 MAXT=MAXT+1 GO TO (710,710,655), INDP </pre>

Program "nbl6" (cont.)

<pre> 3101 11 139816:03:07 nbl6.f Page 17 WRITE (26,770) NUMB,XXX(J1),TNNH(J1) 770 FORMAT(1X,'/ 1X','CARD',13,13X,'XX'='E15.6,/,35X,'TNH'='E15.6') 775 IF(LAP.EQ.2) GO TO 775 780 WRITE(26,780) 785 FORMAT(1X,20X,'//',52X,' WALL DATA ',//, 16X,'X(N)',16X,'Y(N)',16X,'M',//) 790 WRITE(26,790) 795 FORMAT(1X,20X,'//',50X,' CENTERLINE DATA ',//, 16X,'X(N)',16X,'Y(N)',16X,'M',//) 800 CONTINUE 800 RETURN END </pre>	<pre> 3101 11 139816:03:07 nbl6.f Page 18 1110 SH=TN(H)/'TO-1. 1111 AI=5.71*(ABS(SH))**0.182)-51.8 1112 BI=1.51-0.722*(ABS(SH))**0.125 1113 A2=(7.77*SH+16.125)*SH**7.121*SH-2.363 1114 B2=(0.32*SH+0.04)*SH-0.174*SH+0.73 1115 C2=2.6*(SH+1.0) 1116 A3=1.28-1.106*(ABS(SH))**0.964 1117 B3=0.903-0.088*(ABS(SH))**4.533 1118 GNGEQUINE/RHOE 1119 RETURN END SUBROUTINE LAM IT E IMPLICIT DOUBLE PRECISION (A-H, O-Z) CHARACTER 8, FMT DIMENSION X(1000), YY(1000), EME(1000), EMF(1000), HALFA(16), XI(16), XILN(16), 1 DMDS(1000), S(1000), PVOPO(1000), DMDS(1000), FMT(10), 2 DMDS(1000), YY(1000) COMMON CF0V2, CF0V1, CF0V2T, DELRAT, DELTA, DELTH, DHEAT, DTIDS 1.DUDS, EN, ENBAR, ENTRUB, H, INC, OLDDTH, REL, RETH, RETHT, RHOE, THETA, 2.TAUMAL, THBAR, THETA, THOVD, TLE, ULVE, TRCON, THZERO, PO, TO, THALL, 3.GAMMA, OMEGA, WATE, CP, CMIO, SW, A, B1, B2, C2, C3, B3, GRUE, TE, TAD, 4.TADTE, TWE, QUAY, TETO, UE, GRUE, HA, DPO, DL, XINC, X(1000), YY(1000), 5.EME(1000), HALFA(16), XI(16), XILN(16), TM(1000), PVOPO(1000), 6.DMDS(1000), FMT(10), IT, L, N, LINES, COUNT, LAP, NN, INDFC, INDMU, 7.INDTW, INDR, INDC, MAX, MIN, INDFC, MAX, MIN, INDFC, INDMU, INDRG 1210 ENRA=(THETA**2*DUDS)/(GRUE*PVOPO) 1211 HINC2=(ENBAR**2*DUDS)/CFOV2 1212 H=INCG(TETO+(TO-TE))/TE 1213 EL-A3=(ENBAR**B3)+0.22 1214 REPH=REL*THETA 1215 CFOV2=EL/RETH 1216 DUDS=CF0V2 DUDS=0. IF (ENBAR+.3) 10,15,15 10 D5=-3. DDOT=7.9160948*((1130.38170*D5+S9*19725)*S8+ 1 1152.310133*SH+112.21677)*D5+6.13052*D5+(-14.046635*S8+ 2 -30.64551)*SH-4.13355)*SH+8.2910568)*D5+((- 3-3.3482207*SW-0.99306674)*SH+2.254166)*S8 DDOT=DDOT*DDOT THODI=1./ (DOT+(TO/TE-1.)* (HINC*1.)) DELRAT=H*THOVDL 1216 RETURN END SUBROUTINE TRATR IMPLICIT DOUBLE PRECISION (A-H, O-Z) CHARACTER 8, FMT DIMENSION X(1000), YY(1000), EME(1000), EMF(1000), HALFA(16), XI(16), XILN(16), 1 DMDS(1000), S(1000), PVOPO(1000), DMDS(1000), FMT(10), 2 DMDS(1000), YY(1000) COMMON CF0V2, CF0V1, CF0V2T, DELRAT, DELTA, DELTH, DHEAT, DTIDS 1.DUDS, EN, ENBAR, ENTRUB, H, INC, OLDDTH, REL, RETH, RETHT, RHOE, THETA, 2.TAUMAL, THBAR, THETA, THOVD, TLE, ULVE, TRCON, THZERO, PO, TO, THALL, 3.GAMMA, OMEGA, WATE, CP, CMIO, SW, A, B1, B2, C2, A3, B3, GRUE, TE, TAD, 4.TADTE, TWE, QUAY, TETO, UE, GRUE, HA, DPO, DL, XINC, X(1000), YY(1000), 5.EME(1000), HALFA(16), XI(16), XILN(16), TM(1000), PVOPO(1000), 6.DMDS(1000), FMT(10), IT, L, N, LINES, COUNT, LAP, NN, INDFC, INDMU, 7.INDTW, INDR, INDC, MAX, MIN, INDFC, INDMU, INDRG 1310 REPH=REL*THETA GO TO 1311,311,1INDCF 1311 ENTURB=0.85*LOG(RETHT)-1.29 GO TO 1312 1312 ENTURB=-0.9030368*LOG(RETHT)-1.65 1312 IF (IT=4) 1315,131,1313 1313 EN=ENTURB 1314 GO TO 1317 1315 DELRT=RETHT-RETHTER </pre>
--	--

Program "nbl6" (cont.)

```

101 1 906 1633;07
nblc.f

1116 EN=(15.25E-3)-(1.9E-6)*DELTRE*DELTRE*1.25
1117 A=1,-TADE
1118 B=-TADE-TWE
1119 P=TADE-TWE
1120 D 0 1331 J=1,2
1121 SUH=0.
1122 D 0 1124 I=1,16
1123 GIZMO=HALF((1.)*(EXP(XILN(I)*POH)))/(A*X1(I)+B)*X1(I)+TWE)
1124 SUH=SUM(GIZMO)
1125 F(1)=1.328,1.328,1.331
1126 F(2)=1.328,1.328,1.331
1127 GAGET=N*SUM
1128 DEFLAT=-GAGET
1129 POFREN=1.
1130 POFREN=1.

1131 CONTINUE
1132 THVOIL=GADGET-EN*SUM
1133 HE=THVOIL-TRHOIL
1134 DO 1136 I=1,2
1135 TLE=1.-4.68./GAMMA-1.*((1.-ULVE)/((1.-ULVE)**2))
1136 ULVE = 20.*THVOIL/(TLE*(1.-OMEGA)) / RETH) * (1. / (EN-1.1)
      GO TO (1137,1137),INDF
1137 CFVOZ=.00205*TTO*0.5*(TWE/TADE)*0.345/RETH*0.1
1138 GO TO 1138
1139 CFVOZ=((20.*ENTURB)/(1.-ENTURB))*(1.-ENTURB)*(1.-ENTURB)/(1.-OMEGA/RETH)
1140 F(1)=1.328,1.328,1.333
1141 F(2)=1.328,1.328,1.333
1142 QUAY=(CFVOY-CFOVZ)/(RETH*2)
1143 GO TO 1143
1142 CFOV=CFOV2-QUAY/(RETH*2)
1143 RETURN
1144 END

SUBROUTINE OUT
  IMPLICIT DOUBLE PRECISION (A-H, O-Z)
  CHARACTER *8, FM
  DIMENSION X(1000), Y(1000), ENE(1000), HALFA(16), XILN(16),
  1TN(1000), S(1000), POVO(1000), DWD(1000), PRM(10),
  2DELY(1000), YY(1000)
  COMMON CFWOZ,CFVOZ,CFVOY2,DELTA,TDELTA,DELTH,DIBAT,DHDOS
  1,DUEDS,EN,ENBAR,ENTUB,H,HING,OLDDT,BEL,RETH,REHTH,PHGE,THETA,
  2,TAUML,THBAR,THTR,2,THVOIL,TILT,ULVR,TRCON,THIERO,TO,THAL,
  3,GNAMN,OMEGA,WATE,CP,PR,GMDW,SM,AL,BI,A2,R2,C2,A3,B3,GRUE,TE,TAD,
  4,TDATTE,TME,QUAY,TE,U,E,GHU,E,HAD,DL,INC,SE,HE,16,TW110001,S10001,POPO110001,
  5,SEME(1000),HALFA(16),XI(16),TW110001,S10001,POPO110001,
  6,DWD(1000),FTT(10),IT,L,N,LINDE,MOUNT,JAH,NN,INDE,INMMO,INDMO,
  7INDTH,INDTR,INDIC,MAX,MIN,INDOUT,TMES,INDPG,
  XCORX(N),12,
  SECORS(N),12,
  YCOR(Y(N),12),
  BCLAS=L,THETA=L,TAUML=DPOS
  THIN=THETA,12,
  DELSIN=DELTH,12,
  DELIM=DELTHIN,THVOIL,
  THTAITH(N),TAD
  THTOTW(N)/TAD
  TAD=TAD//TO
  CF=CFVOZ/2
  1(IN,GT,MIN) GO TO 12
  4 FORMAT(1X,19,*///,56X,*/* OUTPUT CODE */***/)
  5 FORMAT(20*,(X(1N),10X,'$IN'),10X,YINN),12X, M*,10X,
  6 WRITE(*,6), '(X,RETH),1X,*PO',//)
  15,FORMAT(1X,10X,'$IN'),10X,(TR(R),9X,'$IN'),1X,'RHOE(PSEC2/FT4)',//)
  7 FORMAT(18*,DELTAIN1,'6X,$TRETA1IN1','6X,'DELSTAR1IN1','9X,'H',11X
  1,1,TWT(10X,'$IN'),10X,'$AD1TO',//)
  8 FORMAT(17A,10D(11/FT2),4X,'$DODS(1/SEC)',7X,'$DODS(1/SEC)',6X,
  19,FORMAT(65*,TDAFL(P,FT2),9X,'$IN'),1X,'$CF',11X,'$BTU(P/SEC2)',//)
  9 FORMAT(165*,(8BTU/FT2/SEC)',1X,'$IN'),1X,'$IN(BTU/P/SEC2)',//)

```

Program "nbl6" (cont.)

Jul 11 1996 16:03:07 nbl6.f
Page 22

```
SUBROUTINE LAGINT(X,Y,NPTS,XX,YY,DY)
IMPLICIT DOUBLE PRECISION (A-H, O-Z)
DIMENSION X(1),Y(1)
C1=.1.
DO 40 I=1,NPTS
DY=0.
YY=0.
DO 10 J=1,NPTS
C2=.1.
C1=C1*(XX-X(J))
IF (J .EQ. 1) GO TO 10
C2=C2*(X(1)-X(J))
10 CONTINUE
SUM=0.
DO 30 J=1,NPTS
IF (J .EQ. 1) GO TO 30
C3=.1.
DO 20 K=1,NPTS
IF (K .EQ. 1) OR. K .EQ. 0. J GO TO 20
C3=C3*(XX-X(K))
20 CONTINUE
SUM=SUM+C3
30 CONTINUE
Y1=Y1/C2
Y1=Y1-C1
D1=D1+C1*SUM
40 CONTINUE
RETURN
END
```

LIST OF REFERENCES

1. Kavandi, J.L., Callis, J.B., Gouterman, M., Green, G., Khalil, G., Burns, D. and McLachlan, B.G., "Surface Pressure Field Mapping using Luminescent Coatings", *Experiments in Fluids*, v.14, pp. 33-41, 1993.
2. Kavandi, J.L., Callis, J.B., Gouterman, M., Khalil, G., Wright, D., Green, E., Burns, D. and McLachlan, B.G., "Luminescent Barometry in Wind Tunnels", *Rev. Sci. Instruments*, Vol. 61, No. 5, pp. 3340-3347, November 1990.
3. Peterson, J.I. and Fitzgerald, R.V., "New Technique of Surface Flow Visualization Based on Oxygen Quenching of Fluorescence", *Rev. Sci. Instruments*, Vol. 51, pp.670-671, May 1980.
4. Volland, A. and Alati, L., "A New Optical Pressure Measurement System", 14th International Congress on Instrumentation in Aerospace Simulation Facilities (ICIASF), Paper No. 10, Rockville, Md., October 1991.
5. Morris, M.J., Donovan, J.F., Kegelman, J.T., Schwab, S.D., Levy, R.L. and Crites, R.C., "Aerodynamic Applications of Pressure-Sensitive Paint", AIAA Paper No. 92-0264, 30th AIAA Aerospace Sciences Meeting, Reno, Nevada, January 1992.
6. Morris, M.J., Benne, M.E., Crites, R.C. and Donovan, J.F., "Aerodynamic Measurements Based on Photoluminescence", AIAA Paper No. 93-0175, 31th AIAA Aerospace Sciences Meeting, Reno, Nevada, January 1993.
7. McLachlan, B.G., Bell, J.H., Kennelly, R.A., Schreiner, J.A., Smith, S.C., and Strong, J.M., "Pressure-Sensitive Paint Use in the Supersonic High-Speed Oblique Wing (SHOW) Test", AIAA Paper No. 92-2686, 10th AIAA Applies Aerodynamics Conference, Palo Alto, Ca., June 1992.
8. McLachlan, B.G., Bell, J.H., Espina, J., Gallery, J., Gouterman, M., Demandante, C.G.N. and Bjarke, L., "Flight Testing of a Luminescent Surface-Pressure Sensor", NASA Technical Memorandum 103970, October 1992.
9. Kavandi, J.L., *Luminescence Imaging for Aerodynamic Pressure Measurements*, Doctoral Thesis, Chemistry Department, University of Washington, 1990.
10. Moore, W.J., *Physical Chemistry*, Prentice Hall, Inc., 1962.

11. Pringsheim, P., *Fluorescence and Phosphorescence*, Interscience Publishers, 1949.
12. Calvert, J.G. and Pitts, J.P. Jr., *Photochemistry*, John Wiley and Sons, Inc., 1966.
13. Wayne, R.P., *Photochemistry*, American Elsevier Publishing Company, Inc., 1970.
14. Rice, O.C., *Electronic Structure and Chemical Binding*, Dover Publications, Inc., 1969.
15. Parker, C.A., *Photoluminescence of Solutions*, Elsevier Publishing Company, 1968.
16. Cundall, R.B. and Gilbert, A., *Photochemistry*, Appleton-Century-Crofts, 1970.
17. Wendland, R.A., *Upgrade and Extension of the Data Acquisition System for Propulsion and Gas Dynamics Laboratories*, M.S.A.E. Thesis, Naval Postgraduate School, Monterey, California, June 1992.
18. Adamson, T.C. Jr. and Nicholls, J.A., "On the Structure of Jets From Highly Underexpanded Nozzles Into Still Air", *J. Aero/Space Sciences*, Vol. 26 No. 1, 1959.
19. James H. Bell, (Private Communication) NASA Ames, Moffet Field, CA., January 1994.
20. Instruction and Operating Manuals, *Quartz Tungsten Halogen Lamp Housing Model 66186 and Lamp Controller Model 6405*, Oriel Corporation, 1992.
21. Hord, M.R., *Digital Image Processing of Remotely Sensed Data*, Academic Press, 1982.
22. McLachlan, B.G., and Bell J.H., "Image Registration for Luminescent Paint Sensors", AIAA Paper No. 93-0178, 31st Aerospace Sciences Meeting and Exhibit, Reno, Nevada, January 1993.
23. User's Manual, *EPIX 4MIP - 4MIPTOOL Interactive Image Analysis Software*, EPIX Incorporated, 1993.
24. Perretta, D.A., *Laser Doppler Velocimetry Measurements Across A Normal Shock In Transonic Flow*, M.S.A.E. Thesis, Naval Postgraduate School, Monterey, California, March 1993.
25. Kooi, J.W., "Experiment on Transonic Shock-Wave Boundary Layer Interaction", *Advisory Group for Aerospace Research and Development (AGARD)*, AGARD-CP-168, pp. 30-1, 30-10, November 1975.

26. Sebra, D.K., *Electronic Structure and Chemical Bonding*, Blaisdell Publishing Company, 1964.
27. Rice, O.K., *Electronic Structure and Chemical Binding*, Dover Publications, Inc., 1969.
28. Beynon, J.D.E. and Lamb, D.R., *Charge-Coupled Devices and Their Applications*, McGraw-Hill, 1980.
29. Demo, Jr., W.J., *Cascade Wind Tunnel for Transonic Compressor Studies*, M.S.A.E. Thesis, Naval Postgraduate School, Monterey, California, June 1978.

INITIAL DISTRIBUTION LIST

- | | |
|---|----|
| 1. Defense Technical Information Center
8725 John J. Kingman Rd., STE 0944
Ft. Belvoir, VA 22060-6218 | 2 |
| 2. Dudley Knox Library
Naval Postgraduate School
Monterey, California 93943-5002 | 2 |
| 3. Chairman, Department of Aeronautics and Astronautics
Code AA
Naval Postgraduate School
699 Dyer Road - Room 137
Monterey, California 93943-5106 | 1 |
| 4. Professor R.P. Shreeve
Department of Aeronautics and Astronautics
Code AA/SF
Naval Postgraduate School
699 Dyer Road - Room 137
Monterey, California 93943-5106 | 10 |
| 5. Professor G.V. Hobson
Department of Aeronautics and Astronautics
Code AA/HG
Naval Postgraduate School
699 Dyer Road - Room 137
Monterey, California 93943-5106 | 1 |
| 6. Commander, Naval Air Systems Command
Code Air 4.4 T
1421 Jefferson Davis Hwy
Arlington, Virginia 22243 | 1 |
| 7. Naval Air Warfare Center-Aircraft Division
Code Air 4.4.3.1 [S. McAdams]
Propulsion and Power Engineering Bldg. 100
Patuxent River, Maryland 20670-5304 | 1 |

8. Curricular Officer, 1
Department of Aeronautics and Astronautics
Code 31
Naval Postgraduate School
699 Dyer Road - Room 135
Monterey, California 93943-5106
9. Lieutenant D.L. Seivwright 3
149 Edde Court
Marina, California 93933